

PHYSICO-CHEMICAL STUDIES ON COPOLYMERS OF
2-METHYLENEGLUTARONITRILE AND SELECTED DERIVATIVES

A Thesis submitted to
the University of Stirling
for the Degree of
Doctor of Philosophy

STEPHEN HENRY CREE

Department of Chemistry
November 1985

Nov 85

PREFACE

This thesis is submitted for the degree of Doctor of Philosophy at the University of Stirling, having been submitted for no other degree. It is a record of research undertaken in the Department of Chemistry. This work is wholly original except where due reference is made.

ACKNOWLEDGEMENTS

I wish to thank my supervisor, Professor J. M. G. Cowie, not only for his guidance and advice during this period of study, but also for his encouragement and enthusiasm, generated during many stimulating discussions.

I am also very grateful to Dr. R. Ferguson whose expertise made available to me the computer programs employed in this work. His willingness to spend time on the writing and/or modification of the above programs is much appreciated.

My thanks also go to Dr. I. J. McEwen for his practical assistance and experimental instruction in both synthetic and instrumental techniques.

I must also thank a number, if not all of the members of the Department of Chemistry at Stirling, both academic and services, for their assistance during my period of study. In the latter category special thanks must go to Greta who performed all the C, H, and N analysis and to Mr. G. Castle who was almost always able to provide the desired chemical from a store which he professed did not stock it. As regards this thesis, thanks go once again to Dr. I. J. McEwen for reading the manuscript, Mrs. P. Brown for her patience whilst typing this work, and Ms. Valerie Reid for arranging submission of the finished item.

I wish to express my sincere gratitude to all my family and friends for their encouragement and to DSM Limburg BV for the financial support during the period of this work.

Finally, ".... yet the worker while he cannot ignore past work, cannot allow himself to be overwhelmed by the large volume of patents and journal papers and feel that nothing significant can be done."

J. Boor Jr. (1974)

ABSTRACT

2-Methyleneglutaronitrile (MGN) has been prepared by the catalytic dimerisation of acrylonitrile. The radical homopolymerisation of dinitrile monomer was investigated. As a method of preparing PMGN, radical initiation suffers from the drawback of competing reactions, resulting in the formation of oligomeric material of irregular structure.

The anionic polymerisation of MGN was performed using organo lithium and organo magnesium reagents, PMGN prepared by dipiperidino magnesium initiation was characterised.

The radical copolymerisation of MGN with a variety of comonomers was carried out. The tendency of MGN to form alternating copolymers with "donor" monomers was observed. The spectroscopic, thermal, and thermomechanical properties of selected copolymers was determined.

Proton nmr studies identified the presence of weak electron donor-acceptor comonomer complexes in CCl_4 solutions of MGN/isoprene and MGN/ α -methyl styrene.

The mechanism of the alternating copolymerisations of MGN/isoprene and MGN/ α -methyl styrene were investigated in terms of the possible involvement of such complexes using a non-linear least squares curve fitting analysis of the compositions of copolymers prepared over a wide comonomer composition range. The analysis coupled with a statistical testing method reveals that in both systems, invoking complex participation does not provide a statistically significant improvement, over the standard Mayo-Lewis terminal model, in the ability to describe the experimental data.

The possible origin(s) of the small deviations observed between the experimental copolymer compositions and those predicted by the Mayo-Lewis model are discussed. In the MGN-isoprene systems, such deviations may

be explained by invoking diene propagation in more than one chemically distinguishable form.

A number of derivatives of MGN have been prepared by elementary chemical reactions. The feasibility of preparing liquid crystalline monomers based on one such derivative, 2-methyleneglutaric acid, has been demonstrated.

CONTENTS

	<u>Page</u>
1	
<u>CHAPTER ONE (INTRODUCTION)</u>	
1.1 2-Methyleneglutaronitrile Monomer	1
1.1.1 Homopolymerisation and Copolymerisation of 2-Methyleneglutaronitrile	2
1.2 Radical Chain Copolymerisation	3
1.2.1 The Terminal Model	3
1.2.2 The Penultimate Model	5
1.2.3 The Complex Model	6
1.3 Alternating Copolymers	7
1.4 Liquid Crystalline Materials	7
1.4.1 Low Molecular Weight Liquid Crystals	7
1.4.2 Classification of Liquid Crystals	8
1.4.3 Polymeric Liquid Crystals	10
2.	
<u>CHAPTER TWO (EXPERIMENTAL)</u>	
2.1 The Dimerisation of Acrylonitrile	12
2.1.1 Preparation of 2-Methyleneglutaronitrile	12
2.2 Potential Monomers Derived from 2-Methyleneglutaronitrile	13
2.2.1 2-Methyleneglutaric Acid	13
2.2.2 2-Methyleneglutaric Anhydride	14
2.2.3 Monoesters of 2-Methyleneglutaric Acid	15
2.2.4 2-Methyleneglutaramic Acid	16
2.2.5 2-Methyleneglutaramide	17
2.2.6 2-Methyleneglutarimide	18
2.2.7 N-Ethyl-2-Methyleneglutarimide	
2.3 Homopolymerisation of 2-Methyleneglutaronitrile	19
2.3.1 Radical Polymerisation of 2-Methyleneglutaronitrile	19
2.3.2 Anionic Polymerisation of 2-Methyleneglutaronitrile	20

	<u>Page</u>
2.4 Radical Copolymerisations	22
2.4.1 Radical Copolymerisation of 2-Methyleneglutaronitrile	22
2.4.2 The Copolymerisation of MGN with Selected Monomers in the presence of a Lewis Acid	22
2.5 Monomer-Monomer Donor-Acceptor Complexation	23
2.6 Instrumentation	25
2.6.1 Number Average Molar Mass Determination	25
Vapour Pressure Osmometry	25
Membrane Osmometry	26
2.6.2 Thermal Analysis	27
Differential Scanning Calorimetry	27
Thermogravimetric Analysis	28
2.6.3 Thermomechanical Analysis	28
Torsional Braid Analysis	28
Dynamic Viscoelastic Measurements	29
2.6.4 Spectroscopic Techniques	31
Nuclear Magnetic Resonance	31
Infrared Spectroscopy	31
Ultraviolet Spectroscopy	31
2.6.5 Miscellaneous Techniques	31
Elemental Analysis	31
Polarising Microscopy	31
3. <u>CHAPTER THREE</u>	
3.1 Radical Polymerisation of 2-Methyleneglutaronitrile	32
3.2 Anionic Polymerisation of 2-Methyleneglutaronitrile	37
4. <u>CHAPTER FOUR</u>	
4.1 Copolymerisation of 2-Methyleneglutaronitrile: A General Survey	42
4.2 Mayo-Lewis Treatment of Selected Copolymerisations	46

	<u>Page</u>
4.3 Thermal and Thermomechanical Analysis	53
4.3.1 Location of the T _g of MGN Copolymers by Differential Scanning Calorimetry	
4.3.2 Gravimetric Analysis	
4.3.3 Torsional Braid Analysis	
4.3.4 Viscoelastomeric Analysis	
4.4 Spectroscopic Analysis of MGN Copolymers	
4.4.1 Spectroscopic Analysis of 2-Methyleneglutaronitrile-Isoprene (MGN-IP) Copolymers	58
4.4.2 Spectroscopic Analysis of 2-Methyleneglutaronitrile- α -Methylstyrene (MGN-MS) Copolymers	61
4.5 Mechanistic Considerations	62
5. <u>CHAPTER FIVE</u>	
5.1 Electron Donor-Acceptor Complex Participation	65
5.2 Electron Donor-Acceptor (EDA) Complexes	65
5.3 NMR Analysis of EDA Complexation	66
5.3.1 Theoretical	67
5.3.2 Complex Stoichiometry	70
5.3.3 Determination of the Equilibrium Quotient	71
5.4 Complex Participation: Pertinent Observations	74
5.4.1 The Initial Rate of Polymerisation in MGN-IP and MGN-MS Systems	74
5.4.2 "Spontaneous" Copolymerisation	75
5.4.3 Copolymerisation in the Presence of Lewis Acid	76
5.4.4 Kelen-Tüdös Analysis	77
5.4.5 Polymer Stereochemistry (Complex Geometry)	79
6. <u>CHAPTER SIX</u>	
6.1 The Complex Participation Model	83
6.1.1 Analysis of the Complex Participation Model using Monomer Feed - Copolymer Composition Data	84

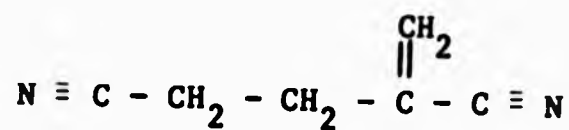
	<u>Page</u>
6.2 Monomer Feed - Copolymer Composition Analysis of the MGN-MS and MGN-IP Copolymerisations	87
6.2.1 Model Discrimination in MGN Copolymerisations on the Basis of Monomer Feed - Copolymer Composition Data	88
6.2.2 The MGN-MS Copolymerisation System	89
6.2.3 The MGN-IP Copolymerisation System	91
6.3 The Mayo-Lewis Terminal Model: Sources of Deviations	92
6.4 The Penultimate Copolymerisation Model	93
6.4.1 Penultimate Model Analysis of the MGN-MS Copolymerisation System	95
6.4.2 Penultimate Model Analysis of the MGN-IP Copolymerisation System	96
6.5 The Copolymerisation of MGN-MS and MGN-IP: Conclusions	98
7. <u>CHAPTER SEVEN</u>	
7.1 Possible Applications of MGN Derivatives	100
7.2 The Proposed Synthesis of Cholesteric Liquid Crystalline Monomers - Polymers	101
7.2.1 Experimental Procedure	103
7.2.2 Discussion	105
7.3 Conclusion	107
Appendix	108
References	109

CHAPTER ONE

INTRODUCTION

1.1 2-METHYLENEGLUTARONITRILE MONOMER

In the early 1960's, U.S. Industrial Chemicals Company (USI)* were actively investigating the growing field of catalytic polymerisation and dimerisation. As a result of these studies, a tertiary phosphine catalysed dimerisation of acrylonitrile was developed which made available for the first time the unique trifunctional compound 2,4-dicyanobut-1-ene (2-methyleneglutaronitrile - MGN).



(I) 2-Methyleneglutaronitrile (MGN)

Subsequently, almost all research on the dimer has been carried out by major chemical concerns.

In 1965, USI issued a bulletin which illustrated the potential variety of commercial products which might be obtained by the chemical transformation of the dinitrile.¹ Enthusiasm within USI was such that a pilot plant was set up at their central research laboratories in Cincinnati to produce around 100,000 lbs per year of MGN. Consequently, numerous patents on the preparation of MGN began to appear in the chemical literature. By 1972 USI,² EI Du Pont de Nemours and Co.,³ Shell Oil Co.,⁴ and Mitsubishi Rayon Co. Ltd.,⁵ were all in possession of patents, while Rhone Poulenc in France⁶ and Mitsubishi Petroleum in Japan⁷ joined USI in producing MGN, by their own patented process, on the pilot plant scale.

Today, however, only Mitsubishi Petroleum produce MGN on a commercial basis. The USI process failed to achieve this level of operation, while the French plant was never restored following a major explosion.

* A division of National Distillers and Chemical Corporation.

1.1.1 Homopolymerisation and Copolymerisation of
2-Methyleneglutaronitrile

Relatively little information concerning the polymerisation properties of MGN is available in the literature. A brief communication by Pritchett and Kamath reported a reluctant radical homopolymerisation but a facile copolymerisation with butadiene, styrene and methyl methacrylate as comonomers⁸. In each case the reactivity ratios were determined from limited analytical data.

In their search for compounds to model branching in polyacrylonitrile, Martinmara et al.⁹ prepared copolymers of acrylonitrile and MGN but again analysis was limited to the determination of the monomer reactivity ratios.

The patent literature reports the anionic polymerisation of MGN in toluene, DMF, and liquid ammonia, initiated respectively by n-butyl-lithium, sodium cyanide, and metallic sodium.¹⁰ However, these reactions were reported to give poor yields of coloured polymers of low intrinsic viscosities.

In 1973 studies carried out by Galin et al.¹¹ in France into the lithium-naphthalene initiated homopolymerisation of MGN showed that such systems yielded a highly polydisperse and branched polymer. Their results were tentatively attributed to chain transfer to polymer via the labile methylene protons α to the nitrile function.

The late sixties and early seventies saw a great deal of patent literature emanating from the Mitsubishi Rayon Co. in Japan^{12,13} concerning the anionic polymerisation of MGN by complex organometallic catalysts such as magnesium bis[(diethyl)(piperidino)aluminate] and the bis(diphenyl amides) of zinc. This interest was primarily stimulated by the potential fibre forming capabilities of a linear polymethyleneglutaronitrile.

However, the homopolymerisation of MGN has never been a wholly satisfactory operation and the more facile copolymerisation reactions are the systems most likely to produce useful and interesting materials.

1.2 RADICAL CHAIN COPOLYMERISATION

By the 1940s considerable progress had been made in interpreting the polymerisation of single monomers, but a systematic study of copolymerisation had been hampered by the absence of a theoretical basis for comparing the behaviour of monomers in such a system. Early research by Staudinger¹⁴ had shown that the composition of a copolymer in most instances differed from that of the comonomer feed and that the relative copolymerisation tendencies of monomers bore little resemblance to their relative rates of homopolymerisation. However, it was not until 1944 that Mayo and Lewis¹⁵ introduced the first successful kinetic analysis of free radical copolymerisation.

1.2.1 The Terminal Model

This was a mathematical treatment of Dostals' hypothesis¹⁶ that the rate of addition of a monomer to a radical is independent of the size and nature of the radical chain and is influenced only by the nature of the radical end group.

The Mayo-Lewis model, or terminal model, recognised four propagation steps (the four combinations of the two chain end radicals and the two monomers, discussed later in chapter 4). This allowed the copolymer composition to be related to the monomer feed composition through two reactivity ratios r_1 and r_2 .

The monomer reactivity ratios provide a measure of the preference a radical exhibits for reacting with its own monomer compared to that of the comonomer. Large values of r (both r_1 and $r_2 \gg 1$) are indicative of a tendency of the monomers to form long homopolymer sequences, whereas

small values of r (both r_1 and $r_2 \approx 0$) imply rapid cross propagation reactions and reflect a tendency for the monomers to alternate in the polymer chain. This latter phenomenon is widespread in copolymerisation¹⁷ and was recognised as early as 1948 by Mayo et al.¹⁸ In a series of papers^{19,20} they stated that this tendency "seems sometimes to be due to steric effects and at other times to dipole effects or specific interactions between monomers". They found that the reactivity of monomers towards attacking radicals could be correlated with the stabilisation of the product radical due to added opportunities for resonance offered by its substituents. Copolymerisation and any alternating tendency was therefore to some extent explained by differences in resonance stabilisation. Generally speaking, it was found that an unstable radical will favour reaction with a resonance stabilised monomer rather than with an unstable monomer and vice versa.

Alternation was also found to be dependent upon any steric hindrance in the system,²¹ especially when considering 1,2 disubstituted ethylene monomers. Such effects were invoked to explain the abnormally low alternating tendency in the diethyl fumarate - vinylidene chloride system²² and for the high alternating tendency in the vinyl acetate - trichloroethylene system.²³

However, alternating effects cannot be explained satisfactorily solely by the difference in resonance stabilisation and by steric effects. A more satisfactory rationale for the tendency to alternate is based on the polarity of the double bonds in the monomers involved.

Polarity is determined by the side group(s) present. Electron withdrawing substituents (eg $-\text{COOR}$, $-\text{CN}$ and $-\text{COCH}_3$) decrease the electron density of the double bond in a vinyl monomer (relative to ethylene), whereas electron donating groups (eg $-\text{CH}_3$, $-\text{OR}$, $-\text{OCOCH}_3$) have the opposite effect. The significant conclusion reached by Mayo

and Walling¹⁹ was that the tendency towards alternation in copolymerisation increases as the difference in polarity between the two monomers increases. Dramatic illustration of this polar effect is evidenced by the facile copolymerisation of monomers which show little or no tendency to homopolymerise, for example maleic anhydride,^{24,25} and diethyl fumarate²⁶.

Therefore alternation, as described by the Mayo-Lewis terminal model, is considered to be a result of transition state stabilisation of the cross propagation reactions by electrostatic interactions between the incoming monomer double bond and the propagating radical chain. This hypothesis has been extended in a semi-quantitative manner by Alfrey and Price in their Q-e scheme.²⁷

The terminal model proved to be extremely successful in accounting for the experimental observations in many copolymer systems, but several systems existed which could not be satisfactorily described.^{28,29,30}

1.2.2 The Penultimate Model

In an attempt to explain some of these deviations, Alfrey et al.³¹ postulated that the reactivity of a propagating chain end radical could in some instances be influenced by the penultimate group in the growing chain. This work was later developed by Barb³² in 1953 and extended by Ham.³³ Barb found evidence for a penultimate effect in the copolymerisation of styrene and sulphur dioxide³⁴ and attributed it to electrostatic repulsion between a penultimate SO₂ unit and a styrene-SO₂ complex. Ham and coworkers³⁵ found that penultimate effects are particularly pronounced with monomers of the type CHX=CHX where X is a polar substituent. More recently Ebdon³⁶ has reported that the styrene-maleic anhydride system may also be described by a penultimate mechanism, although much controversy still exists in this case.³⁷

1.2.3 The Complex Model

An alternative rationalisation of the deviations from the Mayo-Lewis terminal model, in systems which tend to alternate, was proposed by Bartlett and Nozaki³⁸ in 1946. They observed that solutions of some comonomers exhibited a yellow colouration, for example in mixtures of styrene and maleic anhydride, a system known to deviate from the terminal model. This colouration was attributed to the formation of a monomer (1) - monomer (2) charge transfer complex. The authors proposed that this comonomer complex may participate in the propagation reactions to the extent that it adds to the chain end radical as a discrete unit, therefore invalidating the terminal model which considers only four propagation reactions. However, Bartlett and Nozaki did not present any mathematical analysis of the complex model scheme and indeed some subsequent work by Walling et al.³⁹ and Lewis⁴⁰ did not provide evidence which would substantiate the proposed mechanism. These workers found copolymer systems that were characterised by a high degree of alternation but which showed no evidence of monomer (1) - monomer (2) complexation. This, and the lack of dilution effects on the copolymerisation kinetics,⁴¹ suggested that comonomer complexes were not participating in chain propagation. Consequently the complex participation model fell into disfavour. For about three decades the explanation for deviations in the compositional data of copolymers and/or the kinetics of copolymerisation was attempted mainly on the basis of the penultimate model.^{42,43}

In 1971, Seiner and Litt⁴⁴ reported the first mathematical analysis of alternating copolymerisation systems in terms of the participation of a monomer-monomer complex in the propagation reactions. Since then a considerably increased research effort has been devoted to the study of this model, with investigations ranging from the

theoretical treatment of methods used to analyse the experimental data,^{45,46} to the mainly experimental study of alternating systems which may proceed via complex participation.^{47,48}

1.3 ALTERNATING COPOLYMERS

Although the precise mechanism of alternating copolymerisation is an area of intense research and controversy, the alternating copolymers themselves are of interest and utility in a number of ways. Control of the regularity of the copolymerisation may provide copolymers of desired physical or chemical properties in greater consistency. For example, the tensile strength and ultimate elongation at break of poly(acrylonitrile-alt-butadiene) were found to be considerably greater than the random copolymer of similar composition.⁴⁹ A butadiene-propylene alternating copolymer has found use as an industrial elastomer.⁵⁰ This material exhibits a high degree of orientation on stretching, high flex resistance, good resistance towards oxidative degradation and superior stress-strain characteristics compared with conventional rubbers.

Alternating copolymers offer the possibility of distributing potentially reactive side groups regularly along the polymer-backbone. Very little research has been undertaken to exploit this feature which may find use in the fields of catalysis or metal chelation.⁵¹ Such alternating systems could also be used to anchor mesogenic moieties to the polymer chain, for example Finkelmann et al.^{52,53} have demonstrated the feasibility of preparing liquid crystalline polymers by linking conventional low molar mass mesogens to linear polymers.

1.4 LIQUID CRYSTALLINE MATERIALS

1.4.1 Low Molecular Weight Liquid Crystals

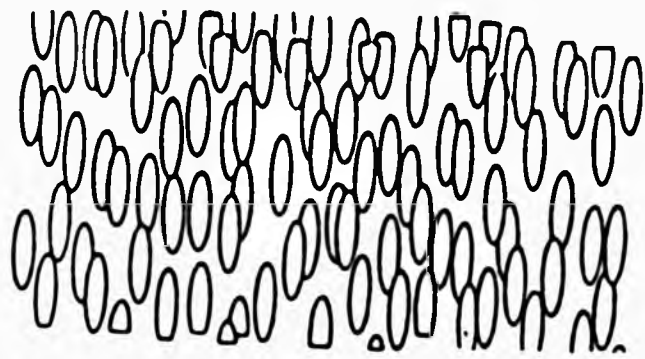
The terms "liquid crystalline" and "mesomorphic state" are used

synonymously to describe a state of matter that is intermediate between a true crystal and a true liquid. The phase has the optical properties of a crystal and the mechanical properties of a liquid. The uniqueness of the mesomorphic state was not recognised until the late 19th century, with the literature at the time containing a number of papers by Reintzer⁵⁴ and Lehmann⁵⁵ in which their relative claims for priority in observing this phenomenon are contested, at times quite acrimoniously.

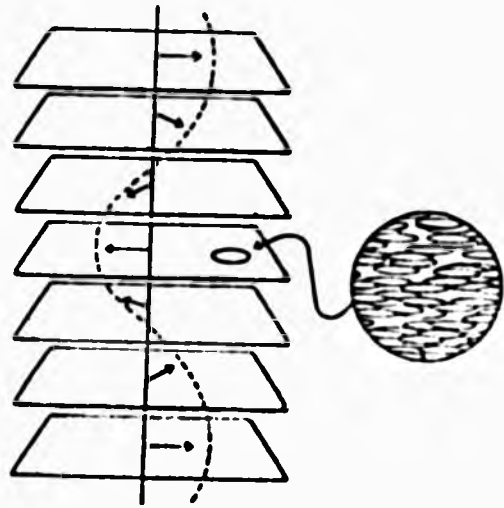
Correlations between the chemical and structural constitution of a molecule and its ability to form a mesophase are largely based on the work of Vörländer,⁵⁶ Wiegand,⁵⁷ and Gray⁵⁸. These investigators determined the general criteria that indicate a molecule's predisposition to forming a liquid crystal. Elongated and rigid rod-shaped, or lathlike, molecules were identified as having the most suitable geometry.⁵⁹ (Chandrasekhar⁶⁰ has discovered "discotic" mesophases composed of large platelike molecules.) For a mesophase to be formed, the cohesive forces operating between the molecules must be anisotropic and of a suitable magnitude. Permanent dipolar groups are present in almost all molecules that form a mesophase, the size and direction of both the total moment and the group moments have been shown to be important.^{61,62} Kast,⁶³ and more recently Demus et al.,⁶⁴ have provided an extensive tabulation of molecules capable of mesophase formation illustrating the large number and variety known.

1.4.2 Classification of Liquid Crystals

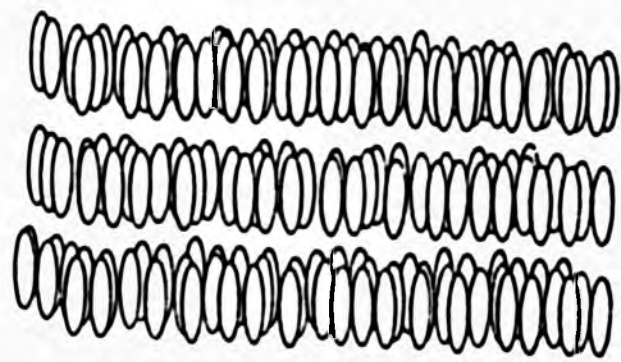
Liquid crystals are termed lyotropic or thermotropic depending upon whether the mesophase is observed by variation of solvent content or by variation of temperature. Thermotropic liquid crystals can be further classified as either nematic, cholesteric (chiral nematic), or smectic, depending upon the arrangement of the molecules in the mesophase.⁶⁵ This is illustrated in Figure 1.1. This classification and terminology



(a)



(b)



(c)

FIGURE 1.1 Schematic representation of (a) nematic (b) cholesteric (chiral nematic) and (c) smectic mesophases.

is based almost entirely on Friedels' observations with the polarising microscope.⁶⁶

In typical nematic liquid crystals the only structural restriction is that the long axes of the molecules maintain a parallel or nearly parallel arrangement over macroscopic distances (Figure 1.1a). Gray⁶⁷ proposed that in cholesteric liquid crystals the molecules are arranged in layers which have a local nematic packing of the molecules. However, the orientation of the molecular axis is displaced regularly in successive layers such that the overall change in orientation describes a helix (Figure 1.1b). There are eleven known smectic structures. With one exception, a smectic phase constitutes a stratified structure in which the molecules are arranged in layers (Figure 1.1c). Each structure possesses a characteristic packing between and within layers. (The exception, smectic D, possesses cubic packing.)

The effect of structure and the chemical constitution of a molecule, on the type of mesophase exhibited, has been extensively studied and has been reviewed recently by Gray.⁵⁸

Such ordered structures are the basis for the practical applications of liquid crystals. For example, the alignment of the molecules can be controlled by magnetic and/or electric fields,⁶⁸ leading to their use in display devices. Cholesteric liquid crystals possess an optical activity, the magnitude of which is without parallel in any solid or liquid. (This is due to the unusual arrangement of molecules and not directly to their asymmetry.) Ferguson⁶⁹ has shown that, due to the helical arrangement of the molecules, cholesteric liquid crystals can behave as a multilayer interference grating, and can selectively reflect incident radiation. The sensitivity of the helical structure to temperature, electric fields, magnetic fields and impurity doping has opened up a host of uses for cholesteric liquid crystals.^{70,71,72}

1.4.3 Polymeric Liquid Crystals

Even before Staudinger had finally recognised the true nature of macromolecular compounds, Vörländer⁷³ had considered the possible mesomorphism of 'infinitely long molecules' and concluded that it must exist. Liquid crystalline properties have been identified in polyethylene melts,⁷⁴ (a smectic structure proposed), polydiethylsiloxane⁷⁵ and polyphosphazenes.⁷⁶ However, such systems exhibit only a distant analogy to the aforementioned low molar mass materials.

In the past few years, numerous research efforts have concentrated on using known mesogenic molecules to prepare liquid crystalline polymers.^{77,78,79} For the preparation of these polymers, the mesogens can be either connected "head to tail" forming liquid crystalline main chain polymers, or linked as side chains to the polymer backbone yielding comblike polymers. This is illustrated in Figure 1.2.

The liquid crystalline main chain polymers⁸⁰ are already commercially used as "high modulus fibres" because the rigid rod like molecules form highly ordered fibres when spun in the anisotropic state.

Compared to the conventional low molar mass liquid crystals, however, these polymers can hardly be ordered in the magnetic or electric field.⁸¹ The liquid crystalline side chain polymers, on the other hand, are more similar to the low molar mass mesogens.

Finkelmann et al.⁸² and Shibaev and coworkers⁸³ have shown that if conventional mesogenic molecules are fixed as side chains to a polymer backbone via sufficient length of "flexible spacer", then nematic, cholesteric, and smectic mesophases can be observed in analogy to the low molar mass derivatives. The flexible spacer (usually an alkyl or alkoxy chain of five or six atoms) is introduced between the polymer backbone and the rigid mesogenic groups in order to decouple the motion of the







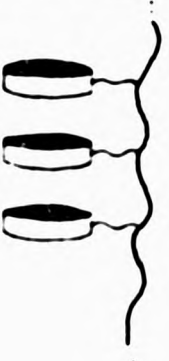
MONOMER UNIT	AMPHIPHILIC	NON AMPHIPHILIC	
		CYLINDRICAL	DISCOTIC
MAIN CHAIN POLYMER			
SIDE CHAIN POLYMER			

FIGURE 1.2 Classification of liquid crystalline monomers and polymers (taken from Ref. 92).

main chain (which tries to achieve a statistical conformation) and the mesogen.⁸⁴ The steric and conformational limitations on the packing of the mesogens are also alleviated. Interestingly, it has been found that in contrast to most low molar mass liquid crystals, the liquid crystalline polymers exhibit a glassy state on cooling. X-ray and polarising microscopy proved that the glassy state of the polymers still shows the macroscopic anisotropic orientation of the mesogens. This procedure may have practical applications as it allows the storage of information.⁸⁵

The synthesis of polymers having mesogenic side chains has taken two approaches.^{86,87} The most convenient method is to introduce into a mesogenic molecule a reactive group capable of undergoing addition polymerisation. A number of polymerisable monomers have been synthesised and have been comprehensively reviewed by Shibaev et al.⁸⁸ and Blumstein and Hsu.⁸⁹ In most cases the polymerisable group is a methacrylate or acrylate moiety.

The second synthetic route starts with preformed reactive polymers which can be modified to mesogenic side chain polymers by using suitably reactive mesogenic monomers. This approach has been employed by Finkelmann⁸² resulting in the smooth addition of vinyl substituted mesogens to poly(hydrogenmethylsiloxane).

Recent research efforts on polymeric liquid crystals have concentrated on three areas. The synthesis of new technologically important materials,⁹⁰ the elucidation of the detailed structure of the mesophases,^{91,92} and the effects of the nature of the polymer backbone, the flexible spacer, and the mesogen, on the mesophase observed.^{93,94}

CHAPTER TWO

EXPERIMENTAL

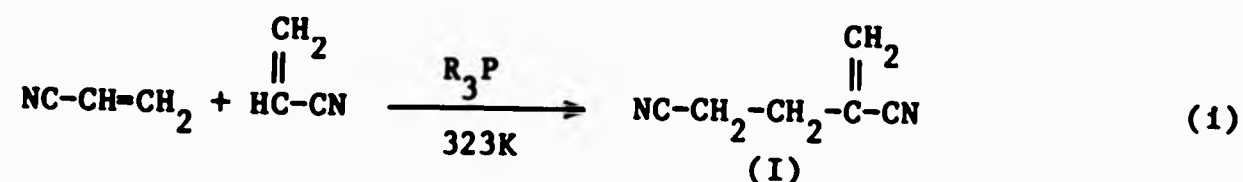
2.1 THE DIMERISATION OF ACRYLONITRILE

Dimers of acrylic compounds have in the past been prepared by heating the monomer in the liquid phase to at least 433K in the presence of a polymerisation inhibitor.⁹⁵ However, when acrylonitrile is heated to 473K by this method, the formation of polyacrylonitrile resin is reported as well as a dimer of unspecified structure.⁹⁶ Heating acrylonitrile to higher temperatures, i.e. 573K, favours the formation of 1,2-dicyanocyclobutanes.⁹⁷

The catalytic dimerisation of acrylonitrile at 298K in the presence of a trialkylphosphine or cycloalkylphosphine was reported by the National Distillers and Chemical Corporation,⁹⁸ to lead to 2,4-dicyanobut-1-ene (MGN) in approximately 35% yield. Appreciable amounts of 1,4-dicyanobut-1-ene (cis and trans) have also been reported to form when triphenylphosphine is used as the catalyst.⁹⁹ In the presence of ruthenium salts and hydrogen, acrylonitrile dimerises to a mixture of 1,4-dicyanobut-1-ene and adiponitrile, the ratios of the two products varying considerably depending on solvent temperature and catalyst.¹⁰⁰ Adiponitrile is the predominant product when cobalt or iron carbonyl are used as catalysts.¹⁰¹

2.1.1 Preparation of 2-Methyleneglutaronitrile (MGN) (I)

By using tri-n-butylphosphine as the tertiary phosphine catalyst, acrylonitrile was dimerised to 2-methyleneglutaronitrile in reasonable yields (equation 1).



Reagents: Toluene was refluxed over CaH₂, distilled and stored over sodium wire. Acrylonitrile was fractionally distilled prior to use. Tri-n-butylphosphine (Aldrich 95%+) was used as supplied.

Procedure: Under a nitrogen atmosphere, 39.5g (0.74 mol) of acrylonitrile was added dropwise to a stirred solution of 0.8g (3.95×10^{-3} mol) of tri-n-butylphosphine in 70 cm^3 toluene at 323K. This addition was accompanied by a discolouration of the solution and the simultaneous formation of brown polymeric resin. The mixture was stirred for a further 30 minutes, cooled to room temperature, and then 100 cm^3 of 1M HCl added to destroy the catalyst. The organic layer was separated, washed twice with water, dried over magnesium sulphate and filtered. The solvent was removed and the residual pale yellow liquid purified by vacuum distillation, giving a 45% yield of colourless MGN distilling at 330-332K/0.2 torr.

Characterisation: The purified monomer was characterised by ^1H and ^{13}C nmr, infrared and ultraviolet spectroscopy. The spectra are shown in Figures 2.1 and 2.2 and the physical properties of MGN are listed in Table 2.1. 2-Methyleneglutaronitrile is miscible with most polar organic solvents and aromatic hydrocarbons. It is, however immiscible with water, aliphatic, and alicyclic hydrocarbons.

2.2 POTENTIAL MONOMERS DERIVED FROM 2-METHYLENEGLUTARONITRILE

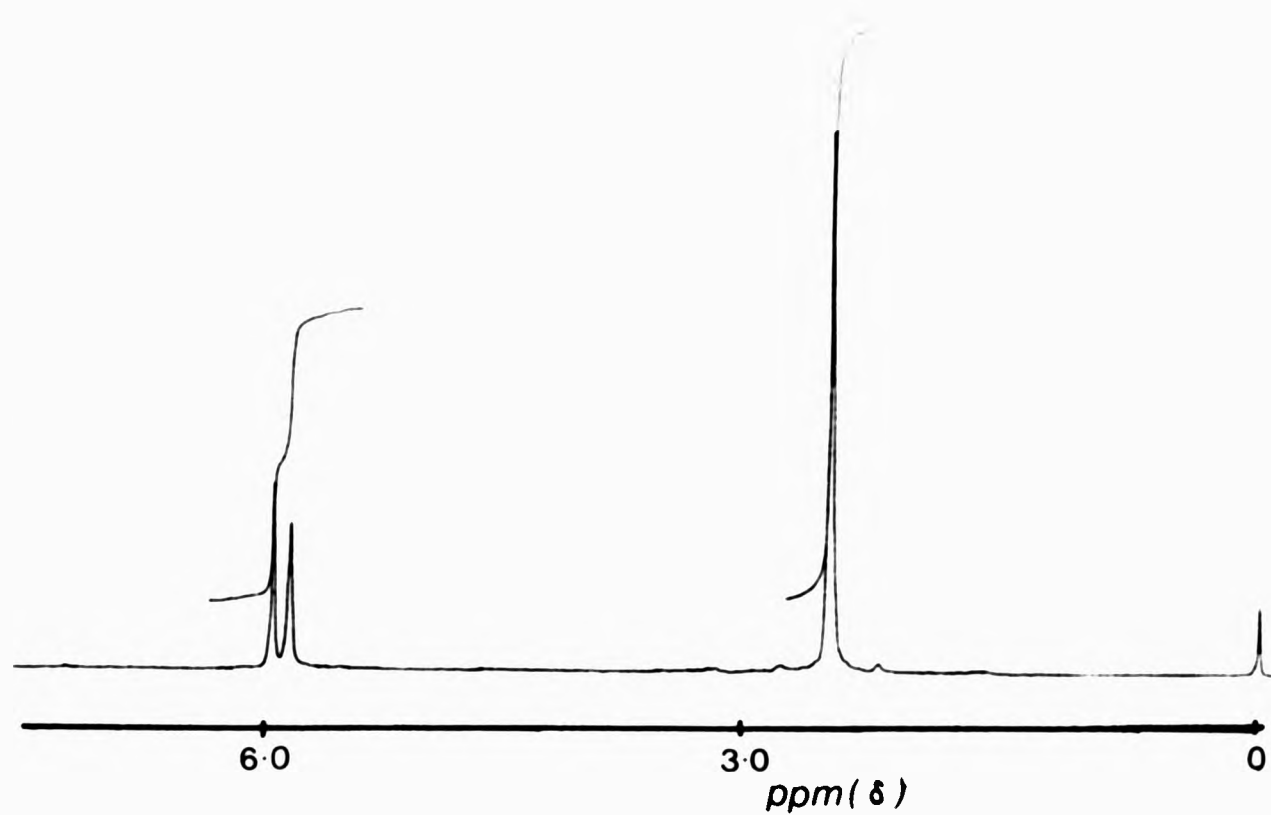
Numerous derivatives of MGN have been prepared by the elementary chemical transformation of the monomer's trifunctional structure. This is illustrated in Figure 2.3.

The application of MGN derivatives is envisaged as twofold.

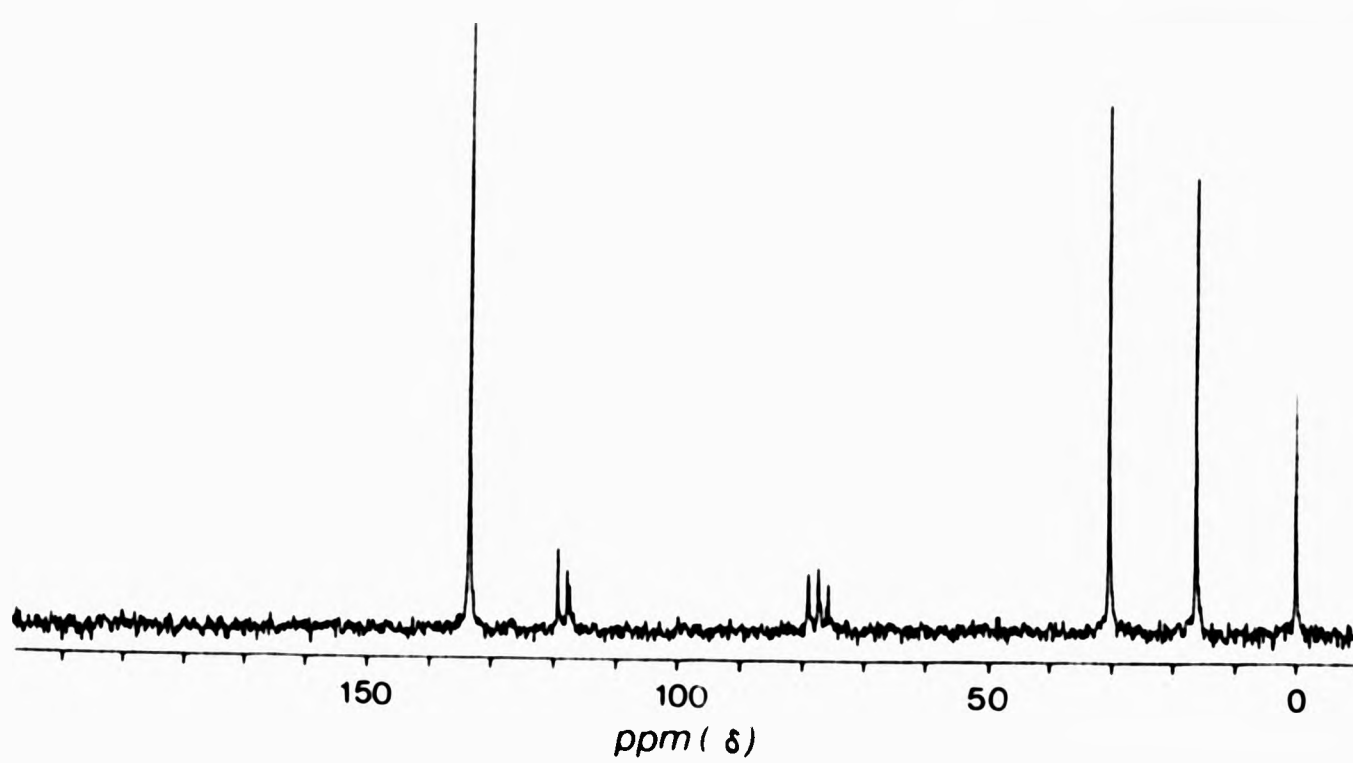
- (a) Their use as monomers in homopolymerisation and/or copolymerisation.
- (b) Their use as the "polymerisable moiety" in the synthesis of potential mesogenic polymers.

2.2.1 2-Methyleneglutaric Acid (II)

This acid has been extensively reported in the literature as the product of numerous and diverse chemical reactions.¹⁰² It has



(a)



(b)

FIGURE 2.1 (a) The ^1H (90MHz) nmr spectrum of MGN.
(b) The ^{13}C nmr spectrum of MGN.

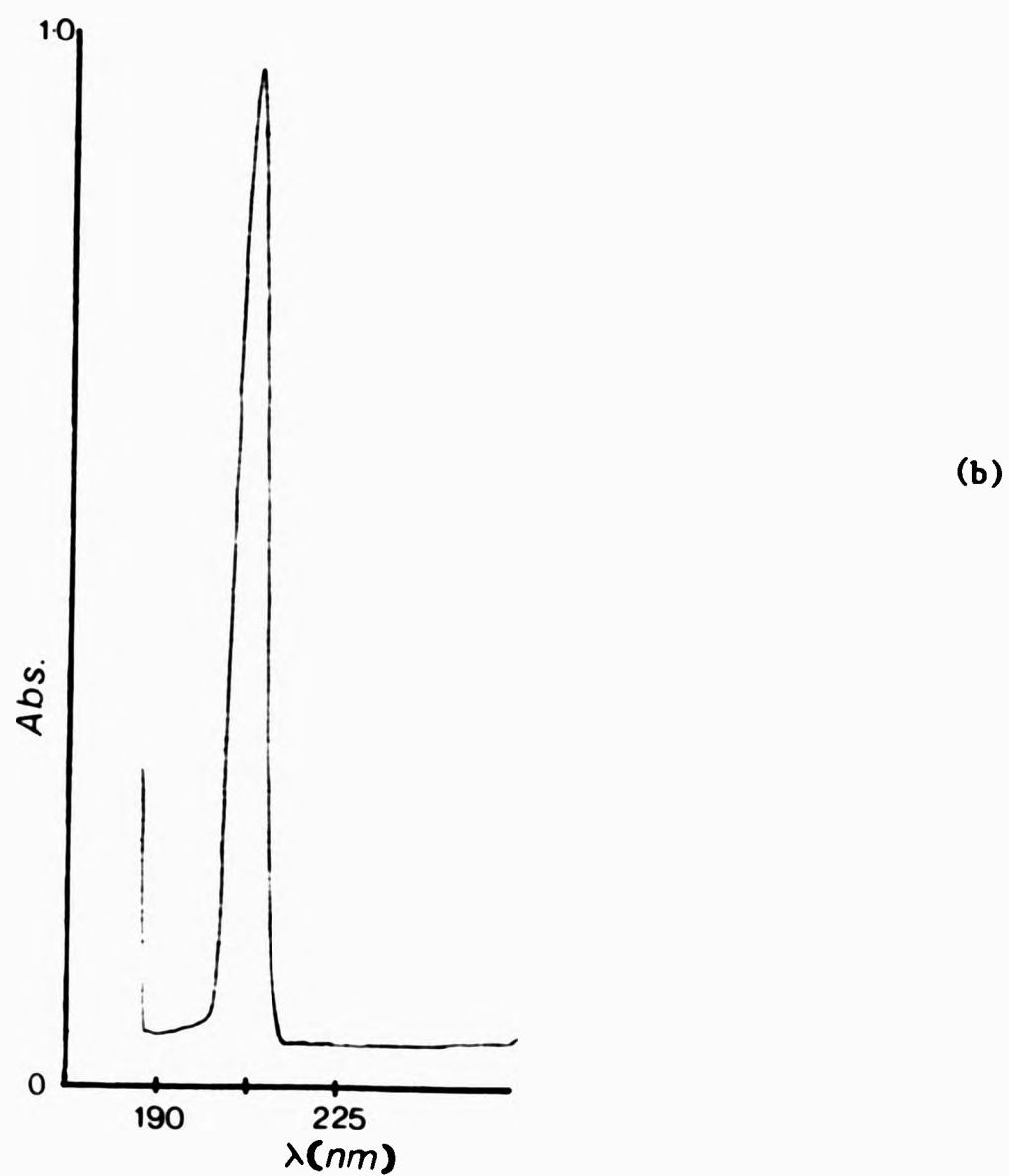
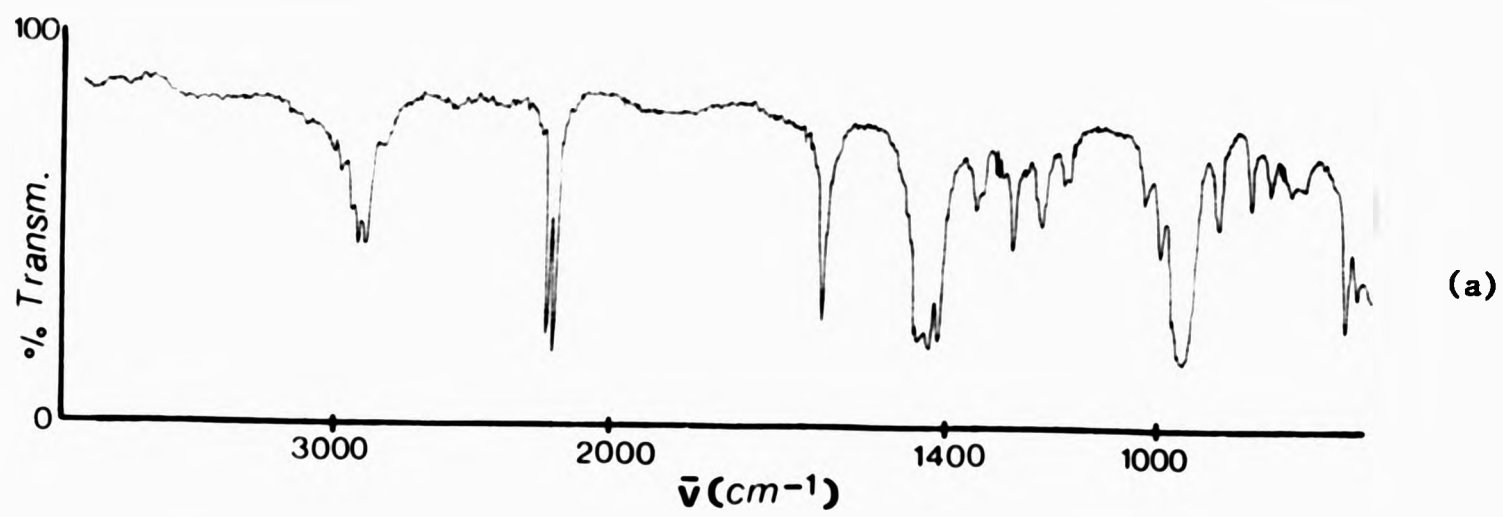


FIGURE 2.2 (a) Infrared spectrum of MGN.

(b) U.V. spectrum of MGN, $\epsilon = 6200$; $\lambda_{\text{max}}^{\text{methanol}} = 205 \text{ nm}$

TABLE 2.1

The Physical Properties of 2-Methyleneglutaronitrile^a

<u>MGN Property</u>	<u>Value</u>
Refractive Index (n_D^{30})	1.4531
Density (D_4^{24})	0.978 g/cm ³
Freezing Point	264.29K
Heat of Fusion	1.85kJ/mol
Specific Heat	0.209 KJ/mol/K
Heat of Vapourisation	75kJ/mol at 383K

a) As reported by U.S.I.

TABLE 2.1

The Physical Properties of 2-Methyleneglutaronitrile^a

<u>MGN Property</u>	<u>Value</u>
Refractive Index (n_D^{30})	1.4531
Density (D_4^{24})	0.978 g/cm ³
Freezing Point	264.29K
Heat of Fusion	1.85kJ/mol
Specific Heat	0.209 KJ/mol/K
Heat of Vapourisation	75kJ/mol at 383K

a) As reported by U.S.I.

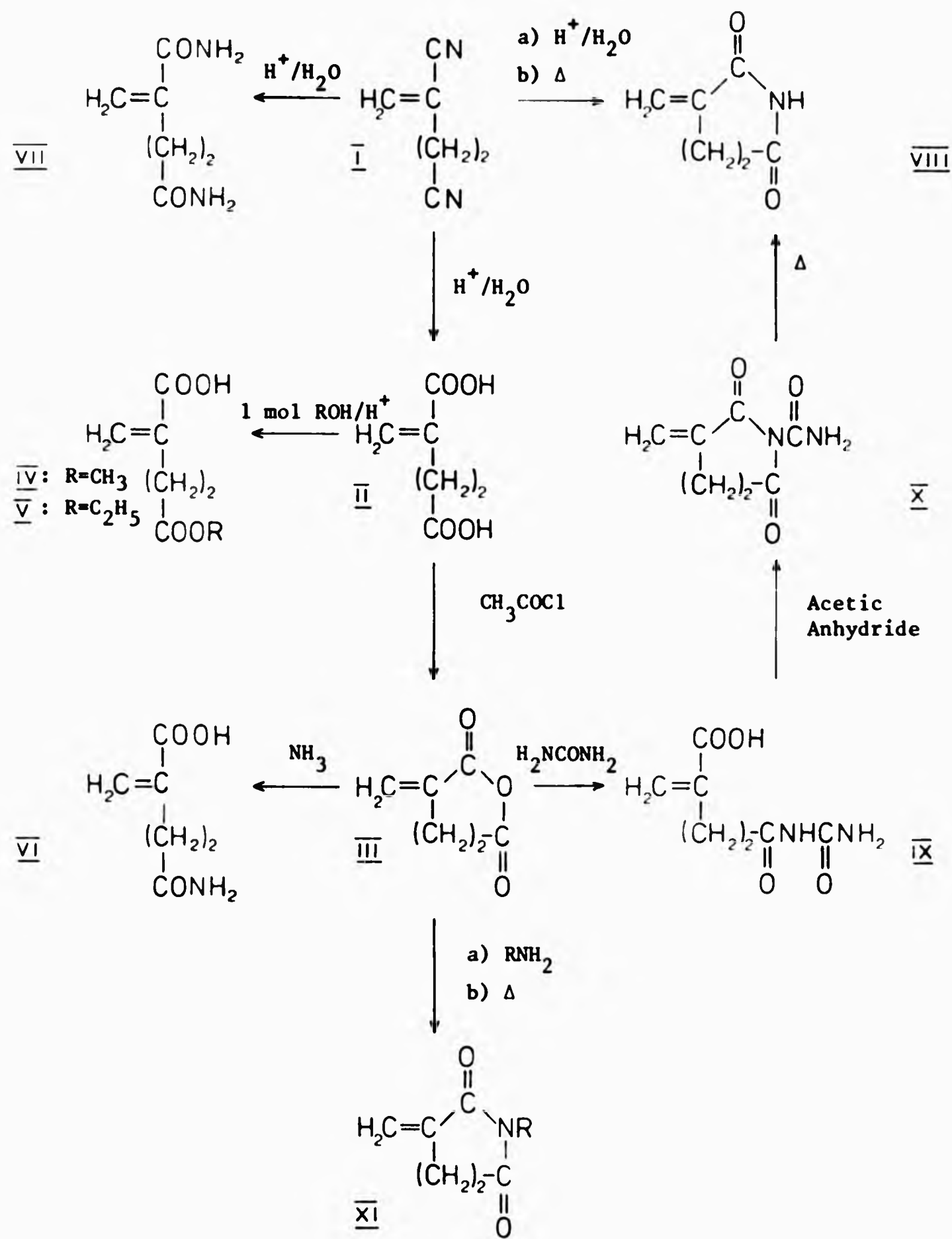


FIGURE 2.3 Preparation of MGN derivatives.

been prepared in this study by the acid catalysed hydrolysis of MGN.
 Procedure: 10.8 cm^3 (0.1 mol) of MGN was added to 20 cm^3 of concentrated hydrochloric acid. The solution was warmed cautiously until the reaction proceeded and the solution began to reflux. Prolonged heating was avoided as it may lead to the formation of the saturated chloro-derivative. On precipitation of ammonium chloride, the mixture was cooled and 20 cm^3 of water added. Extraction of the product with diethyl ether yielded 10.8g (75%) of 2-methyleneglutaric acid, m.pt. = 403-404K. The product was characterised by n m r and i r spectroscopy.
NMR (D_2O) δ ppm: 0.0 (Na TMS), 2.58 (s, 4H), 4.5 (Exchangeable protons), 5.70 (s, 1H), 6.15 (s, 1H).

where s = singlet; d = doublet; t = triplet; q = quartet; m = multiplet.

IR (KBr disc) cm^{-1} : 3250-2600 (b), 1700, 1620 (s).

where b = broad, s = sharp (characterisation absorptions only).

2.2.2 2-Methyleneglutaric Anhydride (III)

The preparation of 2-methyleneglutaric anhydride has been reported in the patent literature and may be accomplished by the dehydration of 2-methyleneglutaric acid using acetyl chloride, thionyl chloride or phosphorus pentoxide.¹⁰³

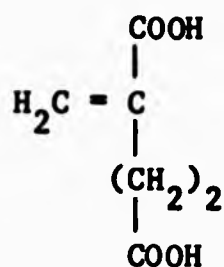
Procedure: Equimolar amounts of II and acetyl chloride were heated at reflux until all the diacid had reacted. The solution was allowed to cool and the acetic acid formed was removed under reduced pressure. The product 2-methyleneglutaric anhydride was obtained in 70% yield by vacuum distillation of the residue, b.pt = 343-348K/0.5 torr, (m.pt. = 332-324K). The anhydride was characterised by n m r and i r spectroscopy.

NMR (CDCl_3) δ ppm: 0.0 (TMS), 3.60 (m, 4H), 5.90 (s, 1H), 6.50 (s, 1H).

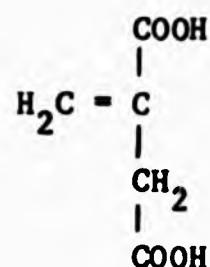
IR (Thin Film) cm^{-1} : 1850 (s), 1765 (s), 1655 (s).

2.2.3 Monoesters of 2-Methyleneglutaric Acid (IV and V)

The close structural similarity between 2-methyleneglutaric acid and itaconic acid is evident.



2-Methyleneglutaric Acid (II)



Itaconic Acid (XII)

The feasibility of the monoesterification of itaconic acid has been thoroughly demonstrated by Baker et al.¹⁰⁴ and in this study the analogous reaction of 2-methyleneglutaric acid is described.

Procedure: The 2-methyleneglutaric acid monomethyl and monoethyl esters (IV and V respectively) were prepared by refluxing a mixture of 2-methyleneglutaric acid and a 3-4 mole excess of the required alcohol with a catalytic amount of acetyl chloride for 20-30 mins. The excess unreacted alcohol was removed rapidly under reduced pressure and the pure monester was isolated and recrystallised from toluene-petroleum ether (1:1). Yields of monester were ca. 60% with m.pt. IV = 339-340K, m.pt. V = 326-327K. The monoesters were characterised spectroscopically.

(IV) NMR (CDCl₃) δppm: 0.0 (TMS), 3.36 (m,4H), 3.71 (s,3H), 5.84 (s,1H), 6.47 (s,1H), 11.5 (s, 1H).

(IV) IR (Thin Film) cm⁻¹: 3200-2800(b), 1730(b), 1700, 1625(s).

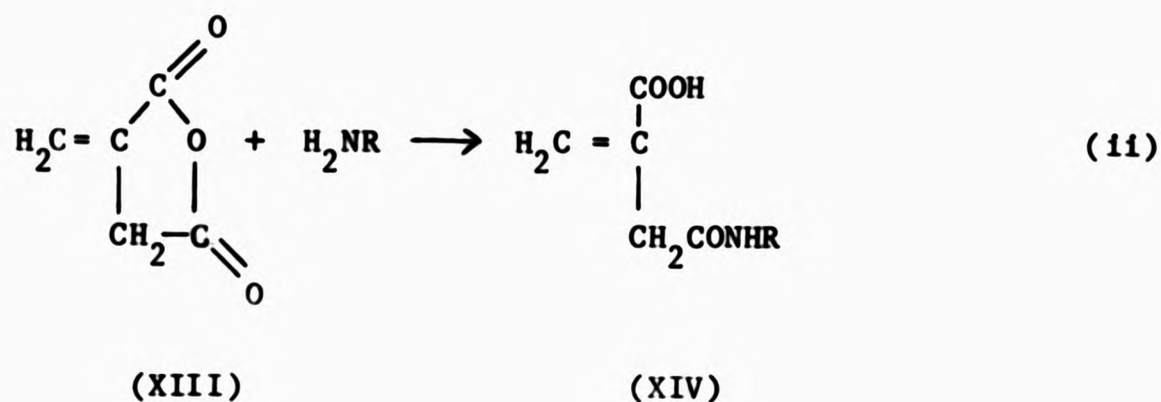
(V) NMR (CDCl₃) δppm: 0.0 (TMS), 1.31 (t,3H), 3.31 (m,4H), 4.25 (q,2H), 5.82 (s,1H), 6.30 (s,1H), 11.45 (s,H).

(V) IR (Thin Film) cm⁻¹: 3200-2800(b), 1730(b), 1700, 1625(s).

2.2.4 2-Methyleneglutaramic Acid (VI)

This potential monomer has not been synthesised previously but synthetic methodology is based upon the analogous reactions of itaconic anhydride.

Zilkha et al.¹⁰⁵ have shown that the ring opening of itaconic anhydride with a molar equivalent of amine results in the preferential formation of 2-methylene-N-alkylsuccinamic acids (equation 11).



This result has been rationalised on the basis of the lowering of the partial positive charge of the α - β unsaturated carbonyl carbon, thus making it less susceptible to nucleophilic attack than the "remote" carbonyl carbon.

Procedure: Excess dry gaseous ammonia was passed into an ice-cooled solution of 2-methyleneglutaric anhydride in chloroform. The ammonium salt which precipitated was filtered, dissolved in water, and heated for a few minutes to expel excess ammonia. The solution was then passed through a column packed with cation exchange resin (nuclear sulphonic acid type resin, Amberlite IR-120). The excess solvent was removed and the crude product was recrystallised from ethanol to give 2-methyleneglutaramic acid, m.pt. = 426-428K, in 45% yield. The monomer was characterised by nmr and ir spectroscopy.

NMR (D_2O) δ ppm: 0.0 (Na TMS), 3.3 (s, 4H), 4.6 (exchangeable protons),

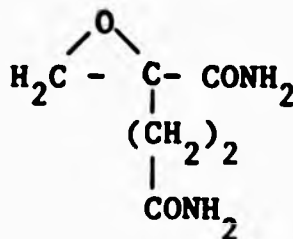
5.86 (s, 1H), 6.33 (s, 1H).

IR (KBr Disc) cm^{-1} : 3380 (b), 3200 (b), 3100-2600 (b), 1700 (s), 1670 (s), 1640 (s), 1590 (s).

2.2.5 2-Methyleneglutaramide (VII)

This interesting material has been reported in the patent literature as the precursor to the saturated derivative 2-methylglutaramide.¹⁰⁶

In this study 2-methyleneglutaramide was prepared by the intermediate hydrolysis of 2-methyleneglutaronitrile. A conventional preparation employing aqueous sodium hydroxide containing 10% H_2O_2 proved unsuccessful due to the addition of hydrogen peroxide across the vinylic system to yield the epoxyamide compound XV.



(XV)

The desired amide VII was however successfully prepared by the hydrolysis of MGN employing (a) concentrated H_2SO_4 or (b) MnO_2 heterogeneous catalysis.

(a) The product resulting from the acid hydrolysis of MGN depends to a large extent on the concentration of the acid employed. The use of dilute sulphuric acid results in the complete hydrolysis of MGN to the corresponding 2-methyleneglutaric acid. When concentrated (85%) sulphuric acid is employed, partial hydrolysis to the diamide VII results. Procedure: 19.0 cm^3 (0.17 mol) of MGN was added to 40g (228 cm^3) of 85% H_2SO_4 at 323K. The reaction mixture was carefully and slowly heated to 338K and held at that temperature for 15 minutes, then poured

into 200 cm³ of isopropanol. Dry ammonia gas was bubbled through the solution until it was neutral. The mixture was filtered and solvent removed to give crude 2-methyleneglutaramide in 45% yield. The diamide was recrystallised from methanol, m.pt. 438-440K, and characterised by ir and nmr spectroscopy.

NMR (D₂O) δppm: 0.0 (Na TMS), 2.60 (m, 4H), 4.5 (exchangeable protons), 5.6 (s, 1H), 5.85 (s, 1H).

IR (KBr Disc) cm⁻¹: 3360 (b), 3250 (b), 1650 (b), 1660 (b), 1600 (s).

(b) 2-Methyleneglutaramide was also prepared by the less drastic heterogeneous hydrolysis using MnO₂.

In this instance the probable mechanism of reaction is considered to be a solid phase catalysis of the hydrolysis by H₂O which is known to be present on the surface of MnO₂. However, the length of the reaction time and the quantity of MnO₂ employed made this procedure unattractive.

Procedure: A 10% solution of MGN in CH₂Cl₂ and a ratio of substrate to MnO₂ of 1:10 by weight was stirred at room temperature for 24 hours. The MnO₂ was washed with methanol, evaporation of which gave 2-methyleneglutaramide in 35% yield.

2.2.6 2-Methyleneglutarimide (VIII)

Attempts to synthesise methyleneglutarimide, a potential cyclic monomer, proved unsuccessful, but the N-ethyl-2-methyleneglutarimide derivative was prepared and characterised (2.2.7). Neither system has been reported previously in the literature.

Attempts to cyclise 2-methyleneglutaramic acid, VI, to the title imide were unsuccessful. Therefore, an alternative procedure using 2-methyleneglutaric anhydride as a precursor was proposed. This route is outlined in Figure 2.3.

This synthesis involved the condensation of 2-methyleneglutaric

anhydride with urea followed by cyclisation to yield the N-carbamyl-2-methyleneglutarimide X, decomposition of which it was hoped would lead to the title imide, VIII.

The first step proceeded smoothly. However, the subsequent cyclisation reaction of IX \rightarrow X was unsuccessful. Proton nmr and ir spectroscopic analysis of the reaction product indicated that nucleophilic attack on the vinyl system of IX had occurred.

2.2.7 N-Ethyl-2-methyleneglutarimide (XI)

Although this cyclic monomer has not been reported in the literature, the analogous preparations of N-substituted maleimide¹⁰⁷ and N-alkylitaconimides are known.¹⁰⁸

Procedure: 56g (0.5 mol) of 2-methyleneglutaric anhydride is dissolved in 250 cm³ of xylene at room temperature and 22.5g (0.5 mol) of ethylamine added dropwise. The water white solution immediately turned deep red. The mixture was refluxed for a further three hours. The solvent was removed and the residue was vacuum distilled to give XI b.pt. = 328K/0.1 torr in low yield (20%).

The product was characterised by nmr and ir spectroscopy.

NMR (CDCl₃) δ ppm: 0.0 (TMS), 1.20 (t, 3H), 3.36 (m, 4H), 3.60 (q, 2H), 5.71 (m, 1H), 6.34 (m, 1H).

IR (Thin Film) cm⁻¹: 3100 (s), 1690 (b), 1640 (b), 1620 (s).

2.3 HOMOPOLYMERISATION OF 2-METHYLENEGLUTARONITRILE

2.3.1 Radical Polymerisation of 2-Methyleneglutaronitrile

The literature contains no information on the radical homopolymerisation of MGN. In this study the radical homopolymerisation was attempted using conventional bulk and emulsion techniques.

The details of the polymerisation conditions are contained in Table 2.2.

TABLE 2.2**Conditions Employed in the Radical Polymerisation of MGN**

<u>System/Sample Ref. No.</u>	<u>Polymerisation System</u>	<u>Initiator/conc.^{a)}</u>	<u>Temperature/ K</u>	<u>Reaction Time/hrs</u>
1	Bulk	AIBN/0.5 mol%	333	72
2	Bulk	AIBN/0.5 mol%	353	72
3	Bulk	AIBN/0.5 mol%	333	96
4	Bulk	AIBN/2 mol%	353	72
5	Emulsion	K ₂ S ₂ O ₈ /1 mol%	333	144
6	Bulk	Dicumyl Peroxide/1 mol%	393	6

a) AIBN = α,α -Azobisisobutyronitrile.

TABLE 2.2

Conditions Employed in the Radical Polymerisation of MGN

<u>System/Sample Ref. No.</u>	<u>Polymerisation System</u>	<u>Initiator/conc.</u> ^{a)}	<u>Temperature/ K</u>	<u>Reaction Time/hrs</u>
1	Bulk	AIBN/0.5 mol%	333	72
2	Bulk	AIBN/0.5 mol%	353	72
3	Bulk	AIBN/0.5 mol%	333	96
4	Bulk	AIBN/2 mol%	353	72
5	Emulsion	K ₂ S ₂ O ₈ /1 mol%	333	144
6	Bulk	Dicumyl Peroxide/1 mol%	393	6

a) AIBN = α,α -Azobisisobutyronitrile.

Bulk polymerisations employed AIBN (α,α' -Azobisisobutyronitrile) or dicumyl peroxide as the initiating species. The emulsion polymerisation of MGN used a conventional recipe¹⁰⁹ which is set out in Table 2.3.

Procedure: Pyrex reaction flasks were charged with the polymerisation ingredients and degassed by two freeze-thaw cycles. The flasks were sealed under vacuum and placed in a thermostated oil bath controlled to $\pm 0.5\text{K}$ for the required reaction period. In the emulsion system, agitation was effected by means of a Griffith flask shaker. The polymer was isolated by precipitation into methanol and purified by a minimum of two reprecipitations from acetonitrile solution into methanol. Polymers were vacuum dried at 303K and characterised by nmr and ir spectroscopy, differential scanning calorimetry and vapour pressure osmometry.

2.3.2 Anionic Polymerisation of 2-Methyleneglutaronitrile

The details of the polymerisation conditions which were employed in the anionic polymerisation of MGN are given in Table 2.4.

Catalysts Pentane solutions of n-butyllithium and t-butyllithium were used as supplied (BDH reagents). These solutions were analysed for active reagent by the back titration method of Gilman.¹¹⁰

Diphenylmethyllithium was prepared by the addition of diphenylmethane to a THF solution of lithium naphthalene according to the procedure of Normant.¹¹¹ The concentration of active catalyst was again determined by Gilman's titration procedure.

The synthesis of the anionic initiators diethylmagnesium and dipiperidinomagnesium is outlined in Figure 2.4. This procedure has been reported briefly by Joh¹¹² and it necessitates the use of an inert atmosphere. The most satisfactory results were obtained by employing a polyethylene glovebag (Aldrich Chemical Company "Atmos Bag") containing petri dishes of P_2O_5 to remove residual moisture.

TABLE 2.3

Typical Formulation for the Emulsion Polymerisation of MGN

<u>Constituent</u>	<u>Quantity/g</u>
Monomer	100
Potassium peroxydisulphate ($K_2S_2O_8$)	2.5
Soap (sodium lauryl sulphate)	5.0
Water	200

TABLE 2.4

Conditions Employed in the Anionic Polymerisation of MGN^a

<u>System/Sample Ref No</u>	<u>Initiator System</u>	<u>Solvent</u>	<u>Polymerisation Temperature/K</u>	<u>Polymerisation Time/hours</u>
7	n-butyllithium	toluene	223	3
8	t-butyllithium	toluene	223	3
9	Diphenylmethyllithium	toluene	223	3
10	Diethylmagnesium	toluene	223	1.5
11	Dipiperidinomagnesium	DMF	223	0.5

a) [Monomer] = 2 M; [Initiator] = 4×10^{-2} M; Solvent = 100 cm³.

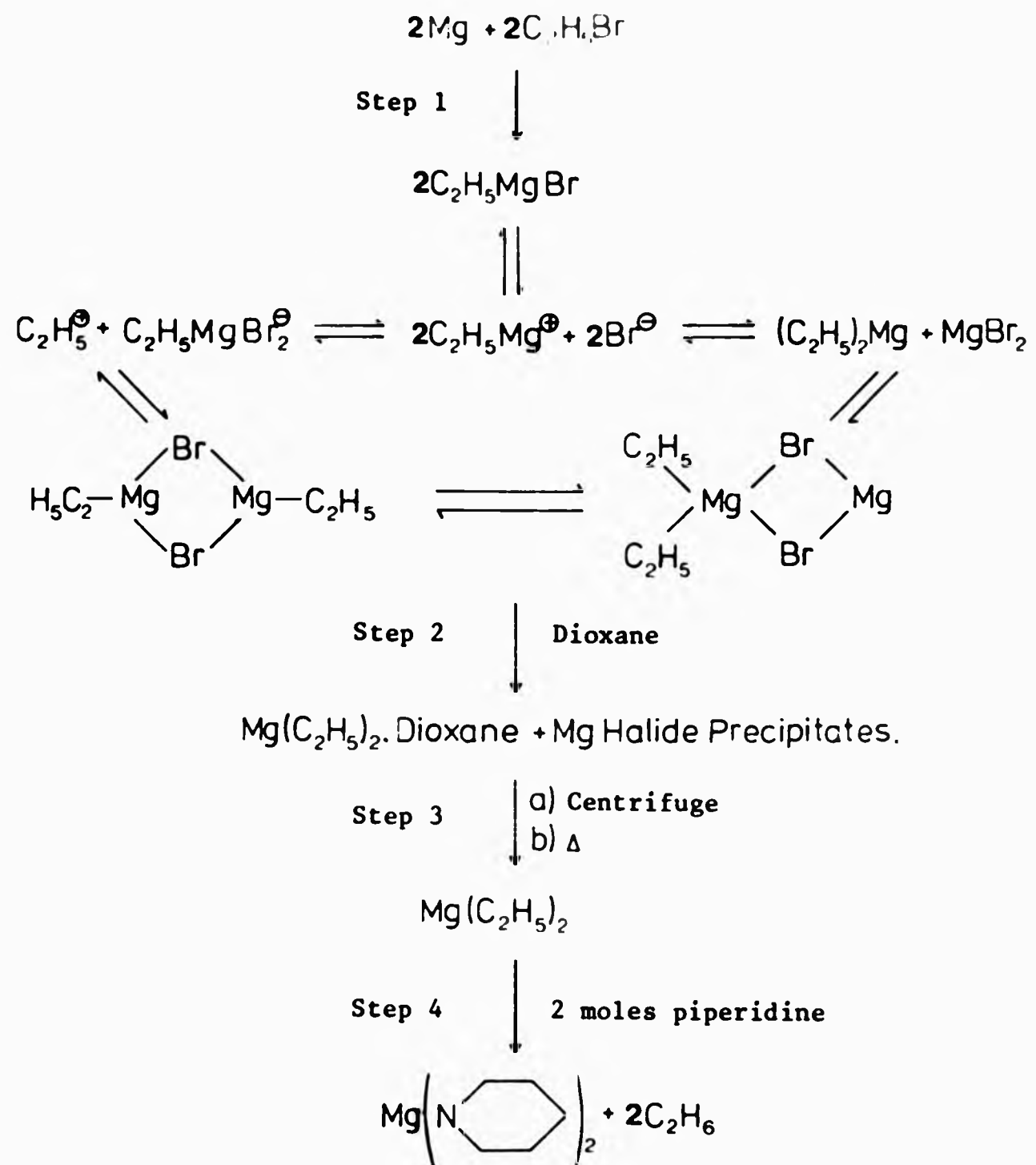


FIGURE 2.4 The synthesis of the anionic initiators diethylmagnesium and dipiperidinomagnesium.

Preparation of Organomagnesium Initiators: Ethylmagnesium bromide was prepared by a standard Grignard procedure and good yields of diethylmagnesium were obtained by the dioxane precipitation method of Dessy.¹¹³ This method involves the addition of dioxane to the Grignard solution and the subsequent removal of the precipitated magnesium halides by centrifugation. Diethyl ether is evaporated from the mother liquor to give the diethylmagnesium-dioxane complex, which upon heating at 393K/0.1 torr for 36 hours, yields the white crystals of diethylmagnesium. Addition of piperidine (2 mol. eq.) to a toluene solution of diethylmagnesium (1 mol. eq.) at 298K results in the depolymerisation of the magnesium alkyl and concurrent evolution of ethane. The yellow crystals of dipiperidinomagnesium were isolated by the evaporation of toluene.

Where possible, the magnesium compounds were characterised by the titrimetric analysis of their hydrolysed solutions.

Polymerisation Procedure: The reaction flasks were flamed and purged with nitrogen. The solvent and monomer were introduced into the reaction flask and the system cooled to the desired temperature. The polymerisation was started by the injection of the initiator solution which, with the exception of the alkyllithium systems, resulted in the formation of an orange colour in the reaction medium. This colouration persisted until the end of the polymerisation. Termination was effected by the addition of methanol to the systems and the crude polymer was purified by repeated precipitation from acetonitrile solution into an excess of methanol and dried under vacuum at 323K for 24 hours. The polymers were characterised by nmr and ir spectroscopy, differential scanning calorimetry, thermogravimetric analysis and osmometry.

2.4 RADICAL COPOLYMERISATIONS

2.4.1 Radical Copolymerisation of 2-Methyleneglutaronitrile

The 2-methyleneglutaronitrile copolymers which have been prepared are listed in Table 2.5, together with the details of the copolymerisation conditions.

The monomers were purified by literature procedures.

Polymerisation Procedure: Copolymerisations were carried out using bulk, solution, or emulsion techniques. A conventional redox emulsion recipe which is given in Table 2.6 was used for the copolymerisations performed at 303K.

The reaction flasks were charged with the required ingredients, evacuated by freeze-thaw cycles, and sealed under vacuum. The flasks were then placed in a thermostat bath controlled to $\pm 0.5K$. Where "instantaneous copolymer composition" data was required, copolymerisations were allowed to continue to a maximum of 10% conversion.

Gravimetric analysis was employed to yield the initial rate of copolymerisation in systems 16 and 19.

All copolymers were isolated by precipitation into methanol and were purified by reprecipitation from an acetone solution into an excess of methanol. The copolymers were vacuum dried at 333K for 36 hours and subsequently fully characterised.

Copolymer compositions were determined both by C, H, and N elemental analysis, and by nmr analysis.

2.4.2 The Copolymerisation of MGN with Selected Monomers in the Presence of a Lewis Acid

The copolymerisations which were carried out in the presence of zinc chloride are listed in Table 2.7, together with the reaction conditions. Procedure: Zinc chloride was heated at 383K/0.1 torr for 24 hours before use. The Lewis acid was dissolved in the comonomer solution and the

TABLE 2.5

Details of the Copolymerisation of MGN with Various Comonomers using Free Radical Initiation

System/Sample Ref. No.	Comonomer ^a	Feed Range (Mole Fraction MGN)	Copolymerisation Medium ^b	Polymerisation Temperature/K
12	Acrylonitrile	0.5	Bulk	333
13	Buta-1,3-diene	0.5	Toluene Solution	333
14	Ethyl vinyl ether	0.1-0.9	Bulk	333
15	Furan	0.5	Bulk	333
16 (a) (b)	Isoprene	0.1-0.9 0.1-0.9	Toluene Solution Emulsion	333 303
17	Itaconic anhydride	0.5	Toluene Solution	333
18	Methyl methacrylate	0.5	Bulk	333
19	α -Methylstyrene	0.1-0.9	Bulk	333
20	Trans-stilbene	0.5	Toluene Solution	333
21	Styrene	0.5	Bulk	333
22	Vinyl acetate	0.5	Bulk	333
23	N-Vinyl carbazole	0.1-0.9	Toluene Solution	333
24	4-Vinyl pyridine	0.5	Bulk	333

a) In the bulk and solution systems 1 mole % AIBN was employed as initiator, emulsion polymerisations employed the redox initiation system reported in Table 2.6.

b) The total concentration of monomers in the solution copolymerisation systems was 5M.

TABLE 2.6

Copolymerisation Redox Emulsion Recipe

<u>Constituent</u>	<u>Quantity/g</u>
Monomer(s)	100.00
Emulsifier/Sodium Lauryl Sulphate	50.00
Sodium Pyrophosphate	0.10
Ferric Sulphate	0.02
H ₂ O ₂ (20%)	0.35
H ₂ O	200.00
Solvent (Toluene)	25.00

TABLE 2.6

Copolymerisation Redox Emulsion Recipe

<u>Constituent</u>	<u>Quantity/g</u>
Monomer(s)	100.00
Emulsifier/Sodium Lauryl Sulphate	50.00
Sodium Pyrophosphate	0.10
Ferric Sulphate	0.02
H ₂ O ₂ (20%)	0.35
H ₂ O	200.00
Solvent (Toluene)	25.00

TABLE 2.7

Details of the Solution Copolymerization of MGN with Selected
Comonomers in the Presence of Zinc Chloride^{a, b}

<u>System/Sample Ref No</u>	<u>Comonomer</u>	<u>Feed Range (Mole fraction)</u>	<u>MGN/ZnCl₂ (Mole ratio)</u>	<u>Polymerisation Temperature/K</u>
25	Isoprene	0.15-0.85	2	333
26	α -Methylstyrene	0.15-0.85	2	333

a) Copolymerisations were carried out in toluene solution, total monomer concentration = 5M.

b) 1 mole % AIBN was employed as initiator.

subsequent copolymerisation procedure used was analogous to that set out in the previous section. Copolymers were isolated and purified by repeated dissolution in acetone and precipitation into methanol. The elimination of ZnCl_2 from the product was confirmed by the addition of the polymer solution to an acetone solution of dithiozone (diphenylthiocarbazone). The copolymers were then fully characterised.

2.5 MONOMER-MONOMER DONOR-ACCEPTOR COMPLEXATION

In this study, the stoichiometry and the equilibrium quotient of monomer-monomer donor-acceptor complexes were determined by proton nmr spectroscopy employing a technique proposed by Hanna and Ashbaugh.¹¹⁴ The theory of this technique and its utilisation in the form of the Benesi-Hildebrand equation (or modifications) is described in Chapter 5.

Complex stoichiometry was determined by the nmr equivalent of the continuous variation method of Job.^{115,116} For this procedure solutions were prepared by mixing $x \text{ cm}^3$ of 1M MGN with $(10-x) \text{ cm}^3$ of 1M donor solution, both in CCl_4 (where x was varied from 1 to 9 cm^3) and the total volume was kept at 10 cm^3 . The ^1H nmr spectrum of the resulting solutions were then recorded for analysis.

To satisfy the criteria for the reliable determination of formation quotients of weak complexes,¹¹⁷ the concentration of the "donor" molecules was increased in the range 2-10M in an inert solvent (in this study CCl_4) while the concentration of the

"acceptor molecule" was kept low and constant at around 0.1M. The ^1H nmr spectrum of the resulting solutions were then recorded and analysed.

Ideally, the reverse system should also be studied, i.e. keeping the concentration of the donor molecule low and constant, while varying the acceptor concentration in the range 2-10M. Unfortunately, due to the limited miscibility of MGN and CCl_4 , such experiments were not possible.

All samples were run on a Perkin-Elmer R32 90 MHz spectrometer. The chemical shifts were measured using tetramethylsilane (TMS) as the reference signal in either an internal or external capacity. The sweep width setting of 100 Hz permitted direct reading to ≈ 1 Hz. A nitrogen stream was used as the temperature control and allowed the system to be studied at selected temperatures.

2.6 INSTRUMENTATION

2.6.1 Number Average Molar Mass (M_n) Determination

Several techniques based on the colligative properties of dilute solutions are available for the determination of the number average molar mass. In this study, vapour pressure osmometry and membrane osmometry were used to determine M_n .

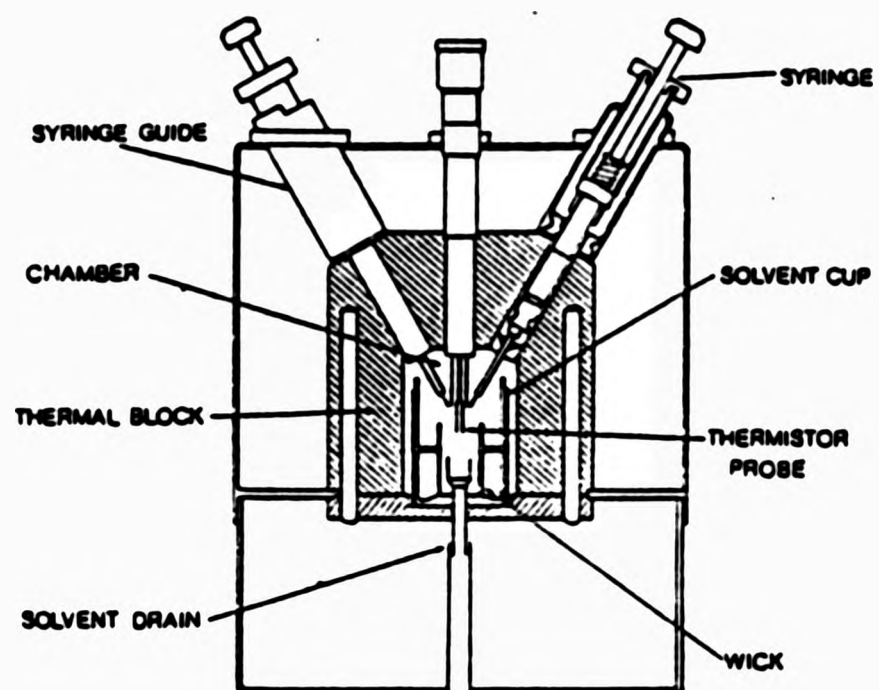
Vapour Pressure Osmometry (VPO). This is a useful method of measuring values of M_n from 50 to 20,000g mol⁻¹. It is a relative method and is calibrated using such low molar mass standards as benzil and methyl stearate. The technique and instrumentation are thoroughly described in the literature.¹¹⁸

The property measured in VPO is the small temperature difference resulting from the different rate of solvent evaporation from, and condensation onto, droplets of pure solvent and polymer solution maintained in an atmosphere of solvent vapour. The temperature difference is detected by two differential matched thermistors which form part of a Wheatstone's bridge, ΔT is thus recorded as a difference in resistance, ΔR . The number average molar mass (M_n) can then be calculated from equation (1) by extrapolating the data to $C=0$.

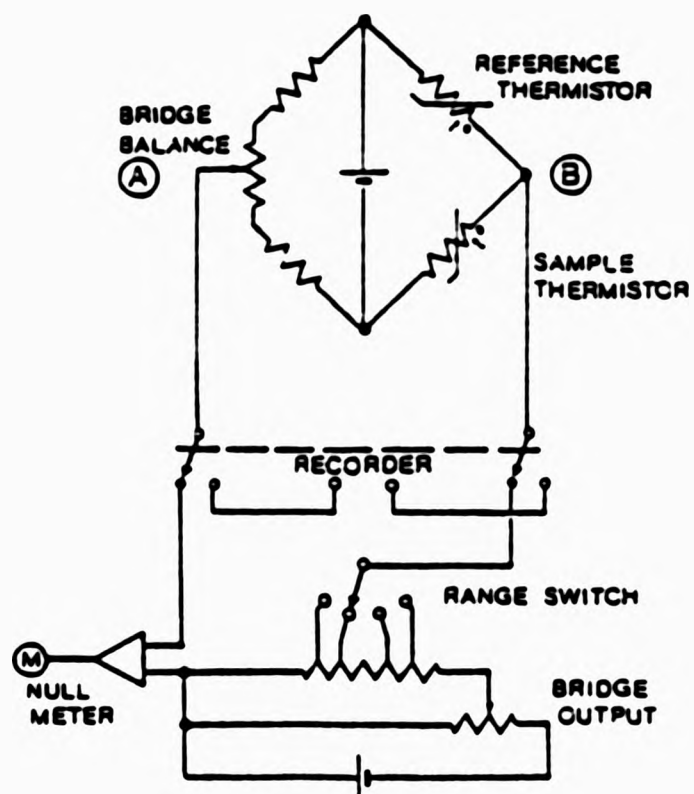
$$K^* = M_n (\Delta R/C)_{C \rightarrow 0} \quad (1)$$

K^* is a calibration constant estimated by measuring ΔR for solutions of known concentration (C) prepared from standard compounds of known molecular weight.

The instrument employed in this work was a Hewlett-Packard Model 302-B Vapour Pressure Osmometer. The basic features of the instrument are shown in Figure 2.5. The operating temperature was 308K and acetonitrile was used as solvent. The system was calibrated using



(a)



(b)

FIGURE 2.5 Schematic diagram of vapour pressure osmometer.
 (a) Thermal chamber showing probe and syringes.
 (b) Simplified circuit diagram.

benzil (Mol.Wt. =210.23), giving a value for K^* the calibration constant of $8.8 \times 10^3 \text{ Vg}^{-1} \text{ dm}^3$. The concentrations of the polymer solutions employed were in the range $1-20 \text{ gdm}^{-3}$.

Membrane Osmometry. Measurements of the osmotic pressure (π) of a polymer solution enables the number average molar mass (M_n) to be determined from equation (2),

$$(\pi/c)_{c \rightarrow 0} = RT/M_n \quad (2)$$

(R is the gas constant and T is the temperature in degrees Kelvin.) This is again a limiting form, valid at infinite dilution. Only under special conditions, when the polymer is dissolved in a pseudo-ideal solvent, e.g. a theta solvent, is (π/c) independent of concentration.

Experimentally, a series of concentrations is studied and the results treated according to a virial expansion, the most familiar of which is equation (3),

$$(\pi/c) = RT(M_n^{-1} + A_2c + A_3c^2 + \dots) \quad (3)$$

where A_2 and A_3 are the second and third virial coefficients respectively. When solutions are sufficiently dilute a plot of (π/c) against (c) is linear ($A_3=0$). The intercept of such a graph at zero concentration gives (RT/M_n) , enabling the number average molar mass to be determined.

In this work a Knauer membrane osmometer and detecting bridge were used. The basic features of this instrument are shown in Figure 2.6. Calibration is by the application of a known external pressure. On addition of polymer solution the pressure change is detected by the diaphragm and a signal proportional to the pressure change is registered

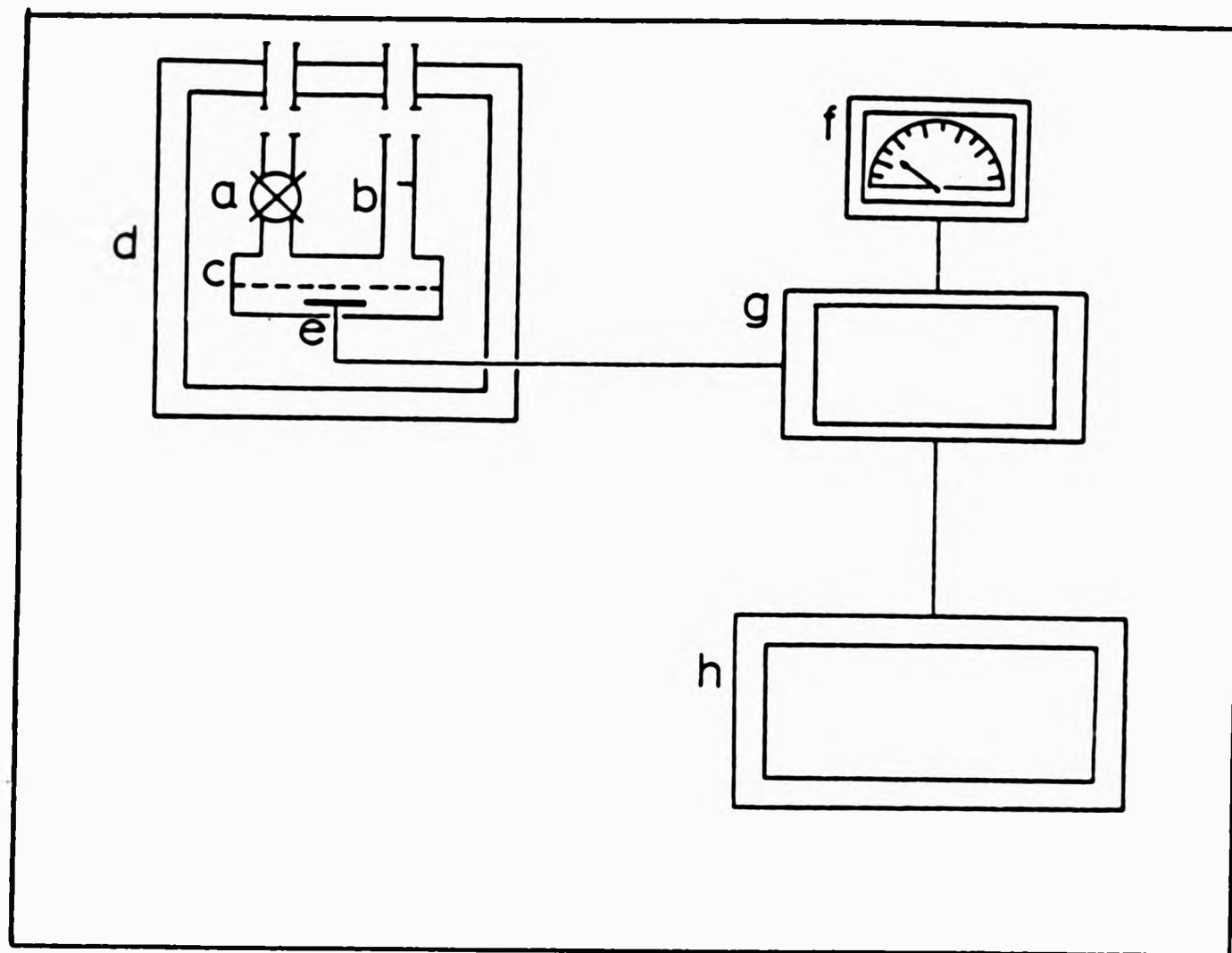


FIGURE 2.6 Schematic of membrane osmometer.

- (a) outlet valve
- (b) inlet valve
- (c) membrane
- (d) thermostatted chamber
- (e) pressure detecting membrane
- (f) osmotic pressure dial
- (g) Wheatstone bridge circuit
- (h) chart recorder.

on a chart recorder.

Membranes (Sartorius, regenerated cellulose) were conditioned to butan-2-one and proved satisfactory for M_n measurements down to ca. $20,000 \text{ g mol}^{-1}$. The operating temperature was 313K and the concentration of the polymer solutions employed were in the range $1\text{-}20 \text{ g dm}^{-3}$.

2.6.2 Thermal Analysis

Differential Scanning Calorimetry (DSC). Perhaps the simplest definition of the glass transition temperature (T_g) is the temperature below which the polymer is glassy and above which it is rubbery. The molecular interpretation of the T_g is widely accepted as the onset of long range cooperative motion of the polymer backbone (macro-Brownian motion) which is frozen in below T_g . From the experimental viewpoint the glass transition temperature of a material may be detected by monitoring any one of a number of properties which can be measured as a function of temperature. These include specific heat, specific volume, dielectric and mechanical behaviour.¹¹⁹⁻¹²⁰ In this study differential scanning calorimetry was employed in the vast majority of cases to locate the T_g of polymers and copolymers.

The system employed was a Perkin-Elmer model DSC-2, equipped with a low temperature mode accessory and capable of measurements in the temperature range 100-1000K.

This instrument records the differential power required to maintain a zero temperature difference between the sample and an inert reference, as the temperature of both is changed at a linear programmed rate. A schematic diagram of the DSC-2 is shown in Figure 2.7. Thus when the sample undergoes a thermal transition, the power to the two heaters is adjusted to maintain their temperatures, and a signal ($\Delta H/dt$) proportional to the power difference is plotted on one axis of an X-Y

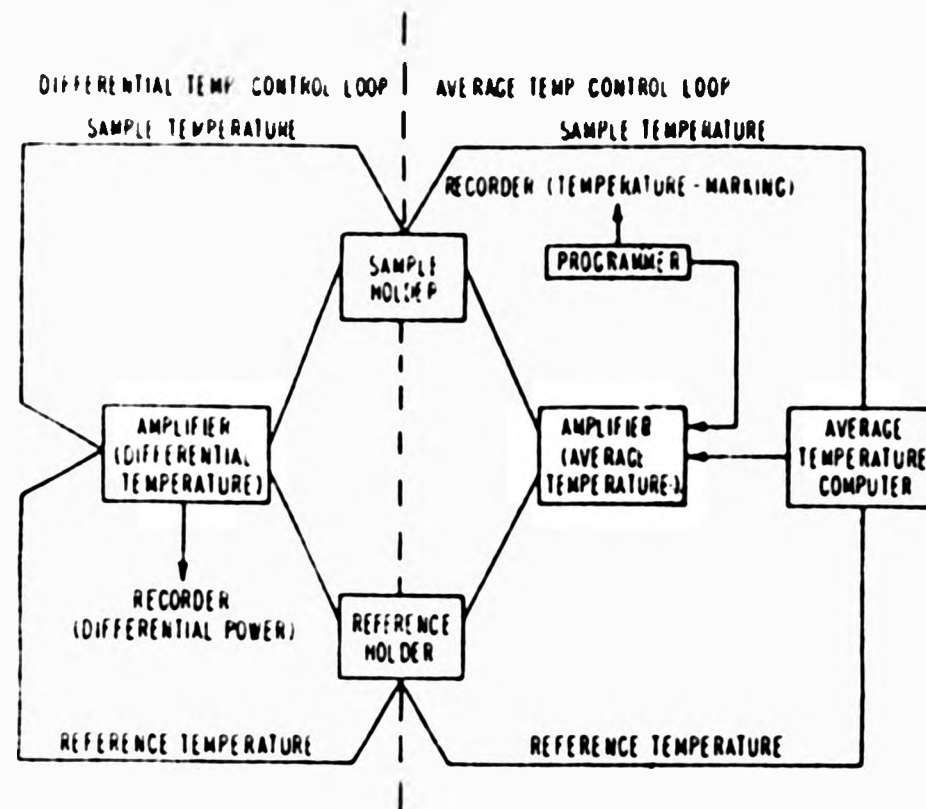


FIGURE 2.7 DSC schematic.

recorder with temperature plotted on the second axis. Details of the theory and design of differential scanning calorimeters have been described by Watson et al.¹²¹ and by O'Neill.¹²²

In experiments involving subambient scans, dry helium was used as the purge gas, with above ambient work being conducted under oxygen free nitrogen. In all cases the scan rate was 20K min^{-1} .

Thermogravimetric Analysis (TGA). This is a dynamic thermal analysis technique in which the weight loss of a material is measured as a function of increasing temperature at a linear programmed rate. Weight loss can also be measured as a function of time at constant temperature if required. The technique was applied to most of the polymer samples prepared in this work in order to evaluate their thermal stability and degradation temperatures.

A Perkin-Elmer Thermogravimetric System model TGS-2 connected to the Perkin-Elmer DSC-2 temperature programmer was used in this study. Thermal degradation of all polymer samples was carried out under a nitrogen atmosphere at heating rates of 20K min^{-1} . The results are displayed as a graph of % sample weight loss against temperature.

2.6.3 Thermomechanical Analysis

Torsional Braid Analysis (TBA). This is a technique used to measure the dynamic thermomechanical properties of polymers over a wide temperature range. TBA was originally developed by Gillham¹²³ from the conventional torsional pendulum. A schematic diagram of the Gillham apparatus is shown in Figure 2.8. Unlike the torsional pendulum, TBA measurements can be made on relatively small (ca. 100mg) amounts of material which are impregnated into a multifilament glass-braid which acts as a support for mechanically weak materials. This allows the study of thermoplastics above their melting or softening points. Perhaps the major disadvantage of the TBA technique is that it cannot

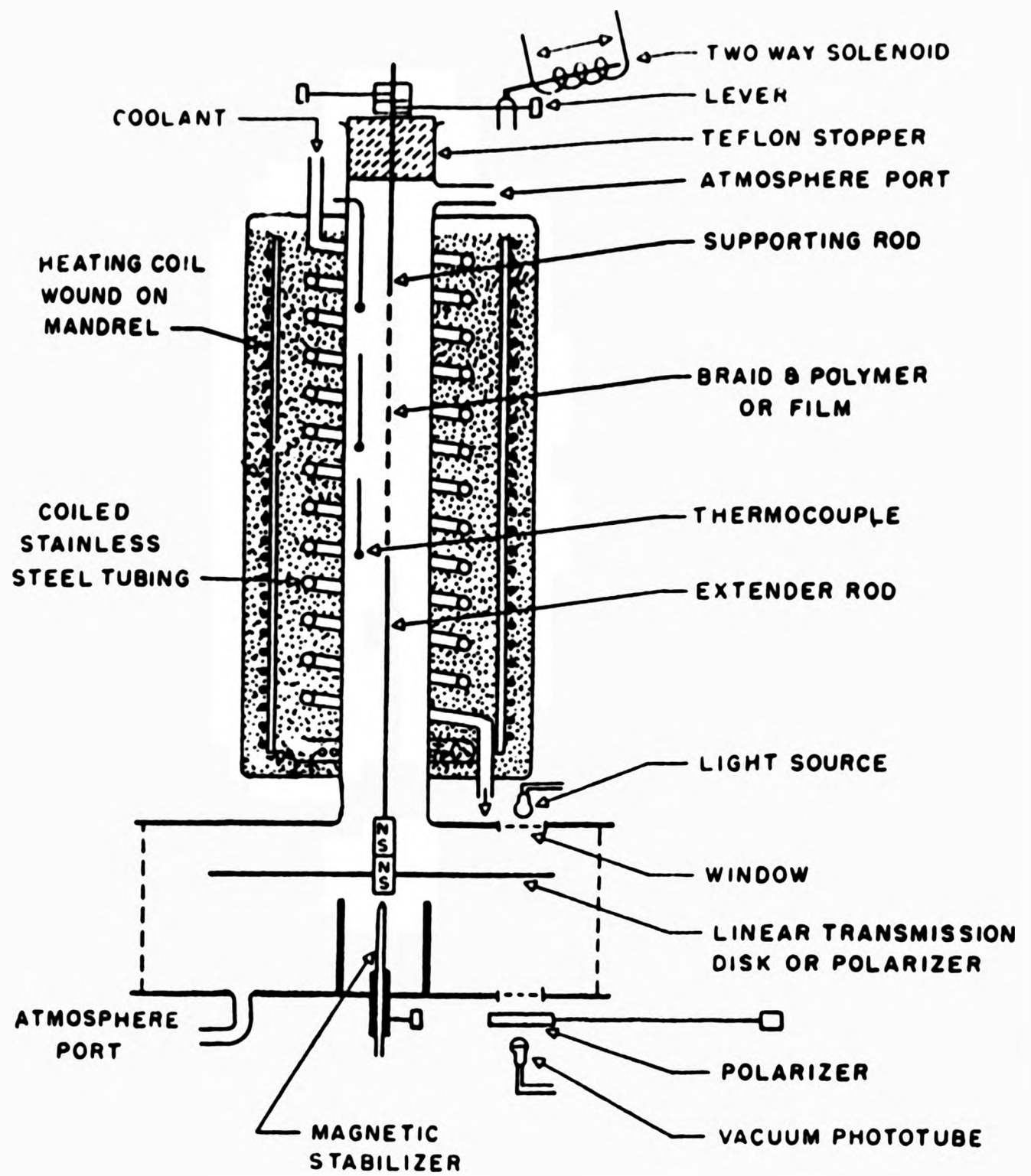


FIGURE 2.8 Torsional pendulum and torsional braid apparatus of Gillham (schematic).

provide absolute measurements (for example, a polymer's mechanical modulus) since the material under test is a composite and not a pure polymer of known dimensions.

The instrument used in this work was a torsional braid analyser model 100-B1, manufactured by Chemical Instruments Corporation of New York. The normal frequency of measurement is approximately 1Hz and it may be operated over the temperature range 83K-773K. The TBA was interfaced to an APPLE II microcomputer in order to facilitate data collection and analysis. The logarithmic decrement, LD, and the relative rigidity, $1/P^2$ (which is proportional to the shear modulus of the polymer/glass fibre composite) were measured for each oscillation along with the temperature e.m.f. from an iron-constantan thermocouple inside the apparatus. About 80 to 120 damped oscillations were collected to construct each TBA-thermogram. The location of the T_g is evidenced by a maximum in the LD and a large drop in the relative rigidity.

Dynamic Viscoelastic Measurements. If a sinusoidal tensile strain is applied at one end of a polymer sample (at a fixed frequency), the resulting stress will also be sinusoidal but will be out of phase when there is energy dissipation or damping in the polymer. This is illustrated in Figure 2.9. Satisfying the condition $|\bar{\alpha}_1| = |\bar{\alpha}_2| = 1$, where α_1 and α_2 are the electrical vectors from the force and displacement transducers, the tangent of the phase angle δ between the stress and strain may be calculated from equation (4).

$$|\bar{\alpha}_1 - \bar{\alpha}_2| = 2 \sin(\delta/2) \approx \tan \delta \quad (4)$$

The operation of adjustment followed by subtraction of the electrical vectors is performed directly in the recording circuit of the

analysing instrument.

The complex elastic modulus E^* is given by equation (5)

$$E^* = (2l/DA) \times 10^8 \text{ Nm}^{-2} \quad (5)$$

where D is the dynamic force obtained directly from the instrument, l is the length of the sample in cm, and A is the sample cross sectional area in cm^2 . The tensile storage and loss moduli E' and E'' respectively, follow from equations (6) and (7),

$$E' = E^* \cos \delta \quad (6)$$

$$E'' = E^* \sin \delta \quad (7)$$

In this study the viscoelastic nature of polymer samples were investigated using a Rheovibron model DDVIIC direct reading dynamic viscoelastomer supplied by Toyo Baldwin Co. Ltd., Japan, and capable of operating at 3.5 Hz, 11 Hz, 35 Hz, and 110 Hz. A schematic of the instrument is shown in Figure 2.10. Analysis using this instrument allows the complex elastic modulus and damping characteristics of the polymer to be obtained.

Polymer samples were prepared by a compression moulding technique using a Moore variable temperature 20 ton hydraulic press.

Dynamic viscoelastometry is sensitive to the onset of molecular motion in the polymer chains and as such it may be used to detect the glass transition temperature of the material. The precise location of the T_g is dependent upon the frequency of the applied force, therefore operating the instrument at the four available frequencies (assuming Arrhenius behaviour) allows the determination of the apparent activation

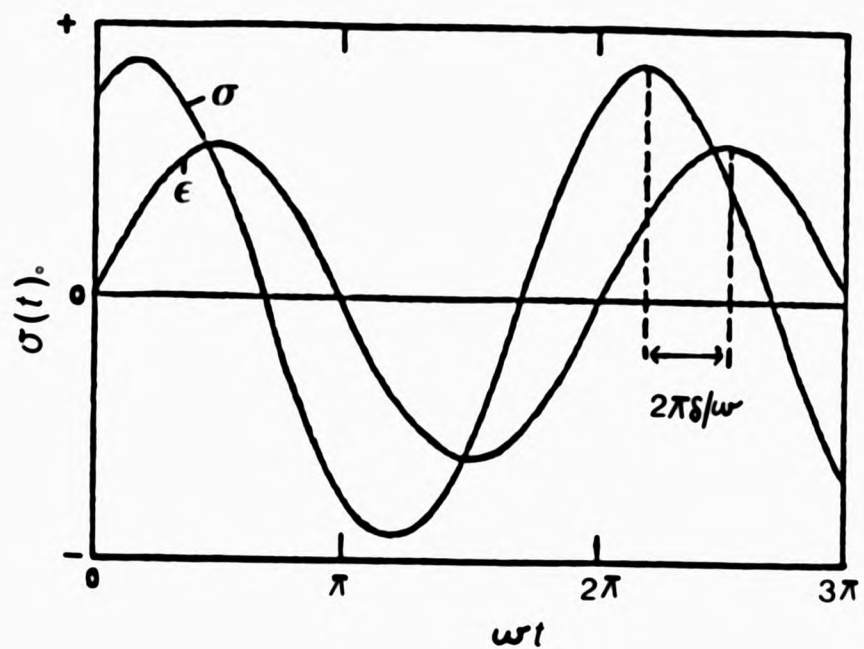


FIGURE 2.9 Stress (σ) and strain (ϵ) as a function of time in the application of a sinusoidal strain to a viscoelastic sample.

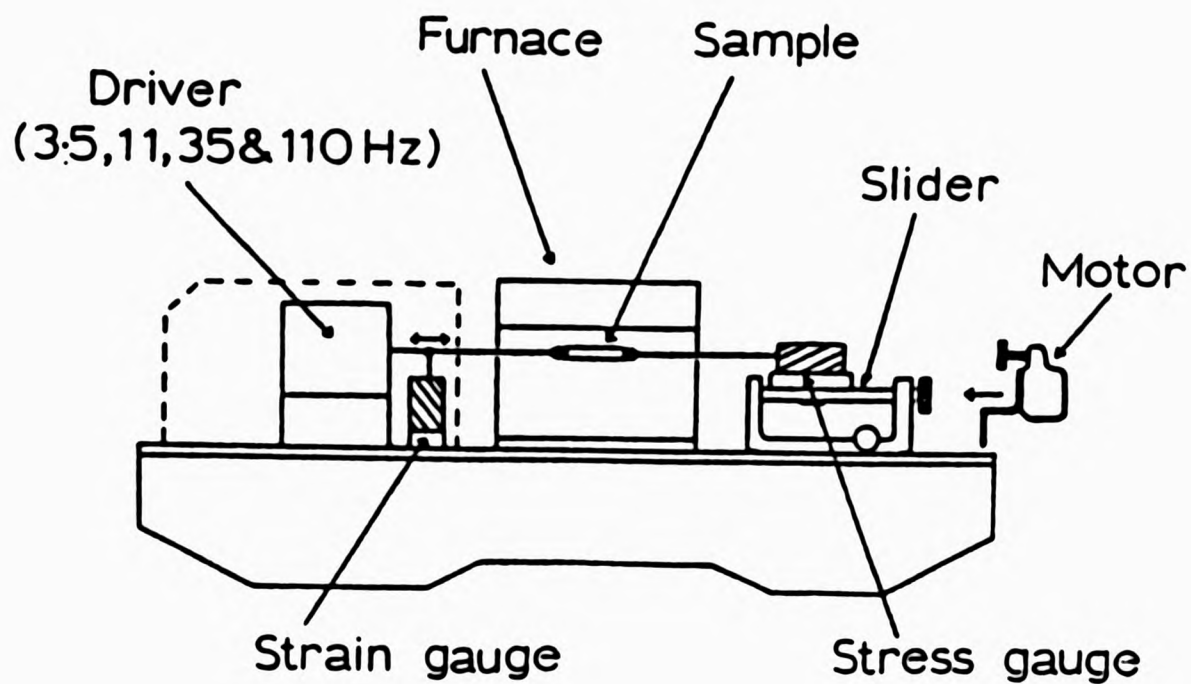


FIGURE 2.10 Schematic diagram of Rheovibron DDV-IIC.

energy of the Tg.¹²⁴

2.6.4 Spectroscopic Techniques

Nuclear Magnetic Resonance. ¹H NMR were recorded either on a Perkin-Elmer R32 (90 MHz) spectrometer or a Bruker WP80 Fourier transform NMR spectrometer.

The former instrument was operated in standard mode and samples were studied as 10-15% wt./vol. solutions in D₂O, or in deuterated chloroform, dimethylsulphoxide, or acetone. Tetramethylsilane (TMS) was used as the internal reference.

¹³-Carbon NMR and Nuclear Overhauser enhancement double resonance experiments were carried out on the Bruker WP80 instrument equipped with an Aspect 2000 minicomputer.

Infrared Spectroscopy. Infrared analysis was carried out using a Perkin-Elmer 577 Grating Infrared Spectrophotometer. Samples were studied either as KBr discs or as films cast on NaCl plates.

Ultraviolet Spectroscopy. UV absorption spectra were run on a Perkin-Elmer 402 ultraviolet-visible spectrophotometer.

2.6.5 Miscellaneous Techniques

Elemental Analysis was carried out on a model 1106 Carlo-Erba Elemental Analyser (Milan, Italy) under standard conditions. Carbon, hydrogen and nitrogen were determined directly and oxygen by difference.

Polarising Microscopy. Transition temperatures of mesomorphic materials were measured by optical microscopy using a Reichert ThermoVar polarising microscope fitted with a hot stage and capable of accommodating a Polaroid Landpack camera model ED-10 on the eyepiece of the instrument.

CHAPTER THREE

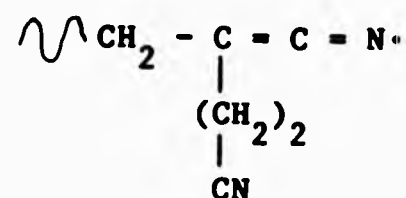
3.1 RADICAL POLYMERISATION OF 2-METHYLENEGLUTARONITRILE

The radical polymerisation of MGN carried out in bulk or emulsion leads to reasonable yields of white or coloured powdery polymethyleneglutaronitrile. However, the reaction time necessary to achieve such yields, 6-144 hrs, illustrates that this is not a particularly facile radical polymerisation. Table 3.1 contains the results of the polymerisations and characterisation of the polymer samples.

The polymer samples 1-5 have solubility properties which are similar to those of radically polymerised polyacrylonitrile, being soluble in dipolar aprotic solvents such as acetonitrile, dimethylformamide, and nitromethane. No solvent was found for sample 6.

A representative infrared spectrum of polymethyleneglutaronitrile is shown in Figure 3.1. Polymer samples 1-6 displayed well defined absorptions which can be identified with "structural irregularities" in the polymer. The absorption at 2000 cm^{-1} is also found in the spectrum of polyacrylonitrile and polymethacrylonitrile and has been identified with the presence of a ketene-imine structure $[\text{C}=\text{C}=\text{N}]$ in the polymer.^{125,126}

In the polymerisation of MGN this structure may arise from a 1-4 propagation mechanism, giving XVI,



(XVI)

or alternatively, from a termination reaction (iii) involving a growing

TABLE 3.1
Results and Analysis of the Radical Polymerisation of 2-Methyleneglutaronitrile

System/Sample Ref.No.	Polymerisation System ^a	Temperature/K	Reaction Time/hrs	Polymer Yield % ^b	Tg/K	$M_n \times 10^{-3} / c$ g mol ⁻¹
1	Bulk/0.5 mol% AIBN	333	72	22W	387	1.8
2	Bulk/0.5 mol% AIBN	353	72	62W	372	1.5
3	Bulk/0.5 mol% AIBN	333	96	43W	375	1.4
4	Bulk/2.0 mol% AIBN	353	72	60Y	367	1.2
5	Emulsion/1.0 mol% K ₂ S ₂ O ₈	333	144	10W	384	2.0
6	Bulk/1 mol% DCP	393	6	30B	395	ND

a) AIBN = α, α' -Azobisisobutyronitrile; DCP = Dicumylperoxide

b) W = white polymer; Y = yellow polymer; B = Brown polymer

c) ND = Not Determined (insoluble material)

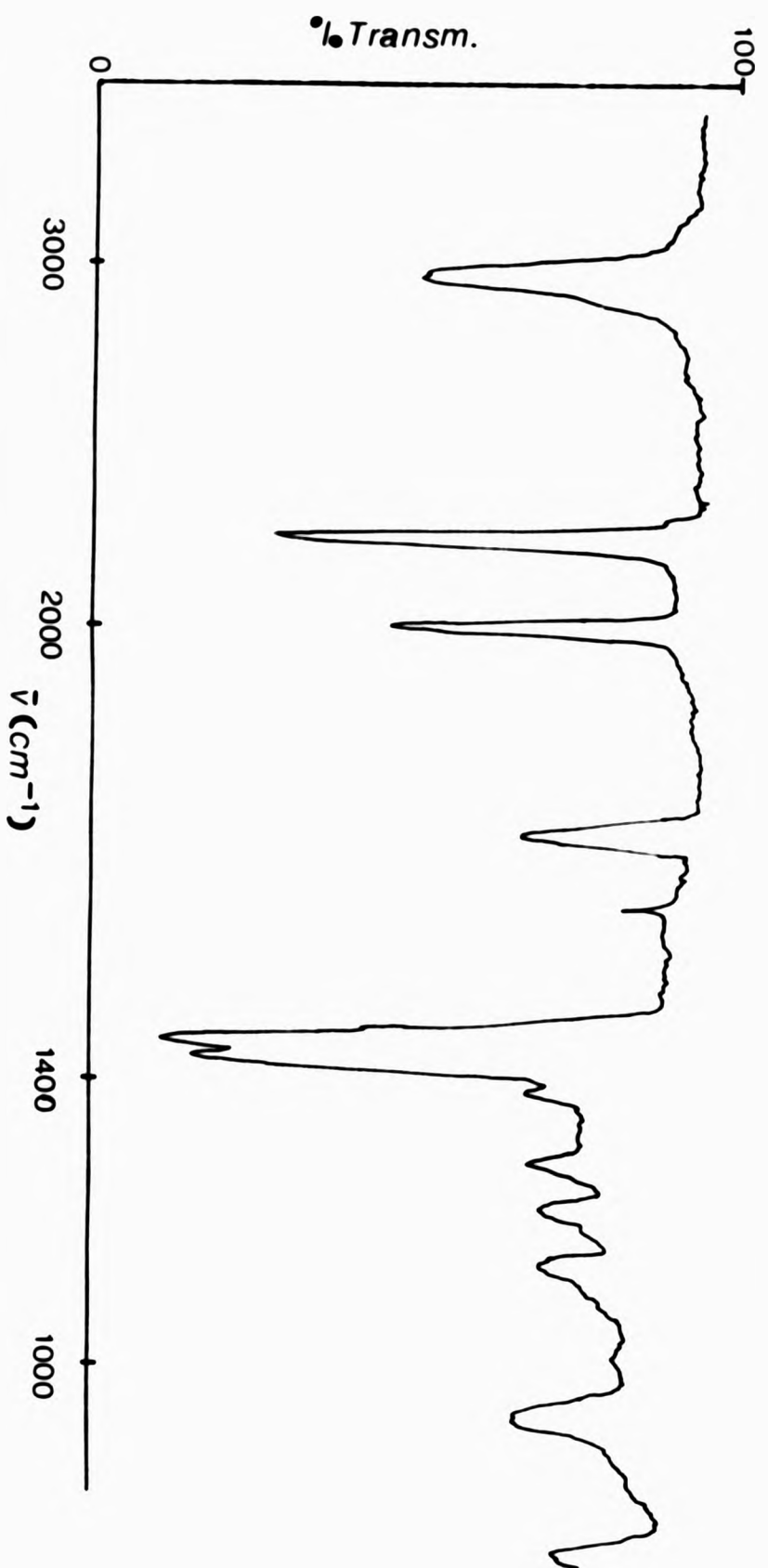
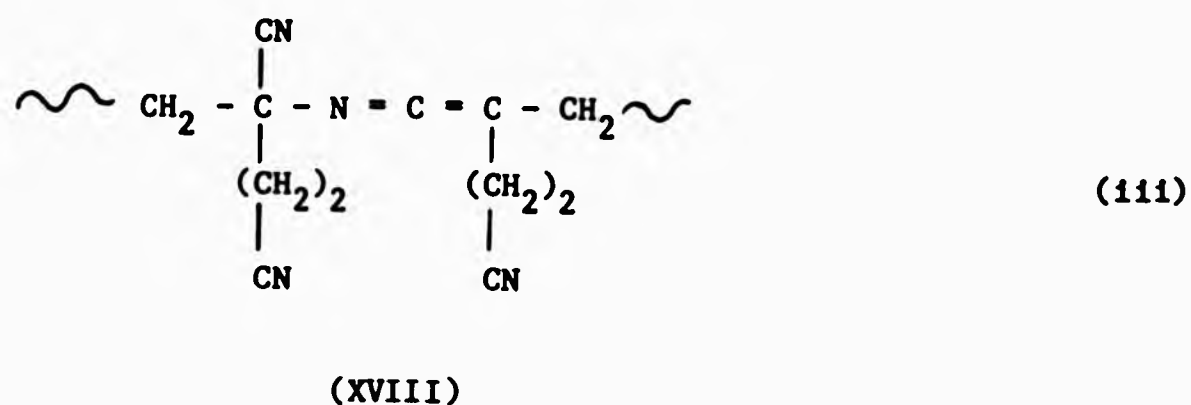
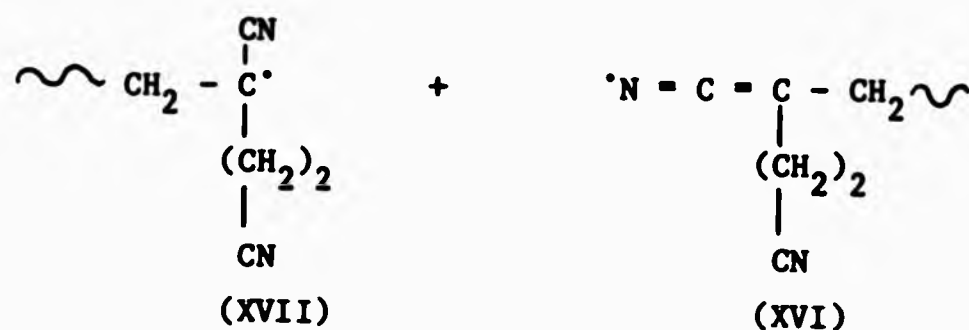
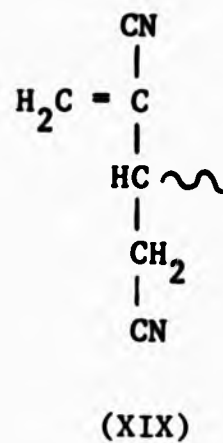


FIGURE 3.1 Representative infrared spectrum of radically polymerised MGN.

chain radical of the form XVII with its resonance hybrid XVI, producing the ketene-imine group XVIII by combination.

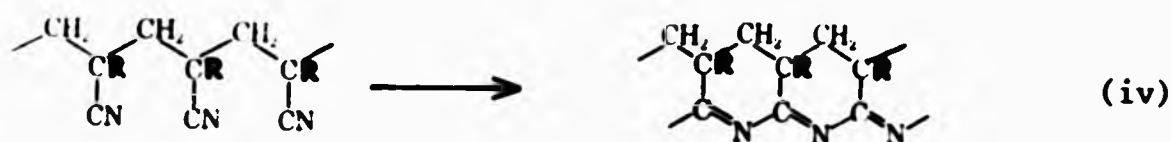


A sharp and well defined absorption at 1630 cm^{-1} is present in the spectrum of all samples and is attributed to the presence of ethylenic double bonds in the polymer. Residual monomer was ruled out as the source of this absorption as repeated precipitation of the polymer samples did not reduce the intensity of the absorption. This unsaturation can arise from both chain transfer to monomer and degradative chain transfer, leading to structures such as XIX.



There is also evidence for the $\begin{array}{c} | \\ -C-H \\ | \end{array}$ methine group vibration at 1320 cm^{-1} in accord with this structure.

In polymer sample 6 the broad and intense absorption at 1660 cm^{-1} is correlated with the presence of a ketimine structure $(C=N)_n$, arising from the cyclisation of the α nitrile groups $XX \rightarrow XXI$.¹²⁷

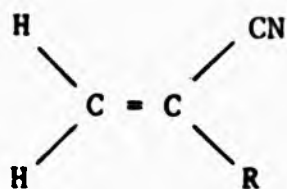


(XX)

(XXI)

This process is known to occur in polyacrylonitrile and has been the subject of a wealth of literature.¹²⁸ It may occur by the thermal treatment of the polymer or by the addition of various chemical reagents, particularly bases. Such structures have been cited as the origin of the discoloration in the polymer.¹²⁹ A more detailed account of this cyclisation reaction will be presented later in section 3.2.

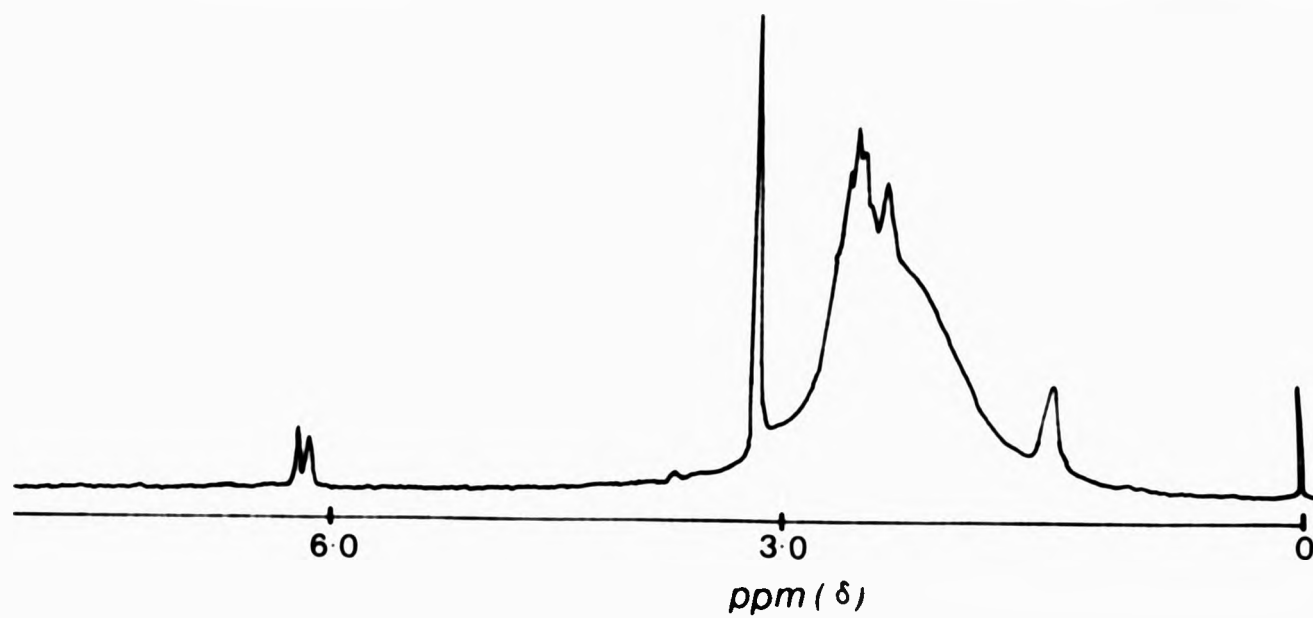
Both the ^{13}C and 1H nmr spectra of samples 1-5 are essentially identical and representative spectra are shown in Figure 3.2. The important feature of the proton nmr spectrum are the signals at 6.1 δ and 6.2 δ arising from ethylenic protons of the type



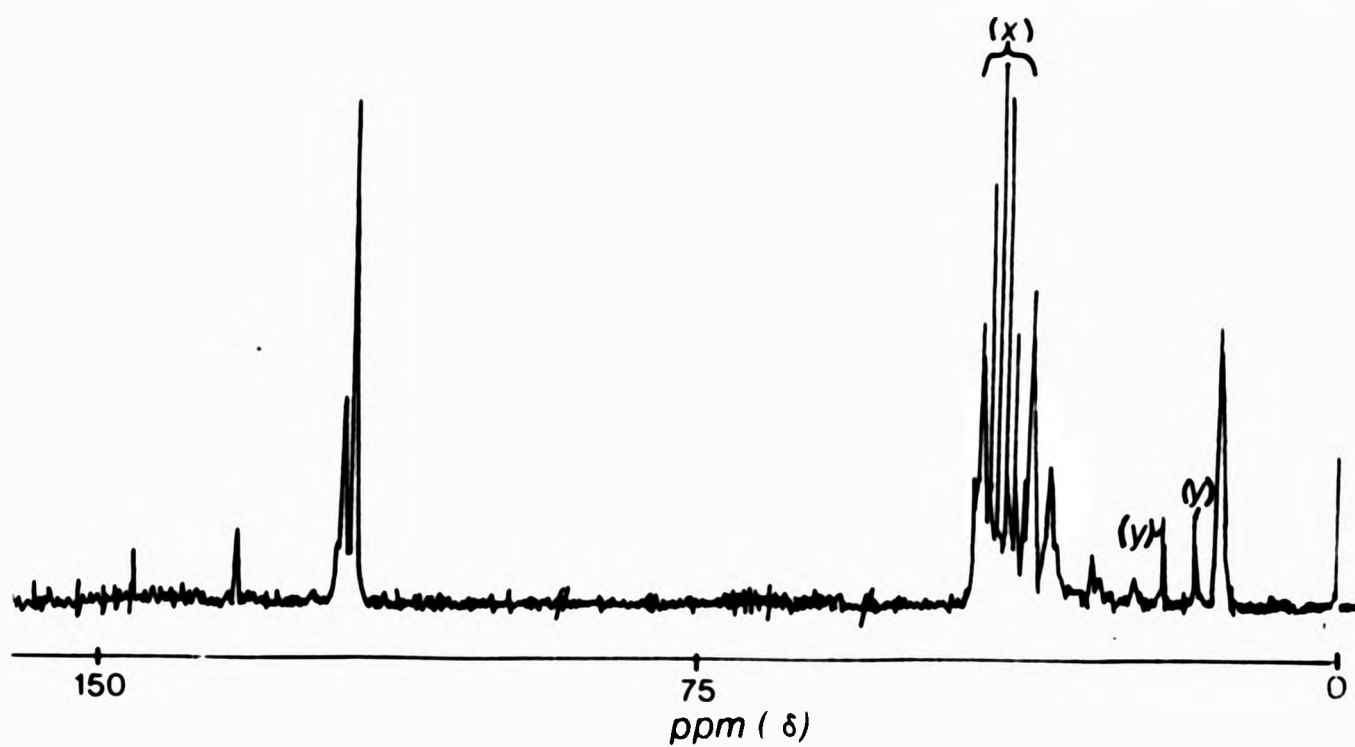
substantiating the infrared

assignment

and confirming the occurrence of chain transfer in the



(a)



(b)

FIGURE 3.2 (a) ^1H (90MHz) nmr spectrum of radically polymerised MGN.
 (b) ^{13}C nmr spectrum of radically polymerised MGN;
 (X) = solvent signals; (Y) = NaTMS signals.

system.

The ^{13}C nmr spectrum is interesting. The weak signals at 135.6 δ and 148.2 δ are due to the carbons of the ketene-imine functionality. The low intensity of the signals is due to the lack of Overhauser effect and the relatively long relaxation time of the quaternary carbons. The nitrile signals at 120.7 δ and 121.9 δ are however very intense and the reason for this is not yet clear.

The measurement of the glass transition temperature of radically initiated MGN shows a wide variation of 365K - 403K. All Tgs were determined by differential scanning calorimetry, leaving two possible, but not mutually exclusive explanations for the variation observed.

The spectroscopic analysis has shown the presence of structural irregularities in the polymers, and the variation in the extent of such structures may, to some degree, explain the variation in Tg.

The second effect, the dependence of the glass transition temperature on the molecular weight of a polymer, is well documented in the literature,¹³⁰ and has resulted in the formation of relationships such as the Flory-Fox Equation (8).

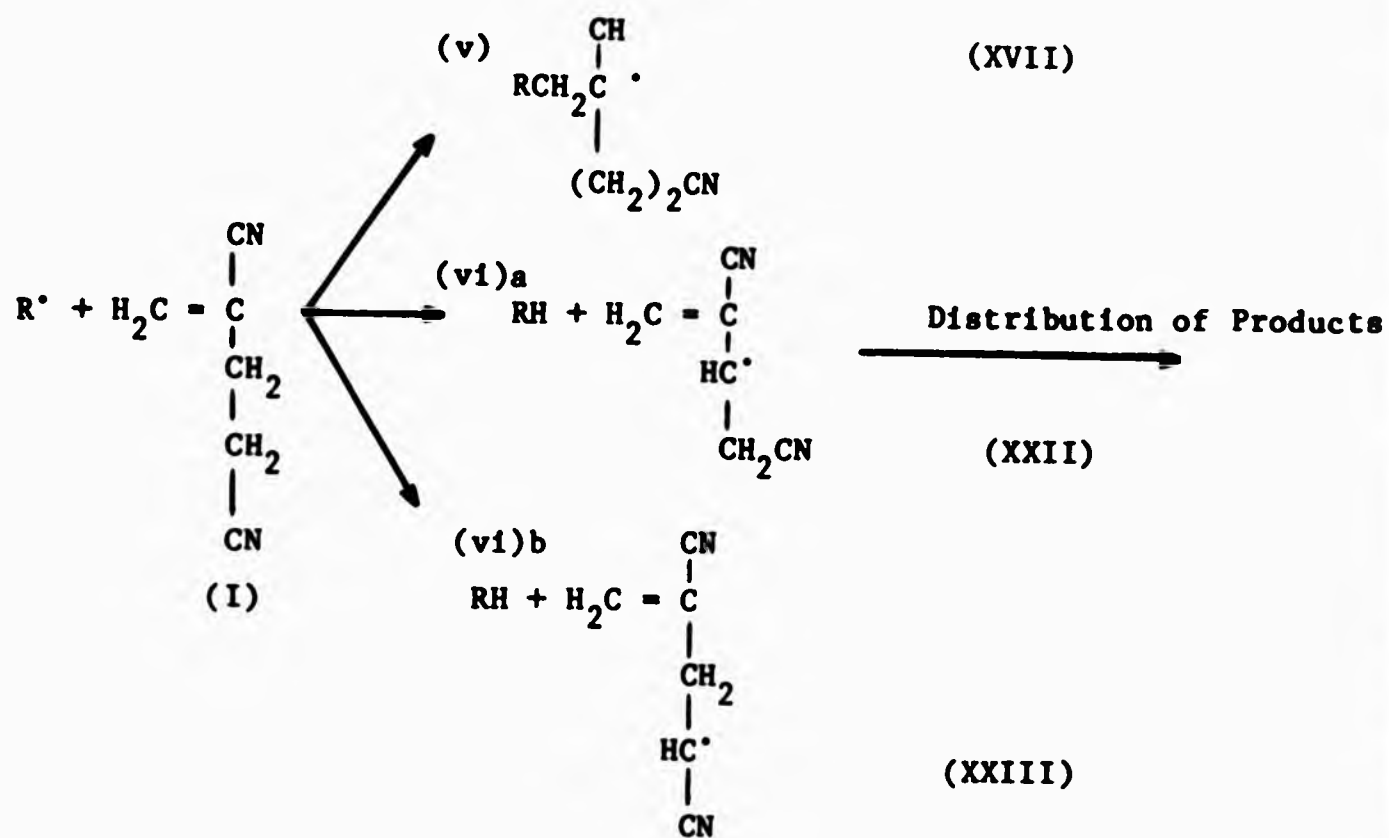
$$T_g = T_{g\infty} - a/M_n \quad (8)$$

(Here "a" is a constant and $T_{g\infty}$ is the glass transition temperature for a polymer of infinite chain length.)

Beevers¹³¹ has observed a large variation in the Tg (325-403K) of polyacrylonitrile for molecular weights in the range $8 \times 10^3 - 3 \times 10^6 \text{ g mol}^{-1}$, with the greatest variation occurring in the oligomeric region. In this present system, the M_n s were determined by vapour pressure osmometry (Table 3.1) and reveal a maximum in the degree of polymerisation of around 20. Although this appears an explanation for

the variation in glass transition temperatures, a direct correlation of M_n with T_g is not observed probably because of the previously mentioned structural variations in the polymers.

The inability of MGN to polymerise radically to high molecular weight material may be rationalised at the basis of reactions (v)-(vi).



This considers two fundamental reactions between a propagating radical R^\bullet and MGN, polymerisation is therefore a competition between radical addition (v) and abstraction reactions (vi). Equation (vi)a illustrates the behaviour of MGN as an allyl monomer, a class of monomer which is notoriously difficult to polymerise radically because of degradative chain transfer.¹³²

In radical polymerisations of this type, the kinetic chain is considered to be terminated by the transfer of an allylic hydrogen atom from a monomer molecule to a growing radical. This results in the

formation of a radical which is resonance stabilised by virtue of its allylic structure and it resists propagating long enough to terminate by bimolecular combination. This is effectively autoinhibition by the monomer, and in fact due to this type of behaviour allyl compounds have found use as inhibitors and stabilisers of prepolymer mixtures.¹³³

In the case of MGN however, this behaviour may be reduced as the resonance promoting nitrile function attached to the ethylenic nucleus tends to increase the reactivity of the monomer toward propagation (v). Nevertheless, the cyanoethyl moiety of MGN does offer potential chain transfer sites capable of reducing the degree of polymerisation in the system. Such reactions are substantiated by the spectroscopic evidence.

The additional possibility that very fast mutual termination of the growing radical chains takes place in the polymerisation of MGN and that this limits the rate and degree and polymerisation, as in the case of 1,3-butadiene,¹³⁴ was discounted on the grounds that the emulsion polymerisation (which isolates and localises the radical species) still yielded oligomeric material.

As a method of preparing polymethyleneglutaronitrile, radical initiation suffers from the drawback that there are competing reactions which results only in the formation of oligomeric material of irregular structure.

It may be possible to reduce the effects of such side reactions by carrying out the polymerisation at low temperatures and/or by employing an alternative method of initiation.

3.2 ANIONIC POLYMERISATION OF 2-METHYLENEGLUTARONITRILE

The electron deficient nature of the vinyl double bond of MGN and the ability of the α -nitrile group to stabilise a propagating anion

suggests that anionic initiators should be used to polymerise MGN. Table 3.2 contains the results of the anionic polymerisation of 2-methyleneglutaronitrile by organolithium and organomagnesium reagents.

Much of the chemistry of organolithium compounds is dictated by the nature of their electron deficient bonding and can be predicted by considering them as carbanion donors.¹³⁵ The alkyllithium initiated polymerisation of MGN results in poor yields of low molecular weight yellow polymer. The increase, albeit small, in M_n when diphenylmethylithium is used may be attributed to a variety of factors such as the greater stability of the anion, leading to greater selectivity in the reactions of the initiator, the greater steric requirements of the reagent or simply related to a difference in the number of actual "active centres" present in the three systems.

Spectroscopic analysis of polymer samples 7, 8 and 9 shows the presence of conjugated ketimine structures. By analogy with polyacrylonitrile, such structures may result from termination by cyclisation, a reaction which is favoured by anionic conditions and an isotactic sequence of nitrile groups.¹³⁶

There is no spectroscopic evidence to suggest a direct attack of the anionic initiator on the nitrile function, a major competing reaction in the anionic polymerisation of polar monomers such as methyl methacrylate.¹³⁷ Abstraction of the cyanoethyl protons of both monomer and polymer are also envisaged as possible side reactions, transfer to polymer would of course lead to branching in the system, a well documented problem in the anionic polymerisation of polyacrylonitrile initiated by the alkyllithiums.¹³⁸

There are numerous publications on the difference in the behaviour of organolithium and organomagnesium reagents towards unsaturated

TABLE 3.2

Results and Analysis of the Anionic Polymerisation of 2-Methyleneglutaronitrile

<u>System/Sample Ref.No.</u>	<u>Polymerisation System (Solvent/Initiator)^a</u>	<u>Temperature/K</u>	<u>Reaction Time/hrs</u>	<u>Polymer Yield %</u>	<u>Tg/K</u>	<u>$M_n \times 10^{-3}/$ $g \text{ mol}^{-1}$</u>
7	toluene/n-butyllithium	223	3	8	381	2.0
8	toluene/t-butyllithium	223	3	10	380	3.5
9	toluene/diphenylmethylolithium	223	3	15	383	15.0
10	toluene/diethylmagnesium	223	1.5	20	388	12.0
11	DMF/dipiperidinomagnesium	223	0.5	85	390	28.0

a) [Monomer] = 2 M; [initiator] = 4×10^{-2} M; Solvent = 100 cm³

compounds. Important in this respect is not only the polarity of the metal-carbon or nitrogen bond but also the degree of molecular association in the compound and the complex equilibria involved. In general organomagnesium initiators have been found to exhibit a relatively lower tendency to undergo various deactivating reactions (as set out above) and therefore led to a situation which is more favourable for polymerisation.^{139,140}

An extremely facile polymerisation of MGN is achieved by the use of the organomagnesium initiators diethylmagnesium and dipiperidinomagnesium. The resulting polymers are off-white powders, soluble in dipolar aprotic solvents such as DMF. The previously unreported glass-transition temperature of PMGN (390K) has been determined and may be compared to that of polyacrylonitrile (370K) and polymethacrylonitrile (393K).

It is impossible to draw any rigorous conclusions about the increase in the rate of polymerisation and molecular weights of PMGN observed in systems 10 and 11 (eg. the concentration or nature of "active centres" is not known) as the preparation of PMGN was the object of the exercise not a kinetic study of the system. However, it is possible to suggest reasons for the dramatic increase in the rate of polymerisation in system 11.

Reaction rates are known to depend on the dielectric constant of the solvent, the resonance stability of the propagating carbanion, the electronegativity of the initiator, and the nature of the gegen-ion and its degree of solvation.¹⁴¹

The major influence in this system is probably the nature of the solvent, the polar solvent promoting ionisation of the already polarised $\text{Mg}^{\text{S}^+} - \text{S}^- \text{NR}_2$ bond. Such an effect has been shown to lead to an

enhancement in the rate of polymerisation in the diethylmagnesium initiated polymerisation of acrylonitrile and a reduction in concurrent side reactions such as attack at the nitrile function.¹⁴² This effect, combined with the ability of DMF to stabilise the propagating chain end anion - gegen ion system may account for the observed polymerisation rate.

The infrared and ¹³C nmr spectra of sample 11 are shown in Figure 3.3. This again shows the difficulty of preparing "pure" PMGN. The broad absorption at 1660 cm⁻¹ is due to the ubiquitous (C=N) structure, the extent of which is unknown but is probably limited to low values (unless the magnesium gegen-ion induces a stereospecific polymerisation) as an isotactic placement of successive α nitriles is required, which would entail increased steric hindrance around the cyanoethyl moieties.

Thermogravimetric analysis of sample 11 was performed in an inert atmosphere and the thermogram is shown in Figure 3.4. This analysis shows little or no evolution of volatiles below 500K with a 60% weight loss in the region 500K-650K. The result of this pyrolysis is the production of a thermally stable residue reminiscent of that obtained in the thermal degradation of polyacrylonitrile.¹⁴³ Further to this work two PMGN-11 samples were heated to 400K and 500K respectively, each for 4 hrs., and examined by infrared spectroscopy. Visually it was found that the increase in the temperature of treatment was accompanied by an increase in the discolouration of the sample, again a similar observation to that found in the degradation of polyacrylonitrile. In the latter system, such discolouration has been attributed to an increase in the number of conjugated ketimine structures, an analogous process may well be involved in the present system as evidenced by Figure 3.5 which shows the ir spectra of three PMGN samples varying in the degree of heat

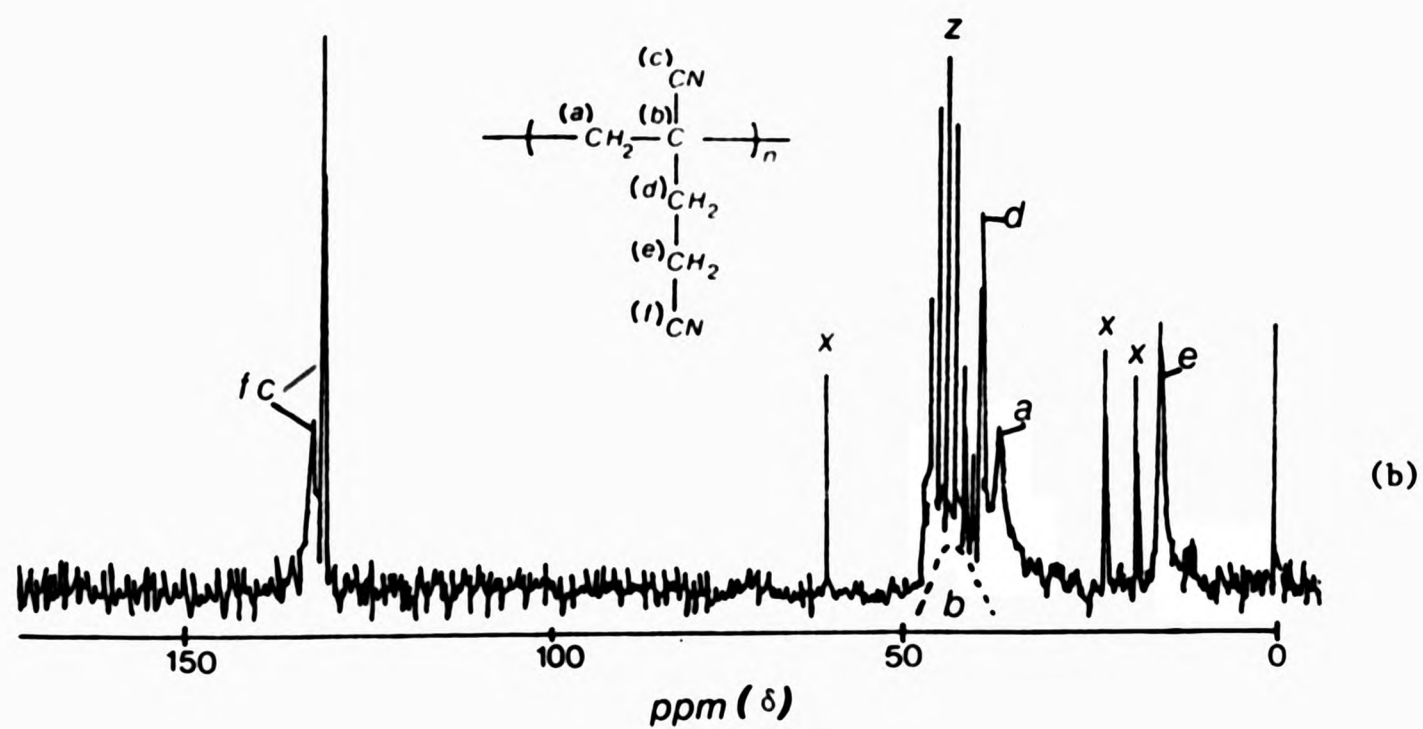
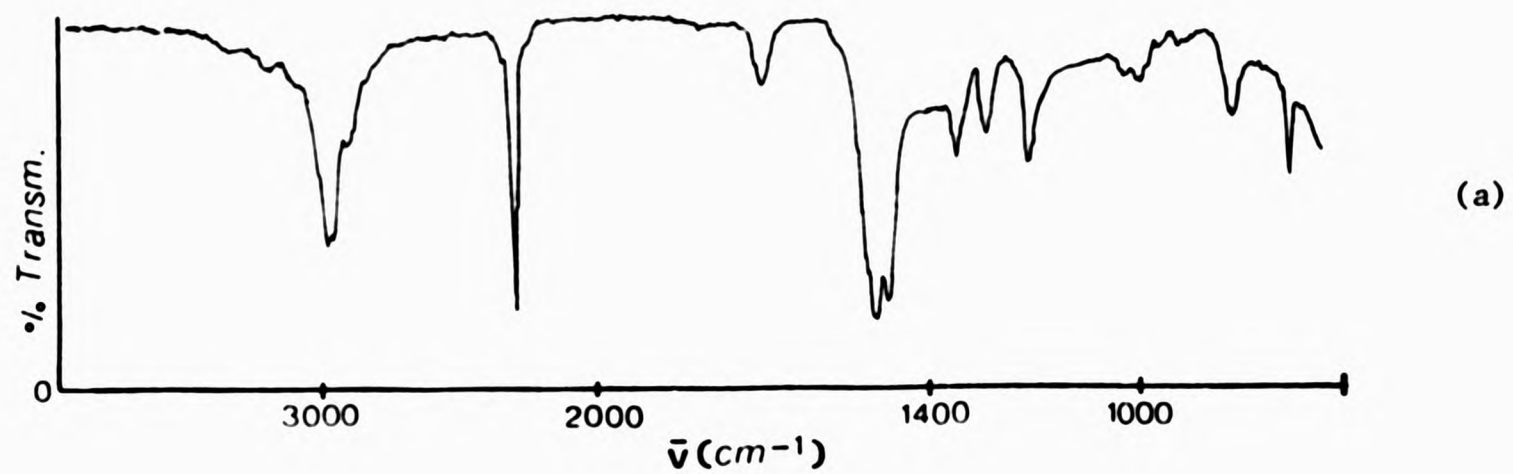


FIGURE 3.3 (a) The infrared spectrum of PMGN-11.
 (b) The ^{13}C spectrum of PMGN-11. (X = NaTMS; Z = DMSO solvent signals).

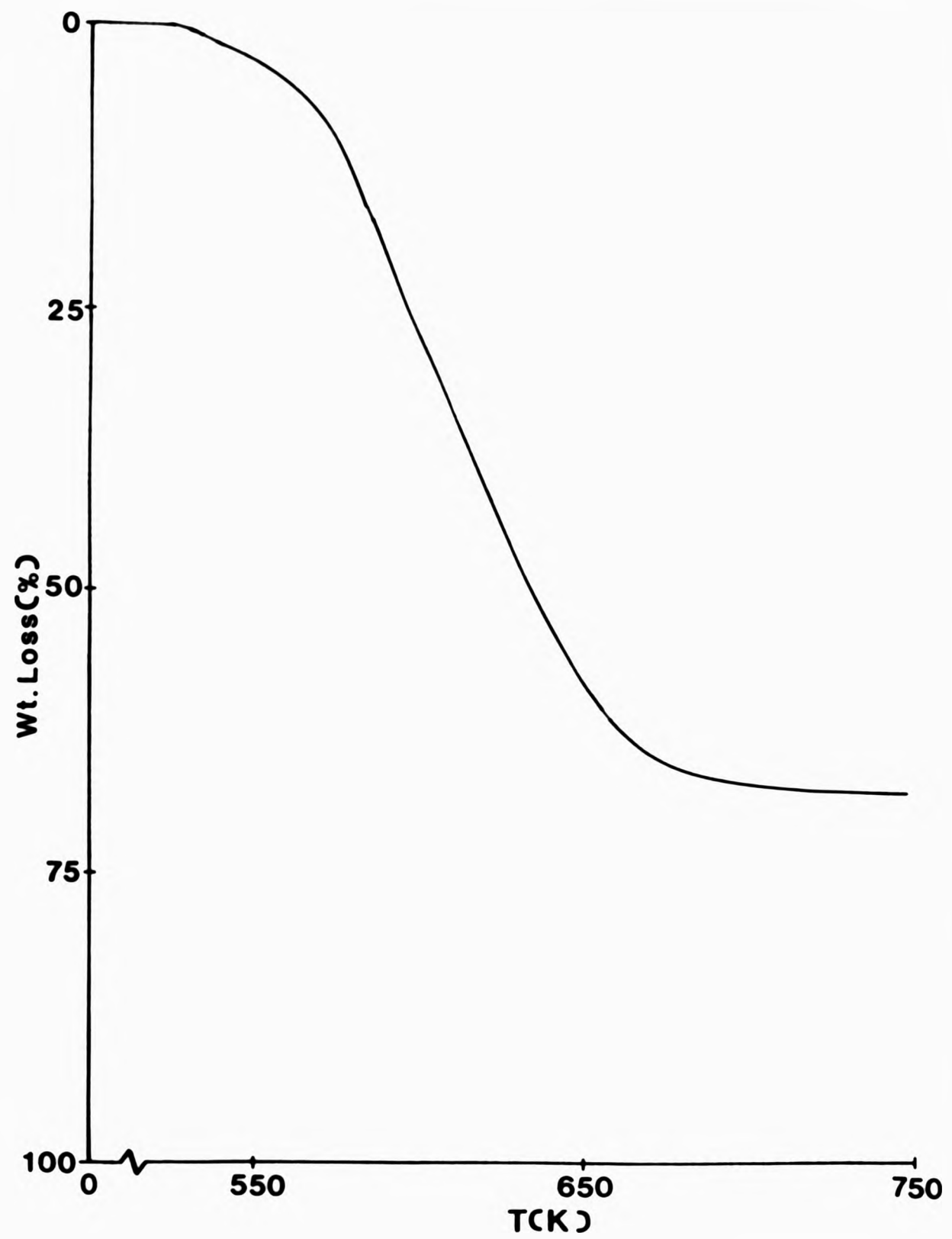


FIGURE 3.4 Thermogram of PMGN-11.

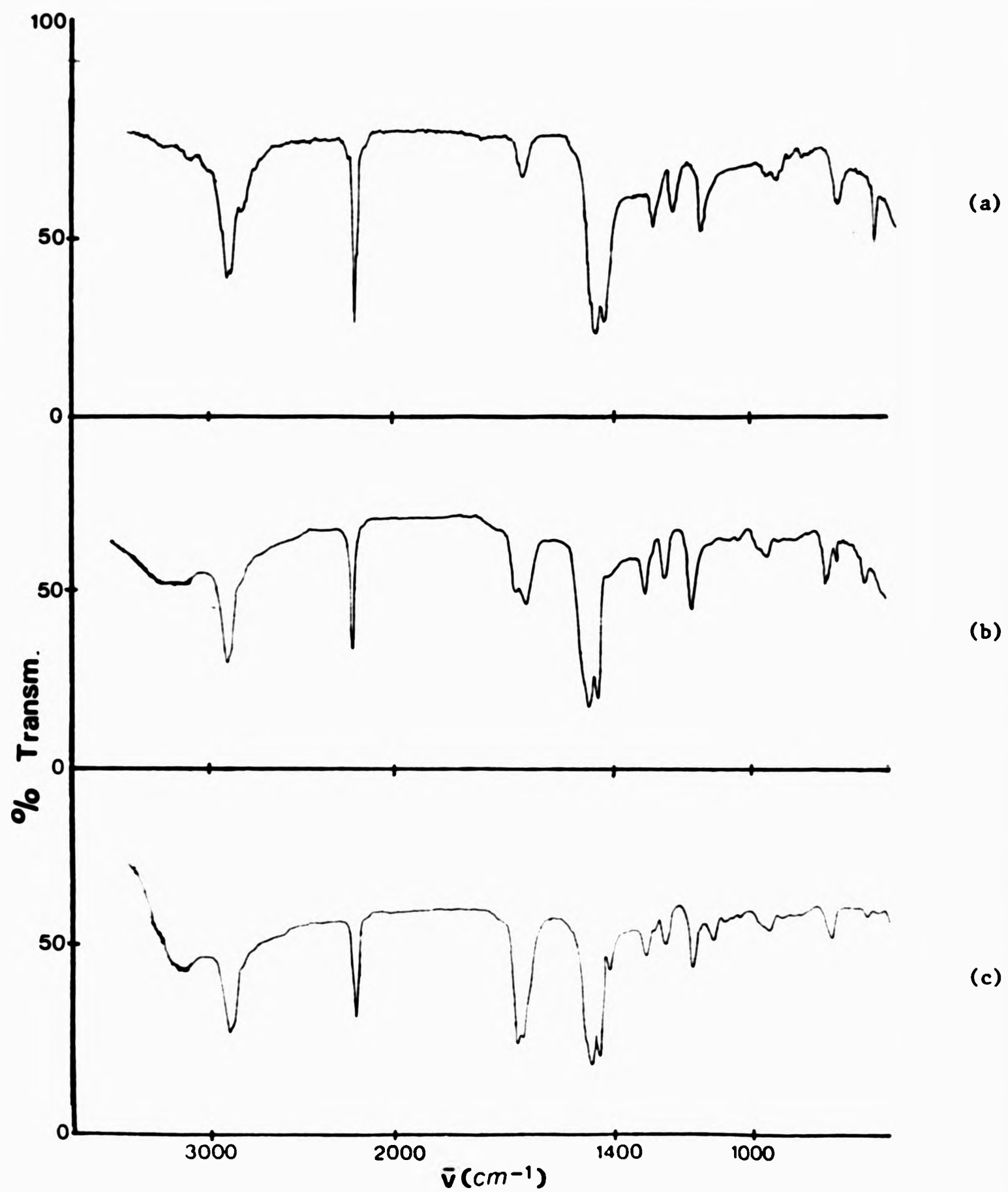
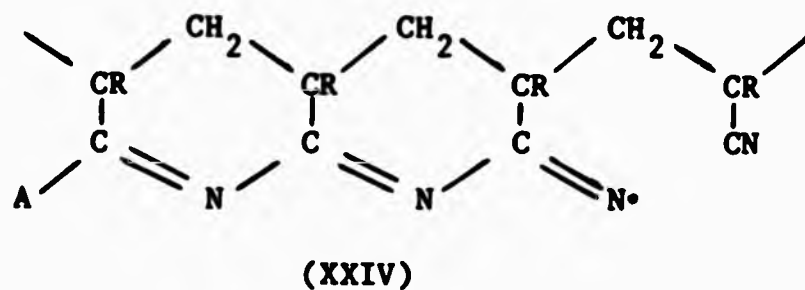


FIGURE 3.5 Thermal treatment of PMGN-11.

- (a) No treatment.
- (b) PMGN-11 heated to 400K for 4 hrs (inert atmosphere).
- (c) PMGN-11 heated to 500K for 4 hrs (inert atmosphere).

treatment and intensity of ketimine absorptions. Although Batty and Guthrie¹⁴⁴ have shown that such sequences alone would not be expected to absorb in the visible region (the terminal function being important, represented by A in structure XXIV). As 10 or 8 atom rings are unlikely, cyclisation should occur predominantly via the nitrile groups to the backbone initiated by some radical species (A).



However, it would be reasonable to assume that the cyanoethyl moieties participate to some extent in the degradative process, for example by a crosslinking reaction which may in itself be part of a ketimine system. Grassie et al.¹⁴⁵ have proposed that the thermal degradation of polyacrylonitrile is a radical process and that the methine hydrogen atoms play an important role in the degradative process. This role in PMGN may be filled by the hydrogen atoms of the cyanoethyl moiety.

The poor thermal stability of PMGN above its T_g would obviously limit any potential use for the material although it would be possible to temper such a deficiency and prepare more interesting materials by copolymerising MGN with a variety of monomers.

The similarity between polymethyleneglutaronitrile and polyacrylonitrile is very much in evidence and not all together surprising.

CHAPTER FOUR

4.1 COPOLYMERISATION OF 2-METHYLENEGLUTARONITRILE: A GENERAL SURVEY

Thermal studies on PMGN-11 have shown the propensity of polymethyleneglutaronitrile to discolour and degrade at temperatures above its glass transition temperature. Therefore rather than turning to more sophisticated initiating systems (such as modified Zeigler-Natta catalysts) in an attempt to prepare higher molecular weight material ($\sim 10^5 \text{ g mol}^{-1}$), an investigation into the copolymerisation behaviour of MGN was thought to be more promising.

The polymerisation of a single monomer is relatively limited as far as the number of different products that can be prepared is concerned. Copolymerisation greatly increases the number and type of products possible, by variations in the nature and relative amount of the two monomer units in the copolymer.

Thirteen speculative copolymerisations, encompassing a wide spectrum of comonomers, were performed at equimolar monomer feeds. The systems investigated, together with the analysis of the resulting copolymers, are contained in Table 4.1. It is evident that MGN exhibits a wide variation in its copolymerisation behaviour, ranging from the facile MGN-1,3-diene systems to the unsuccessful MGN-trans-stilbene and MGN-itaconic anhydride systems.

The inability of MGN and trans-stilbene to copolymerise under the conditions employed may be rationalised on the basis of a steric interaction between the molecules which would hinder the approach of one molecule to another and, additionally, impose a strain on the bonds being established in the transition state. Unlike the successful copolymerisation of maleic anhydride and trans-stilbene,¹⁴⁶ the favourable polar interactions in this system do not seem to overcome such steric restrictions.

TABLE 4.1

The Results of the Equimolar Copolymerisation of 2-Methyleneglutaronitrile with Selected Monomers^a

System/Sample Ref. No.	Comonomer	Copolymerisation System	Polymerisation Time (hrs)	% Conversion ^d	Mole Fraction ^e MGN in Copolymer	T _g /K	Mn x 10 ⁻⁴ / g mol ⁻¹
12	Acrylonitrile	B	16(P)	10.5	0.65	368	0.4
13	Buta-1,3-diene	S	10	2.3	0.48	283	10.0
14	Ethyl vinyl ether	B	15	7.5	0.60	357	2.3
15	Furan	B	48	10.2	0.96	365	0.2
16	Isoprene	S	1.5	2.5	0.46	288	12.0
17	Itaconic Anhydride	S	168	Nil	-	-	-
18	Methyl Methacrylate	B	1.0	7.0	0.38	385	1.2
19	α-Methylstyrene	B	6	1.2	0.48	430	3.8
20	Trans-stilbene	S	72	Nil	-	-	-
21	Styrene	B	2.0	23.2	0.45	380	6.1
22	Vinyl Acetate	B	168	50.1	0.63	345	0.8
23	N-Vinyl Carbazole	S	2.5(P)	3.3	0.52	480	4.2
24	4-Vinyl Pyridine	B	4.0	40	0.48	391	4.1

a) Initiator = 1 mol% AIBN; Temperature = 333K.

d) Determined gravimetrically.

b) B = Bulk, S = Toluene Solution; [Total Monomer] = 5M.

e) Determined from elemental analysis and nmr measurements.

c) P = copolymer precipitated during polymerisation.

Also unsuccessful was the MGN-itaconic anhydride copolymerisation. Both these monomers possess allylic hydrogen atoms, therefore one might expect degradative chain transfer to play a part in this system (both monomers are reluctant to homopolymerise, essentially forming oligomeric material). Additionally, unlike the majority of copolymerisation systems in Table 4.1, there is no favourable polar interaction between a chain end radical (1) with a monomer molecule (2). Both monomers being considered to possess "electron poor" vinyl bonds (relative to ethylene). A similar situation was encountered by Gilberts et al.¹⁴⁷ who noted the reluctant copolymerisation of vinylidene cyanide with maleic anhydride.

The low reactivity of the vinyl bond of vinyl acetate towards free radicals, compared with other well known monomers, was reported as far back as 1948 by Mayo et al.¹⁴⁸ The copolymerisation of acrylonitrile with vinyl acetate was shown by these authors to be a sluggish reaction and in fact comonomer solutions comprising ca. 15% acrylonitrile failed to polymerise. Therefore, the slow copolymerisation of MGN and vinyl acetate is not surprising.

The copolymerisation of furan, essentially the cyclic analogue of divinyl ether, with "electron poor" vinyl monomers such as maleic anhydride has been found to yield equimolar copolymers.^{149,150} Although the subject of much controversy, it has been postulated that such copolymerisations are actually homopolymerisations of a Diels-Alder adduct and that furan shows no propensity to copolymerise in the conventional manner.¹⁵¹ From the analysis of sample 15, the attempted copolymerisation of furan and MGN results only in the formation of oligomeric PMGN. One can only assume that no Diels-Alder adduct is formed under the conditions employed here, resulting only in the homopolymerisation of MGN.

Samples isolated from the successful copolymerisations were subjected to elemental analysis and/or nmr measurements allowing the copolymer composition to be obtained (see Table 4.1). However, direct correlation between the comonomer feed ratio and the copolymer composition can only be made (excepting azeotropic copolymerisations) for systems terminated at a low degree of conversion ($\ll 10\%$), where the comonomer feed is relatively unchanged from its known initial value. With conversions greater than this, composition drift cannot be ruled out.¹⁵² In this situation the comonomer feed changes in composition as one of the monomers preferentially enters the copolymer. Therefore there is a drift in the comonomer feed towards the less reactive monomer as the degree of conversion increases. This results in a similar variation of copolymer composition with conversion.

The solubility characteristics of the copolymer samples are shown in Table 4.2.

The previously unreported infrared spectra of the MGN copolymers are shown in Figure 4.1 (a-j). All spectra (excluding that of sample 15) show the characteristic absorptions expected for their respective copolymers. Especially interesting are the spectra of samples 12, 14, 18 and 22. All exhibit, in varying intensities, an absorption at 2000 cm^{-1} . This absorption was observed in the infrared spectrum of radically polymerised MGN and was ascribed to the presence of ketene-imine structures $[\text{C}=\text{C}=\text{N}]$ in the polymer. Without doubt this is the source of the present absorption, the structures again arising from propagation or termination reactions involving the resonance structures XVI and XVII.

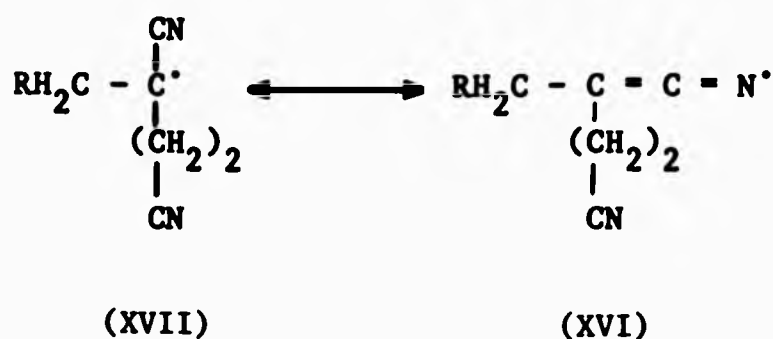


TABLE 4.2**Solubility Characteristics of 2-Methyleneglutaronitrile Copolymers^a**
at 298K

<u>System/Sample</u> <u>Ref. No.</u>	<u>Dioxane</u>	<u>Chloroform</u>	<u>Acetone</u>	<u>Butan-2-one</u>	<u>DMF</u>	<u>Acetone</u>
12	S	0	0	0	S	S
13	+	+	S	S	S	S
14	0	S	S	S	S	S
16	+	+	S	S	S	S
18	S	S	S	S	S	S
19	0	S	S	S	S	S
21	S	S	S	S	S	S
22	0	0	S	0	S	S
23	0	0	S	S	S	0
24	0	0	0	0	S	0

a) 0 = Not soluble; + = Swells; S = Soluble

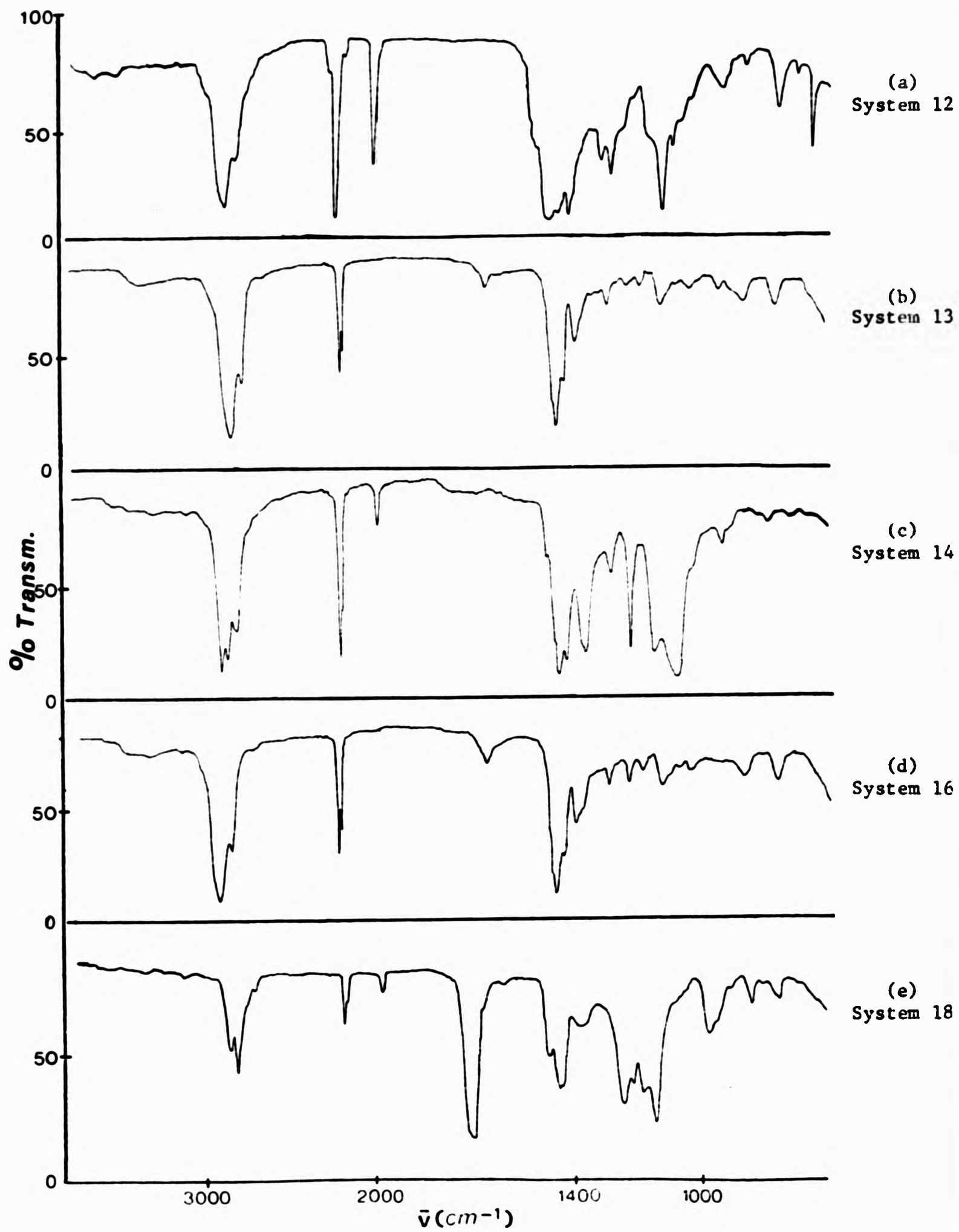


FIGURE 4.1 (a-j) Infrared spectra of MGN copolymers.

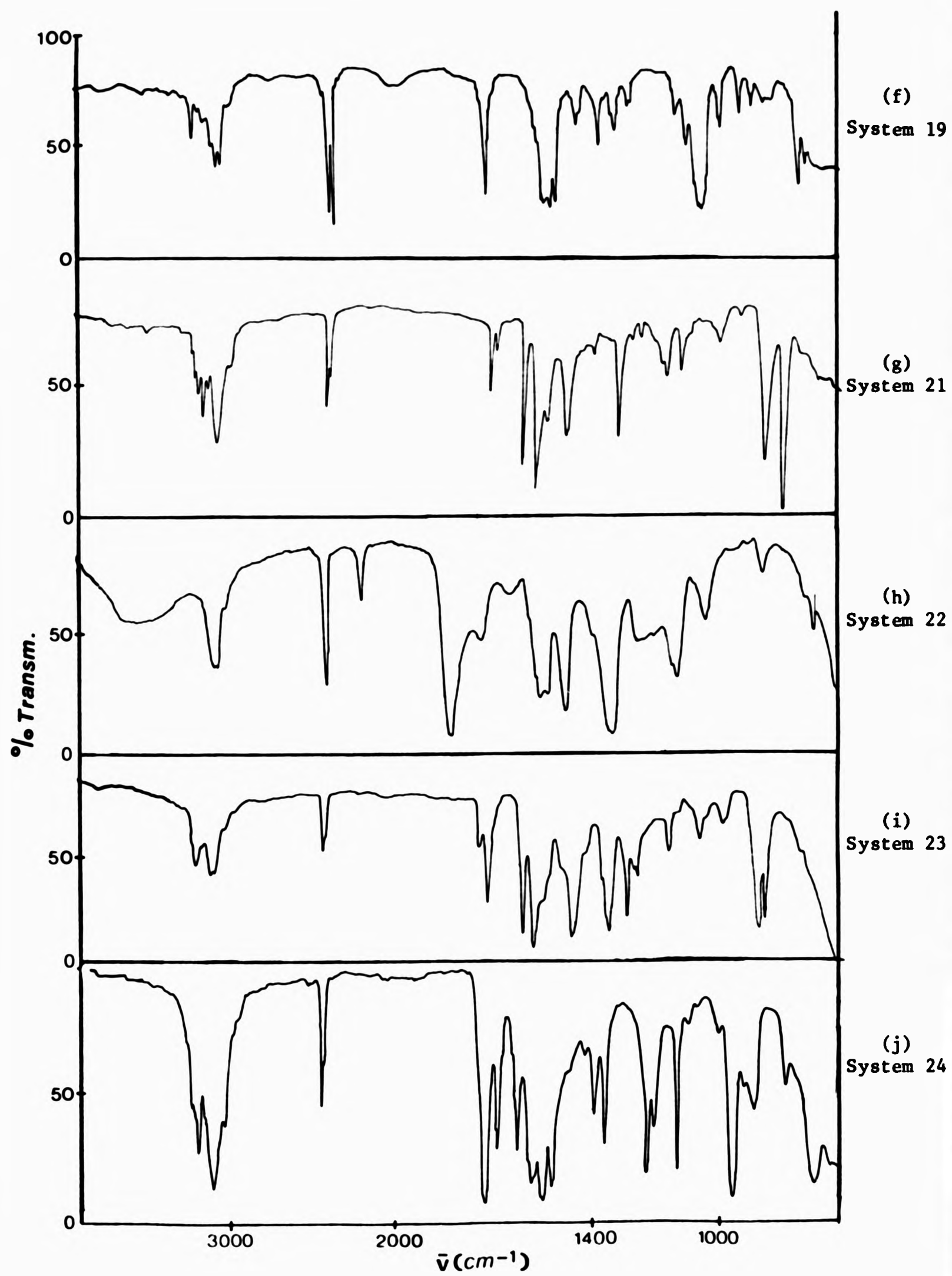
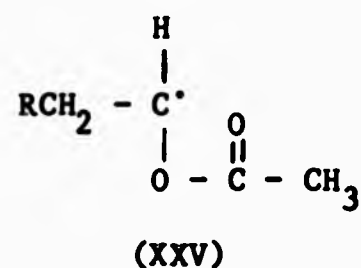


FIGURE 4.1 (a-j cont.)

Chain growth in the copolymerisation of conjugated dienes may proceed in a number of ways leading to geometric isomerisation in the copolymer. Infrared spectroscopy has been employed to identify such isomeric structures in isoprene and butadiene homopolymers,¹⁵³ however this was not found to be a satisfactory method in this copolymerisation study. A detailed discussion of this problem and a thorough analysis of the copolymer structure is presented later in section 4.4.

Number average molar masses were determined by vapour pressure osmometry and membrane osmometry. This analysis showed samples 12, 15, 18 and 22 to be of rather low molar mass. Although no kinetic studies were undertaken here, this is probably the result of extensive chain transfer in these systems. Certainly in the copolymerisation of vinyl acetate and MGN, one has a combination of an unstable/reactive radical (the vinyl acetate radical XXV) and potential chain transfer sites on



both monomers. For example, the allylic hydrogen atoms of MGN and the acetoxy hydrogen atoms of vinyl acetate are prime targets for chain transfer to monomer (both would result in the formation of a resonance stabilised radical).

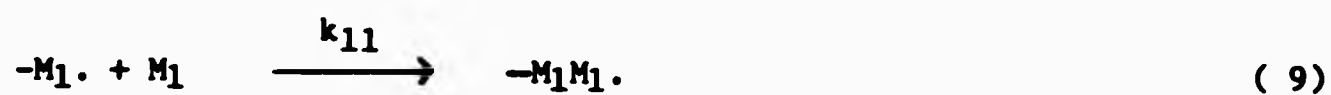
Provided that comonomer pairs do not have a tendency to form blocks of "homopolymer" upon copolymerisation i.e. $(M_1-M_1)_n-(M_2-M_2)_m$, copolymers will exhibit a single Tg which normally lies between the values of the Tg for the two homopolymers. At this stage the connectivity of the monomers in the copolymer samples has not been established, but the copolymers do show a single Tg in the temperature regions expected. Copolymerisation of MGN with a 1,3-diene moiety

(isoprene and butadiene) yields a tough flexible thermoplastic with a T_g around room temperature. The addition of rigid bulky side groups to the polymer backbone results in a restriction to rotation imposed by steric restraint, this decreases the flexibility of the polymer chain leading to an increase in T_g .¹⁵⁴ The effect is accentuated by increasing the size of the side group (there is some evidence to suggest a correlation between T_g and the molar volume of a pendant side group¹⁵⁵) and therefore we observe an increase in the T_g of MGN copolymers in the order 21, < 19, < 23.

This exploratory study has shown the facile copolymerisation of MGN with certain monomers, and the possibility of preparing high molecular weight copolymers free of the "structural irregularities" found in polymethyleneglutaronitrile. In this category are the copolymerisations of MGN with styrene and related monomers, the MGN-1,3-diene systems and the copolymerisation of MGN with the electron-rich N-vinyl carbazole monomer.

4.2 MAYO-LEWIS TREATMENT OF SELECTED COPOLYMERISATIONS

In the polymerisation of two monomers, the rate at which the two monomers add to the growing chain determines the composition and hence the properties of the resulting copolymer. The order as well as the ratio of amounts in which monomers add are determined by their relative reactivities in the chain growth step. The terminal model or Mayo-Lewis model of copolymerisation¹⁵ assumes that chain growth is influenced only by the nature of the chain end radical and of the monomer; this therefore results in the four propagation reactions, 9-12.



where k_{11} and k_{22} are the rate constants for the self-propagating reactions and k_{12} and k_{21} are the corresponding cross-propagation rate constants. Under steady state conditions one can derive a copolymer equation relating the instantaneous composition of copolymer being formed, $d[M_1]/d[M_2]$, to the monomer concentrations:

$$d[M_1]/d[M_2] = ([M_1]/[M_2]) (r_1[M_1] + [M_2]) / ([M_1] + r_2[M_2]) \quad (13)$$

where $k_{11}/k_{12} = r_1$ and $k_{22}/k_{21} = r_2$.

The parameters r_1 and r_2 are the monomer reactivity ratios. They are the ratios of the rate constants for a given radical adding its own monomer to that for it adding the other monomer. A value of $r > 1$ means that the radical prefers to add its own monomer, and vice versa.

Reactivity ratios are obviously the factors which control the composition of the copolymer and therefore one must obtain reliable values of r_1 and r_2 for each pair of monomers if copolymerisation systems are to be understood and controlled.

The parameters r_1 and r_2 may be determined by analysing the composition of the copolymers formed from a number of monomer feed ratios at low conversions, and employing this data in one or other of the mathematical transformations of equation 13, as enumerated by

Mortimer.¹⁵⁶

The copolymerisation study of MGN with isoprene, α -methyl styrene, N-vinyl carbazole, and ethyl vinyl ether, was extended to cover a wide range of monomer feed compositions allowing the determination of the monomer reactivity ratios for these systems.

The comonomers MGN and isoprene are not totally miscible over the monomer feed range investigated (333K) as shown by the cloud point curve, Figure 4.2, obtained from turbidity measurements on MGN-isoprene mixtures. The copolymerisation of MGN and isoprene was therefore carried out in toluene solution. Solvent was also employed in the redox emulsion copolymerisation of this monomer pair. In both systems the copolymers were obtained as tough white materials. Tables 4.3 and 4.4 summarise the results of the copolymerisations.

The bulk copolymerisation of MGN and α -methyl styrene at 333K and employing 1 mol% AIBN led, in the majority of cases, to low molecular weight or oligomeric material. This observation may be the result of a number of mechanistic considerations, such as a thermally reversible polymerisation,^{157,158} steric hinderance to successive placements of α -methyl styrene units in the polymer chain,¹⁵⁹ degradative chain transfer to monomer,¹⁶⁰ and to generation of a relatively stable α -methyl styrene radical characterised by a low rate of propagation of the free radical kinetic chain.^{161,162} Successful copolymerisations were achieved, to the detriment of the polymerisation rate, by carrying out the reactions in bulk at 323K using 0.25 mole% AIBN. The redox emulsion technique at 298K did not produce copolymer within the time scale of the experiment (96 hrs). MGN- α -methyl styrene copolymers were obtained as white powders and the results of the copolymerisations are summarised in Table 4.5.

The analogous results for the MGN-N-vinyl carbazole and MGN-ethyl

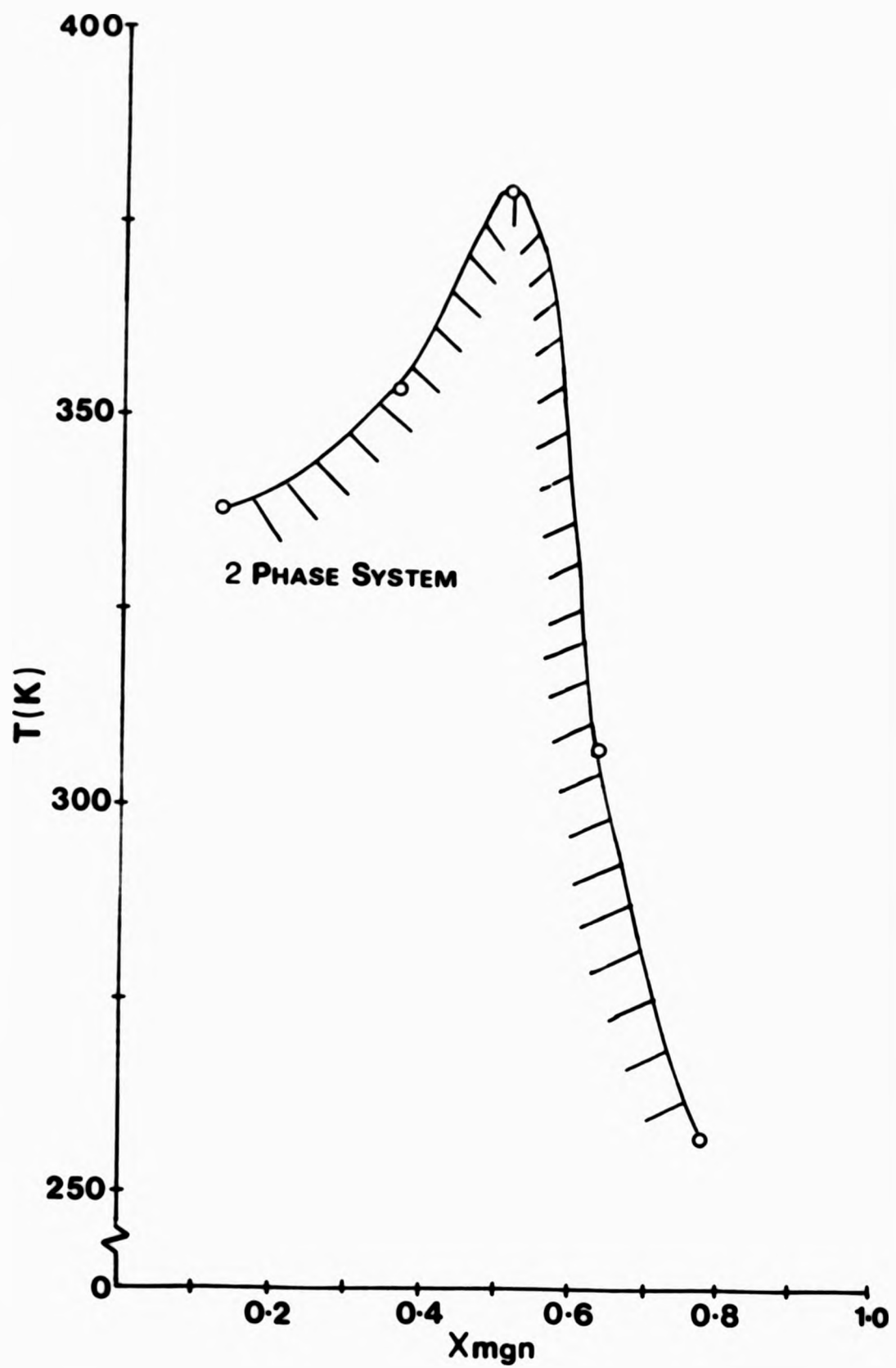


FIGURE 4.2 Cloud point curve of MGN-IP mixtures illustrating the limited miscibility of the monomers. (X_{mgn} = mole fraction MGN)

TABLE 4.3
Redox Emulsion Copolymerisation of MGN with Isoprene at 298K^a

Monomer Feed (Mole Fraction MGN)	Polymerisation Time (hrs)	% Conversion ^b	Elemental Analysis			Copolymer Composition (Mole Fraction MGN)	Mn x 10 ⁻⁴ g mol ⁻¹	Tg/K ^c
			%H	%C	%N			
0.10	3.5	2.4	8.4 ₁	79.1 ₁	14.1 ₄	0.425	3.8	282
0.20	3.75	2.5	8.2 ₆	76.3 ₉₈	14.3 ₅	0.433	5.5	284
0.30	3.75	1.9	8.1 ₉	76.0 ₁	15.0 ₁	0.458	10.9	287
0.40	4.0	3.1	8.6 ₇	78.1 ₀	14.7 ₅	0.448	10.0	287
0.50	3.5	2.8	8.0 ₁	75.8 ₇	15.1 ₇	0.464	8.8	288
0.60	4.0	2.5	8.1 ₀	75.4 ₀	15.5 ₁	0.477	9.6	288
0.70	3.5	3.5	7.9 ₈	75.2 ₀	15.8 ₁	0.489	10.5	289
0.80	3.5	1.5	7.6 ₉	75.0 ₃	16.4 ₄	0.515	7.1	294
0.90	4.75	1.6	8.0 ₇	75.8 ₂	17.0 ₂	0.538	5.1	298

a) Employing the recipe set out in Table 2.6.

b) Determined gravimetrically.

c) Determined from DSC thermograms by the extrapolated onset method.

TABLE 4.4
Copolymerisation of MGN with Isoprene in Toluene at 333Ka

Monomer Feed (Mole Fraction MGN)	Polymerisation ^b Time (hrs)	% Conversion ^c	Elemental Analysis ^d			Copolymer Composition (Mole Fraction MGN)	Mnx10 ⁻⁴ g mol ⁻¹	Tg/K ^e
			%H	%C	%N			
0.10	8.5 ^P	2.3	9.9 ₆	78.8 ₉	11.6 ₅	0.336	0.9	272
0.20	3.5 ^P	2.2	8.6 ₁	78.3 ₄	13.6 ₅	0.407	2.2	282
0.30	1.5	3.6	8.3 ₁	77.5 ₁	14.3 ₈	0.434	9.7	287
0.40	0.5	1.6	8.3 ₆	77.3 ₂	14.7 ₃	0.447	10.4	288
0.50	0.33	1.2	7.9 ₀	77.0 ₈	15.0 ₁	0.475	12.2	288
0.60	0.50	1.3	8.1 ₉	76.4 ₄	15.4 ₆	0.458	10.2	290
0.70	0.50	1.1	8.6 ₅	75.9 ₆	16.3 ₇	0.475	9.2	292
0.80	0.66	1.0	7.7 ₁	76.1 ₁	16.3 ₇	0.489	6.8	296
0.90	1.00	2.1	7.6 ₀	75.7 ₃	16.9 ₃	0.534	2.1	300

a) Total monomer concentration = 8M; Initiator = 1 mol % AIBN.

b) P = Precipitation of polymer during reaction.

c) Determined gravimetrically (mean value).

d) Each set of CHN values are the mean from (on average) three separate copolymerisations for that feed ratio.

e) Determined from DSC thermograms by the extrapolated onset method.

TABLE 4.5
Bulk Copolymerisation of MGN with α -Methyl Styrene at 323K^a

Monomer Feed (Mole Fraction MGN)	Polymerisation Time (hrs)	Conversion ^b %	Elemental Analysis ^c		Copolymer Composition (Mole Fraction MGN)	Mnx10 ⁻⁴ g mol ⁻¹	Tg/K ^d
			%H	%C			
0.1	120	0.72	7.6 ₉	83.8 ₆	0.351	0.8	410
0.2	34	0.9	7.0 ₁	82.5 ₂	0.404	1.2	417
0.3	26	1.4	7.6 ₀	81.4 ₃	0.445	1.5	420
0.4	18	1.5	8.0 ₅	80.9 ₁	0.460	2.8	426
0.5	12	1.2	6.9 ₀	81.2 ₅	0.481	3.8	429
0.6	12	1.1	6.0 ₁	80.9 ₇	0.490	3.3	424
0.7	9	0.8	6.4 ₅	80.3 ₂	0.509	2.2	424
0.8	7	0.45	6.1 ₁	79.9 ₀	0.531	1.8	420
0.9	4	0.15	6.0 ₁	78.8 ₅	0.601	1.4	418

a) Total monomer: 0.2 moles; Initiator concentration = 0.25% AIBN.

b) Determined gravimetrically (mean value).

c) Each set of CHN values are the mean from, on average, 3 separate copolymerisations.

d) Determined from DSC thermogram by the extrapolated onset method.

vinyl ether copolymerisations are presented in Tables 4.6 and 4.7 respectively.

Experimental copolymer composition data may be analysed by a number of methods to yield values of the monomer reactivity ratios (MRR). In a critical review Tidwell and Mortimer¹⁶³ pointed out the defects of the various linear methods and suggested the use of a non-linear least squares procedure. The superiority of the non-linear analysis was reiterated by Leicht et al.¹⁶⁴

Consequently, this study utilised a Fortran non-linear least squares curve fitting procedure employing a standard Newton Raphson algorithm (N.A.G. subroutine E04FDF) to analyse the copolymer composition data of Tables 4.3-4.7. In this procedure it is first necessary to define a goodness of fit parameter τ (taken as the residual sum of the squares of the experimental-calculated copolymer compositions) and to successively change the estimated input values of the monomer reactivity ratios in a patterned manner so as to locate the minimum value of τ on its hypersurface. The values of the MRR which correspond to this minimum can then be said to best fit the experimental data. In this manner the topography of the hypersurface in the region of the minimum can be examined in order to gauge how well each parameter has been defined by the data fit. Assigning a limit on τ of twice its value at the minimum gives each parameter a plausible range of values consistent with an adequate representation of the experimental data. This procedure was performed on a VAX 11/780 computer and the results of these analyses are shown in Figures 4.3-4.7. For systems 16a and 19, the experimental error in the copolymer compositions established from repeated copolymerisations is ca. $\pm 0.8\%$. However, no such multiple analyses were performed on the remaining three systems. In each case the error involved in the value of the monomer feed is considered small enough, in

TABLE 4.6

Copolymerisation of MGN with N-Vinyl Carbazole in Toluene at 333K^a

<u>Monomer Feed (Mole Fraction MGN)</u>	<u>Polymerisation^b Time (hrs)</u>	<u>% Conversion^c</u>	<u>Copolymer Composition^d (Mole Fraction MGN)</u>	<u>Mnx10⁻³ g mol⁻¹</u>	<u>Tg/K^e</u>
0.10	12.5 ^P	1.5	0.37	2.6	488
0.20	10.5 ^P	1.9	0.46	3.0	482
0.30	6.0 ^P	2.3	0.49	2.5	480
0.40	5.5 ^P	2.5	0.51	3.8	479
0.50	2.5 ^P	3.3	0.52	4.2	480
0.60	2.5 ^P	3.5	0.54	3.7	471
0.70	2.0	3.0	0.57	2.8	468
0.80	1.5	3.0	0.63	1.8	469
0.90	1.5	3.8	0.67	0.90	465

a) Total monomer concentration = 5M; Initiator concentration = 1 mol % AIBN.

b) P = Precipitation of polymer during reaction.

c) Determined by gravimetric analysis.

d) Determined by ¹H nmr spectroscopic analysis from the ratio of aromatic:aliphatic signal integrals.

e) Determined from DSC thermograms by the extrapolated onset method.

TABLE 4.7
Bulk Polymerisation of MGN with Ethyl Vinyl Ether at 333K^a

Monomer Feed (Mole Fraction MGN)	Polymerisation		Elemental Analysis ^c			Copolymer Composition		Mnx10 ⁻³ g mol ⁻¹	T _g /K ^d
	Time (hrs)	% Conversion	%H	%C	%N	%O	(Mole Fraction MGN)		
0.10	12	0.5	7.8 ₂	67.9 ₆	15.2 ₂	9.4 ₀	0.48	12.2	338
0.20	12	1.2	7.7 ₁	68.4 ₅	16.2 ₄	8.6 ₀	0.52	15.7	-
0.30	18	2.4	7.2 ₅	67.9 ₁	16.7 ₃	8.8 ₁	0.54	15.1	344
0.40	18	4.4	7.4 ₁	69.7 ₄	17.2 ₂	7.6 ₃	0.56	21.1	-
0.50	18	3.1	7.3 ₀	67.1 ₁	18.4 ₂	6.6 ₆	0.61	23.2	357
0.60	18	3.2	7.1 ₀	66.4 ₁	19.3 ₄	5.1 ₅	0.65	17.4	-
0.70	18	2.9	6.8 ₂	67.6 ₅	20.4 ₆	5.0 ₁	0.70	14.0	370
0.80	24	2.6	6.6 ₄	66.6 ₄	21.5 ₀	4.1 ₈	0.75	4.9	-
0.90	24	4.1	6.4 ₃	65.7 ₆	22.5 ₈	3.2 ₁	0.80	4.1	382

a) Total moles of monomer = 0.2 moles; Initiator concentration = 1 mol % AIBN.

b) Determined gravimetrically.

c) %O determined by difference.

d) Determined from DSC thermograms by the extrapolated onset method.

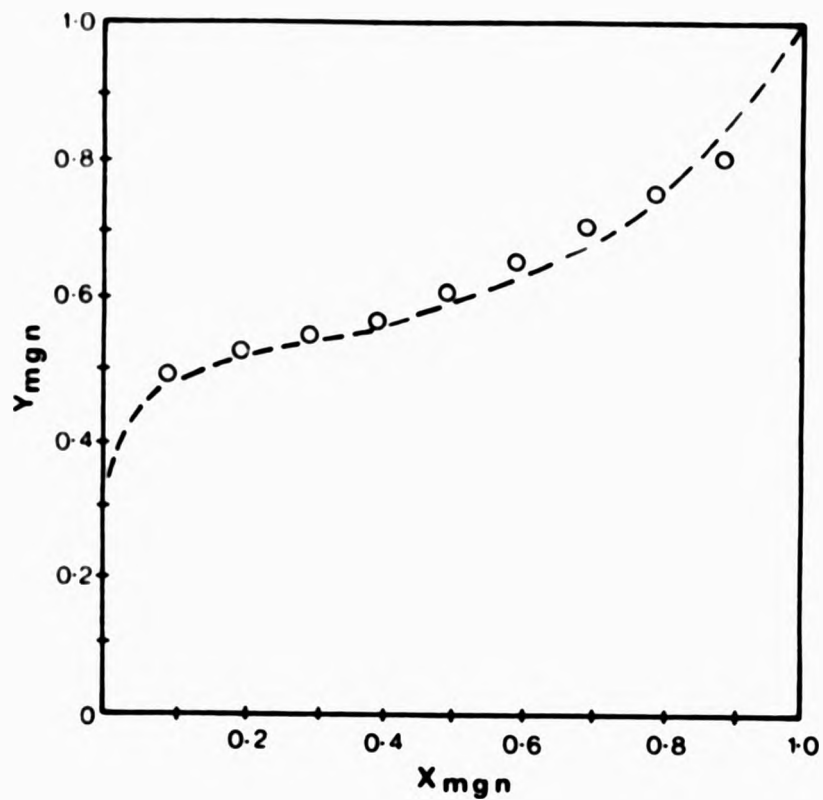


FIGURE 4.3

Copolymer composition curve for the copolymerisation of MGN and ethyl vinyl ether (system 14) in bulk at 333K.

(Y_{MGN} = mole fraction MGN in copolymer; X_{MGN} = mole fraction MGN in monomer feed.)

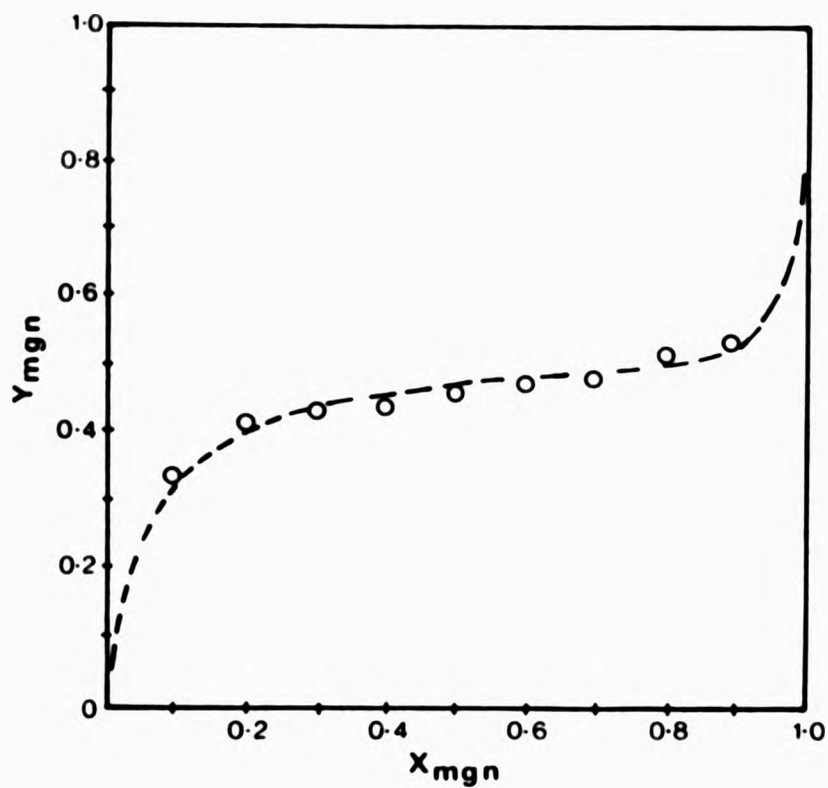


FIGURE 4.4

Copolymer composition curve for the solution copolymerisation of MGN and isoprene (system 16a) at 333K. (Y_{MGN} = mole

fraction MGN in copolymer; X_{MGN} = mole fraction in monomer feed.)

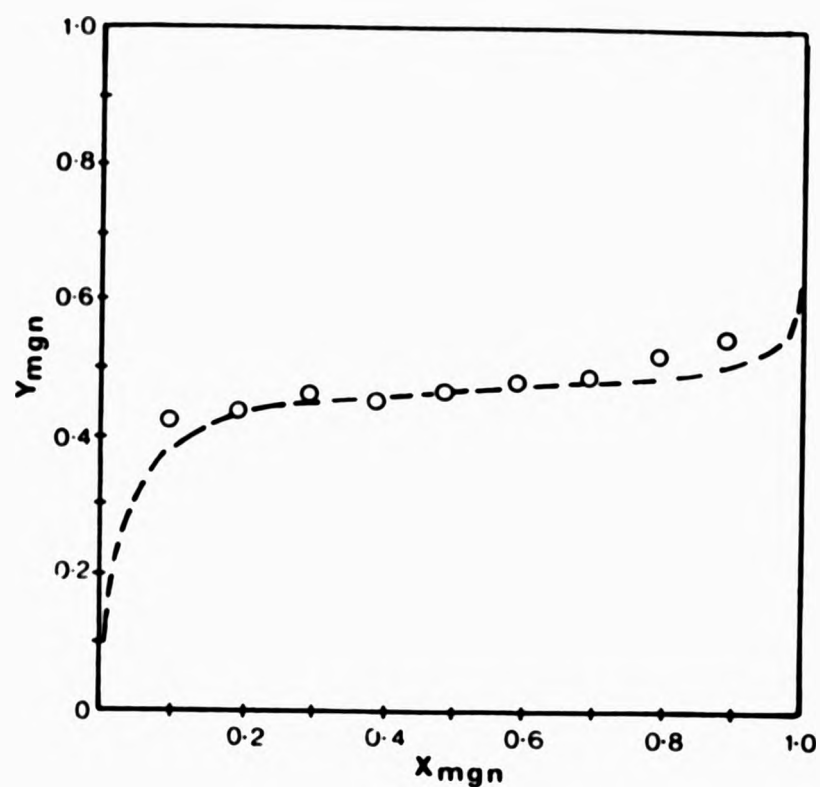


FIGURE 4.5

Copolymer composition curve for the redox emulsion copolymerisation of MGN and isoprene (system 16b) at 303K. (Y_{MGN} = mole fraction MGN in copolymer; X_{MGN} = mole fraction MGN in monomer feed.)

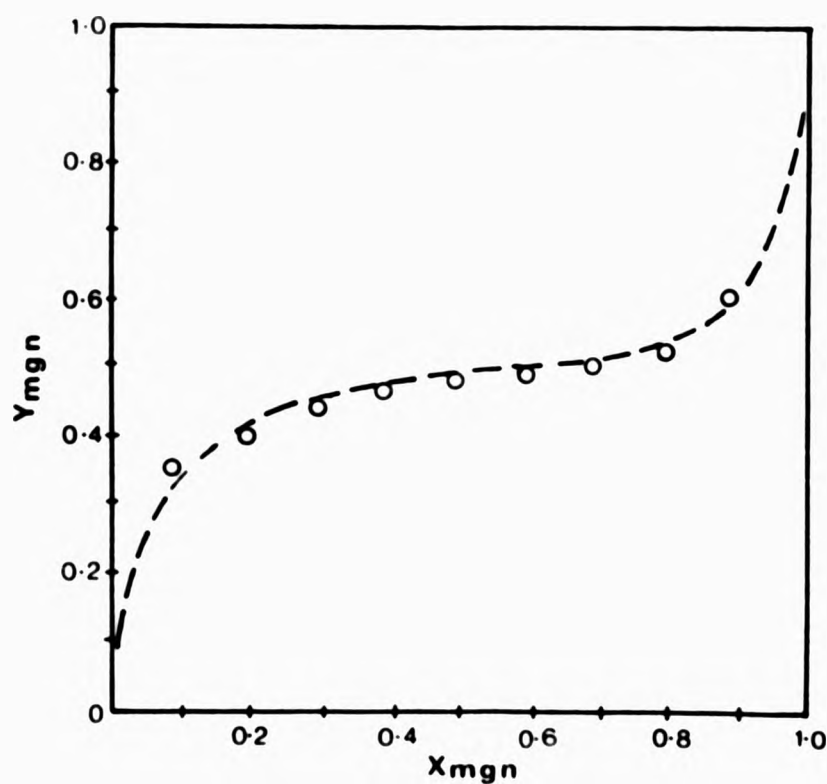


FIGURE 4.6

Copolymer composition curve for the copolymerisation of MGN and α -methyl styrene (system 19) at 323K. (Y_{MGN} = mole fraction MGN in copolymer; X_{MGN} = mole fraction MGN in monomer feed.)

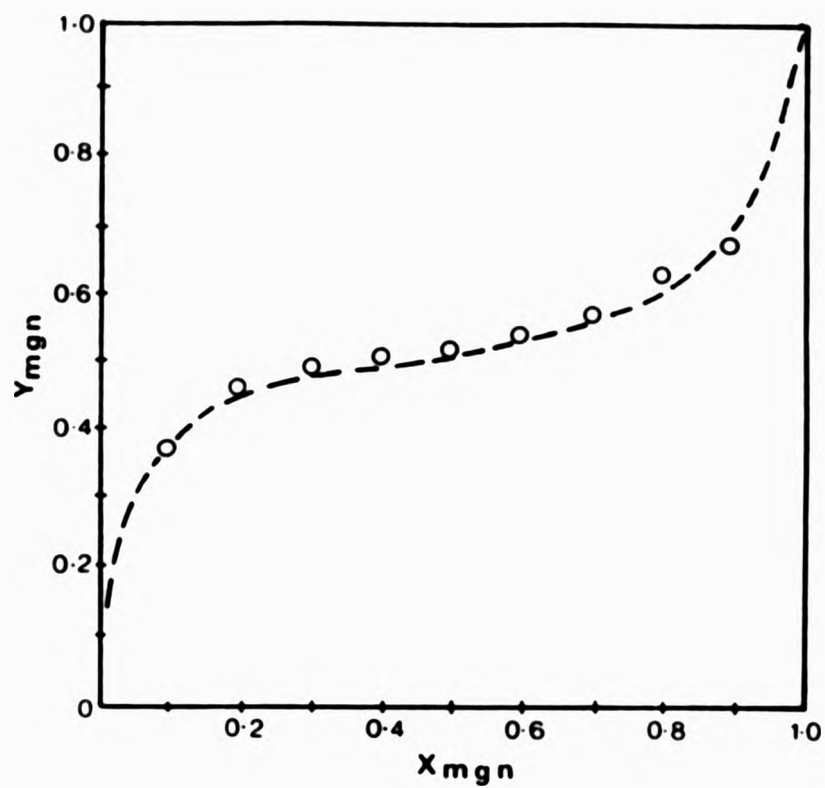


FIGURE 4.7

Copolymer composition curve for the solution copolymerisation of MGN and N-vinyl carbazole (system 23) at 333K.

(Y_{MGN} = mole fraction MGN in copolymer; X_{MGN} = mole fraction MGN in monomer feed.)

comparison, to be neglected. The monomer reactivity ratios obtained by the non-linear least squares curve fitting procedure are summarised in Table 4.8.

Generally speaking, monomer reactivity ratios are essentially independent of the reaction medium in radical copolymerisation.¹⁶⁵ Occasionally, however, emulsion copolymerisations do result in copolymer compositions which are different from those obtained from bulk or solution polymerisation, e.g. when the comonomer composition at the reaction site (the micelle in emulsion copolymerisations) is different from that in the solution copolymerisation.¹⁶⁶ This may arise for a number of reasons, for example, if diffusion of one of the monomers (or solvent) into the micelle is slow. The absolute monomer reactivities are unchanged in such systems and the "discrepancy" in copolymer compositions, such as that between systems 16a and 16b, may simply be due to the altered concentration of monomers at the reaction sites.

Also interesting are the results of the MGN-ethyl vinyl ether system. Unlike the strictly alternating copolymerisation of maleic anhydride and ethyl vinyl ether,¹⁶⁷ which also involves two monomers that have no great propensity to homopolymerise, system 14 shows a greater similarity to acrylonitrile-ethyl vinyl ether copolymerisation.¹⁶⁸ Over the wide monomer feed range, system 14 yields copolymers rich in the nitrile monomer and consequently the product tends to reflect the characteristics of PMGN.

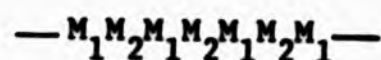
Copolymerisations are generally classified according to the values of r_1 , r_2 , and the product $r_1 r_2$. All four copolymerisation systems studied here (14, 16, 19 and 23) have r_1 and r_2 values < 1 with the products $r_1 r_2$ of the order 10^{-3} . This is indicative of a tendency of the monomers to alternate during the copolymerisation reaction and results in copolymers whose structure tends towards that of XXVI.

TABLE 4.8

MGN (M₁)-Comonomer (M₂) Reactivity Ratios

<u>System Ref.No.</u>	<u>Comonomer M₂</u>	<u>r₁ (MGN)</u>	<u>Error^a Range</u>	<u>r₂ (comonomer)</u>	<u>Error^a Range</u>	<u>r₁r₂</u>
14 (Bulk)	Ethyl vinyl ether	0.495	0.381-0.621	0.014	0 -0.040	6.93x10 ⁻³
16(a) Solution Copoly.	Isoprene	0.015	0.003-0.029	0.121	0.097-0.146	1.82x10 ⁻³
16(b) Emulsion Copoly.	Isoprene	0.013	0 -0.041	0.058	0.028-0.091	7.54x10 ⁻⁴
19 (Bulk)	α-Methyl Styrene	0.050	0.036-0.065	0.109	0.086-0.129	5.45x10 ⁻³
23 (Bulk)	N-Vinyl Carbazole	0.144	0.105-0.184	0.068	0.045-0.101	9.79x10 ⁻³

a) Error range calculated as described in section 4.2.



(XXVI)

The connectivity of the monomers along the copolymer chain in systems 16(a) and 19 is confirmed directly by nmr analysis (section 4.4) to exclude any unusual arrangement of the monomers in the copolymer which would yield similar elemental analysis, for example a tendency towards $\text{---(M}_1\text{M}_1\text{M}_1\text{)}_n\text{---(M}_2\text{M}_2\text{M}_2\text{)}_m\text{---}$ or $\text{---(M}_1\text{M}_1\text{M}_2\text{M}_2\text{M}_1\text{M}_1\text{M}_2\text{M}_2\text{)}_n\text{---}$ structures. Although realistically such behaviour is encountered in only a few copolymerisations, involving the sequential addition of the two monomers in the presence of coordination catalysts.¹⁶⁹

Attempts to place copolymerisation on a quantitative basis in terms of correlating structure and reactivity have met with limited success. A generally useful correlation is the Alfrey-Price "Q-e" scheme,²⁷ which defines the rate constant for the radical ($M_1\cdot$) - monomer (M_2) reaction as

$$k_{12} = P_1 Q_2 \exp(-e_1 e_2) \quad (14)$$

where P_1 and Q_2 are a measure of the reactivities or resonance effects of the radical and monomer respectively, and e_1 and e_2 are a measure of the polarity of the radical ($M_1\cdot$) and monomer (M_2). Extending this treatment (assuming that a monomer and its radical have the same e value) gives the relationships for r_1 and r_2 .

$$r_1 = (Q_1/Q_2) \exp(-e_1(e_1 - e_2)) \quad (15)$$

$$r_2 = (Q_2/Q_1) \exp(-e_2(e_2 - e_1)) \quad (16)$$

Transposing equations 15 and 16 into equations 17 and 18,

$$\ln r_1 r_2 = -(e_1 - e_2)^2 \quad 17$$

$$\ln Q_1 = \ln r_1 + \ln Q_2 + e_1(e_1 - e_2) \quad 18$$

allows the Alfrey-Price Q-e parameters for MGN to be determined using the data contained in Table 4.8. The results of the four independent calculations of the Q and e values for MGN are given in Table 4.9.

These values may be compared with the literature values reported by Greenley¹⁷⁰, Q = 0.41; e = 1.25, which were calculated from the limited data of Pritchett and Kamath.⁸

The spread in the values of these parameters is by no means peculiar to this study,¹⁴⁷ such variations are a result of both the inherent inadequacies of the Q-e scheme (for example it does not explicitly take into account steric factors which may affect monomer reactivity, particularly in the case of 1,1-disubstituted ethylenes like MGN) and the experimental errors involved in the determination of the monomer reactivity ratios. Nevertheless, the mean values of Q and e calculated for MGN are consistent with the structure of the monomer. Monomers possessing substituents capable of conjugation with the olefinic double bonds tend to have a value of Q > 0.5 and the positive value of e correlates with the polarisation of the vinyl system caused by the nitrile function. For comparison the corresponding values for acrylonitrile are Q = 0.6, e = 1.2¹⁷¹ and methacrylonitrile Q = 1.12, e = 0.8.¹⁷²

Although essentially only a useful approximation, the Q-e values of MGN can be used to predict the copolymerisation behaviour of MGN in previously untried systems.

TABLE 4.9

Calculated Alfrey Price Q and e Values for MGN^a

<u>System Ref.No.</u>	<u>Comonomer (M₂)</u>	<u>Comonomer</u>		<u>MGN</u>	
		<u>e₂</u>	<u>Q₂</u>	<u>e₁</u>	<u>Q₁</u>
14	Ethyl Vinyl Ether	-1.17	0.03	1.06	0.16
16(a)	Isoprene	-1.22	3.33	1.29	1.27
19	α-Methyl Styrene	-1.27	0.98	1.01	0.49
23	N-Vinyl Carbazole	-1.40	0.41	<u>0.75</u>	<u>0.30</u>
	Mean value:			<u>1.03</u>	<u>0.56</u>

a) In the Alfrey-Price scheme styrene is assigned the arbitrary values of Q = 1.0 and e = -0.8.

4.3 THERMAL AND THERMOMECHANICAL ANALYSIS

One of the most important properties of a high polymer is its thermal behaviour. Knowledge of this is essential for the full characterisation of the material's physical and mechanical properties and an indication of the possible end-use of the polymer.

4.3.1 Location of the Tg of MGN copolymers by differential scanning calorimetry

The Tgs of random copolymers are usually predicted by additive relationships such as the Fox equation (19)¹⁷³.

$$(1/TgP) = (W_A/TgA) + (W_B/TgB) \quad (19)$$

where TgP is the Tg of a copolymer containing weight fraction W_A and W_B of the two monomer units A and B, for which the homopolymers have glass transition temperatures of TgA and TgB. There are, however, copolymer systems which are known to deviate from the Fox equation and, according to Hirooka et al.,¹⁷⁴ such deviations appear to be magnified in the case of the corresponding alternating copolymer. These observations have prompted researchers to conclude that, when predicting the Tg of a copolymer, it is necessary to take into account the sequential distribution of the monomers in the copolymer.¹⁷⁵

For the majority of materials in the copolymer systems 14, 16(a), 19 and 23, the Tg was located and defined by the DSC extrapolated onset method. The results of these analyses, summarised in Tables 4.4-4.7, permit an evaluation of the Fox relationship.

Examination of the data (Table 4.7) for system 14 reveals that the molar masses are too low for the Tg values to be characteristic of the corresponding high polymer. Additionally the infrared spectra of a number of these MGN-EVE copolymers at extreme feed ratios show the presence of irregular structures in the materials. It would therefore

be unwise to correlate the T_g measurements with copolymer composition in this system. The molar mass data of Tables 4.5 and 4.6 also dictate a restricted analysis of these systems. This apart, it is still possible to draw some primary conclusions.

Figure 4.8 shows the T_g data vs copolymer composition for three MGN copolymer systems plotted on the basis of the Fox equation. The MGN-MS system is shown to conform essentially to the Fox relationship. On the other hand, systems 16(a) and 23 exhibit negative and positive deviations respectively. Such deviations are a manifestation of the inherent simplifying assumptions made by the Fox equation. The Fox and similar equations do not take into consideration the effect on the steric and energetic relationships of adjacent dissimilar monomer units in the copolymer backbone, and assume that the freedom of rotation and free volume contributed to a copolymer by a given monomer will be the same as its contribution in the homopolymer. In fact, Johnston¹⁷⁶ has noted that the T_g contribution of many bulky di- α -substituted monomers changes dramatically when these monomers are copolymerised with monomers not similarly substituted. Further analysis of the MGN copolymer composition/ T_g behaviour is not warranted by the data presented here.

4.3.2 Thermogravimetric Analysis (TGA)

The thermal stability of a copolymer can seldom be predicted from the stabilities of the corresponding homopolymers. The incorporation of a small amount of comonomer into a material may influence the stability either favourably or adversely and, in the limiting case of alternating copolymers, such materials may be considered as essentially homopolymers, exhibiting their own thermal behaviour.¹⁷⁷

In the present study TGA (see section 2.6.2) allows an evaluation of the thermal stability of 3 MGN copolymers. The thermograms are presented in Figure 4.9, which shows the % weight loss as a function of temperature.

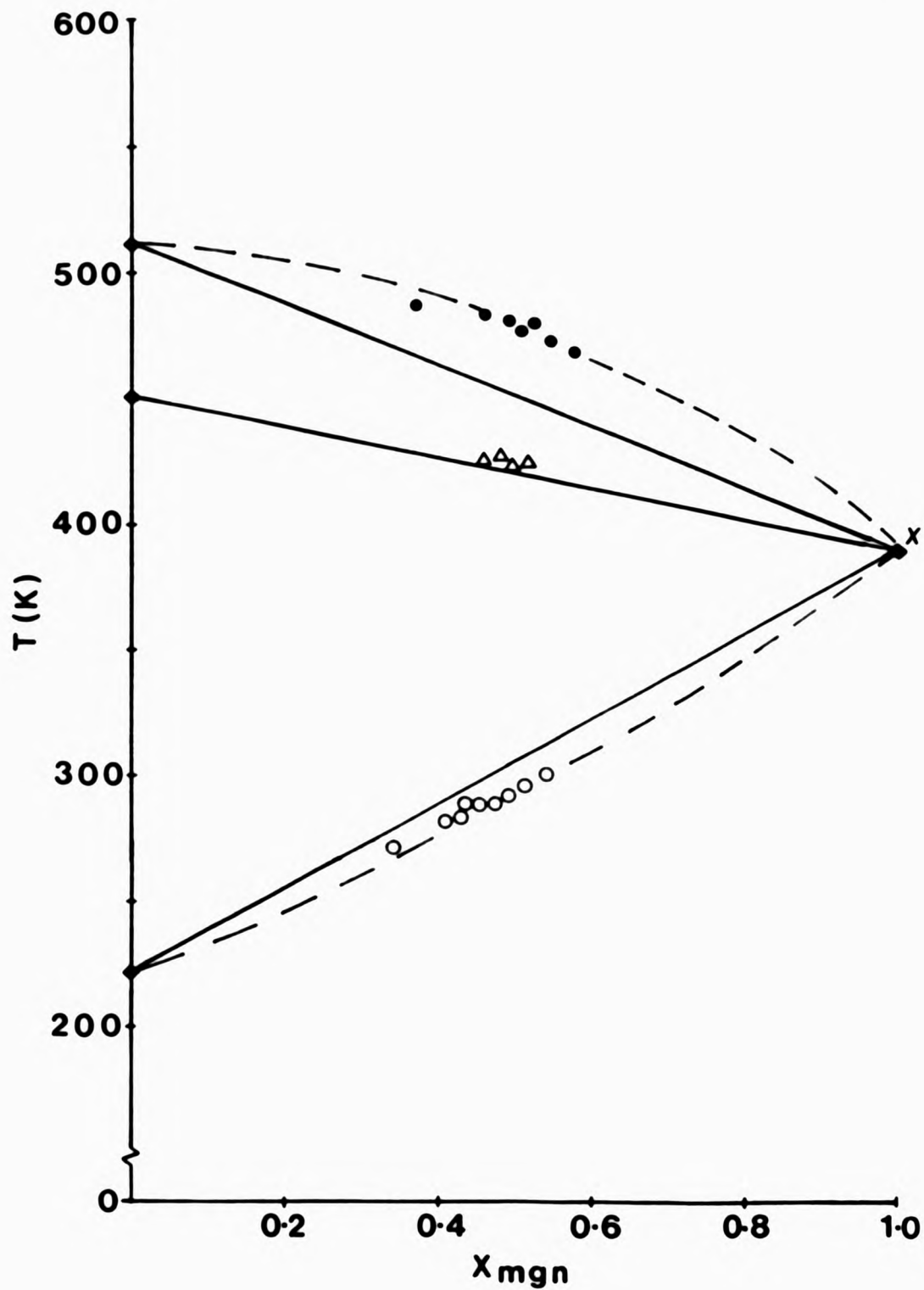


FIGURE 4.8

MGN copolymer Tg/copolymer composition data plotted according to the FOX equation (19).

(-----) = experimental fit; (——) = Fox equation predicted fit.

● = MGN-NVC copolymer system.

▲ = MGN-MS copolymer system.

○ = MGN-IP copolymer system.

× = Tg of PMGN-11.

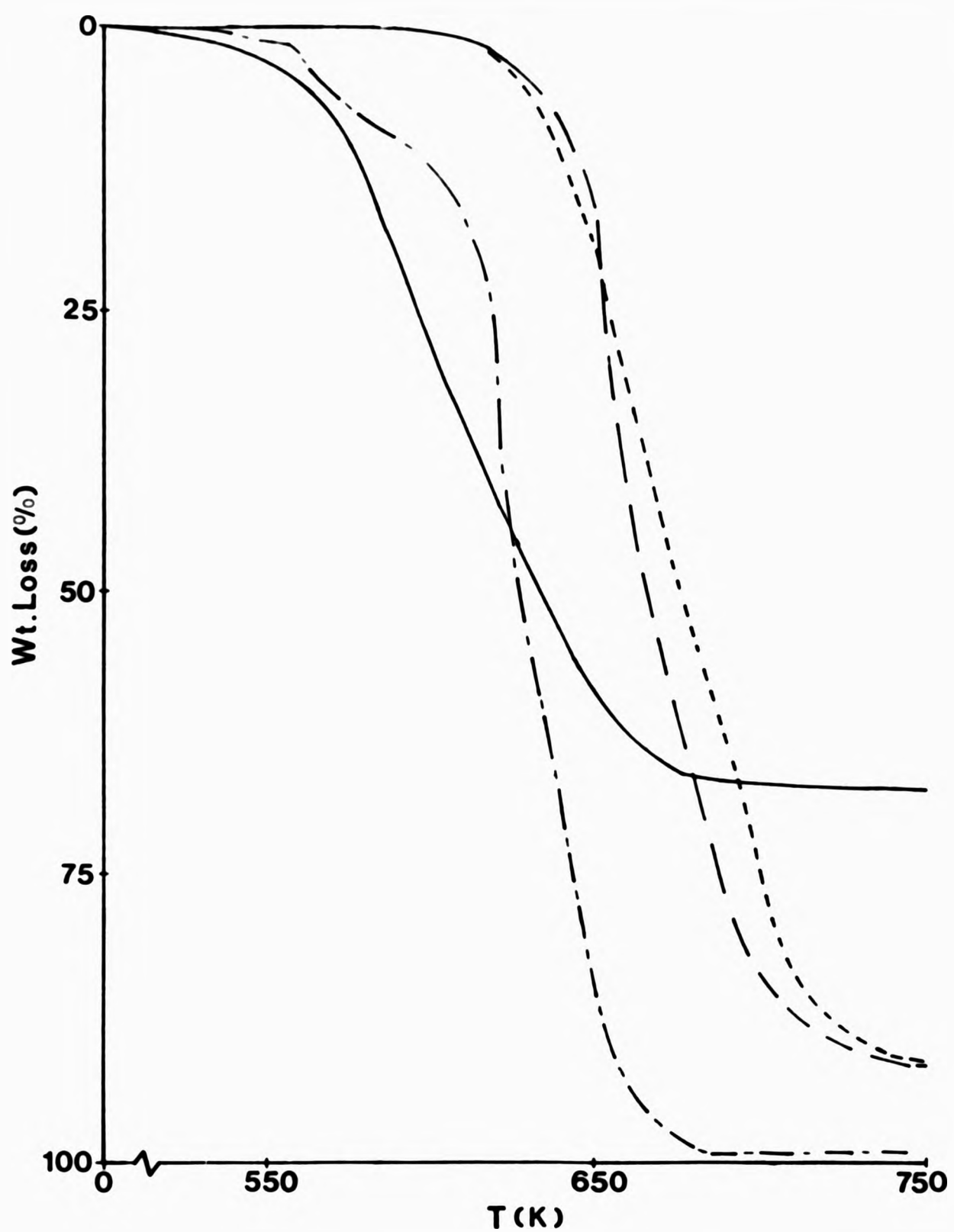


FIGURE 4.9 Thermogravimetric analysis curves for MGN polymers.
 (—) = PMGN-11.
 (---) = MGN-IP (45.8/54.2) copolymer.
 (---) = MGN-NVC (48/52) copolymer.
 (- - -) = MGN-MS (48.1/51.9) copolymer.

A number of observations are worth noting. In both the MGN/NVC (52/48) and MGN/IP (45.8/54.2) systems, the materials are stable up to a temperature of 600K, some 50K above the temperature at which extensive degradation of PMGN itself is observed. Figure 4.9 also reveals that, unlike the homopolymer, both copolymers are almost totally volatilised at 750K.

The MGN/MS (48.1/51.9) copolymer is found to be the least thermostable copolymer of the three, with the onset of degradation occurring 100K above its T_g , at 530K. This thermogram seems to indicate a two step degradative process, (a) an initial 10% weight loss occurring in the region 530K-580K, followed by (b) extensive main chain scission over the range 580-710K, again resulting in almost complete volatilisation at 750K.

The Perkin-Elmer TGS2 used in this work was not employed in conjunction with an additional analytical system such as pyrolysis gas chromatography, therefore little other than the basic thermal stability of the polymeric materials can be obtained.

However, from the comparison of the % weight loss at 750K of the three copolymers to that of the homopolymer it could be argued that the copolymer degradation pattern points to the possibility that the three copolymers are comprised predominantly of alternating comonomer sequences. Such a microstructure would inhibit the nitrile condensation reaction which has been shown to lead to the formation of thermally stable ring systems ca. above 570K (cf. chapter 3.2).

4.3.3 Torsional Braid Analysis (TBA)

Two MGN copolymer samples (an MGN/IP and MGN/MS copolymer) were analysed by TBA, the use of which is described in chapter 2.6.3, and the resulting thermograms are presented in Figures 4.10 and 4.11, with temperature as the abscissa, and the logarithmic decrement (L.D.) and

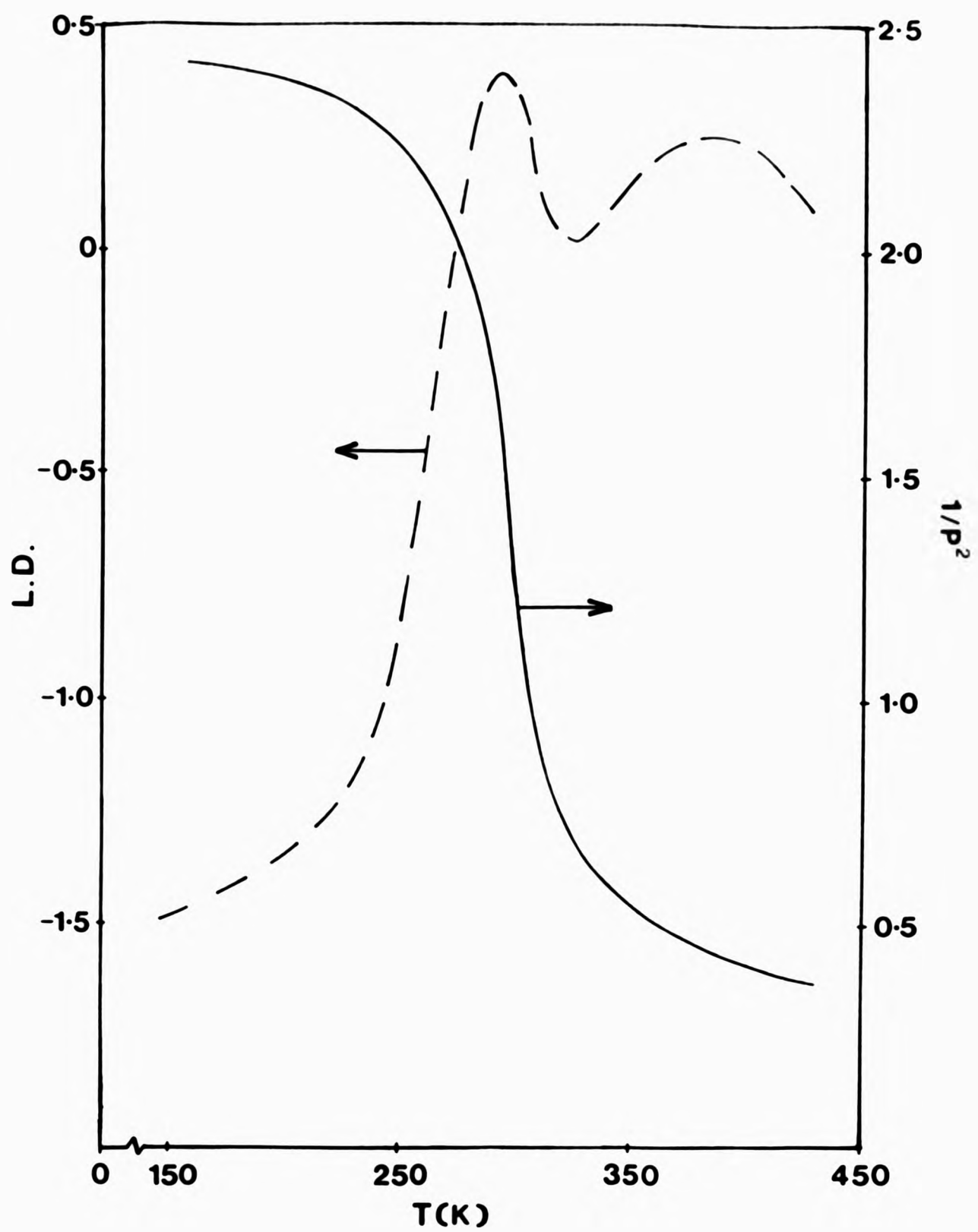


FIGURE 4.10 Plots of the logarithmic decrements (L.D.) and the relative rigidity ($1/p^2$) for MGN-IP (45.8/54.2) copolymer.

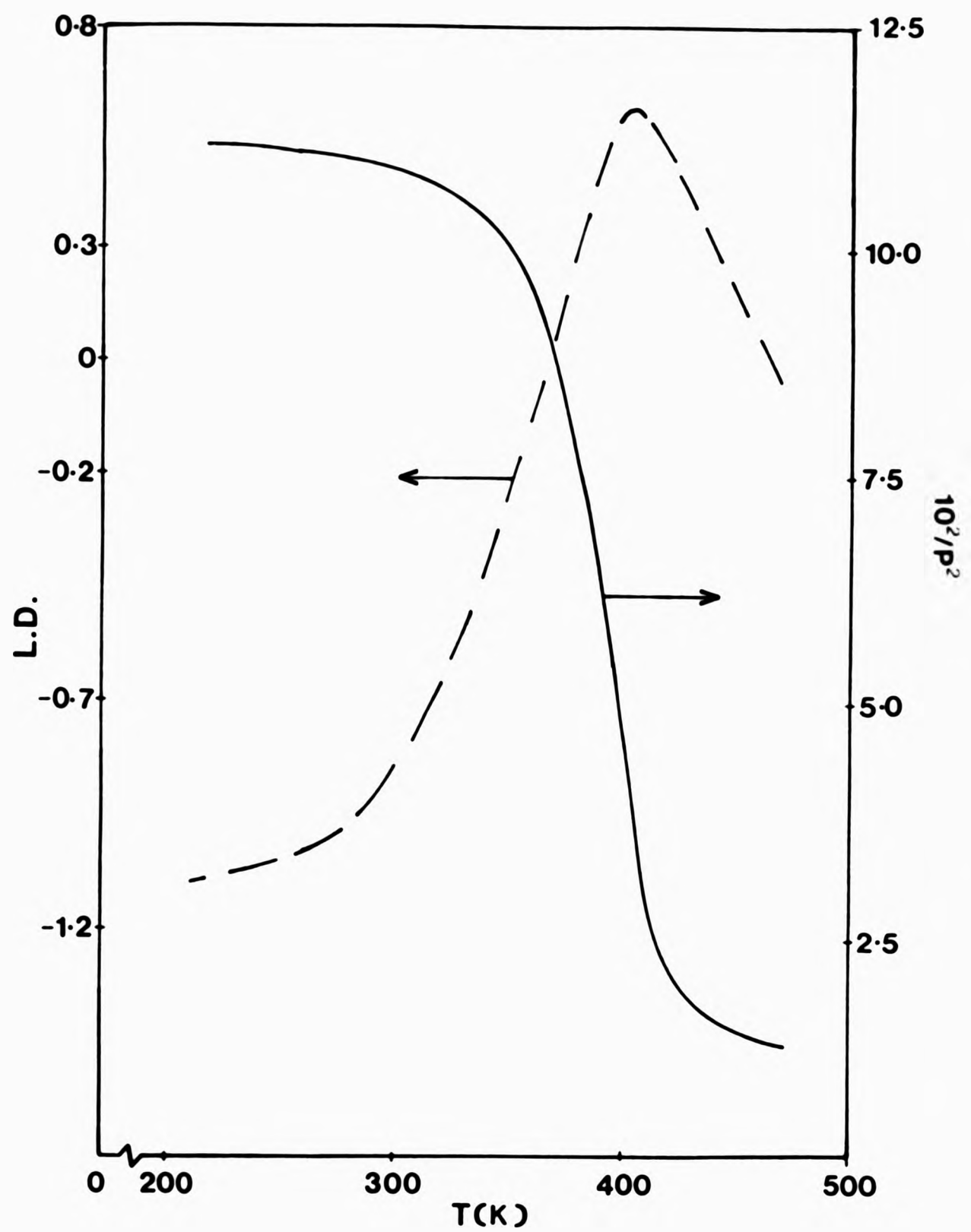


FIGURE 4.11 Plots of the logarithmic decrements (L.D.) and the relative rigidity ($1/p^2$) for MGN-MS (48.1/51.9) copolymer.

relative rigidity ($1/p^2$) as the ordinates.

The T_g of each sample is estimated from the maximum in the L.D. and/or from the corresponding points of inflection in the $1/p^2$ curve. Since the nominal frequency of the TBA instrument used is relatively low (ca. 1Hz) The observed T_g s are broadly in accord with those obtained by DSC (cf. Tables 4.4 and 4.5).

Dynamic mechanical procedures have been shown to be sensitive to the molecular mechanisms giving rise to secondary transitions.¹⁷⁸ For example, the local main chain motions which give rise to the β -transition of poly-(vinyl chloride)¹⁷⁹ and the β -transition of the poly-(methacrylates)¹⁸⁰ which arise from motions in the side group. With regards to the TBA of the two MGN copolymers (Figures 4.10 and 4.11) no transitions were observed below their respective T_g s indicating the absence of discrete localised modes in these samples. Attention is, however, drawn to the TBA loss peak at 390K in the MGN-IP copolymer thermogram. Such super- T_g events have been named by Boyer¹⁸¹ as T_{II} transitions although the exact origin of such transitions is still a matter of great controversy. The wealth of literature surrounding this debate is concerned with whether or not such TBA peaks are in fact due to a change from segmental motion to coordinated motion involving the entire polymer chain, as proposed by Boyer,¹⁸¹ or merely that such observations are an artifact caused by the glass fibre braid support.¹⁹² The present study can add little to this debate.

4.3.4 Rheovibron Viscoelastic Analysis

Polymers are viscoelastic materials, therefore when they are subjected to a periodic stress their deformation shows a phase lag with respect to the stress. This phase difference between stress and deformation affords information about the molecular processes taking place in the material. The dynamic mechanical properties of MGN/IP

(45.8/54.2) copolymer were measured using a Rheovibron dynamic viscoelastometer (see chapter 2.6.3) over the temperature range 200K-340K at a frequency of 11Hz.

The variation of $\tan \delta$ (dissipation factor) and of the complex elastic modulus E^* as a function of temperature are shown in Figure 4.12. As is typical for an amorphous polymer below its T_g , the MGN/IP copolymer has a complex modulus of ca. 10^9 Nm^{-2} . The transition region includes the T_g which is taken here as the point of inflection of the E^* curve (or by the maximum in the $\tan \delta$ plot). In this region the complex elastic modulus drops by ca. three orders of magnitude before reaching the "rubbery plateau" where the value of the modulus remains roughly constant over an extended temperature range. Under the present conditions the extent of this plateau, which precedes liquid flow (providing the material does not degrade), could not be determined.

The behaviour of E' , the tensile storage modulus, and E'' , the loss modulus, as a function of temperature are also established by the Rheovibron experiment. The results obtained for the present sample are given in Figure 4.13.

From this analysis, it is evident that the T_g of this MGN copolymer, defined as the maximum in $\tan \delta$, is 308K, 20K above the value determined for the same copolymer sample by DSC.

Such a difference arises from the effective rate of measurement in each technique and the inherent kinetic aspect of the glass transition phenomenon. (In general dynamic techniques yield a value of a T_g 10K-40K above that obtained by static procedures).

By studying the shift of the $\tan \delta$ maximum as a function of frequency, the apparent activation energy for the molecular mechanism responsible may be calculated by employing the Arrhenius relationship (20)

$$\ln v = \ln v_0 - E_A/RT \quad (20)$$

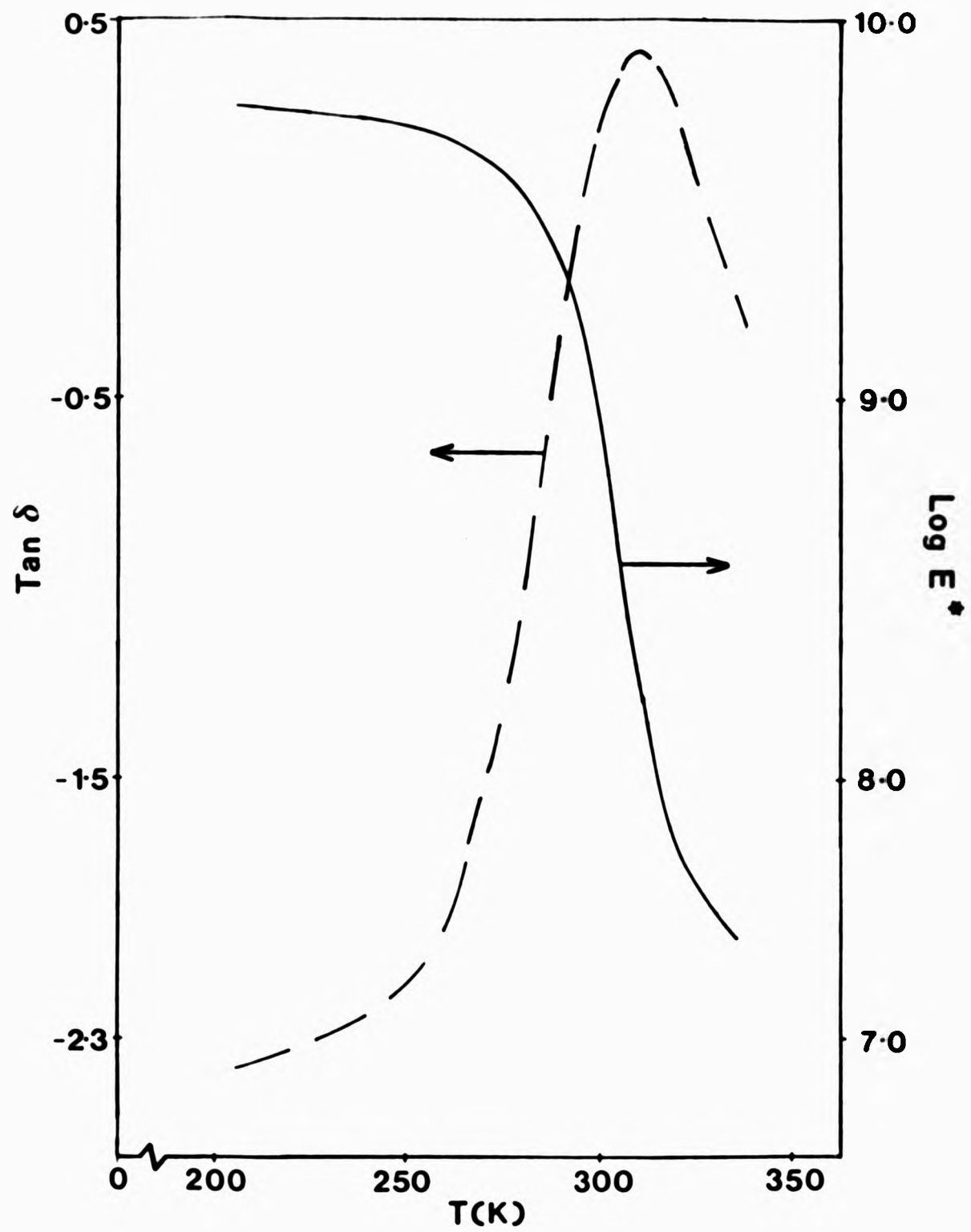


FIGURE 4.12 Plots of $\tan \delta$ and $\log E^*$ vs. temperature for MGN-IP (45.8/54.2) copolymer.

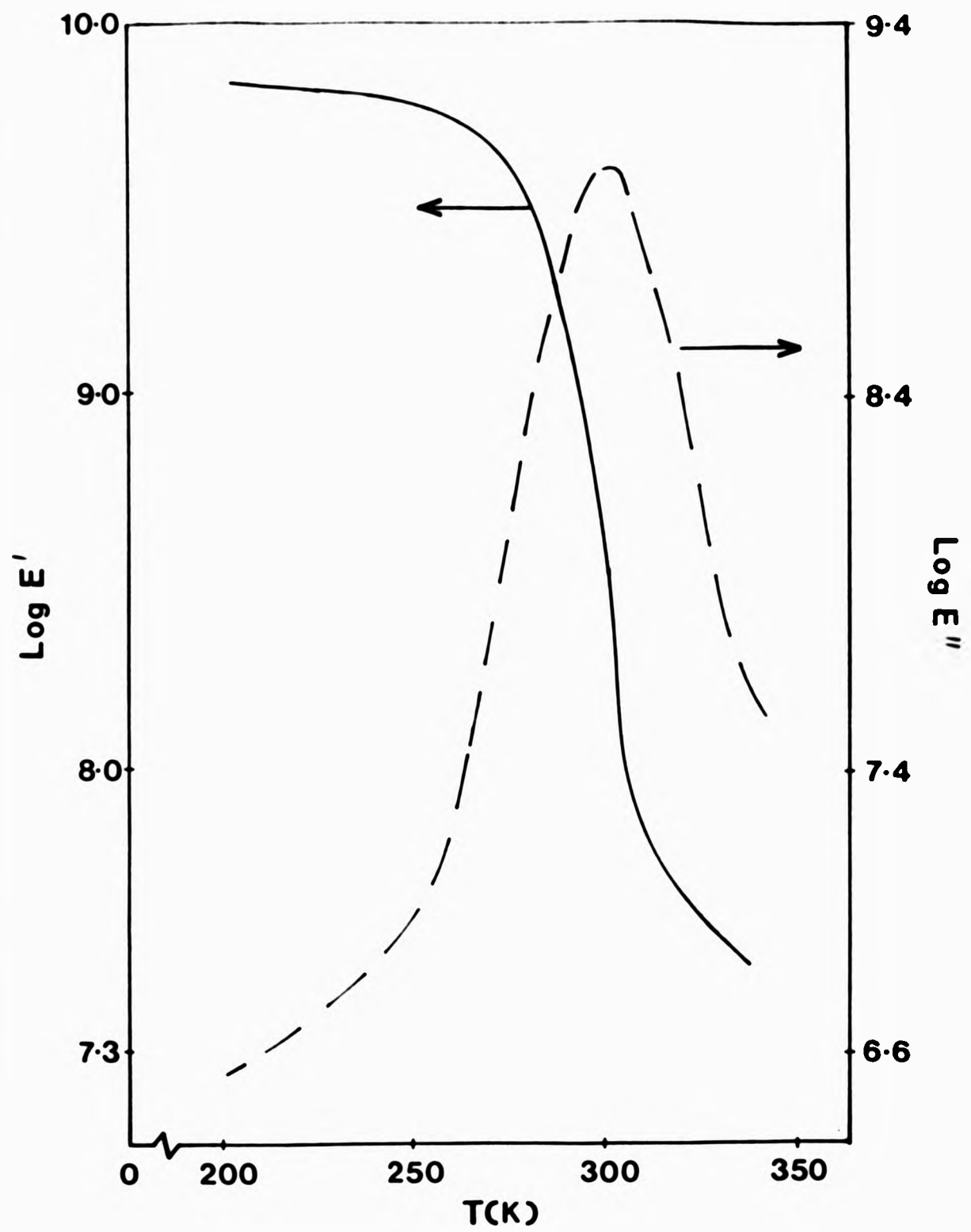


FIGURE 4.13 Plots of the dynamic modulus (E') and the loss modulus (E'') vs. temperature for the MGN-IP (45.8/54.2) copolymer.

where ν is the frequency of the measurements, E_A the apparent activation energy, R the gas constant and T_m the temperature of the $\tan \delta$ maximum obtained from a plot of $\tan \delta$ vs. temperature. Figure 4.14 shows the variation in the damping maximum for the MGN-IP copolymer as a function of temperature at the four operational frequencies of the Rheovibron viscoelastometer. The data, utilised in an Arrhenius plot, shown in Figure 4.15, yields an apparent E_a for the glass transition of the MGN-IP (45.8/54.2) copolymer of 160 kJ mol^{-1} . This value for an α -transition may be compared with that of *cis*-1,4 poly(isoprene) $E_A = 95 \text{ kJ mol}^{-1}$ ($T_g = 200\text{K}$), atactic poly(styrene), $E_A = 364 \text{ kJ mol}^{-1}$ ($T_g = 373\text{K}$), and poly(methyl methacrylate) $E_A = 436 \text{ kJ mol}^{-1}$ ($T_g = 378\text{K}$)¹⁸³ and is therefore in accord with the empirical correlation, the greater the E_A of the α -transition for a polymer, the higher the polymer's glass transition temperature is located.

4.4 SPECTROSCOPIC ANALYSIS OF MGN COPOLYMERS

The spectroscopic analysis of 2-methyleneglutaronitrile copolymers is limited to the two systems which will form the major part of this study.

4.4.1 Spectroscopic Analysis of 2-Methyleneglutaronitrile-Isoprene (MGN-IP) Copolymers (16a).

(a) Stereochemistry of the isoprene vinyl bond. Copolymerisation of isoprene may lead to a number of isomeric structures resulting from the mode of addition to the diene monomer (Figure 4.16). An examination of the infrared spectrum of an MGN-IP copolymer, prepared from an equimolar feed and analysed to contain 45.8% MGN, identified the predominant mode of radical addition to the isoprene monomer as a 1,4-addition. This assignment is made on the basis of the absorption at 850 cm^{-1} and the absence of absorptions at 890 cm^{-1} (CH bend of

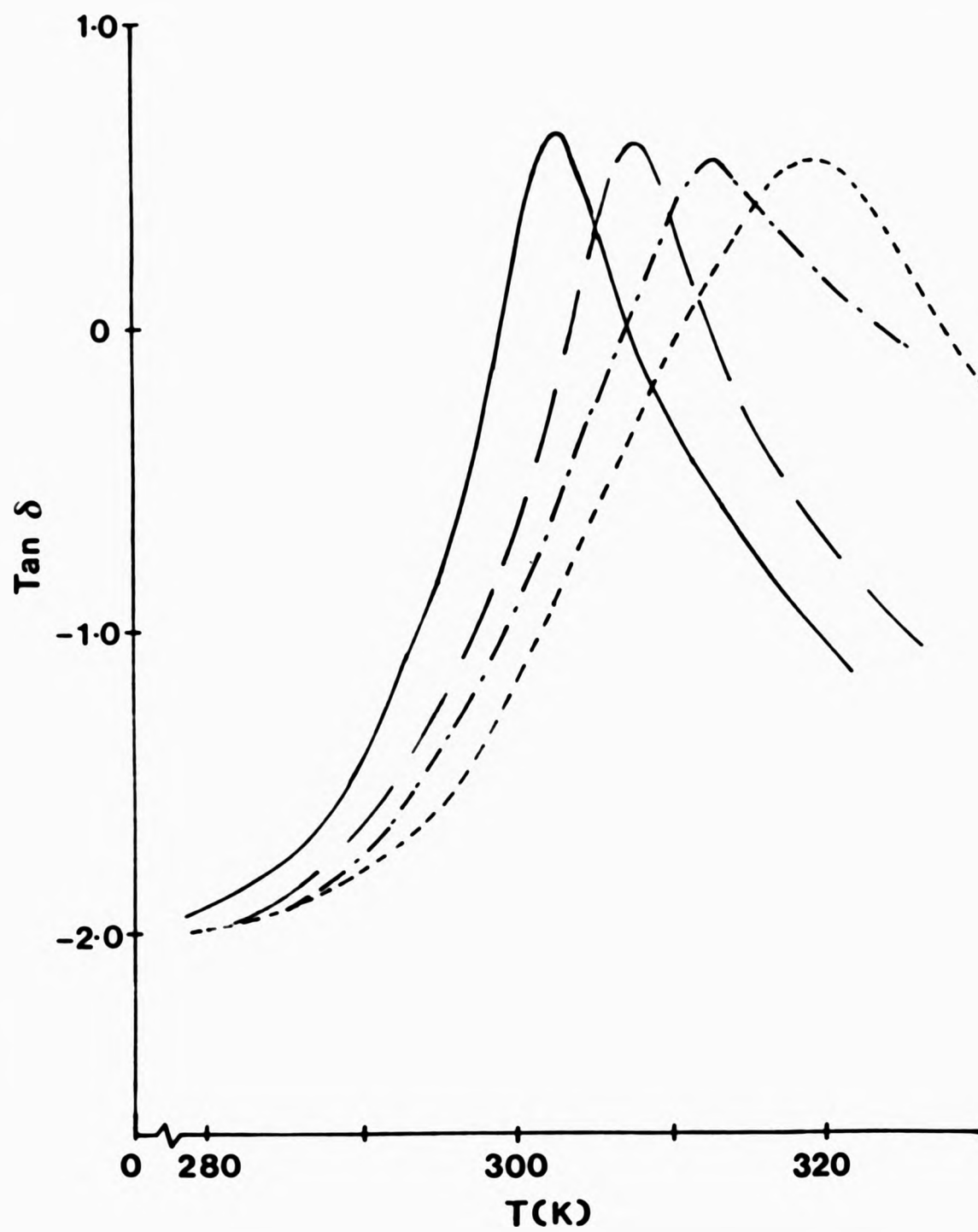


FIGURE 4.14 The loss tangent ($\tan \delta$) as a function of temperature for the MGN-IP (45.8/54.2) copolymer at four frequencies.

(—) = 3.5 Hz; (— —) = 11 Hz;
 (---) = 35 Hz; (- - -) = 110 Hz.

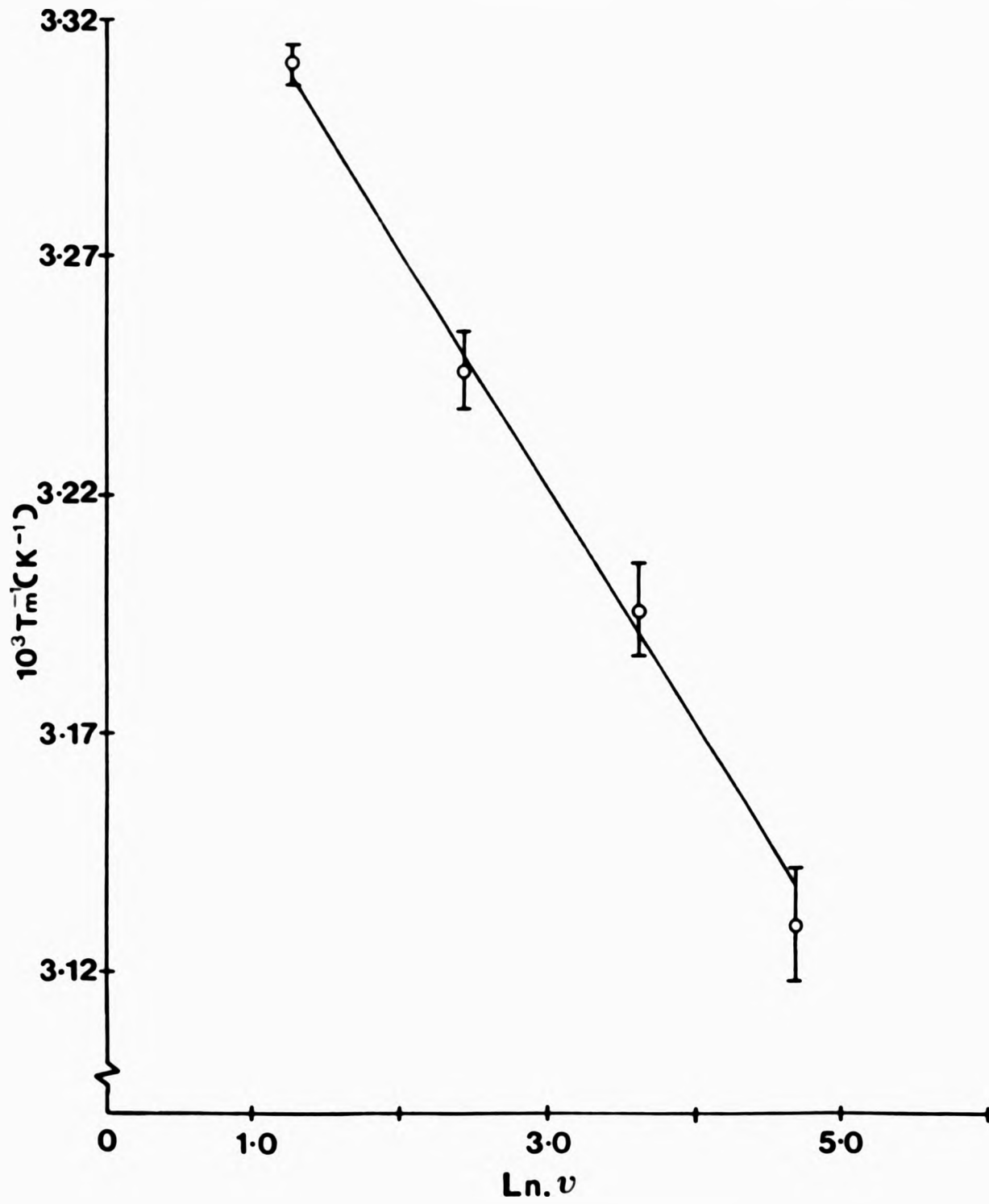


FIGURE 4.15 Arrhenius plot of the α -transition for the MGN-IP (45.8/54.2) copolymer obtained from the variation in $\tan \delta$ as a function of temperature at four operational frequencies.

<u>Operational Frequency:</u>	3.5 Hz	11 Hz	35 Hz	110 Hz
<u>Tan δ Maximum:</u>	302K	308K	313K	319K

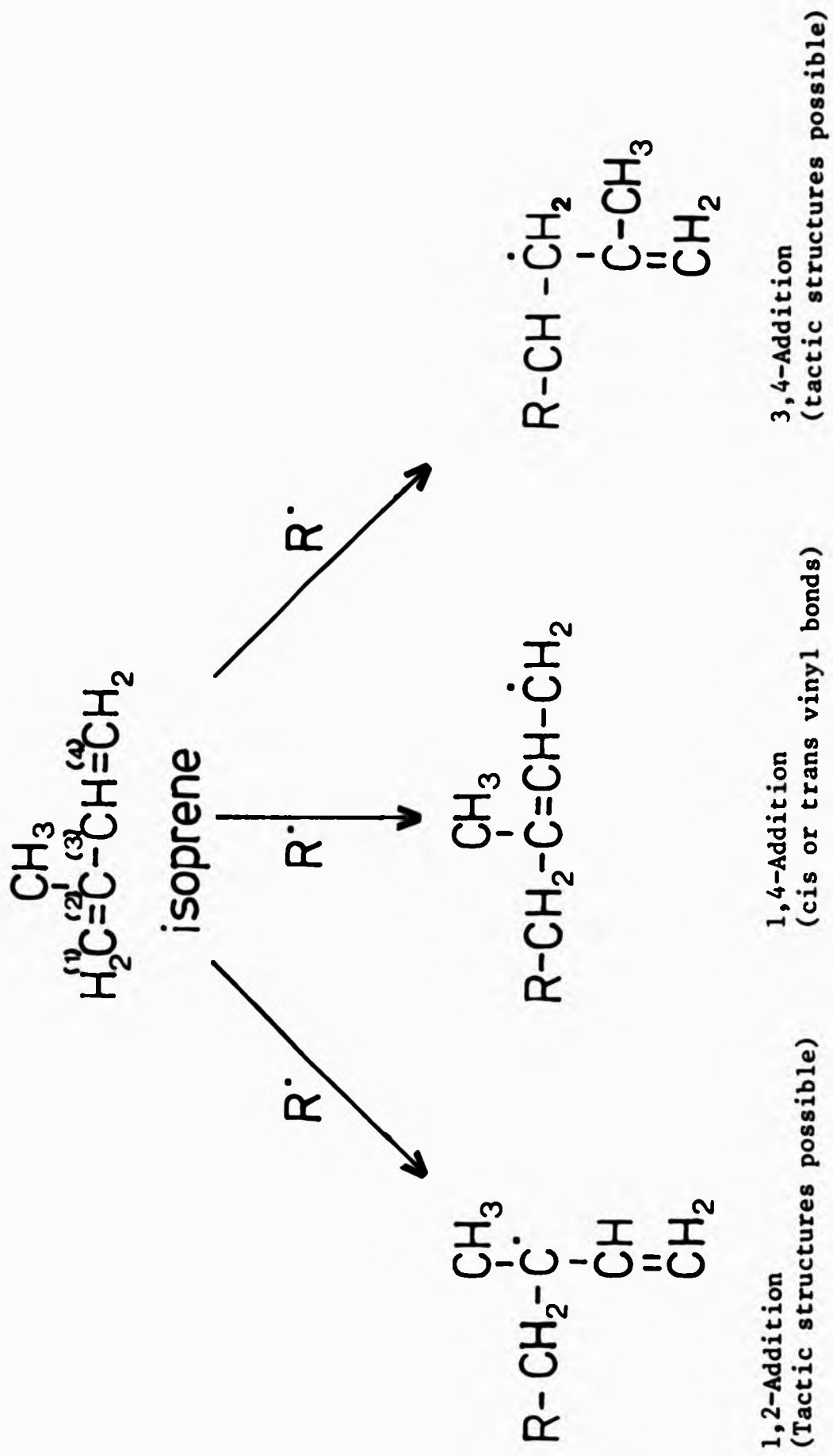


FIGURE 4.16 Possible modes of linear radical addition to isoprene monomer.

3,4-addition) and 909 cm^{-1} (CH bend of 1,2-addition). The infrared spectrum alone does not allow the stereochemistry of the vinyl bond in the copolymer to be established. The $90\text{ MHz } ^1\text{H}$ nmr spectrum is shown in Figure 4.17(a). This confirms the infrared assignment, no resonances due to 3,4- or 1,2- isoprene structures can be observed. In homopolyisoprenes the cis and trans-1,4 configurations may be differentiated by the methyl resonance, the latter being about 0.1ppm more shielded.¹⁸⁴ In the present copolymer, methyl protons appear as a singlet at 1.85δ indicative of one prominent stereochemistry, but assignment is difficult. The stereochemistry was established by performing nOe (nuclear Overhauser enhancement) experiments on standard samples of cis-1,4-polyisoprene, trans-1,4-polyisoprene and the MGN-IP copolymer. Very briefly, nOe effects (and the rates at which they grow and decay) are measures of the strength of "through space" dipole-dipole interaction between the spins involved.¹⁸⁵ For example, if two protons (Ha and Hb), or sets of protons, are close enough to allow through-space interaction of their fluctuating magnetic vectors then each can contribute to the others spin lattice relaxation process. Provided Hb makes a significant contribution to the spin lattice relaxation of Ha, then double irradiation of Hb causes an increase in the intensity of the Ha signal. In this study, the procedure involved double irradiation of the methyl protons of the isoprene moiety in the three polymers and in each case the enhancement, or lack of enhancement, in the olefinic proton signal was monitored. The results are shown in Figure 4.18. An 8% nOe was observed for the cis-1,4-polyisoprene standard with no detectable nOe found for the trans-isomer. Double irradiation of the methyl protons (1.85δ) of the MGN-IP copolymer also resulted in no observable nOe. The technique applied to the weak resonances at 1.92δ and 1.82δ (possible cis methyl group) also proved negative. These experiments lead to the

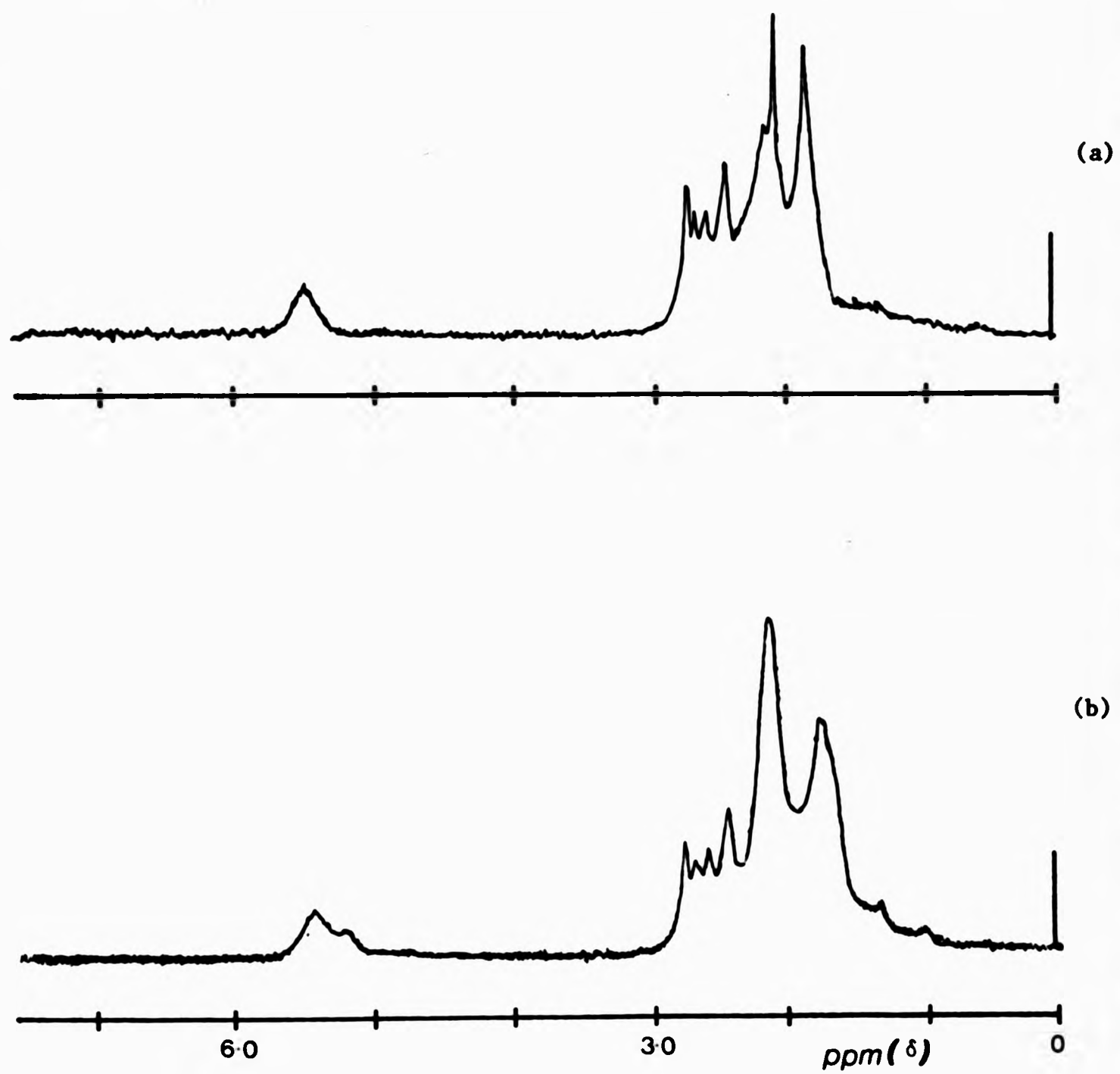


FIGURE 4.17 ¹H 90 MHz nmr spectra of MGN-IP copolymers.

(a) An MGN-IP (45.8/54.2) copolymer.

(b) An MGN-IP (33.6/66.4) copolymer.

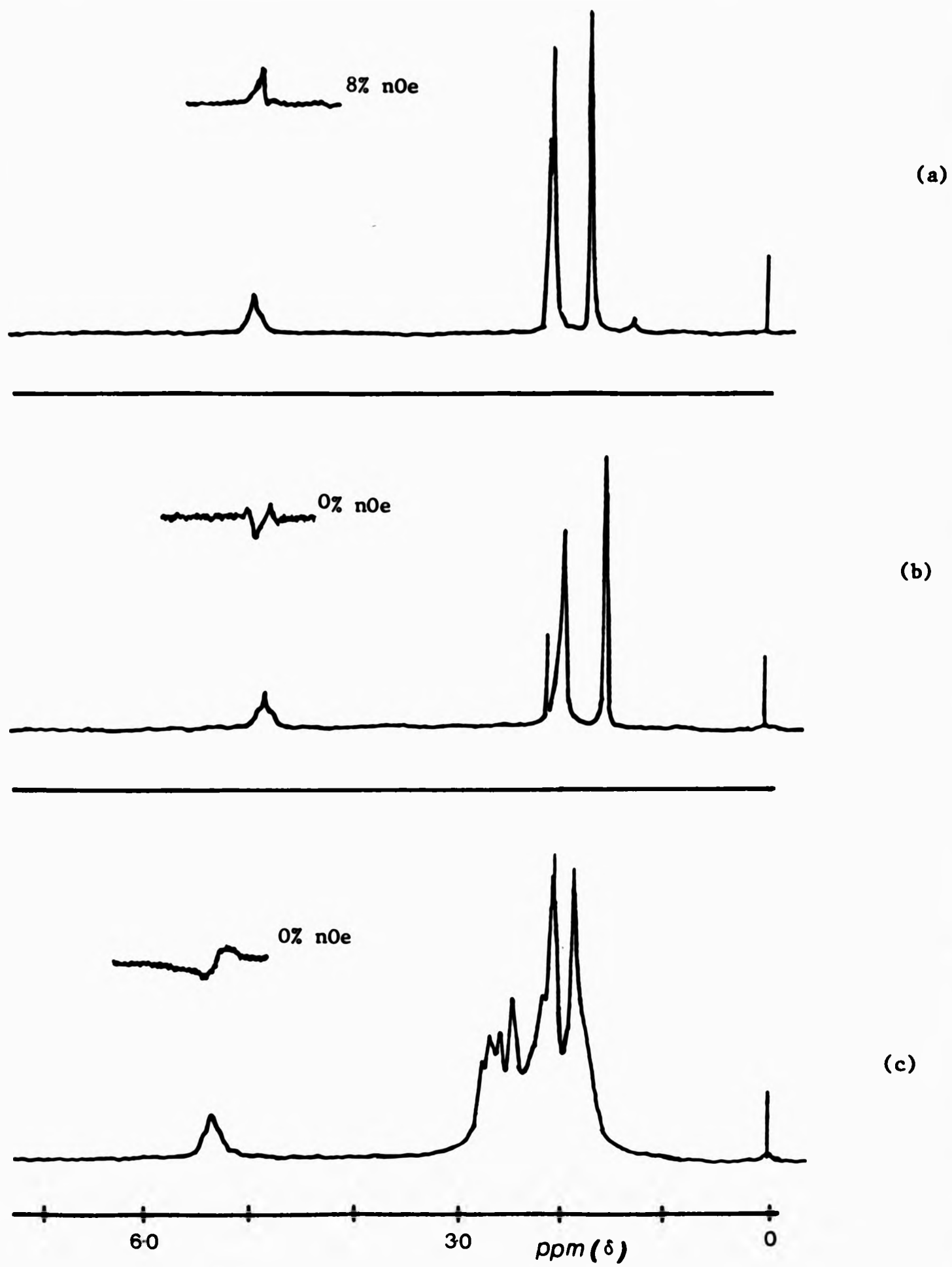
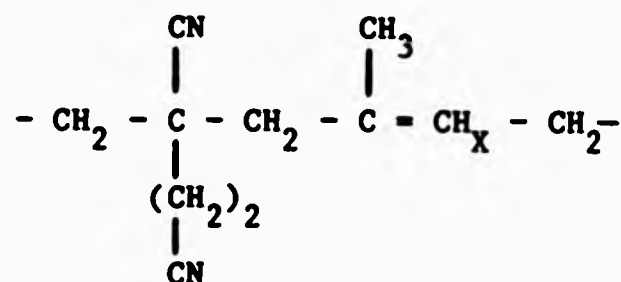


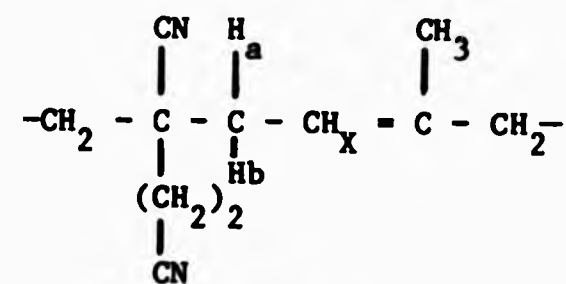
FIGURE 4.18 nOe ^1H nmr spectra.
 (a) cis-1,4-polyisoprene.
 (b) trans-1,4-polyisoprene.
 (c) MGN-IP (45.8/54.2) copolymer.

conclusion that in the MGN-IP copolymer the isoprene moiety is predominantly in the trans-stereochemistry.

(b) The direction of addition of the comonomers. The 90 MHz ^1H nmr spectrum shown in Figure 4.17 does not allow one to discern between the two structures XXVII and XXVIII, both of which are in principle possible in this copolymerisation.



(XXVII)



(XXVIII)

(The actual structure formed being determined by the mode of addition of the MGN propagating radical to the isoprene monomer). Addition at the 4-position of isoprene results in structure XXVIII, whereas addition at the 1-position gives structure XXVII. A 360 MHz spectrum is shown in Figure 4.19 which permits such an assignment and is also indicative of a predominantly alternating copolymer.

Of particular interest in this spectrum are the resonances at 1.85 δ and 5.45 δ . The former signal is a sharp singlet and is assigned to the methyl protons of isoprene in an MGN-IP-MGN triad sequence. The weak resonances at 1.92 δ and 1.82 δ are assigned to other (irregular) sequences. The resonance at 5.45 δ is due to the olefinic proton of isoprene resulting from 1,4-radical addition. This signal is observed as a triplet, indicating that the proton H_x is coupled with two equivalent protons and is indicative of structure XXVII being the likely mode of addition in the copolymer. The other assignments have been tentatively made.

(c) ^{13}C nmr analysis. The assignment of an alternating MGN-IP copolymer of structure XXVII is substantiated by the ^{13}C nmr spectrum

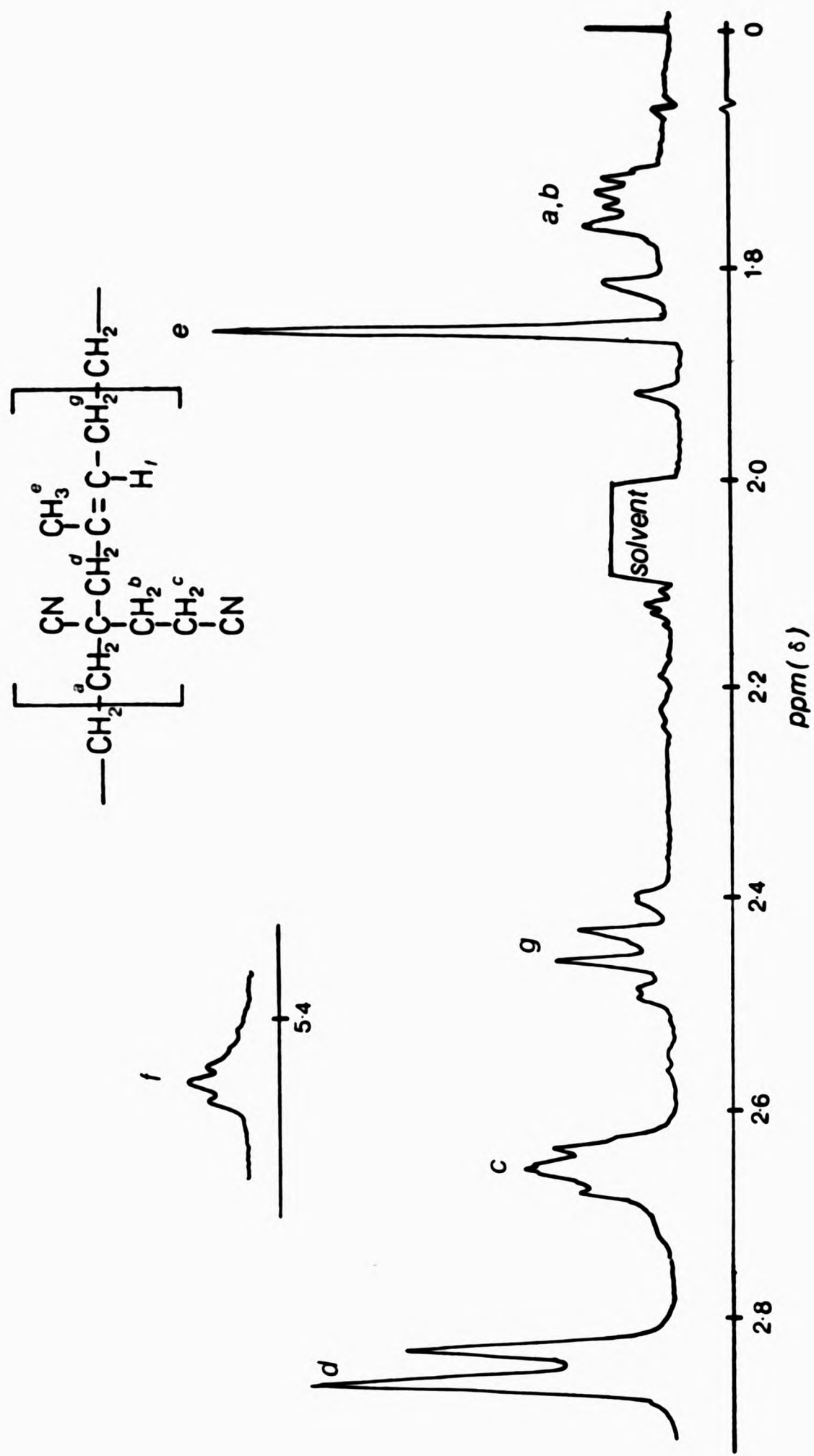


FIGURE 4.19 360 MHz ^1H nmr spectrum of MGN-IP (45.8/54.2) copolymer.

shown in Figure 4.20(a).

This spectrum consists essentially of 11 sharp lines corresponding to the eleven carbon atoms of the uniquely situated MGN and IP units within the alternating sequences. Characteristic 1,4-vinylic resonances are evident, with only minor signals due to 1,2- and 3,4-placements (136ppm and 140ppm). The predominantly trans stereochemistry of the vinyl moiety in the copolymer is in agreement with the chemical shift observed for a methyl carbon in such a configuration, cf. poly(acrylonitrile-alt-trans-1,4-polyisoprene) exhibits this resonance at 16.00ppm. (The methyl signal in cis-1,4-polyisoprene appears at 23.4ppm and at 16.1 in trans-1,4-polyisoprene).¹⁸⁶

The spectra reported here are representative of the majority of MGN-IP copolymers. However, copolymers prepared from extreme (~90%) IP feeds do exhibit differences in their ^1H nmr (Figure 4.17(b)) and ^{13}C nmr (Figure 4.20(b)) spectra, indicating deviations from an alternating structure and the presence of isoprene moieties other than the trans-1,4-structure.

4.4.2 Spectroscopic Analysis of 2-Methyleneglutaronitrile- α -Methyl Styrene (MGN-MS) Copolymers

The 90MHz proton nmr spectrum of the equimolar copolymer, shown in Figure 4.21, does not allow the extent of alternation in the sample to be determined. However, the ^{13}C nmr spectrum is rather more informative. This spectrum has been assigned and is shown in Figure 4.22(a) together with the chemical shifts reported in the literature for poly- α -methyl styrene.¹⁸⁷ The first observation is that the chemical shifts for the equimolar copolymer carbon atoms are different to those observed for the MS homopolymer, indicating no significant amounts of MS homopolymer sequences.

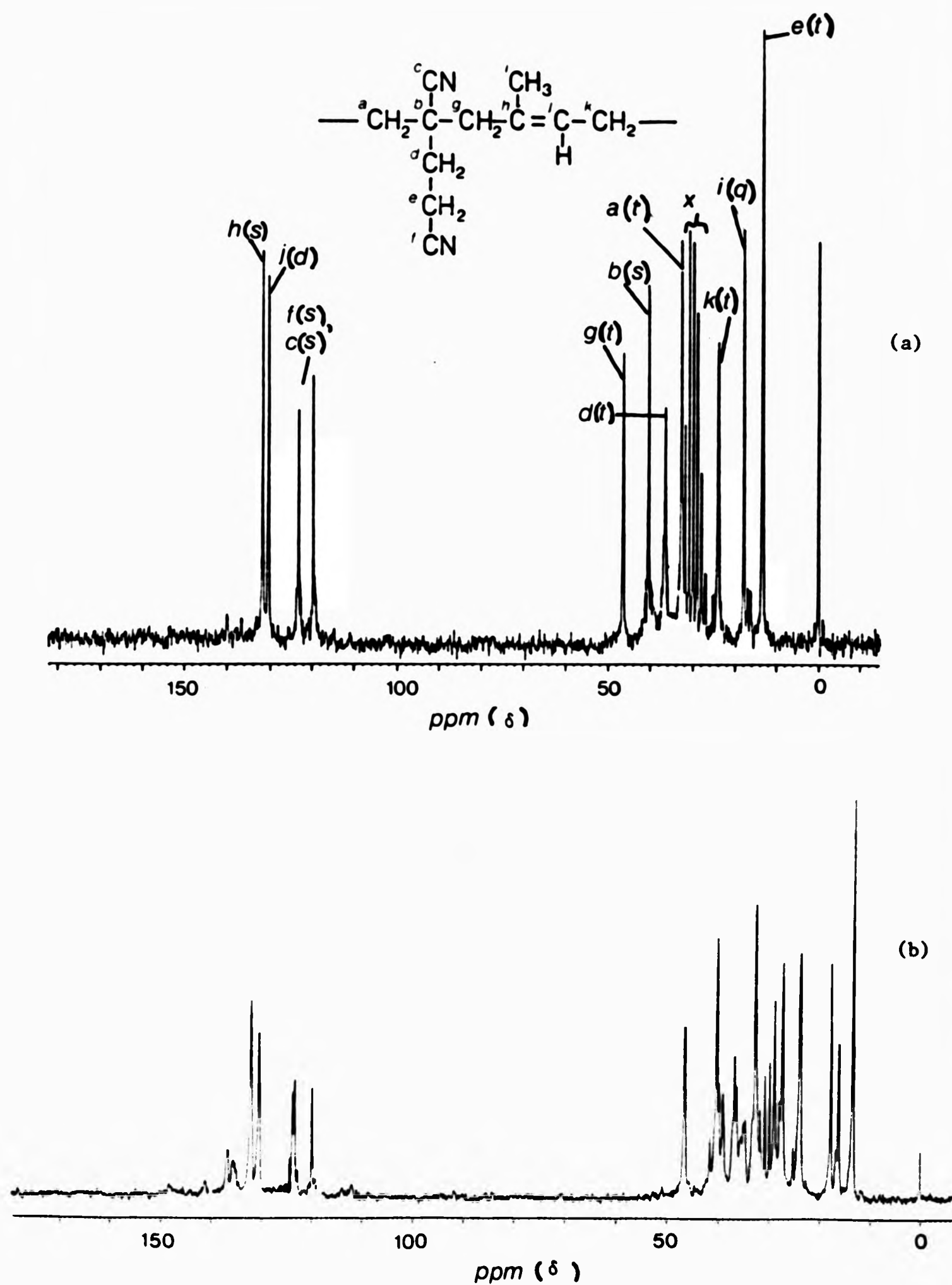


FIGURE 4.20 a) ^{13}C nmr proton decoupled spectrum of MGN-IP (45.8/54.2) copolymer.
 b) ^{13}C nmr proton decoupled spectrum of MGN-IP (33.6/66.4) copolymer.
 (Off resonance spectrum has signal multiplicity; (s) = singlet; (d) = doublet; (t) = triplet; (q) = quartet.)

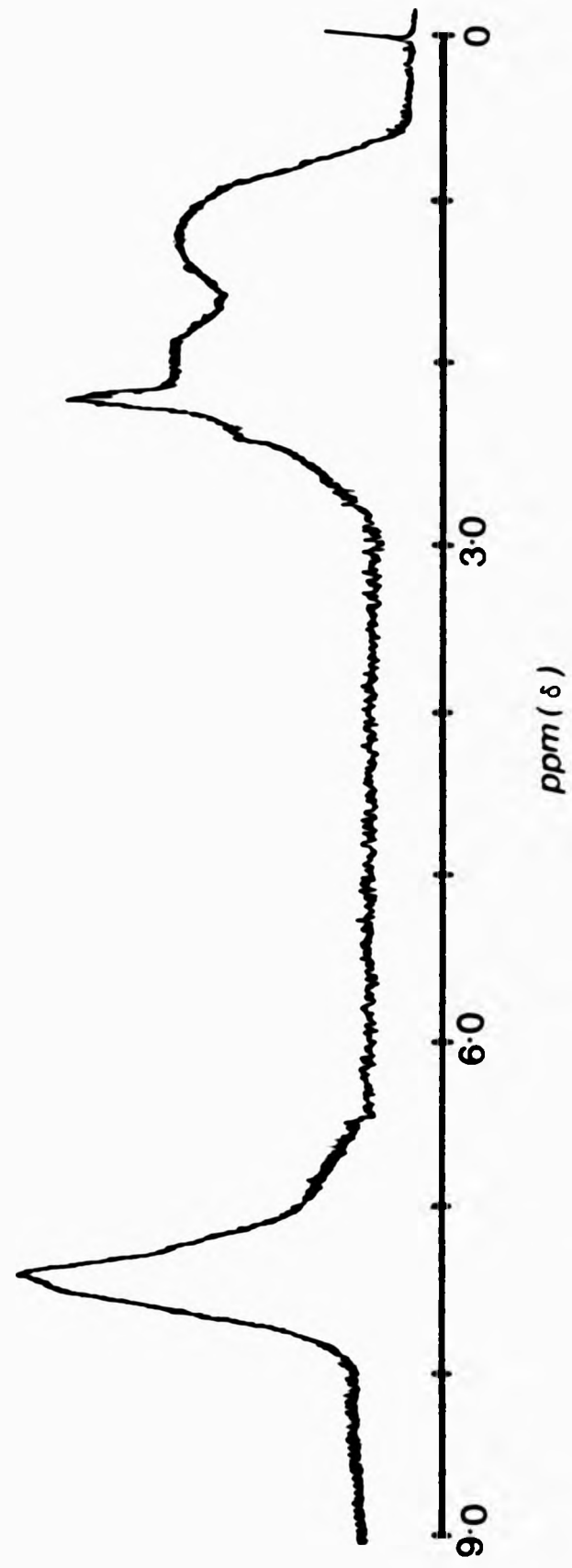


FIGURE 4.21 The ¹H 90 MHz nmr of MGN-MS (48.1-51.9) copolymer.

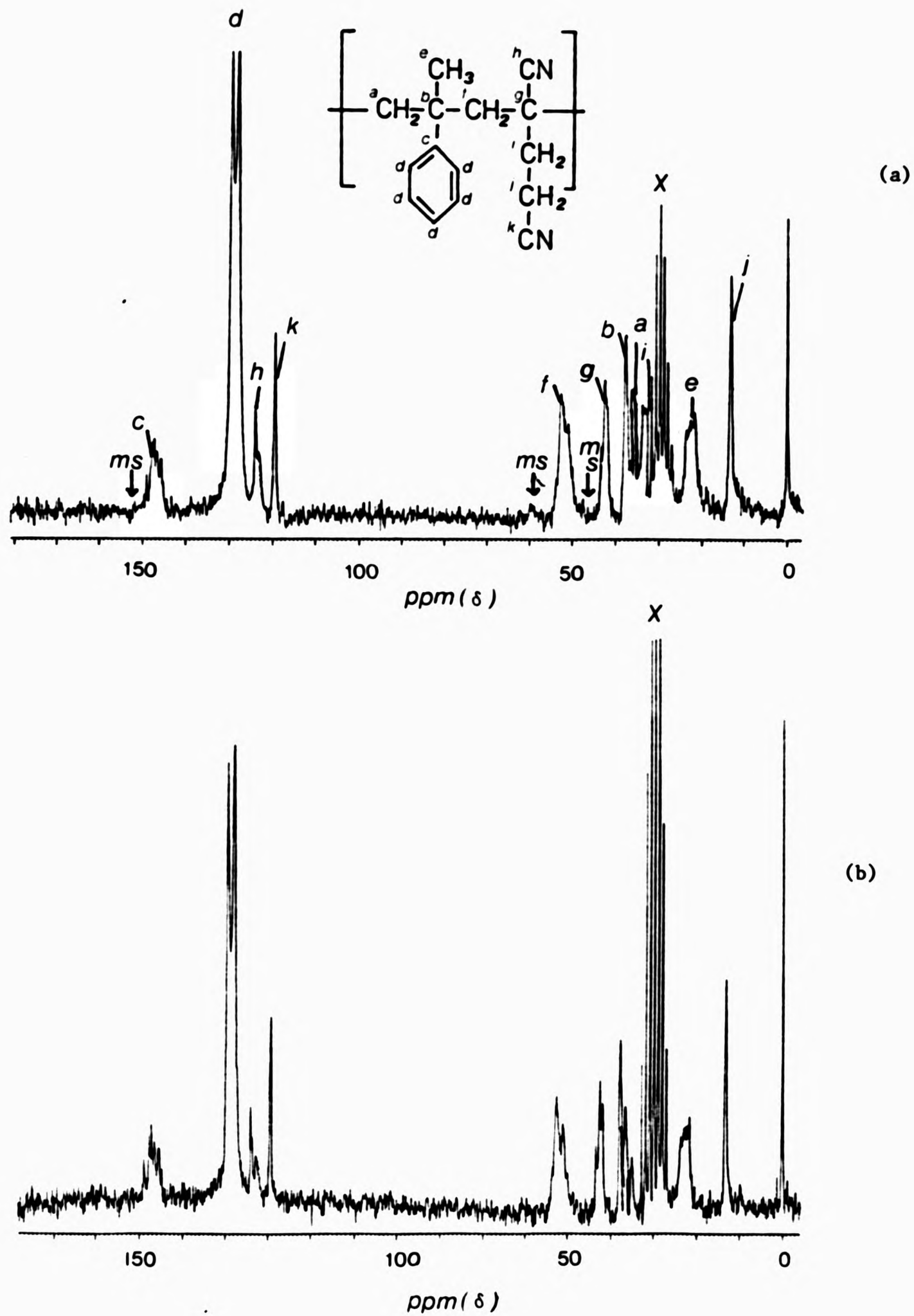


FIGURE 4.22 ^{13}C proton decoupled nmr spectra of
 (a) MGN-MS (48.1/51.9) copolymer.
 (b) MGN-MS (49.0/51.0) copolymer prepared in the presence of ZnCl_2 .
 (MS = poly-(α -methyl styrene) resonances; X = solvent signals).

Secondly, the multiplicity of the resonances of this copolymer most likely reflect differences in steric placement, a consequence of the MGN and MS "asymmetric" sites.

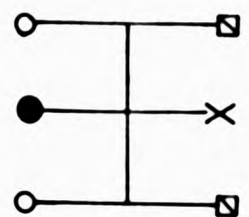
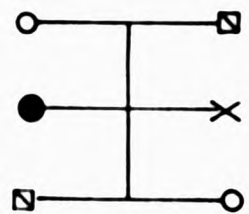
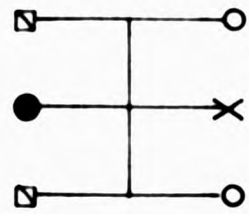
Nearest neighbour interactions give rise to three potentially different chemical shifts as illustrated in Figure 4.23. If second nearest neighbours have a measurable effect on the chemical shifts, then triads become pentads with ten potentially different shifts. Such phenomena can therefore lead to very complex spectra.

The ^{13}C spectrum of an MGN-MS equimolar copolymer, prepared in the presence of ZnCl_2 (see 5.4.3) is shown in Figure 4.22(b) for comparison with the above system. Copolymerisations such as this, performed in the presence of a Lewis Acid, are well known to increase the degree of alternation in the copolymer.¹⁸⁸ There is no reason to doubt this hypothesis for the MGN/MS/ ZnCl_2 ternary system. A comparison of spectra 4.22(a) and 4.22(b) reveals little if any difference between them, which leads one to conclude that the conventional radical copolymerisation of MGN and MS also leads to a predominantly alternating copolymer.

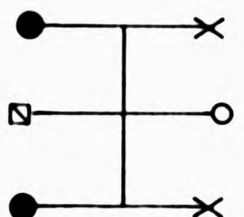
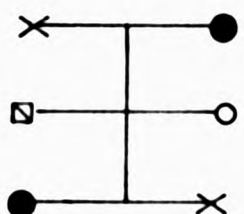
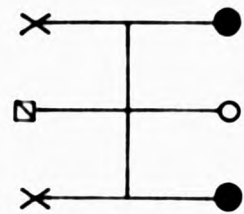
The spectroscopic data presented here on the copolymers of systems 16 and 19 are therefore not at variance with their copolymer composition curves which identified the tendency of MGN to copolymerise in a predominantly alternating fashion with isoprene and α -methyl styrene.

4.5 MECHANISTIC CONSIDERATIONS

The probability of forming a regular alternating copolymer via a random process is very low. However, in the early investigations of copolymerisation it was clearly recognised that a relationship existed between alternating copolymerisation and the resonance and polar



TRIADS CENTRED ON α MS



TRIADS CENTRED ON MGN

● = CH_3 ; X = C_6H_5 ; O = CN; ◻ = $(\text{CH}_2)_2\text{CN}$.

FIGURE 4.23 Triads for the MGN-MS alternating copolymer.

properties of the olefin monomers involved.^{19,20} It was found, for monomers of similar Q values, that a strongly electron donating monomer tends to undergo alternating copolymerisation with a strongly electron accepting monomer.²⁴ This has led over the years to the advancement of two hypotheses in an attempt to explain the alternating tendency in copolymerisation.

(a) The "free monomer" postulate,²⁴ proposes that the monomer molecules add predominantly to "unlike" macroradicals because the inherent polarity differences would lower the activation energy of the cross-propagation reactions (10 and 11) by stabilisation of the transition state, a stabilisation not open to the homopropagation reactions (9 and 12). Such a hypothesis is accommodated by the classical Mayo-Lewis copolymerisation model.

(b) The alternative hypothesis is that the electron donating monomer and the electron accepting monomer form a donor-acceptor charge-transfer complex, which, due to an inherently higher reactivity compared to either monomer, adds preferentially to a propagating chain as a single unit.³⁸ Such a mechanism is, of course, not consistent with the classical scheme of copolymerisation and has led to the development of the "complex participation" model of alternating copolymerisation.

Such postulates represent extreme cases. It is possible that each mechanism operates exclusively in specific systems, however in the majority of cases where comonomer complexes are known to exist, alternating copolymerisation probably proceeds via both mechanisms.

In this study the strong tendency of MGN to copolymerise in an alternating fashion with isoprene and α -methyl styrene is observed. The fact that 2-methyleneglutaronitrile may be classified as an electron accepting monomer, and both isoprene and α -methyl styrene as strongly electron donating systems, raises the possibility of complex

participation in these copolymerisations.

The question of a donor-acceptor comonomer complex existing between the monomer pairs is addressed in the following chapter and the possible involvement of such complexes in the alternating copolymerisations 16a and 19 is assessed in Chapter 6.

participated in the
The
The
involved
and 19

CHAPTER FIVE

5.1 ELECTRON DONOR-ACCEPTOR COMPLEX PARTICIPATION

The recent resurgence of interest in the study of free radical copolymerisations, which lead to predominantly alternating copolymers, has been the result of the hypothesis that such a tendency arises from the participation of a 1:1 monomer (1) - monomer (2) donor-acceptor complex in the propagation reactions.

There are a number of features of alternating copolymerisations which have been considered as evidence for such complex participation.

- (a) A comonomer complex is formed under polymerisation conditions.
- (b) There is a tendency for the copolymerisation system to result in alternating copolymers over a wide monomer feed composition.
- (c) The initial rate of polymerisation is at a maximum around the equimolar monomer feed composition.
- (d) Apparently "spontaneous" initiation of copolymerisation can often be observed.
- (e) A high degree of stereoregularity in the alternating copolymers formed is obtained without recourse to a template species.
- (f) There are deviations from the copolymer compositions predicted by the Mayo-Lewis terminal model of copolymerisation in systems where a comonomer complex is known to exist.

In order to study the possible participation of a donor-acceptor complex in the copolymerisation of MGN with isoprene and α -methyl styrene, it is of course necessary to establish that such species exist.

5.2 ELECTRON DONOR-ACCEPTOR COMPLEXES

The term electron donor-acceptor (EDA) complex is used to describe a wide variety of intermolecular complexes, ranging from those involving weak dispersion forces to those interactions strong enough to result in the isolation of the crystalline complex. Such interactions may be

represented by equation 21 whereby the magnitude of the formation quotient may be taken as a measure of the strength of the interaction.



The criterion for the existence of an EDA complex has been taken to be the appearance of a new (or shifted) absorption band in the ultraviolet/visible spectra of donor-acceptor mixtures, which can be analysed mathematically to give a single non zero value of the equilibrium constant K_Q .¹¹⁷ Alternatively, a change in the chemical shift of the 1H nmr resonances of the donor and/or acceptor molecules can be analysed by similar procedures to yield a value for K_Q and therefore used to provide evidence for complex formation.¹¹⁴

The nature of the solvent plays an important part in the determination of K_Q . Accurate complexation studies require the use of an "inert solvent", i.e. a solvent which will not complex with the donor or acceptor molecule. The preferred solvents for EDA complexation study are therefore materials such as n-hexane and CCl_4 . The immiscibility of MGN /n-hexane, and MGN /n-hexane/donor mixtures, precluded UV analysis using this solvent. Miscibility problems are also encountered, although to a lesser extent, with CCl_4 , but the major problem here is that the UV cut-off point of the solvent (absorption = 1.0 at 265nm) does not permit analysis of the monomer absorbances which themselves lie at shorter wavelengths. This effectively renders the UV technique redundant. Fortunately the present systems proved amenable to analysis by the equivalent nmr method.

5.3 NMR ANALYSIS OF EDA COMPLEXATION

The ideal system for a 1H nmr study of EDA complexes should possess the following properties.

- a) Both the donor and acceptor molecules should contain proton(s) which give rise to a single sharp signal.
- b) It should be possible for both the donor and acceptor concentrations to be made large with respect to the other components.
- c) The ^1H nmr resonances of the donor molecule or solvent should not overlap the signals of the acceptor molecule (vice versa if donor shifts are being studied).

If these conditions hold it should be possible to obtain, in two separate experiments, two estimates of K_Q which allow a check on the consistency of the method. However, such conditions are rarely, if ever, met. Indeed, in the present systems the limited miscibility of MGN and CCl_4 meant that only the chemical shifts of the acceptor could be studied. Fortunately, the MGN ^1H nmr spectrum is ideally disposed to nmr EDA complexation analysis, the spectrum exhibits two sharp and well defined singlets at 540Hz and 530 Hz corresponding to the vinylic proton resonances (90 MHz instrument). The chemical shift of either of these signals, relative to tetramethylsilane (TMS) may then be monitored as a function of the concentration of donor molecules. Tetramethylsilane was employed as reference standard in both internal and external modes (sealed in a separate microtube placed in the nmr sample tube), which within the experimental error for the system, were found to yield the same results.

5.3.1 Theoretical

Consider the equilibrium



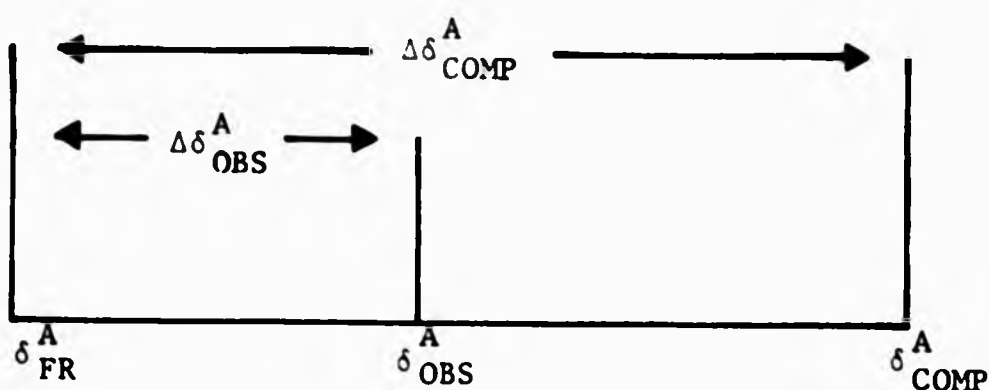
where A and D represent the acceptor and donor molecules respectively and

where AD represents the complex. The equilibrium quotient K_Q is then given by

$$K_Q = \frac{[AD]}{[A][D]} = \frac{[AD]}{([A]_0 - [AD])([D]_0 - [AD])} \quad (23)$$

where $[A]_0$ and $[D]_0$ are the initial concentrations of acceptor and donor molecules.

In weak EDA complexes the molecules are undergoing rapid exchange between the complexed and uncomplexed states.¹⁸⁹ Hence the chemical shifts of the A protons are each observed as a single peak, corresponding to the weighted average of the shift due to the free molecules of A and that due to the complexed molecules of A. The relationship is shown schematically below and given by equation 24.



$$\delta_{OBS}^A = \delta_{FR}^A \frac{[A]}{[A] + [AD]} + \delta_{COM}^A \frac{[AD]}{[A] + [AD]} \quad (24)$$

where δ_{FR}^A is the shift of the acceptor protons in the free or uncomplexed form, δ_{COM}^A is the shift of acceptor protons in the pure complex, and δ_{OBS}^A is the observed shift of acceptor protons in the complexing medium.

Defining

$$\Delta\delta_{\text{OBS}}^{\text{A}} = \delta_{\text{FR}}^{\text{A}} - \delta_{\text{OBS}}^{\text{A}} \quad (25)$$

and

$$\Delta\delta_{\text{COM}}^{\text{A}} = \delta_{\text{FR}}^{\text{A}} - \delta_{\text{COM}}^{\text{A}} \quad (26)$$

equation 23 becomes

$$\frac{1}{[\text{D}]_0} = \Delta\delta_{\text{COM}}^{\text{A}} K_{\text{Q}} \frac{1}{\Delta\delta_{\text{OBS}}^{\text{A}}} - K_{\text{Q}} \left(1 + \frac{[\text{A}]_0}{[\text{D}]_0} \left(1 - \frac{\Delta\delta_{\text{OBS}}^{\text{A}}}{\Delta\delta_{\text{COM}}^{\text{A}}} \right) \right) \quad (27)$$

which on writing in reciprocal form, gives

$$\frac{1}{K_{\text{Q}}} = [\text{D}]_0 \left(\frac{\Delta\delta_{\text{COM}}^{\text{A}}}{\Delta\delta_{\text{OBS}}^{\text{A}}} - 1 \right) - [\text{A}]_0 \left(1 - \frac{\Delta\delta_{\text{OBS}}^{\text{A}}}{\Delta\delta_{\text{COM}}^{\text{A}}} \right) \quad (28)$$

Equation 28 predicts that a plot of $1/K_{\text{Q}}$ vs $\Delta\delta_{\text{COM}}^{\text{A}}$ for a given pair of $[\text{A}]_0$ and $[\text{D}]_0$ gives a curve. For every pair of $[\text{A}]_0$ and $[\text{D}]_0$ the corresponding curve is obtained individually and K_{Q} and $\Delta\delta_{\text{COM}}^{\text{A}}$ can be determined from their cross points.

On the other hand, when one component is in a large excess the experimental data can be utilised in a linear plot. Therefore when $[\text{A}]_0 \ll [\text{D}]_0$ equations 23 and 24 may be recast as

$$\frac{1}{[\text{D}]_0} = \Delta\delta_{\text{COM}}^{\text{A}} K_{\text{Q}} \frac{1}{\Delta\delta_{\text{OBS}}^{\text{A}}} - K_{\text{Q}} \quad (29)$$

Equation 29 is analogous to the Benesi-Hildebrand equation¹⁹⁰ employed in the UV analysis of EDA complexation except that in this instance the concentration of the acceptor molecule does not appear, and $\Delta\delta_{\text{OBS}}^{\text{A}}$ and $\Delta\delta_{\text{COM}}^{\text{A}}$ are used instead of the absorbance and the molar extinction coefficients respectively. Thus a plot of $1/[\text{D}]_0$ vs

$1/\Delta\delta_{\text{OBS}}^{\text{A}}$ should give a straight line of gradient $\Delta\delta_{\text{COM}}^{\text{A}} K_{\text{Q}}$ and intercept K_{Q} .

Modification of equation 29 gives the nmr equivalent of the Scatchard relation,¹⁹¹ equation 30.

$$\frac{\Delta\delta_{\text{OBS}}^{\text{A}}}{[\text{D}]_0} = -\Delta\delta_{\text{OBS}}^{\text{A}} K_{\text{Q}} + \Delta\delta_{\text{COM}}^{\text{A}} K_{\text{Q}} \quad (30)$$

5.3.2 Complex Stoichiometry

Prior to the determination of the formation quotients for the present EDA systems, it is necessary to establish the stoichiometry of any molecular complexes formed (cf. the Benesi-Hildebrand equation and its modifications assume the formation of a 1:1 molecular complex).

Although making a number of simplifying assumptions, (eg. multiple equilibria are neglected) the method of continuous variations, or Jobs method,¹¹⁵ enables the composition of molecular complexes to be determined from an analysis of their mixtures. This method is normally associated with ultra-violet analysis, however, Sahai et al.¹¹⁶ have applied the Job method to ^1H nmr analysis. The procedure reported by Sahai et al.¹¹⁶ is employed in the present study.

Equimolar solutions of donor and acceptor are mixed in varying proportions to constant volume and the chemical shift of either of the MGN vinyl protons is monitored. The experimental results for the two EDA systems are presented in Table 5.1.

Sahai et al.¹¹⁶ have shown that for a 1:n complex if the concentration of EDA complex is a maximum, $\Delta\delta_{\text{OBS}}^{\text{MGN}} \cdot [\text{MGN}]_0$ would also be a maximum at $\chi_{\text{donor}} = n/n+1$, where $[\text{MGN}]_0$ = the initial concentration of MGN in the mixture and χ_{donor} = mole fraction donor in the mixture. Thus by plotting $\Delta\delta_{\text{OBS}}^{\text{MGN}} [\text{MGN}]_0$ against χ_{donor} the maximum will occur at $\chi_{\text{donor}} = n/n+1$.

The experimental results contained in Table 5.1 have subsequently

TABLE 5.1
¹H NMR Continuous Variation Experiment^a

Volume MGN Soln. ^b (cm ³)	Volume Donor Soln. ^b (cm ³)	Mole Fraction Donor (x _D)	Observed Change in ^{c,d} Chemical Shift (H _z) (Δδ ^{MGN} _{OBS})	[MGN] ₀ ^{Δδ} MGN c,d,e OBS
			Donor: (IP)	Donor: (IP)
			(MS)	(MS)
9.0	1.0	0.1	0.5	0.45
7.0	3.0	0.3	1.0	0.70
5.0	5.0	0.5	2.5	1.25
3.0	7.0	0.7	3.25	1.02
1.0	9.0	0.9	5.0	0.5

a) 90MHz spectrometer; TMS internal reference standard.

b) 1M solutions in CCl₄.

c) Δδ^{MGN}_{OBS} is defined in equation 25.

d) Tabulated values are upfield shifts of the MGN vinylic resonance which unperturbed has δ = 540 Hz.

e) [MGN]₀ = Initial concentration of MGN in donor/acceptor solution.

been plotted according to Sahai et al.¹¹⁶ in Figure 5.1. It is evident that the two curves each exhibit a maximum at $x_{\text{donor}} = 0.5$, which indicates that in each system there is the formation of a 1:1 molecular complex.

5.3.3 Determination of the Equilibrium Quotient (K_Q)

Person¹¹⁷ has carried out a critical examination of the use of the Benesi-Hildebrand equation in obtaining the equilibrium quotient of weak complexes. The author pointed out that the Benesi-Hildebrand plots would give zero intercepts despite a moderately large value of K_Q if the equilibrium concentration of the complex is not of the same order of magnitude as the equilibrium concentration of the more dilute components. Deranleau¹⁹² and Drago et al.¹⁹³ have come to the same conclusion. Therefore to satisfy the criteria for the reliable determination of the equilibrium quotient of weak EDA complexes, the initial concentration of the acceptor molecule must be kept low and constant at ca. 0.1M while the initial concentration of the donor molecule is varied in the range 1M-9M (or vice versa).

Person's criterion was employed in this study. The results of the nmr analysis are given in Tables 5.2 and 5.3, and representative ^1H nmr spectra of the MGN-IP system are shown in Figure 5.2 to illustrate the procedure.

In each case it is observed that, on complex formation, the MGN vinylic resonances shift to higher field. There are a number of possible explanations for such an effect, the most rational of which is that the observed shift originates largely from the magnetic anisotropy of the donor molecules.

This suggests a preferred orientation of the MGN molecule in which the vinylic protons of MGN experience a shielding anisotropic effect. This leads to the "amplification" of the small proton chemical shifts

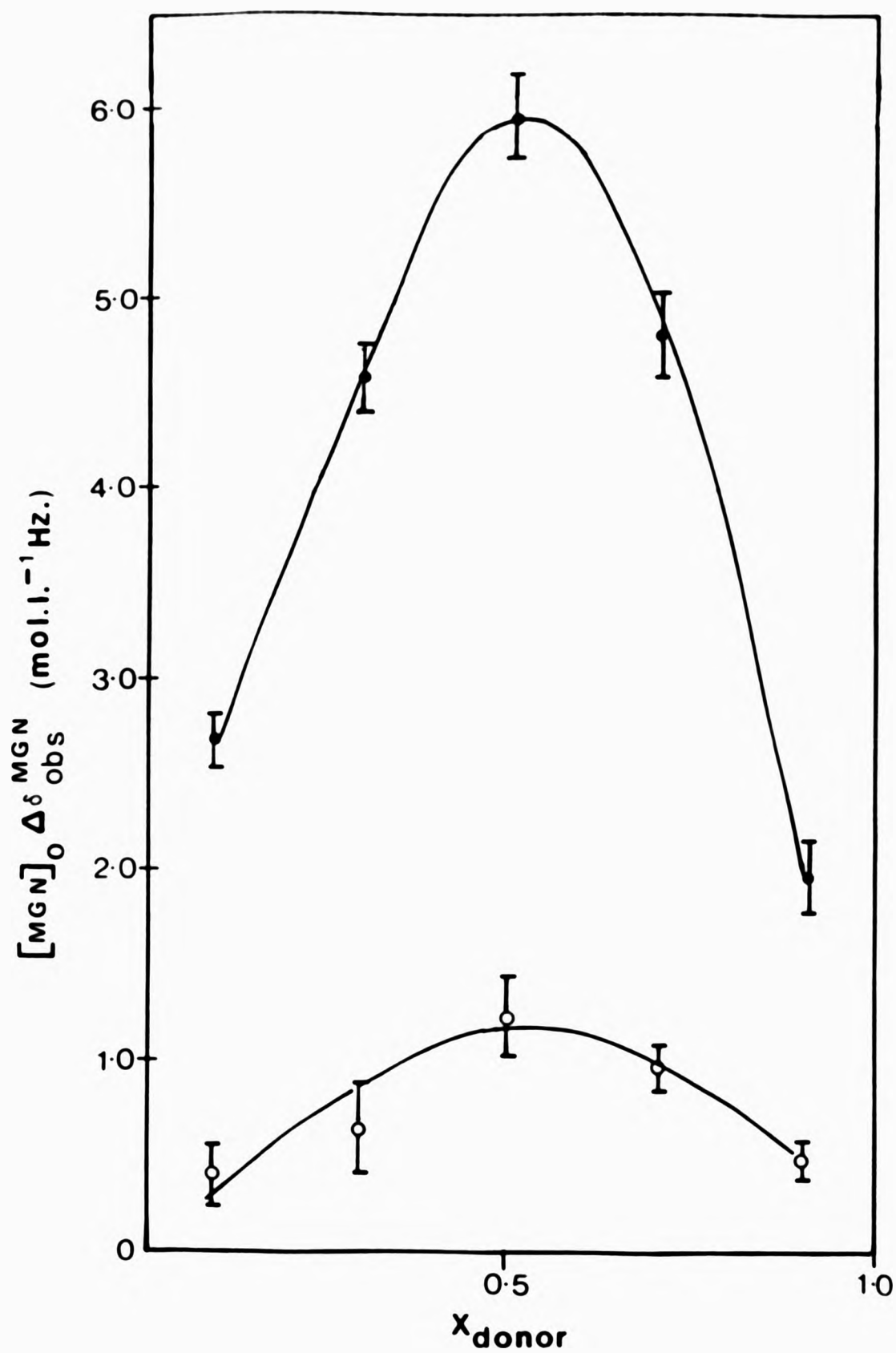


FIGURE 5.1

Stoichiometric determination of EDA complex by the nmr continuous variation method.¹¹⁶ (x_{donor} = mole fraction donor molecules in donor-MGN mixtures.)

(●) = MS-MGN system.

(○) = IP-MGN system.

TABLE 5.2
Values of $\Delta\delta_{\text{OBS}}^{\text{MGN}}$ for the MGN-Isoprene System at 273K, 288K and 306K^a

MGN Conc. (mol/dm ³)	Isoprene Conc. (mol/dm ³)	$\delta_{\text{OBS}}^{\text{MGN}}$ (Hz) ^b			$\Delta\delta_{\text{OBS}}^{\text{MGN}}$ (Hz) ^c		
		273K	288K	306K	273K	288K	306K
0.08	2.66	527.6	528.9	529.3	12.4	11.1	10.7
0.08	3.40	525.1	526.3	526.9	14.9	13.7	13.1
0.08	4.80	520.4	522.1	522.5	19.6	17.9	17.5
0.08	6.60	516.2	517.8	518.7	23.8	22.2	21.3
0.08	8.00	513.7	515.0	515.6	26.3	25.0	24.4
0.08	8.50	512.2	513.7	514.4	27.8	26.3	25.6

a) Performed on a 90 MHz instrument using TMS as the internal standard.

b) The chemical shift quoted is that of the lower field MGN vinylic resonance (Figure 5.2).

c) Calculated from equation 25: $\delta_{\text{FR}}^{\text{MGN}} = 540 \text{ Hz}$.

TABLE 5.3
Values of δ_{OBS}^{MGN} for the MGN- α -Methyl Styrene System at 306K, 318K and 323K^a

MGN Conc. (mol/dm ³)	α -Methyl Styrene Conc. (mol/dm ³)	δ_{OBS}^{MGN} (Hz) ^{b,c}			$\Delta\delta_{OBS}^{MGN}$ (Hz) ^d		
		306K	318K	323K	306K	318K	323K
0.1	1.54	509.7	511.4	513.7	30.3	28.6	26.3
0.1	2.31	498.3	500.8	503.0	41.7	39.2	37.0
0.1	3.08	488.7	492.4	494.5	51.3	47.6	45.5
0.1	3.85	482.9	484.5	487.4	57.1	55.5	52.6
0.1	4.61	(-)	(-)	(-)	(-)	(-)	(-)

- a) Performed on a 90MHz instrument using TMS as the internal standard.
- b) The chemical shift quoted is that of the lower field MGN vinylic resonance (Figure 5.2).
- c) The symbol (-) indicates that the MGN vinylic resonance is overlapped by the MS olefinic proton signal.
- d) Calculated from equation 25: $\delta_{FR}^{MGN} = 540$ Hz.

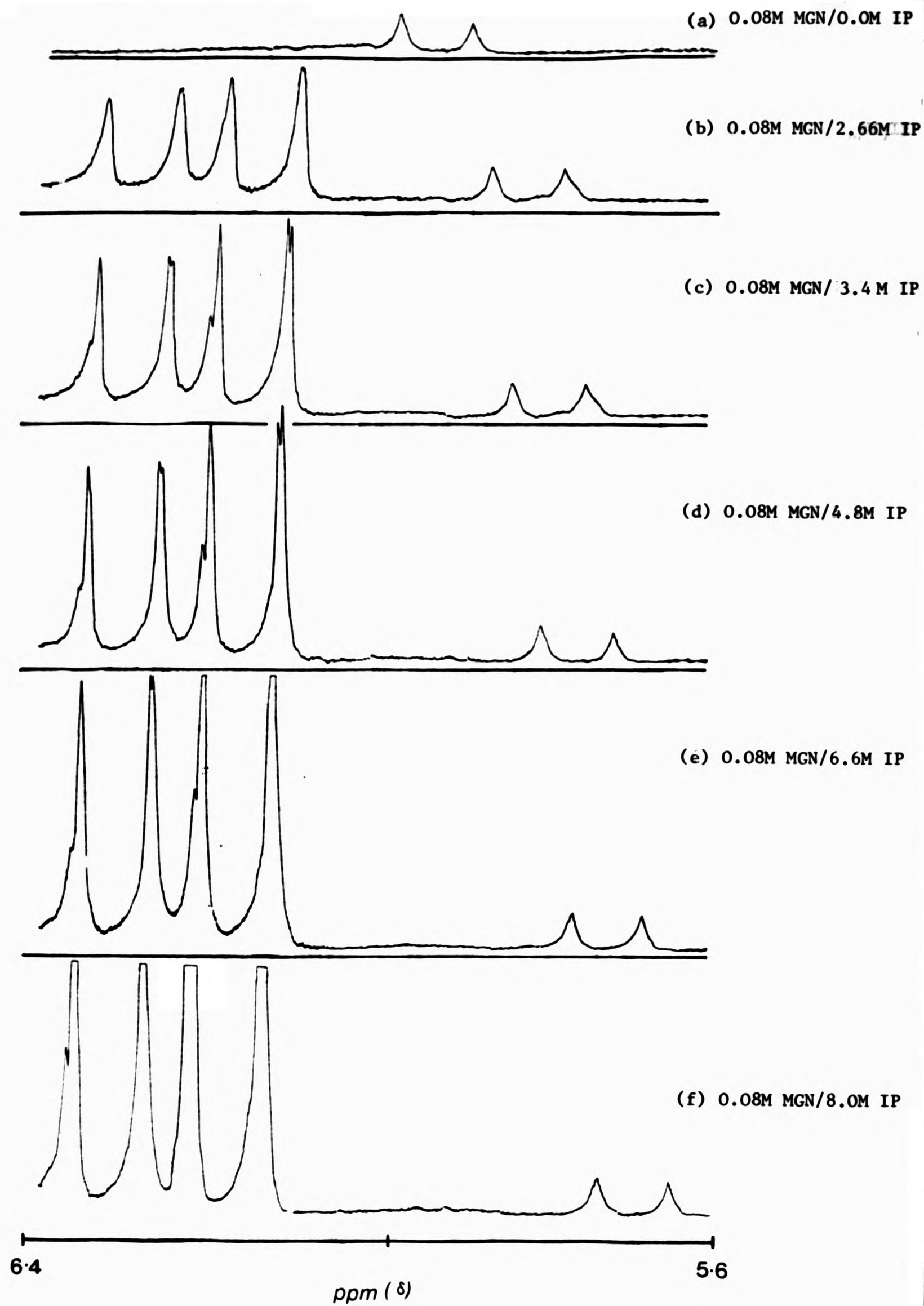


FIGURE 5.2 ^1H nmr spectra of MGN-IP solutions in CCl_4 at 306K illustrating the high field shifts of the MGN vinylic resonances upon complexation with IP.

resulting from EDA complexation by the large magnetic anisotropy of the donor molecules.

Unfortunately the MGN-MS system could not be analysed over the entire donor concentration range because of the overlap of the monitored MGN signals with the MS vinylic resonances. However, the system is still amenable to analysis over a restricted donor concentration range.

The data of Tables 5.2 and 5.3 may be analysed in terms of the Benesi-Hildebrand equation (29), enabling the determination of K_Q for each system at the specified temperature. The plots are shown in Figures 5.3 and 5.4. It can be seen that good linear relationships are observed in all cases. However, the Benesi-Hildebrand equation has been the focus of a great deal of criticism over the past few years from the point of view that it is insensitive to the presence of complexes of more than one stoichiometry. For example, Johnson and Bowen¹⁹⁴ found that such plots were still linear when significant concentrations of complexes of the type D_2A were present. Deranleau¹⁹² has shown that curvature, if present, is most easily seen on the Scatchard plot, therefore the data contained in Tables 5.2 and 5.3 were replotted in terms of the Scatchard equation (30). The resulting plots are shown in Figures 5.5 and 5.6. Again essentially linear plots are obtained allowing the value of the equilibrium quotient to be determined directly from the gradient. The values of K_Q obtained by this method and the Benesi-Hildebrand procedure are summarised in Table 5.4. In each instance the magnitude of the parameter K_Q is of the order expected and in accord with comparable literature systems.

At this juncture it is pertinent to ask whether such equilibrium quotients are indeed meaningful and due to EDA complexation or merely the result of a general solvent effect. This question may be answered by appealing to the existing literature.

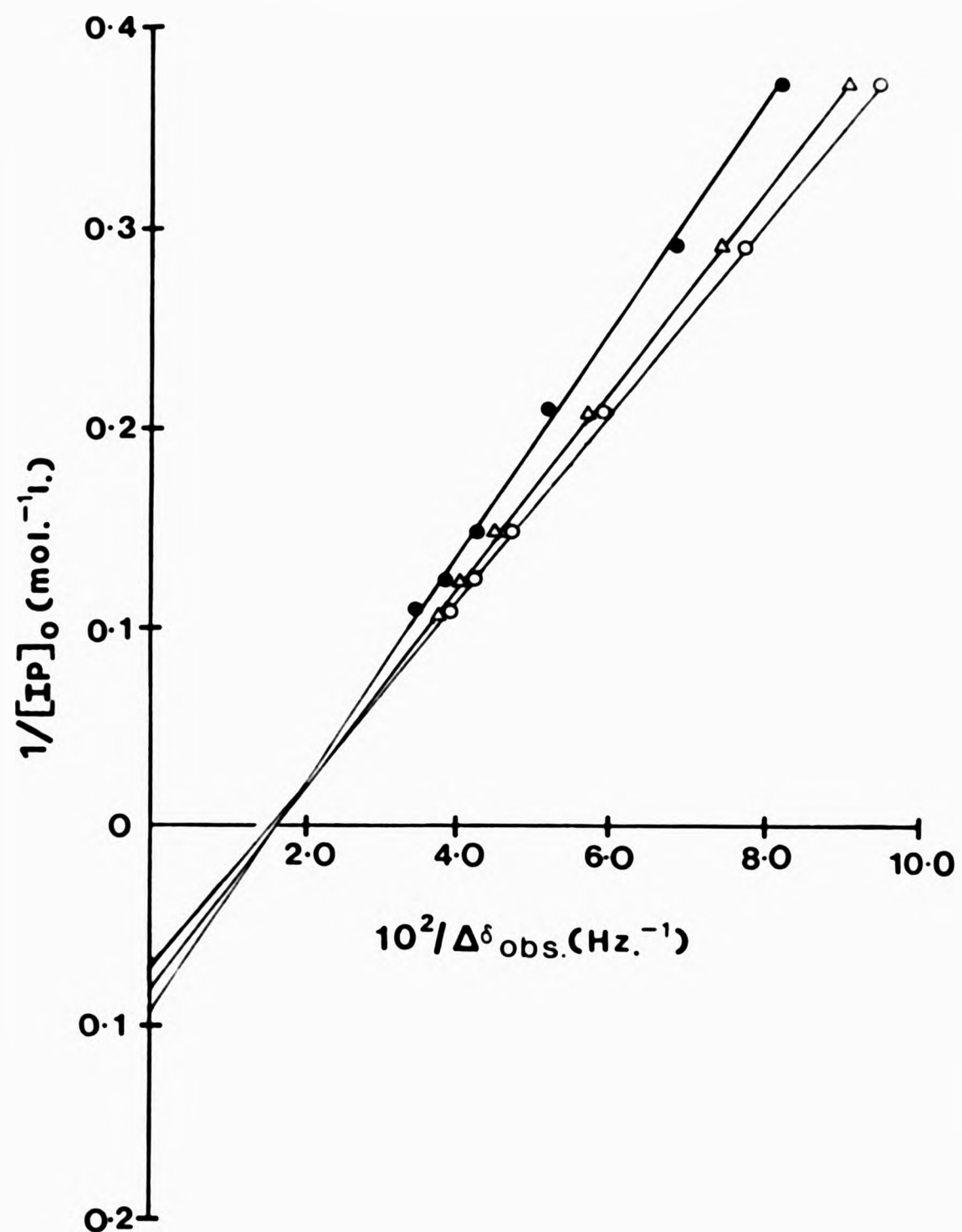


FIGURE 5.3 ^1H nmr determination of the equilibrium quotient (K_Q) for MGN-IP EDA complexation in CCl_4 by the nmr Benesi-Hildebrand equation. ● = 273K; △ = 288K; ○ = 306K.

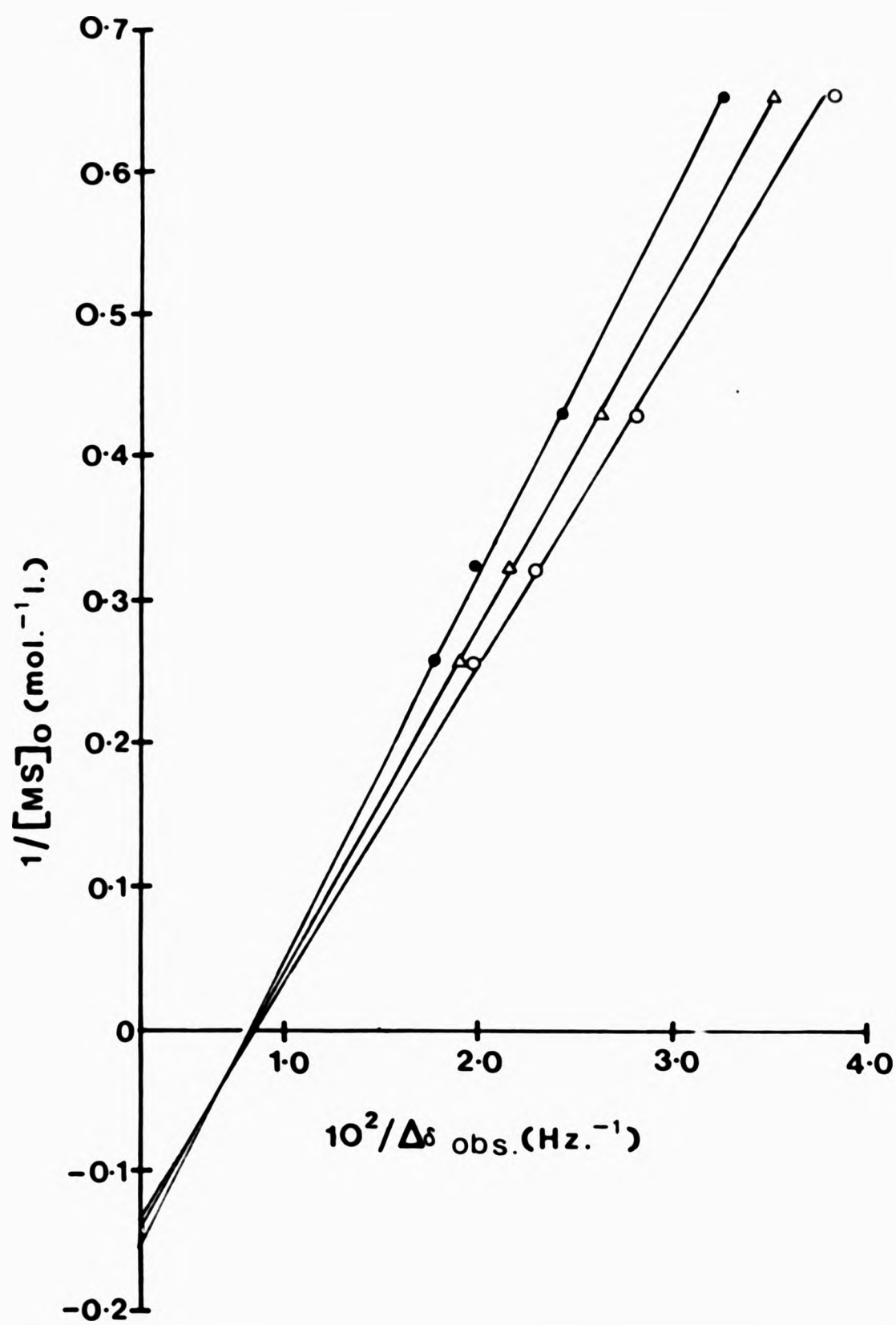


FIGURE 5.4 ^1H nmr determination of the equilibrium quotient (K_Q) for MGN-MS EDA complexation in CCl_4 by the nmr Benesi-Hildebrand equation. ● = 306K; Δ = 318K; ○ = 323K.

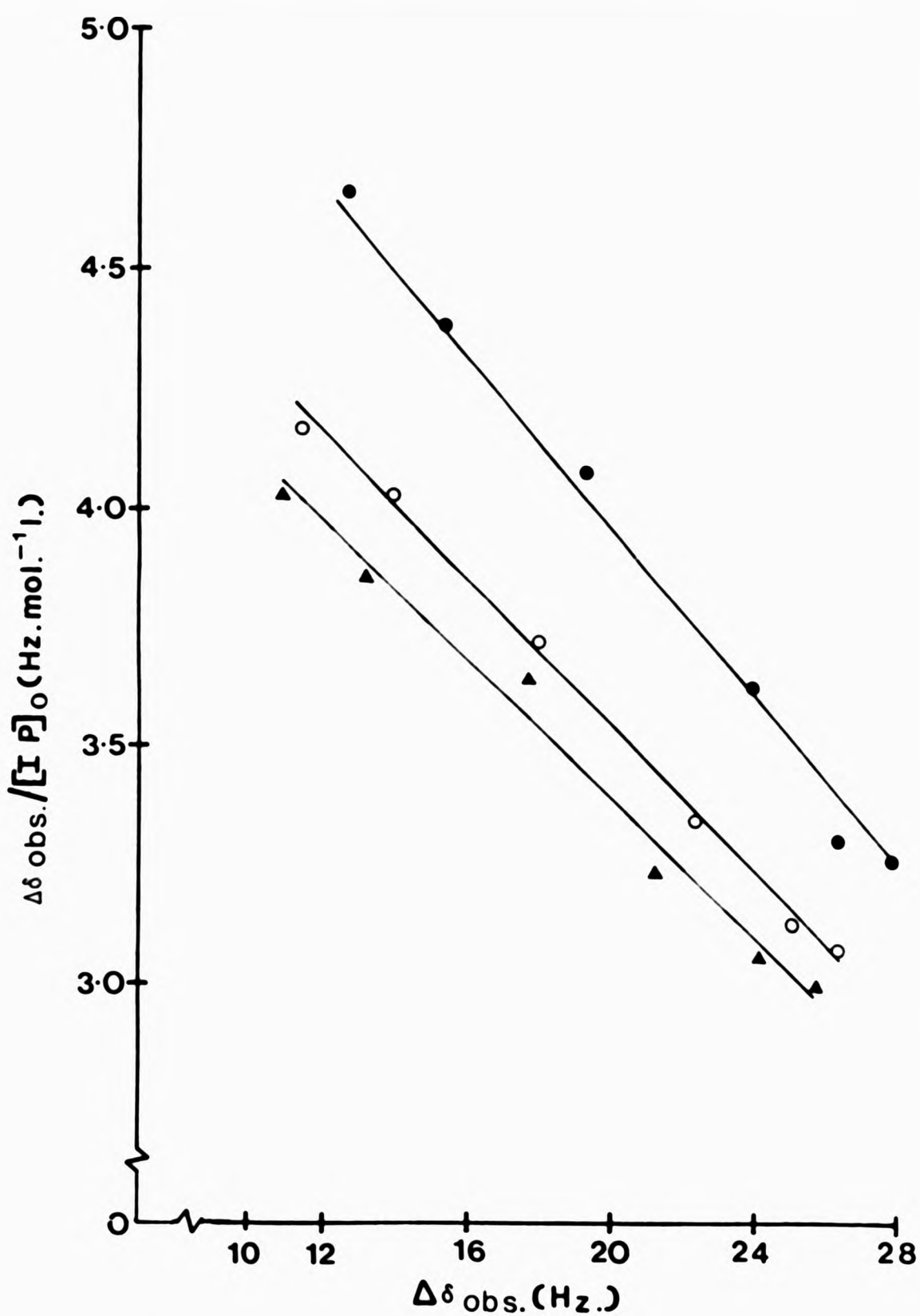


FIGURE 5.5

^1H nmr determination of the equilibrium quotient (K_Q) for MGN-IP EDA complexation in CCl_4 by the nmr Scatchard equation. ● = 273K; ○ = 288K; ▲ = 306K.

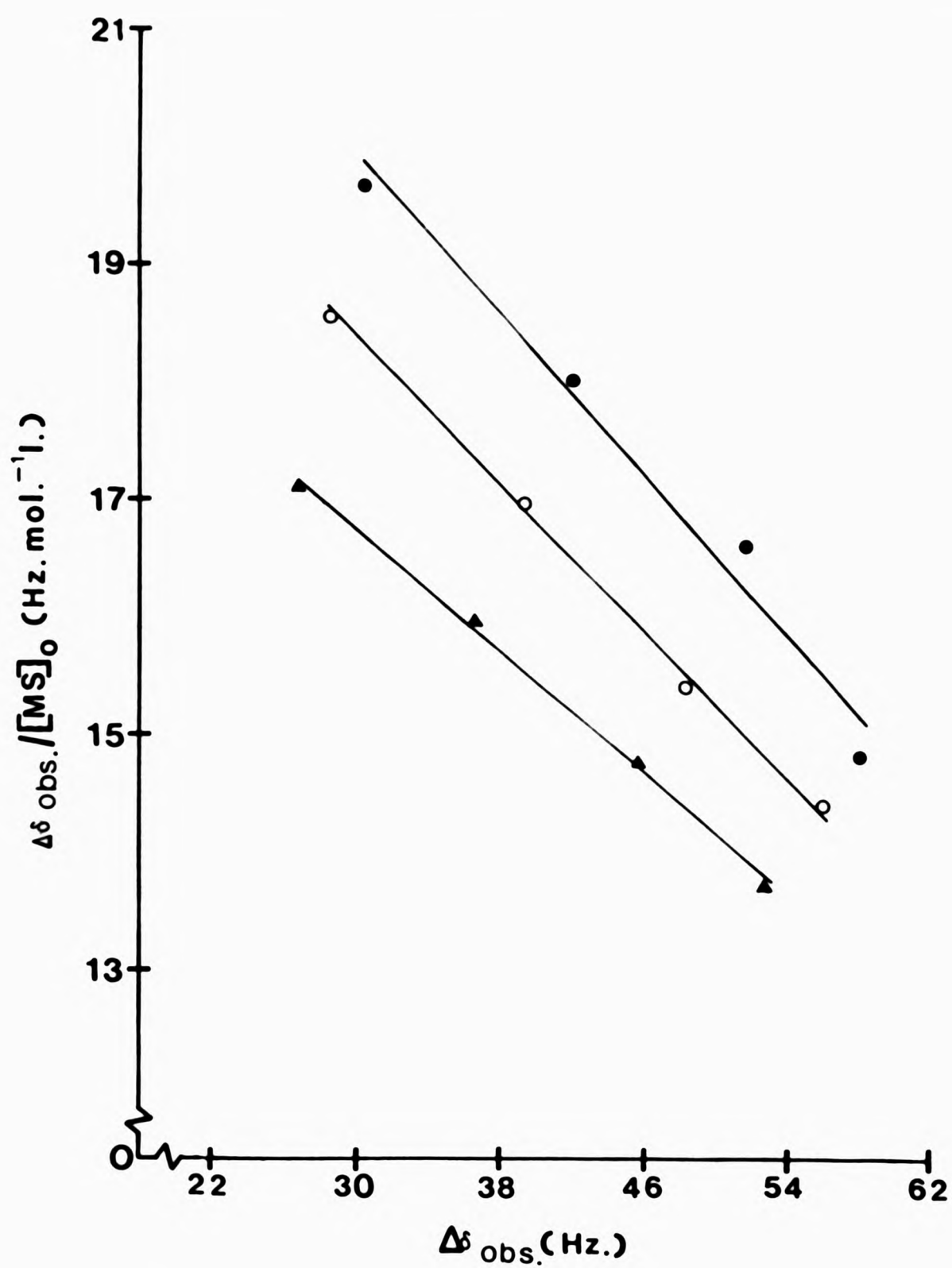


FIGURE 5.6 ^1H n m r determination of the equilibrium quotient (K_Q) for MGN-MS EDA complexation in CCl_4 by the nmr Scatchard equation. ● = 306K; ○ = 318K; ▲ = 323K.

TABLE 5.4

Thermodynamic Parameters for EDA Complexes of MGN calculated from ^1H NMR Data^a

Electron Donor/ Acceptor System	Temp. (K)	K_Q (dm ³ mol ⁻¹)		ΔH (kJ mol ⁻¹)	ΔS (JK ⁻¹ mol ⁻¹)	ΔG (kJ mol ⁻¹)
		Benesi-Hildebrand Analysis	Scatchard Analysis			
α -Methyl styrene/MGN	306	0.16	0.17	-7.2	-38.6	4.6
	318	0.15	0.16			
	323	0.14	0.14			
Isoprene / MGN	273	0.09	0.09			
	288	0.08	0.08			
	306 (333)	0.07 (0.05) ^b	0.07 -	-6.5	-43.1	6.7

a) Error analysis indicates that in each case the uncertainty in K_Q is $\pm 5\%$ with larger errors in the values of ΔH , ΔS and ΔG .

b) Value determined via extrapolation (Figure 5.9).

Hanna and Ashbaugh¹¹⁴ considered a series of complexes between 7,7,8,8-tetracyanoquinodimethane (TCNQ) and various methyl-substituted benzenes and analysed their results by means of the nmr Benesi-Hildebrand method. The authors found that as the ionisation potential of the donor molecule became lower, the equilibrium quotient calculated increased (this is also observed in the present case). Additionally, where comparison with equilibrium quotients obtained from UV measurements was possible, the agreement was good. Their final point was that no change in the chemical shifts of the monitored proton signal was observed when TCNQ was replaced by an aromatic molecule which was not expected to complex with the donor molecule, for example toluene. Similar nmr techniques were used by Schneider¹⁹⁵ to demonstrate directed molecular interaction between polar solute molecules and benzene. Such facts argue against the observed change in chemical shifts being due to a general solvent effect.

The vast majority of approaches to the study of weak EDA complexes have made the assumption that equation 32 holds true

$$\gamma_{AD}/\gamma_A \cdot \gamma_D = 1 \quad (32)$$

where γ_i refers to the activity coefficient of the species; or that the quotient $\gamma_{AD}/\gamma_A \cdot \gamma_D$ remains constant over the range of solutions studied. If one accepts this assumption (with reservations!) and providing that δ_{COM}^{MGN} does not vary with temperature over the temperature range studied (which indeed seems to be the case from Figures 5.3 and 5.4) then the thermodynamic parameters, ΔH (the heat of complex formation), ΔS the entropy change, and ΔG the free energy change, may be determined according to equations 33, 34 and 35.

$$-\ln K = \Delta H/RT + c \quad (33)$$

$$\Delta G = -RT \ln K \quad (34)$$

$$\text{and } \Delta G = \Delta H - T\Delta S \quad (35)$$

The plots of $-\ln K$ against $1/T$ for the MGN-IP and the MGN-MS systems are shown in Figures 5.7 and 5.8. Extrapolation of the MGN-IP data to 333K, allows the determination of K_Q at the temperature which the solution copolymerisations were performed.

The thermodynamic parameters for both systems have been calculated and are summarised in Table 5.4. In each case the values obtained for ΔH and ΔS are in accord with an associative mechanism and are of the order of magnitude consistent with the operation of the weak charge-transfer interactions. The values also compare favourably with those reported in the literature for the EDA complexes of maleic anhydride.¹⁹⁶

5.4 COMPLEX PARTICIPATION PERTINENT OBSERVATIONS

Naturally, the existence of an EDA complex does not necessarily imply its actual participation in the alternating copolymerisation. However, where such complexes are known to exist, a number of experimental observations have been cited as evidence for complex participation. In this respect, it is worthwhile reporting the following observations (5.4.1 - 5.5.4).

5.4.1 The Initial Rate of Copolymerisation

In both the MGN-IP¹⁹⁷ and MGN-MS systems, the initial rate of copolymerisation (determined gravimetrically) was found to exhibit a maximum around the equimolar monomer feeds, i.e. the feeds corresponding to a maximum concentration of comonomer complex. The results are illustrated in Figure 5.9. Rate profiles such as these are typical of

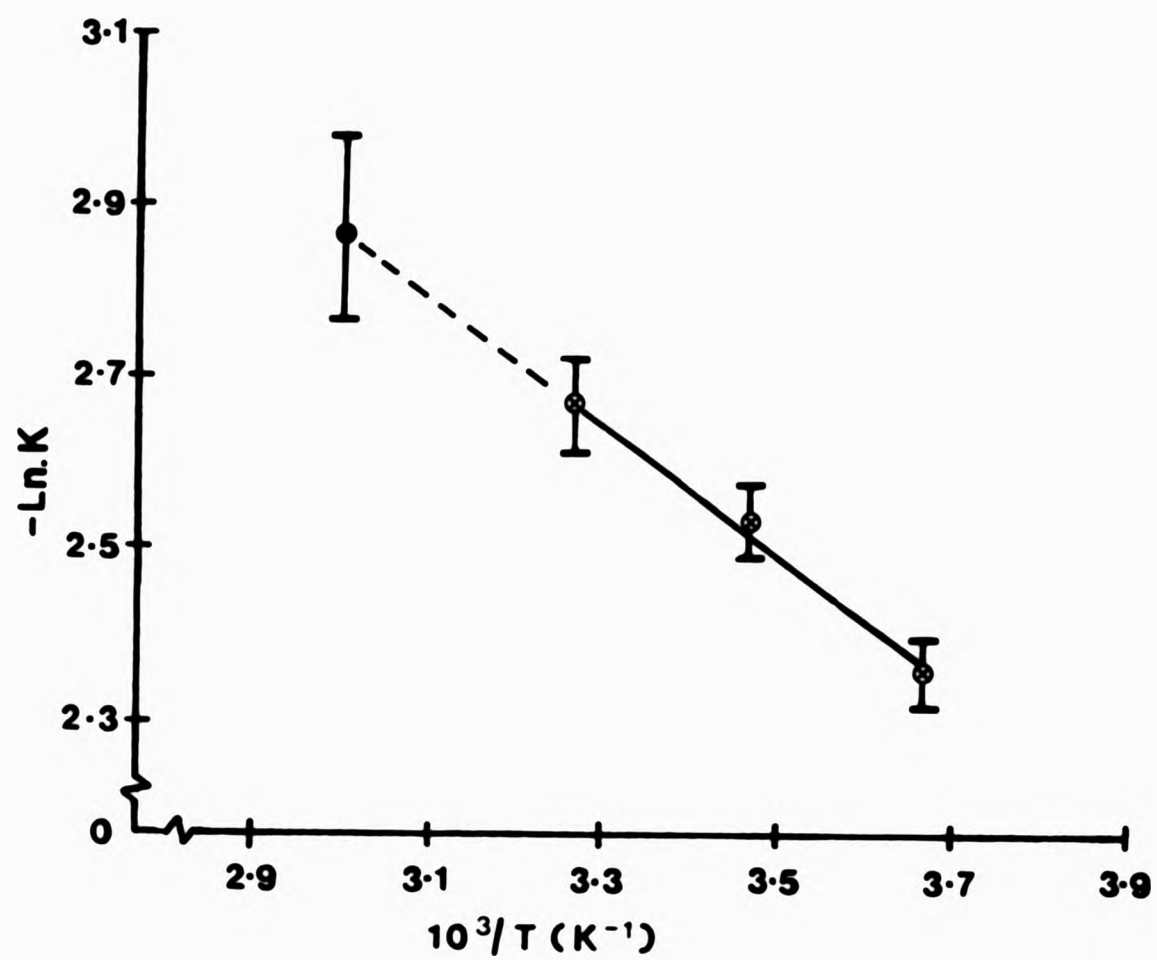


FIGURE 5.7 Determination of ΔH , the heat of complex formation, for the EDA MGN-IP species. Extrapolation to 333K allows the determination of K_Q at the copolymerisation temperature.

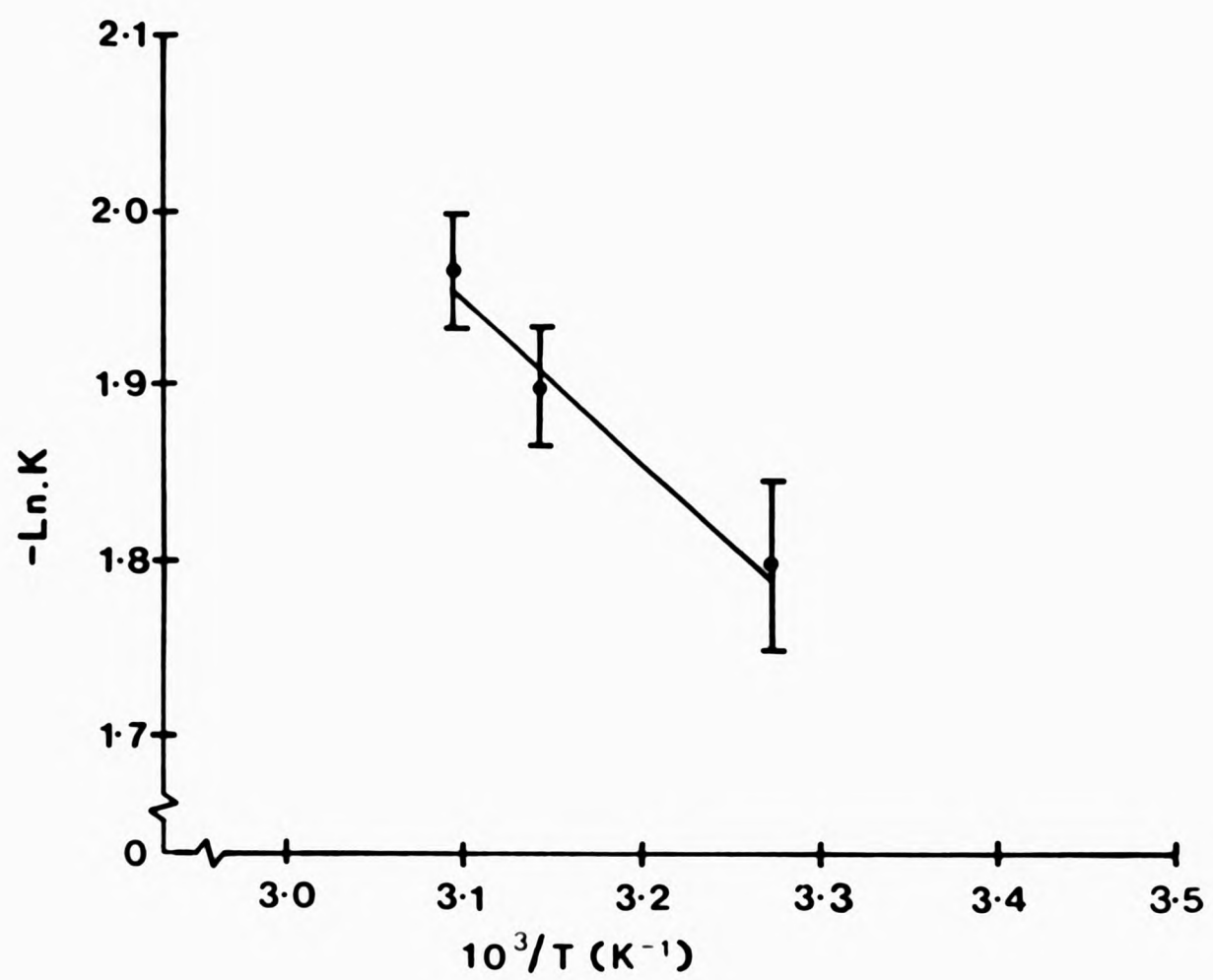


FIGURE 5.8 Determination of ΔH , the heat of complex formation, for the EDA MGN-MS species.

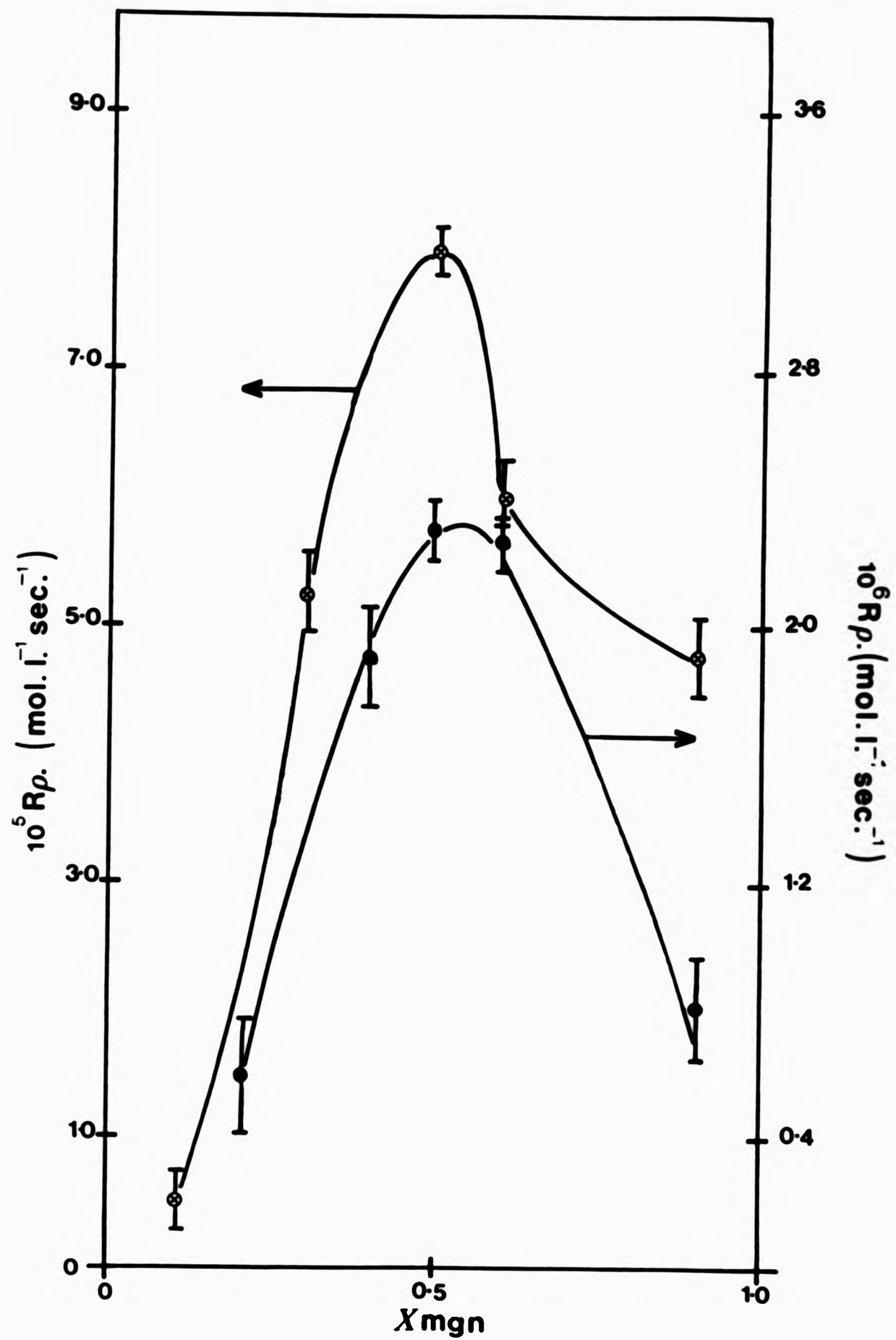


FIGURE 5.9

Plots of the initial copolymerisation rate vs. mole fraction MGN (x_{MGN}) for the MGN-IP (⊗) and MGN-MS (●) systems.

comonomer pairs that polymerise in an alternating fashion.¹⁹⁸

However, mathematical analysis of equation 36, which defines the rate of copolymerisation on the basis of the terminal model (diffusion controlled termination is assumed) shows that a maximum in the rate of copolymerisation at the equimolar feed can also be accommodated by the classical model of copolymerisation.

$$R_p = \frac{(r_1[M_1]^2 + 2[M_1][M_2] + r_2[M_2]^2)R_i}{k_{t(1,2)} \left(\frac{r_1[M_1]}{k_{11}} + \frac{r_2[M_2]}{k_{22}} \right)} \quad (36)$$

where r_1 , r_2 , M_1 , M_2 , k_{11} and k_{22} have the definitions set out previously (4.2), R_i is the rate of initiation and $k_{t(1,2)}$ is the cross termination rate constant.

5.4.2 "Spontaneous" Copolymerisation.

During the study of MGN-IP and MGN-MS copolymerisations it was found that the bulk comonomer solutions increased dramatically in viscosity over the period of a few days, ostensibly as a result of copolymerisation.

In a more quantitative manner, vacuum sealed flasks containing equimolar feed ratios of the distilled monomers were placed in an oil bath and thermostated at 333K (no added initiator). After 48 hrs the MGN-IP system yielded 90% of essentially equimolar copolymer with the MGN-MS system giving ~ 10% yield of ca. 50/50 copolymer after 96 hrs.

Such examples of "spontaneous" copolymerisation are well documented in the literature although there is much debate on the possible mechanism.^{199,200}

Very few monomers are known to exhibit pure thermal initiation, the classic examples being styrene and methyl methacrylate, but as long ago as 1949 Walling²⁰¹ observed that certain pairs of monomers, such as

styrene and maleic anhydride, show an unusually high propensity for what the author proposed was thermal initiation. Walling attributed such phenomena to large polar interactions between the monomers leading to an "extreme case of favourable cross-initiation". A similar situation was anticipated by Walling between buta-1,3-diene and carbonyl or nitrile conjugated monomers.

Alternatively, Gaylord²⁰² has attributed "spontaneous" copolymerisation in certain systems to the formation of comonomer complexes, which he hypothesised to polymerise via the excited state (exiplex).

Additionally, Ellinger²⁰³ and Scott²⁰⁰ independently reported that N-vinyl carbazole was polymerised spontaneously through the formation of charge-transfer complexes which were formed in the presence of a variety of electron acceptors. Subsequent research^{204,205} however, has illustrated the striking influence of impurities upon this and a number of other polymerisation systems, to the extent that they have been deemed to be the source of the initiation.

Clearly great caution is required before any mechanistic conclusions can be drawn from "spontaneity".

5.4.3 Copolymerisation in the Presence of Lewis Acid

In copolymerisations which may involve the participation of a comonomer complex, the addition of a compound which enhances complexation or which complexes preferentially with one of the monomers, may also affect the composition of the resulting copolymers and/or the rate of copolymerisation.

Since the first demonstrations by Bamford and coworkers²⁰⁶ that metal salts can influence the kinetics of radical polymerisations, and by Hirooka and colleagues²⁰⁷ that organometal halides can catalyse the production of alternating copolymers from mixtures of donor and acceptor

monomers, there have been several hundred reports concerned with the study of the influences of Lewis acids upon radical homo- and copolymerisations.

In this work the effects of ZnCl_2 upon the MGN-IP and MGN-MS copolymerisation systems over a wide comonomer feed was established. The results presented in Table 5.5 reveal that the addition of Lewis acid to the MGN copolymerisation systems leads to an increase of both the alternating tendency and the (qualitative observations) rate of copolymerisation. Caution must be exercised as regards this latter point as the effect of ZnCl_2 on the decomposition of AIBN is uncertain.²⁰⁸

Again one may rationalise such observations by invoking (a) either a terminal model mechanism, whereby complexation of MGN with ZnCl_2 enhances the electrophilic character of the double bond of the monomer and increases cross propagation rate constants, or (b) by invoking a ternary complex mechanism whereby the enhanced electrophilic character of the MGN-ZnCl_2 vinyl bond increases the equilibrium constant for MGN-donor complexation, the alternating copolymerisation is thus a result of the homopolymerisation of the ternary complex.^{209,210}

No unambiguous evidence concerning the MGN-IP and MGN-MS copolymerisation mechanisms may therefore be gleaned from the present Lewis acid ternary systems. The parallel between the controversy surrounding the mechanism of a copolymerisation both in the presence and in the absence of a Lewis acid is evident.

5.4.4 Kelen-Tüdös Analysis

Kelen and Tüdös have proposed a simple graphically evaluable linear method for the determination of monomer reactivity ratios in radical copolymerisations.²¹¹ The authors also stated that its applicability "held important clues as to the copolymerisation mechanism", in as much

TABLE 5.5
MGN-IP and MGN-MS Copolymers Prepared in the Presence of ZnCl₂, a, b, c

MGN Feed (Mole fraction)	Polymerisation time		Yield (%)		Copolymer Composition ^d (Mole fractions MGN)		$\bar{M}_n \times 10^{-5}$ (gmol. ⁻¹)		Tg (K)	
	MGN-IP (Hrs)	MGN-MS	MGN-IP	MGN-MS	MGN-IP	MGN-MS	MGN-IP	MGN-MS	MGN-IP	MGN-MS
0.15	2.0	12	8	8	0.48	0.49	0.9	0.3	290	429
0.5	0.5	10	20	15	0.50	0.50	1.5	0.7	295	430
0.85	0.5	10	15	9	0.50	0.52	1.2	0.5	294	425

- a) Toluene solution copolymerisation, total [Monomer] = 5M, [AIBN] = 1 x 10⁻³M.
- b) All copolymerisations carried out at 333K.
- c) Mole ratio of MGN:ZnCl₂ = 2:1.
- d) Possible composition drifts limits direct correlation between comonomer feed and copolymer composition.

as it may invalidate the terminal model of copolymerisation.²¹²

The Kelen Tüdös equation (37) is based on the differential form of the copolymer equation (13) and is suitable for low conversion data (<5%).

$$\text{Kelen-Tüdös (K-T) Equation: } \eta = \left(r_1 + \frac{r_2}{\alpha}\right) \epsilon - \frac{r_2}{\alpha} \quad (37)$$

$$\text{where } \eta = \frac{G}{\alpha+F}; \quad \epsilon = \frac{F}{\alpha+F}; \quad G = \frac{x(y-1)}{y}; \quad F = \frac{x^2}{y}; \quad x = \frac{m_1}{M_2}; \quad y = \frac{m_1}{m_2}$$

m_1 and m_2 are the molar concentrations of the designated monomer in the feed, and M_1 and M_2 are the molar concentrations of the designated monomer in the resulting copolymer, α is an appropriately chosen constant to obtain a uniform spread of the data (where $r_1 \approx r_2$, α is given the value 1).

Thus by plotting η versus ϵ according to the linear equation (37), a straight line is obtained and extrapolation to $\eta = 0$ and $\epsilon = 0$ gives $-r_2/\alpha$ and r_1 (both as intercepts).

Kelen and Tüdös have postulated that if this plot is linear for the copolymerisation in question, the Mayo-Lewis copolymer equation (13) holds and the simple two parameter classical model is a satisfactory description of the system. However, if the plot is curved, a more complicated situation arises and the classical model cannot hold. To this extent, the authors viewed the K-T equation as a diagnostic tool in the elucidation of the copolymerisation mechanism.

The copolymer data previously reported in Tables 4.4 and 4.5 were therefore plotted in terms of the K-T equation. The plots are presented in Figures 5.10 and 5.11.

It is immediately obvious that in both systems there is a systematic

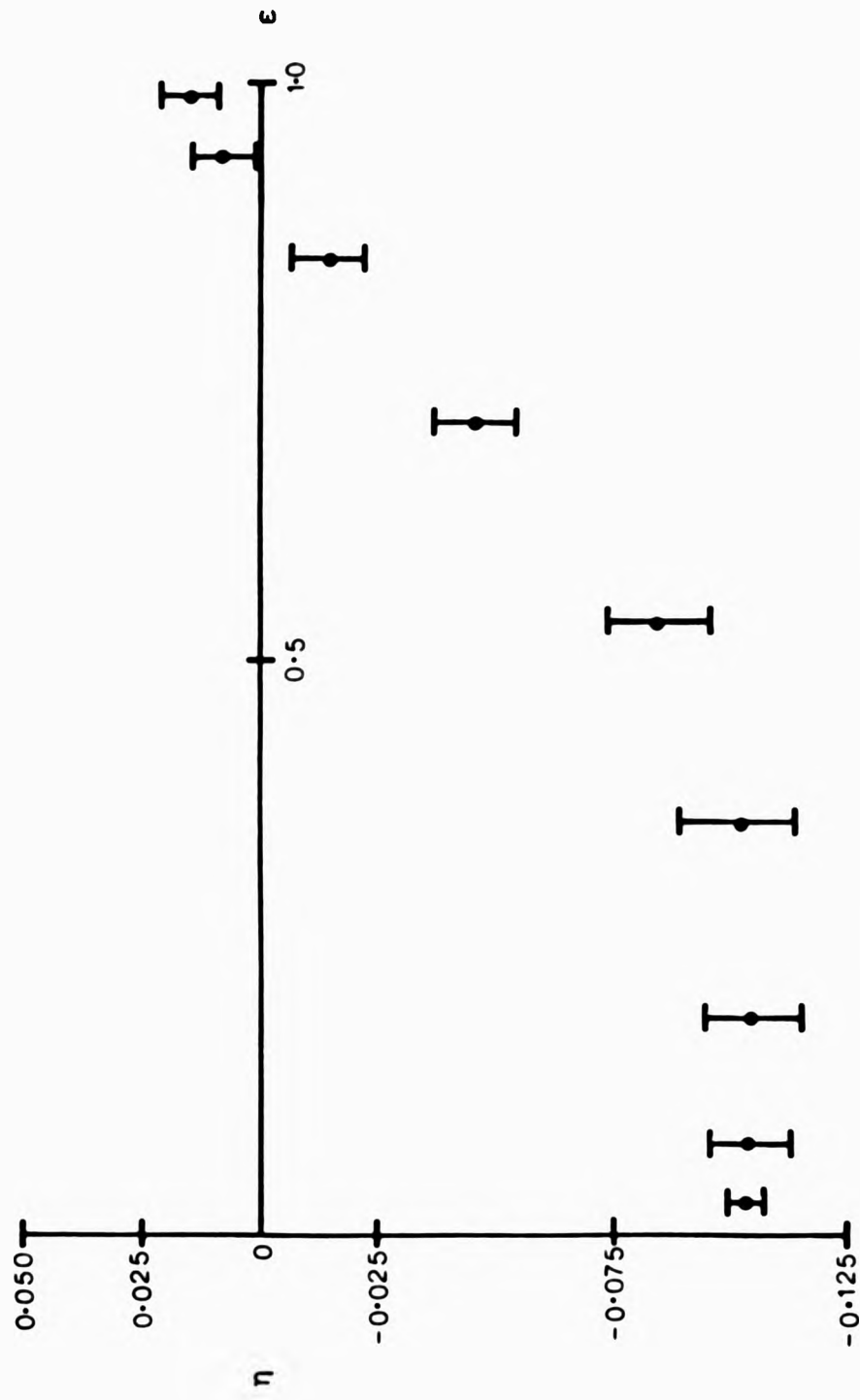


FIGURE 5.10 Kelen-Tüdös plot of the MGN (M_1)-IP(M_2) system 16a.

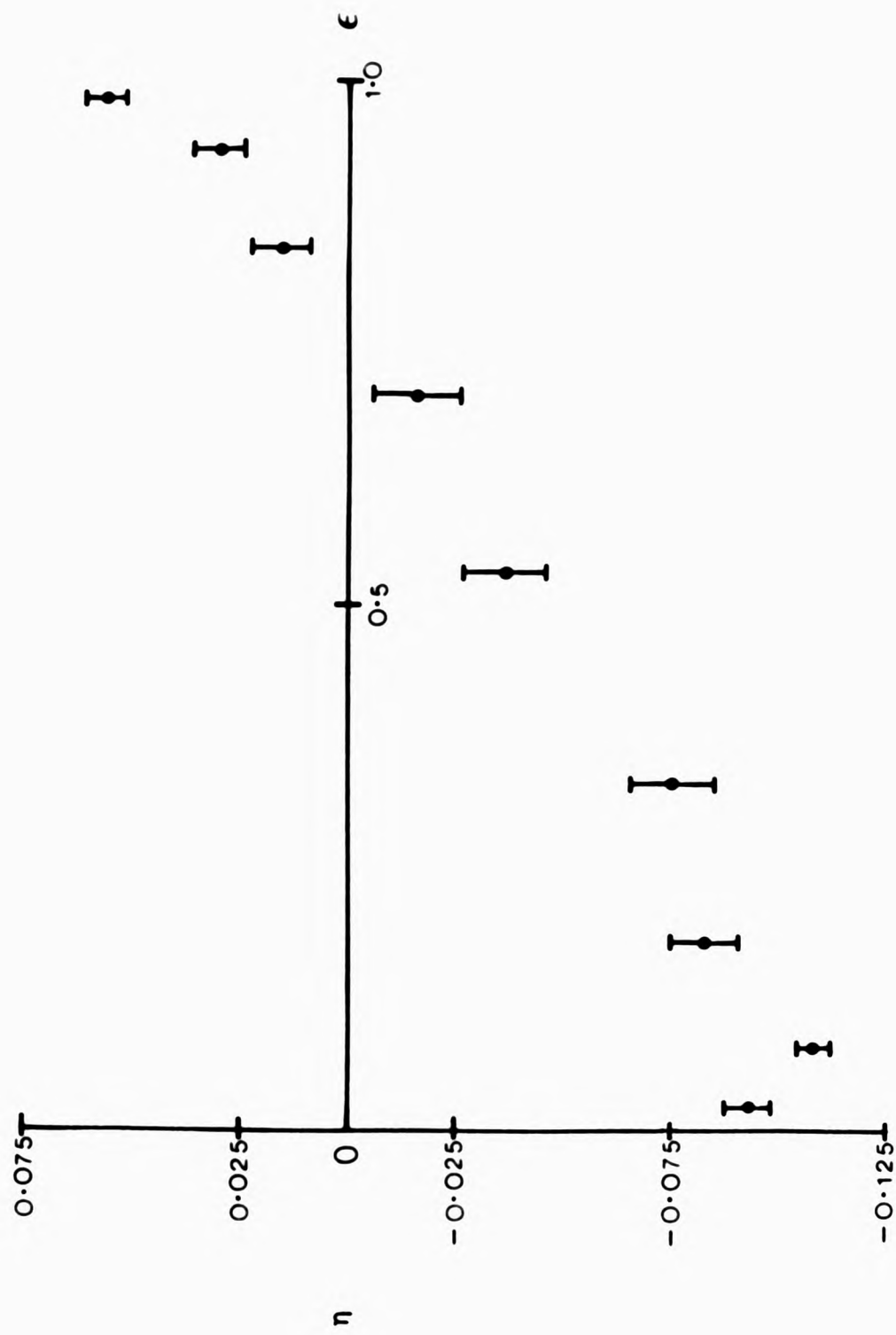


FIGURE 5.11 Kelen-Tudös plot of the $MGN(M_1) - MS(M_2)$ system 19.

deviation from linearity. However, before drawing any conclusions from this observation, the possible sources of such deviations should be realised.

The effect of random errors on a K-T plot has been considered by O'Driscoll,²¹³ who has shown that systematic deviation from the rectilinear K-T plot may stem from the nature of the K-T plot and the error structure of the experimental data.

An examination of the mathematics leading to the K-T equation shows that the variance of the dependent variable η is a complicated function of α , ϵ , γ and x . (eqn. 38)

$$\text{Var } \eta = \left[\frac{(\gamma-1)(1-\epsilon)}{\alpha\gamma} \right]^2 \text{ var } x \quad (38)$$

O'Driscoll has shown that starting from perfect copolymer composition data, generated from preselected monomer reactivity ratios, the imposition of a random error of (say) 3% may result in the line of best fit being a curve. This invalidates the statement made by Kelen et al.²¹² that curvature of a K-T plot indicates that the classical two parameter model of copolymerisation is unsuitable for the description of the copolymerisation system in question.

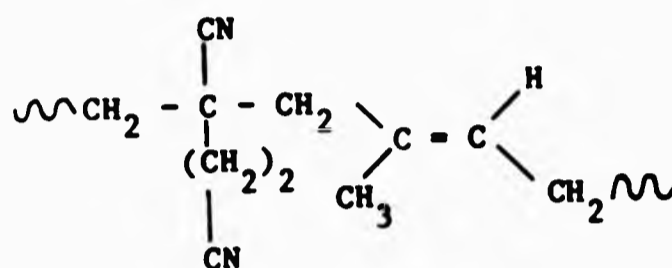
Figures 5.D and 5.11 do however exhibit deviation outwith the estimated experimental errors. This raises the possibility of effects, not accommodated by the Mayo-Lewis treatment of copolymerisation, being present and observed by the K-T treatment of the results. The possible cause(s) of such deviations are numerous and are detailed in the context of the present study in Chapter 6.3.

5.5.4 Polymer Stereochemistry

According to Muliken²¹⁴ any EDA complex is expected to have a

preferred geometry and from this it may be postulated that, if an EDA comonomer complex adds to the propagating radical chain in a concerted manner, a certain amount of stereochemistry may be introduced into the polymer chain.

In this study, the radical copolymerisation of MGN and isoprene resulted in an alternating copolymer with a high degree of stereoregularity (4.4.1), shown as XXVII below. The isoprene unit is



(XXVII)

present predominantly (>90%) in the trans 1,4-configuration, and the MGN and IP moieties are arranged in what might be described as a "head to head" fashion. Such a structure may suggest a copolymerisation mechanism in which complexation of the diene is important.

Just as the outer shell of electrons of an atom is regarded as especially significant in determining the chemistry of that atom, so it is reasonable that the highest occupied molecular orbital (HOMO) of a molecule is the key to determining its reactivity. This is the frontier orbital approach.²¹⁵ Consequently, the HOMO and the LUMO (lowest unoccupied molecular orbital) of isoprene (both cis and trans) and MGN were calculated in an attempt to predict the most favourable interaction and possible geometry of any comonomer complex.

Very briefly, the procedure involves the use of the Allinger "Strain" program package,²¹⁶ which minimises the total energy of a molecule, to obtain its most stable geometry and subsequently inputting

these atomic coordinates to the IBM program package "Gaussian 79"²¹⁷ to determine the relevant wave equations.

The "Gaussian 79" program involves ab initio self consistent field calculations using Roothaan theory but employing Gaussian type orbitals as basis functions (a minimum basis set was used). All work was performed on a VAX 11/780 computer.

Table 5.6 reports the HOMO and LUMO wave functions for isoprene and MGN.

Considering such a frontier orbital approach, one would expect the interaction between MGN and isoprene to be greatest where the molecular orbitals of each monomer are a) closest in energy, b) of the same symmetry, and c) overlap is sterically possible. In the light of these criteria, Figure 5.12 illustrates two of the more likely EDA comonomer interactions. Of these, structure XXIX, an MGN-trans 1P interaction, has the more favourable geometric arrangement, although this structure involves the interaction of π orbitals of lower electron density than the MGN-cis 1P species XXX. This point may be academic as examination of both structures reveals that it is rather difficult to rationalise the established MGN-1P copolymer structure (XXVII) in terms of such comonomer interactions. The copolymer stereochemistry may however be explained without recourse to EDA complex formation. Specifically, the Raman spectrum of isoprene indicates an equilibrium between the S (planar) cis and S trans forms with the S trans content being 85% at 323K.²¹⁸ Consequently, the microstructure of radically polymerised (323K) isoprene comprises 15% cis-1,4-1P, 5% 1,2-1P, 5% 3,4-1P and 75% trans 1,4-1P units.²¹⁹ Thus one would expect a high trans-1,4-1P content in radical copolymerisation empirically.

The "head to head" arrangement of the MGN-1P copolymer may also be accounted for by a "free" monomer mechanism. It has been postulated

TABLE 5.6

The HOMO and LUMO Wave Function Coefficients for MGN and isoprene^a

MGN:

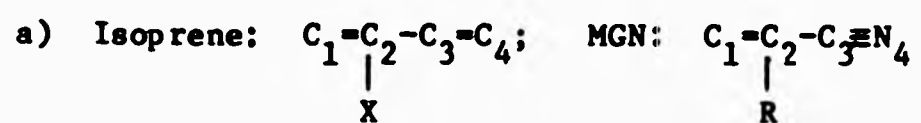
$$\begin{aligned} \text{HOMO } (\Psi_{28}) &= -0.58p\pi_1 - 0.54p\pi_2 + 0.23p\pi_3 + 0.37p\pi_4 \\ \text{LUMO } (\Psi_{29}) &= +0.74p\pi_1 - 0.61p\pi_2 - 0.32p\pi_3 + 0.44p\pi_4 \end{aligned}$$

cis-isoprene:

$$\begin{aligned} \text{HOMO } (\Psi_{19}) &= -0.57p\pi_1 - 0.40p\pi_2 + 0.37p\pi_3 + 0.52p\pi_4 \\ \text{LUMO } (\Psi_{20}) &= -0.63p\pi_1 + 0.43p\pi_2 + 0.45p\pi_3 - 0.65p\pi_4 \end{aligned}$$

trans-isoprene:

$$\begin{aligned} \text{HOMO } (\Psi_{19}) &= -0.56p\pi_1 - 0.38p\pi_2 + 0.39p\pi_3 + 0.53p\pi_4 \\ \text{LUMO } (\Psi_{20}) &= -0.64p\pi_1 + 0.46p\pi_2 + 0.41p\pi_3 - 0.64p\pi_4 \end{aligned}$$



where X = CH₃; R = -(CH₂)₂CN.

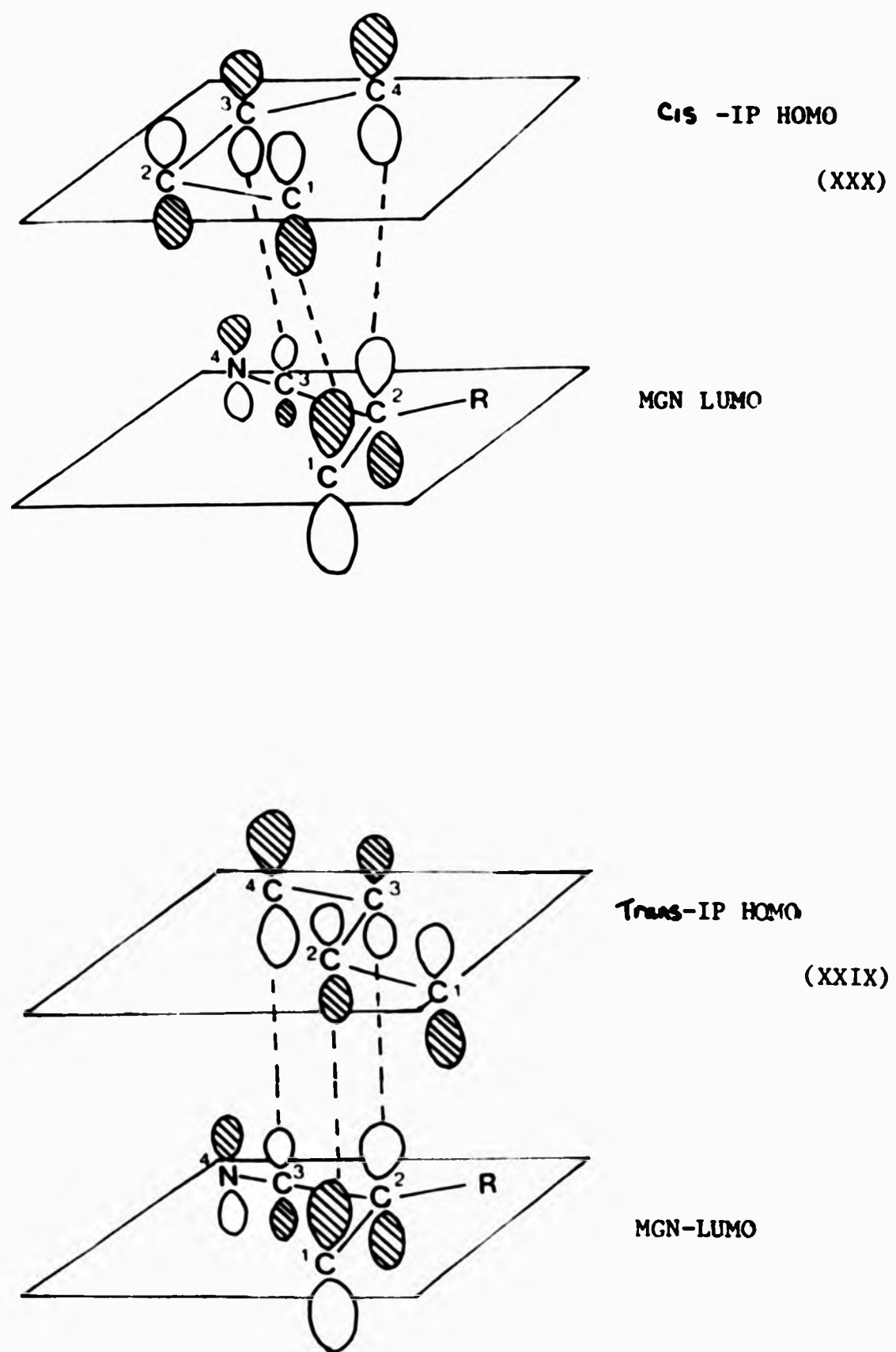
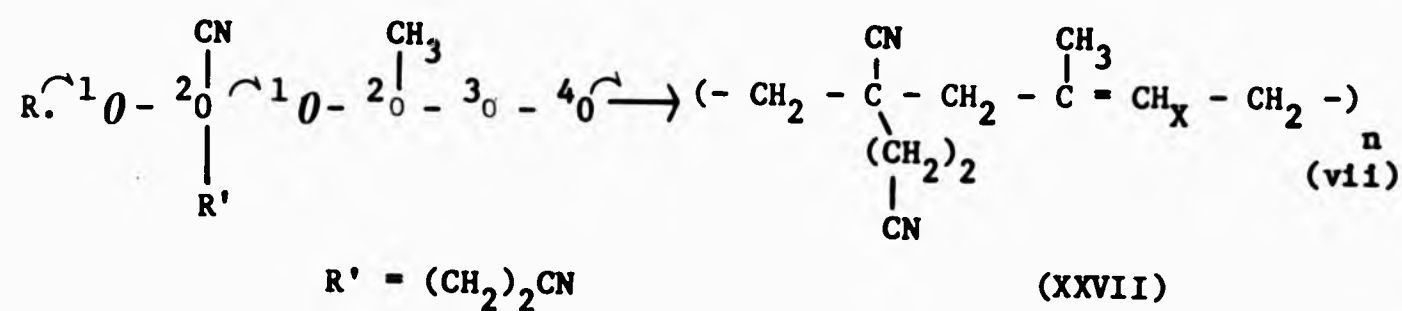


FIGURE 5.12 Possible EDA interaction of MGN LUMO and IP HOMO. (R = (CH₂)₂CN)

that the propagation step of polymerisation occurs between a chain end radical and the position of a monomer having the largest calculated frontier electron density (FED).²²⁰ (The FED is proportioned to the square of the atomic orbital coefficient, cf. Table 5.7.) The FED is greatest in both isoprene and MGN at what has been designated the 1-position. This therefore predicts scheme (vii) for the alternating copolymerisation of MGN with IP.



(where R. is a propagating radical and the size of the node 0 is indicative of the FED.)

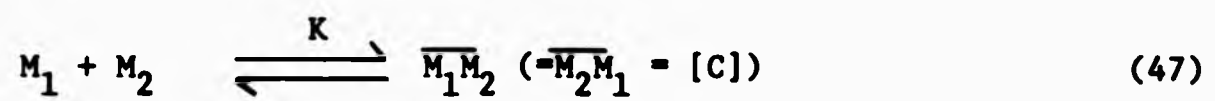
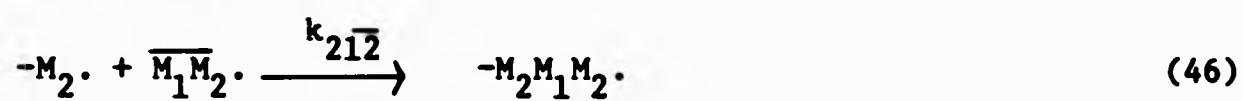
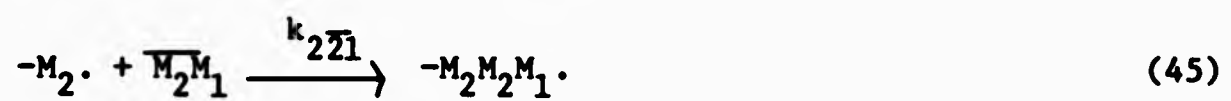
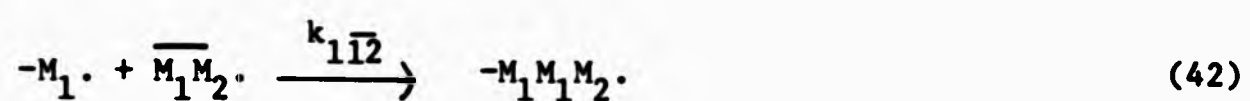
The results and observations contained in this chapter illustrate the difficulty in obtaining unambiguous experimental evidence for or against the participation of a comonomer complex in alternating copolymerisation. The usual practice of appealing to the existing experimental literature can yield data published by careful workers which illustrates techniques which appear to support whichever mechanism, free monomer or comonomer complex, advocated by the researcher!

However, there are two procedures which do enable the determination of the extent of complex participation in alternating copolymerisation, one of which has been employed in this study to analyse the MGN-IP and MGN-MS systems and is the subject of the following chapter.

CHAPTER SIX

6.1 THE COMPLEX PARTICIPATION MODEL

The generalised complex participation model of Seiner and Litt⁴⁴ allows for the participation of both monomers and the comonomer complex and is therefore not limited to a consideration of strictly alternating copolymers. The Seiner and Litt model can be described by eight kinetic equations and an equilibrium constant (equations 39-47).



where k_{11} is the rate constant for addition of propagating radical M_1 to monomer M_1 , and $k_{12\bar{1}}$ is the rate constant for addition of propagating radical M_1 to the M_2 side of the comonomer complex and so on.

In order to examine the applicability of this, or any other model, to a particular copolymer system, two main approaches have been employed. The first is to examine the variation in copolymer composition and/or monomer sequence distribution, as the monomer feed composition is varied over the entire range.²²¹ The second approach, a purely kinetic analysis, studies the variation in the maximum initial polymerisation rate and the mole ratio of the two monomers at this maximum point, with the total monomer concentration.^{46,47}

The former approach was used in this study.

6.1.1 Analysis of the Complex Participation Model using Monomer-Feed-Copolymer Composition Data

Theory

Using a conditional probability approach, Seiner and Litt⁴⁴ derived an equation (48 below), expressing the instantaneous copolymer composition in terms of the free monomers M_1 and M_2 , and the comonomer complex $\overline{M_1M_2}$ from the kinetic scheme 39-47.

$$\frac{d[M_1]}{d[M_2]} = \frac{1 + \left(\frac{r_{21}}{r_{221}} + \frac{r_{21}}{r_{212}} \right) \frac{[C]}{[M_1]} + \left(\frac{r_{12}}{r_{121}} \frac{[C]}{[M_2]} \right) \left| \frac{1 + \left\{ \frac{r_{21}}{r_{221}} \frac{[C]}{[M_1]} \right\}}{1 + \left\{ \frac{r_{12}}{r_{112}} \frac{[C]}{[M_2]} \right\}} \right|}{r_{21} \frac{[M_2]}{[M_1]} + 1 + \left(\frac{2r_{21}}{r_{221}} + \frac{r_{21}}{r_{212}} \right) \frac{[C]}{[M_1]} + \left(\frac{r_{12}}{r_{121}} \frac{[C]}{[M_2]} \right) \left| \frac{1 + \left\{ \frac{r_{21}}{r_{221}} \frac{[C]}{[M_1]} \right\}}{1 + \left\{ \frac{r_{12}}{r_{112}} \frac{[C]}{[M_2]} \right\}} \right|} \quad (48)$$

$$\frac{d[M_1]}{d[M_2]} = \frac{1 + \left(\frac{r_{12}}{r_{112}} + \frac{r_{12}}{r_{121}} \right) \frac{[C]}{[M_2]} + \left(\frac{r_{21}}{r_{212}} \frac{[C]}{[M_1]} \right) \left| \frac{1 + \left\{ \frac{r_{12}}{r_{112}} \frac{[C]}{[M_2]} \right\}}{1 + \left\{ \frac{r_{21}}{r_{221}} \frac{[C]}{[M_1]} \right\}} \right|}{r_{12} \frac{[M_1]}{[M_2]} + 1 + \left(\frac{2r_{12}}{r_{112}} + \frac{r_{12}}{r_{121}} \right) \frac{[C]}{[M_2]} + \left(\frac{r_{21}}{r_{212}} \frac{[C]}{[M_1]} \right) \left| \frac{1 + \left\{ \frac{r_{12}}{r_{112}} \frac{[C]}{[M_2]} \right\}}{1 + \left\{ \frac{r_{21}}{r_{221}} \frac{[C]}{[M_1]} \right\}} \right|}$$

$$\text{where } r_{12} = \frac{k_{11}}{k_{12}}, \quad r_{21} = \frac{k_{22}}{k_{21}}, \quad r_{1\bar{1}\bar{2}} = \frac{k_{11}}{k_{1\bar{1}\bar{2}}}, \quad k_{2\bar{1}\bar{2}} = \frac{k_{22}}{k_{2\bar{1}\bar{2}}}, \quad r_{1\bar{2}\bar{1}} = \frac{k_{11}}{k_{1\bar{2}\bar{1}}} \text{ and}$$

$$r_{2\bar{2}\bar{1}} = \frac{k_{22}}{k_{2\bar{2}\bar{1}}}.$$

This equation can be made more tractable providing one is willing to make a number of assumptions. Even so it still suffers from a number of disadvantages. This study therefore chose to employ the alternative treatment of Cais et al.,⁴⁵ who redefined the reactivity ratios as

$$r_1 = \frac{k_{11}}{k_{12}}; \quad r_2 = \frac{k_{22}}{k_{21}}; \quad p_1 = \frac{k_{1\bar{1}\bar{2}}}{k_{1\bar{2}\bar{1}}}; \quad p_2 = \frac{k_{2\bar{2}\bar{1}}}{k_{2\bar{1}\bar{2}}}; \quad s_1 = \frac{k_{1\bar{2}\bar{1}}}{k_{12}} \text{ and}$$

$$s_2 = \frac{k_{2\bar{1}\bar{2}}}{k_{21}}$$

The transition probabilities for the events given by equations 39-47 were represented by P_{11} , P_{12} , $P_{1\bar{1}\bar{2}}$, P_{21} , P_{22} , $P_{2\bar{2}\bar{1}}$ and $P_{2\bar{1}\bar{2}}$ respectively and defined on the basis of equations 49 and 50.

$$P_{11} + P_{12} + P_{1\bar{2}\bar{1}} + P_{1\bar{1}\bar{2}} = 1 \quad (49)$$

$$P_{22} + P_{21} + P_{2\bar{2}\bar{1}} + P_{2\bar{1}\bar{2}} = 1 \quad (50)$$

It follows that the individual transition probabilities can be represented by the relationships 51 or 52.

$$P_{1x} = \frac{\text{RATE OF ADDITION OF SUBSTRATE } x \text{ to } \text{---}M_1}{\sum_x (\text{RATE OF ADDITION OF SUBSTRATE } x \text{ to } \text{---}M_1)} \quad (51)$$

$$P_{2x} = \frac{\text{RATE OF ADDITION OF SUBSTRATE } x \text{ to } \overline{M_2}}{\sum_x (\text{RATE OF ADDITION OF SUBSTRATE } x \text{ to } \overline{M_2})} \quad (52)$$

where $x = 1, 2, \overline{12}$ or $\overline{21}$.

Consequently, the transition probabilities can be expressed in terms of the reactivity ratios, and the instantaneous concentrations of monomers and comonomer complex as shown below,

$$P_{11} = r_1[M_1]/\Sigma M_1; \quad P_{12} = [M_2]/\Sigma M_1; \quad P_{1\overline{21}} = s_1[\overline{M_1M_2}]/\Sigma M_1;$$

$$P_{1\overline{12}} = s_1 p_1 [\overline{M_1M_2}]/\Sigma M_1; \quad P_{21} = [M_1]/\Sigma M_2; \quad P_{22} = r_2[M_2]/\Sigma M_2;$$

$$P_{2\overline{21}} = s_2 p_2 [\overline{M_1M_2}]/\Sigma M_2; \quad P_{2\overline{12}} = s_2 [\overline{M_1M_2}]/\Sigma M_2$$

where $[M_1]$, $[M_2]$ and $[\overline{M_1M_2}]$ are the concentrations of the monomers M_1 , M_2 , and the comonomer complex; and ΣM_1 and ΣM_2 are given by the relationships 53 and 54.

$$\Sigma M_1 = r_1[M_1] + [M_2] + s_1[\overline{M_1M_2}] ([M_2] + p_1) \quad (53)$$

$$\Sigma M_2 = [M_1] + r_2[M_2] + s_2[\overline{M_1M_2}] ([M_1] + p_2) \quad (54)$$

This approach has enabled Cais et al.⁴⁵ to recast the expression for the copolymer composition in a much simpler form than that of the Seiner and Litt relationship, specifically

$$\frac{d[M_1]}{d[M_2]} = \frac{(1 - P_{12})(P_{21} + P_{2\overline{21}}) + (1 - P_{22})(P_{12} + P_{1\overline{12}})}{(1 - P_{11})(P_{21} + P_{2\overline{21}}) + (1 - P_{21})(P_{12} + P_{1\overline{12}})} \quad (55)$$

Following Cais et al.,⁴⁵ this study employs equation 55 together with

copolymer composition data, in conjunction with a minimisation technique (cf. Chapter 4.2) to yield "best estimates" of the transition probabilities, and hence of the reactivity ratios.

6.2 MONOMER FEED-COPOLYMER COMPOSITION ANALYSIS OF THE MGN-MS AND MGN-IP COPOLYMERISATIONS.

In attempting to define the best model by which a copolymerisation may be described, the discrimination must involve extremely careful analysis. As the copolymerisation mechanism becomes more involved, the number of parameters describing the system increases, making more demands on the quality of the experimental measurements. Consequently, as evaluation of copolymerisation models will be made on the ability of each model to describe the experimental monomer feed-copolymer composition data, it was deemed necessary to expand the experimental data contained in Tables 4.4 and 4.5. To this end four additional copolymerisations (each performed at least twice) for both the MGN-MS and the MGN-IP systems were carried out at MGN monomer feed ratios of 0.15, 0.35, 0.65 and 0.85. Tables 6.1 and 6.2 contain this expanded copolymer composition data, together with the comonomer complex concentration calculated from the nmr studies of Chapter 5. (NB These data and the following analysis of the copolymerisation models neglects the presence of any solvent-monomer complexation in system 16 although, on the basis of the ionisation potential of toluene, such MGN-toluene complexation may occur. However, other than altering the concentration of the MGN-IP complex, it is assumed that such a solvent interaction will exert little influence on the copolymer composition.³⁶)

The data contained in Tables 6.1 and 6.2 reveal the maximum concentration of comonomer complex in systems 19 and 16 to be around 18% and 7% respectively. That such a relatively low concentration of

TABLE 6.1

Expanded MGN-MS Monomer Feed-Copolymer Composition Data^a

LOADED		MONOMER FEED COMPOSITION			COPOLYMER COMPOSITION ^b	
MGN (mol.dm ⁻³)	MS (mol.dm ⁻³)	MGN (mol.dm ⁻³)	MS (mol.dm ⁻³)	Comonomer Complex (mol.dm ⁻³)	Mole Fraction MGN ^d (x _{MGN})	Mole Fraction MGN (x _{MGN})
0.78	7.04	0.39	6.65	0.39	0.10	0.351
1.18	6.70	0.64	6.16	0.54	0.15	0.382
1.59	6.36	0.88	5.66	0.70	0.20	0.404
2.43	5.67	1.47	4.71	0.96	0.30	0.445
2.86	5.31	1.79	4.24	1.07	0.35	0.462
3.30	4.94	2.15	3.79	1.15	0.40	0.460
4.19	4.19	2.94	2.94	1.25	0.50	0.481
5.12	3.42	3.91	2.21	1.21	0.60	0.490
5.60	3.02	4.44	1.86	1.16	0.65	0.502
6.09	2.61	5.00	1.52	1.09	0.70	0.509
7.09	1.77	6.26	0.94	0.83	0.80	0.531
7.61	1.34	6.90	0.63	0.71	0.85	0.555
8.13	0.90	7.67	0.44	0.46	0.90	0.601

a) Bulk polymerisation at 323K; 0.25 mol.% AIBN.

b) Mean values from repeated measurements.

c) Calculated using value of $K_Q = 0.14 \text{ dm}^3 \text{ mol}^{-1}$ (cf. Chapter 5.3.3).

d) Calculated from the LOADED monomer feed data.

TABLE 6.2
Expanded MGN-IP Monomer Feed-Copolymer Composition Data^a

<u>LOADED</u>		<u>MONOMER FEED COMPOSITION</u>			<u>COPOLYMER COMPOSITION^b</u>	
MGN (mol dm ³)	IP (mol dm ³)	MGN (mol dm ³)	IP (mol dm ³)	<u>CALCULATED^c</u> Comonomer Complex (mol dm ³)	Mole Fraction MGN ^d (x _{MGN})	Mole Fraction MGN (x _{MGN})
0.80	7.20	0.60	0.21	0.21	0.10	0.336
1.20	6.80	0.91	6.51	0.30	0.15	0.375
1.60	6.40	1.23	6.03	0.37	0.20	0.407
2.40	5.60	1.91	5.11	0.49	0.30	0.434
2.80	5.20	2.27	4.67	0.53	0.35	0.447
3.20	4.80	2.64	4.24	0.56	0.40	0.440
4.00	4.00	3.42	3.42	0.58	0.50	0.458
4.80	3.20	4.24	2.64	0.56	0.60	0.475
5.20	2.80	4.67	2.27	0.53	0.65	0.480
5.60	2.40	5.11	1.91	0.49	0.70	0.489
6.40	1.60	6.03	1.23	0.37	0.80	0.511
6.80	1.20	6.51	0.91	0.30	0.85	0.523
7.20	0.80	6.99	0.60	0.21	0.90	0.534

a) Solution Copolymerisation; Total monomer concentration = 8M; 1 mol% AIBN; Polymerisation temperature 333K.

b) Mean values from repeated measurements.

c) Calculated using the value of $K_Q = 5.5 \times 10^{-2} \text{ dm}^3 \text{ mol}^{-1}$ (cf. Chapter 5.3.3).

d) Calculated from the LOADED monomer feed data.

complexed species may compete effectively in a copolymerisation has been rationalised on the basis of the enhanced reactivity of an EDA complex. It is postulated⁴⁴ that, as an EDA complex has a larger π electron system than either monomer, it will be more polarisable, and consequently will interact more readily with an approaching radical of the correct polarity than an individual monomer can. This is still, however, a debated point.

6.2.1 Model Discrimination in MGN Copolymerisations on the Basis of Monomer Feed-Copolymer Composition Data

The choice between the terminal model and the complex participation model, as the best description of the mechanism of the MGN-IP and MGN-MS copolymerisation systems is made on the ability of each model to describe the experimental monomer feed-copolymer composition data. This "goodness" of fit is gauged by examining the residual sum of squares of the non-linear least squares fit to the corresponding copolymer equation (13 or 55).

In both the MGN-IP and MGN-MS systems the terminal model was analysed in terms of the "loaded" monomer feed-copolymer composition data. Inherent in this approach are a number of assumptions.

- Either (a) There is no comonomer complex formed per se.
 or (b) The concentration of any such complex is low, complexation does little if anything to alter the reactivity of either monomer, and upon radical attack the complex immediately dissociates releasing one of the monomers.

The latter point raised in (b) has arguably some validity in view of the relative magnitude of the enthalpy of complex formation ca. 6.5 kJ mol^{-1} and that of the enthalpy of polymerisation, ca. $30\text{--}60 \text{ kJ mol}^{-1}$ (for the addition of one monomer), i.e. it is possible that the resulting high vibration at the end of the propagating end of the chain may dissociate a

weakly complexed species making the simultaneous addition of a comonomer complex unlikely.²²²

6.2.2 The MGN(1)-MS(2) Copolymerisation System

In the analysis of both the terminal and complex participation models, the Fortran program requires the user to input a realistic starting set of reactivity ratios. For the terminal model fit, the minimisation program was found to converge rapidly from various estimated starting values of r_1 and r_2 to a unique minimum defined by the model parameters given in Table 6.3. In fitting the complex participation model to the experimental data, the six reactivity ratios were allowed to assume "best values". However, the equilibrium constant was fixed at the value determined by the nmr complexation analysis described in Chapter 5.3.3. (NB. The Fortran program employs the equilibrium constant defined in terms of mole fractions.) Using this model the program converged on various local minima each defined by their own set of reactivity ratios. In this case the set of parameters which yielded the lowest residual sum of squares was considered best to describe the data and these parameters are also presented in Table 6.3.

Figure 6.1 displays the non linear least squares fit of both models to the experimental data and Figure 6.2 the corresponding residuals.

Only a small difference separates the two curves of Figure 6.1, although the complex model is in better agreement with the experimental data over the entire composition range, and has no discernible structure to the deviations of the experimental points about the calculated curve as shown by Figure 6.2 - ie. apparently random deviations result.

The reactivity ratios calculated for the complex participation model are not unrealistic, r_1 , r_2 , p_1 and p_2 are all < 1 . The values of the parameters s_1 and s_2 should give an indication of the extent of complex participation in the predominantly alternating

TABLE 6.3

Reactivity Ratios^{a,b} derived using the Terminal or Complex Participation Models for the Bulk Copolymerisation of MGN and α -Methyl Styrene at 323K.

<u>Copolymerisation Model</u>	<u>Parameter</u>	<u>Value</u>	<u>Error Range^c</u>
Terminal Model	r_1	0.049	(0.034-0.065)
	r_2	0.109	(0.09 - 0.13)
	S.S. ^d	8.56×10^{-4}	-
Complex Participation Model	r_1	0.041	(0.042-0.047)
	r_2	0.138	(0.121-0.163)
	P_1	0.162	(0.00 -0.605)
	P_2	0.160	(0.072-0.273)
	S_1	0.249	(0.00 -0.615)
	S_2	1.654	(1.321-2.108)
	S.S. ^d	3.03×10^{-4}	-
	K_x^e	1.03	-

- a) Defined for the terminal model in Chapter 4.2 and for the complex participation model, in Chapter 6.1.
- b) The subscript 1 (in the reactivity ratios) denotes the MGN parameter, subscript 2 the comonomer, ie.
$$r_1 = \frac{k_{MGN \cdot + MGN}}{k_{MGN \cdot + \alpha MS}} \text{ etc}$$
- c) Calculated as defined in Chapter 4.2.
- d) S.S. = Residual Sum of Squares defined as $SS = \sum (Y_{exp} - Y_{calc})^2$.
- e) Defined as the mole fraction equilibrium constant fixed at the value determined by nmr analysis.

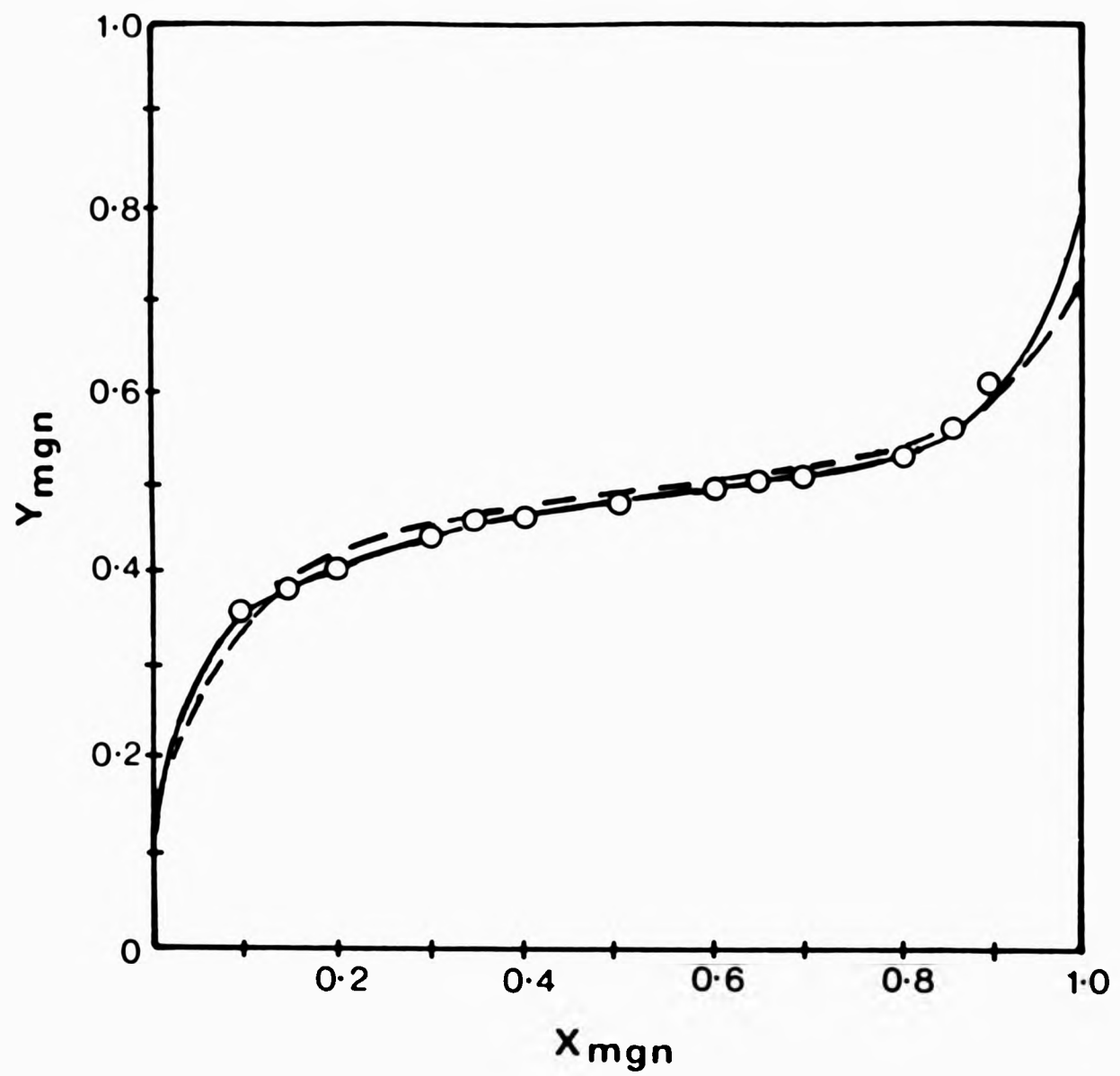


FIGURE 6.1 Copolymer composition curve for the copolymerisation of MGN and α -MS in bulk at 323K. (Y_{MGN} = mole fraction of MGN in copolymer; X_{MGN} = mole fraction MGN in the monomer feed; (O) = experimental data; (---) = terminal model fit and (—) = complex model fit).

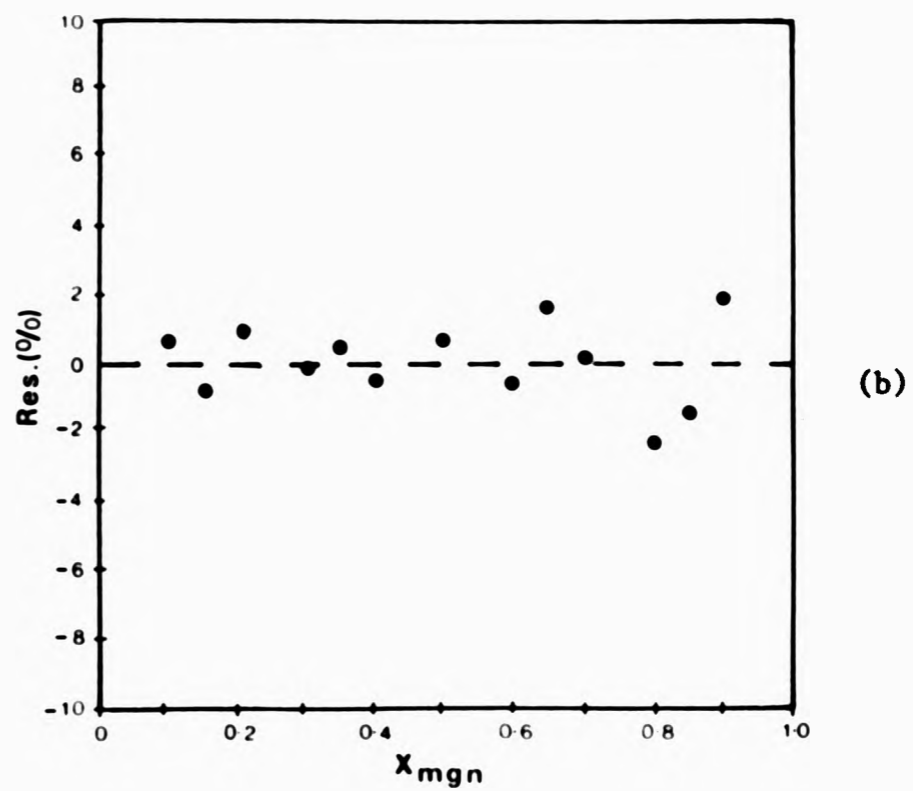
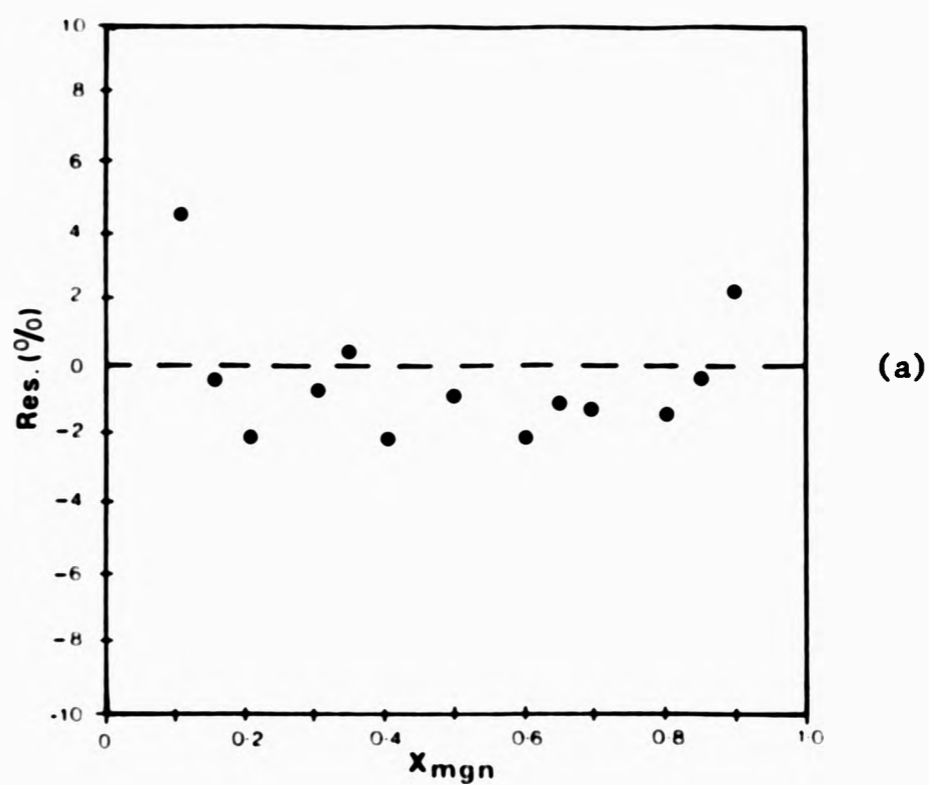


FIGURE 6.2

Residuals from (a) the terminal model fit, and (b) the complex participation model fit. Residuals are calculated in the form;

$$\text{Res} = \frac{(Y_{\text{calc}} - Y_{\text{exp}})}{Y_{\text{exp}}} \times \frac{100}{1}$$

copolymerisation. The value of $s_1 < 1$ suggests free MS more likely to add to a propagating MGN radical than a complexed MS monomer.

As regards the MS chain end radical, a value of s_2 ca. 1-2, indicates an almost equal propensity to add free and complexed MGN. Neither the magnitude of S_1 nor S_2 suggests a highly reactive comonomer complex although it does infer the participation of the complex in the copolymerisation.

The ability to calculate reactivity ratios implying complex participation and of the model to describe the experimental data to a more satisfactory degree than the Mayo-Lewis treatment does not inevitably lead to the conclusion that there is complex participation in the MGN-MS system. Hill and O'Donnell²²¹ have proposed the use of objective statistical tests such as the F-test,²²³ in an attempt to decide whether the improvement of curve fit of the complex participation model over the terminal model is statistically significant or merely due to the inherent use of an increased number of parameters (although it is realised that an increase in the number of parameters does not necessarily improve the fitting procedure).

The F-test is based on the ratio F of the residual sum of squares of the two models being compared according to the formula 56, (Implicit in the F-test is the assumption that the errors are normally distributed with constant variance),

$$F = \frac{(SS_A - SS_B)/(P_A - P_B)}{SS_A/(n - P_A)} \quad (56)$$

where model B (in this study the complex participation model) is a special case of model A (the terminal model). P_A and P_B are the number of variable parameters in the respective model and n is the number

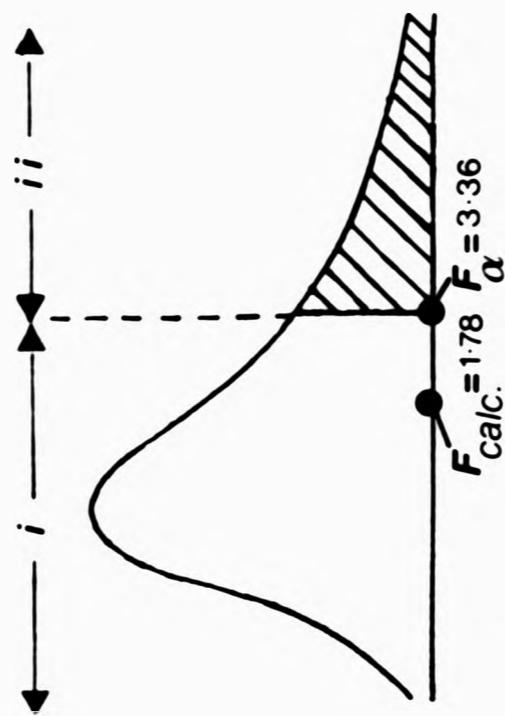
of experimental data points. The value of F calculated by equation 56, is compared to a critical value of F , F_{α} , which is documented in statistical probability tables (Appendix 1). The data are then considered statistically significant if $F > F_{\alpha}$ holds. Applying this test in a comparison of the fit of the terminal and complex participation models to the MGN-MS experimental data yields an F_{calc} value of 1.78 which may be compared at the 0.05 significance level, with $F_{\alpha} = 3.36$ (see Appendix 1). This is shown graphically in Figure 6.3(a). From this analysis one may conclude that there is no statistically significant improvement in the fit to the experimental data on going from the terminal model analysis to the higher order complex participation model.

6.2.3 The MGN(1)-IP(2) Copolymerisation System

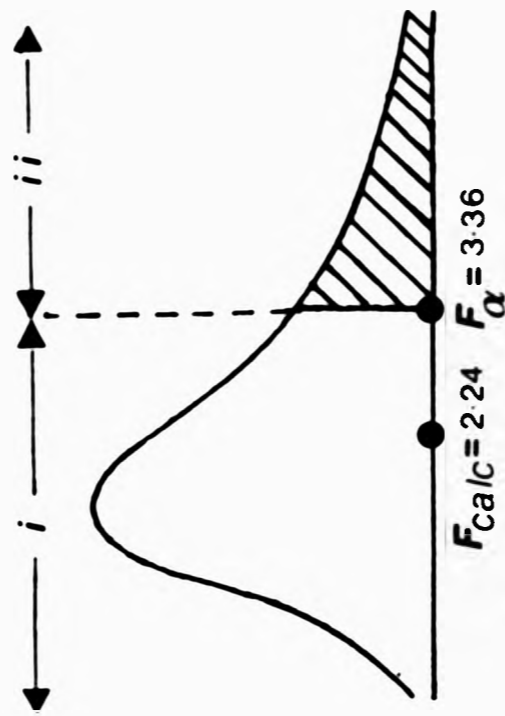
The best fit of the terminal model and of the complex participation model to the MGN-IP experimental data are shown in Figure 6.4. Again only a small difference between the curves is evident, although the terminal model fit does possess some structure to the residuals as illustrated in Figure 6.5. The corresponding reactivity ratios are presented in Table 6.4 together with their estimated error range.

The reactivity ratios for the complex participation model are chemically realistic, r_1 , r_2 , p_1 and $p_2 < 1$. Additionally, the non-zero values of s_1 and s_2 suggest complex involvement in the copolymerisation. As with the MGN-MS system $S_2 > 1$, which could be explained by the fact that it is more favourable to have the more stable comonomer (IP or MS) as the resulting radical when MGN adds to the comonomer ended propagating chain.

As to whether or not the improvement in fit of the complex participation model over the terminal model is statistically significant again requires application of the F test. This yields $F_{\text{calc}} = 2.24$ which may be compared to the critical F_{α} value (at the 0.05 significance



(a) The MGN-MS system.



(b) The MGN-IP system.

FIGURE 6.3 The F probability distribution at the 0.05 significance level: the value of F calculated from equation 56, for the terminal model vs. complex participation model (F_{calc}) is compared with the critical value of F_{α} (see Appendix 1).
 Region (i) = A 0.95 probability that there is no significant improvement employing the higher order model.
 Region (ii) = A 0.95 probability that there is a significant improvement employing the higher order model.

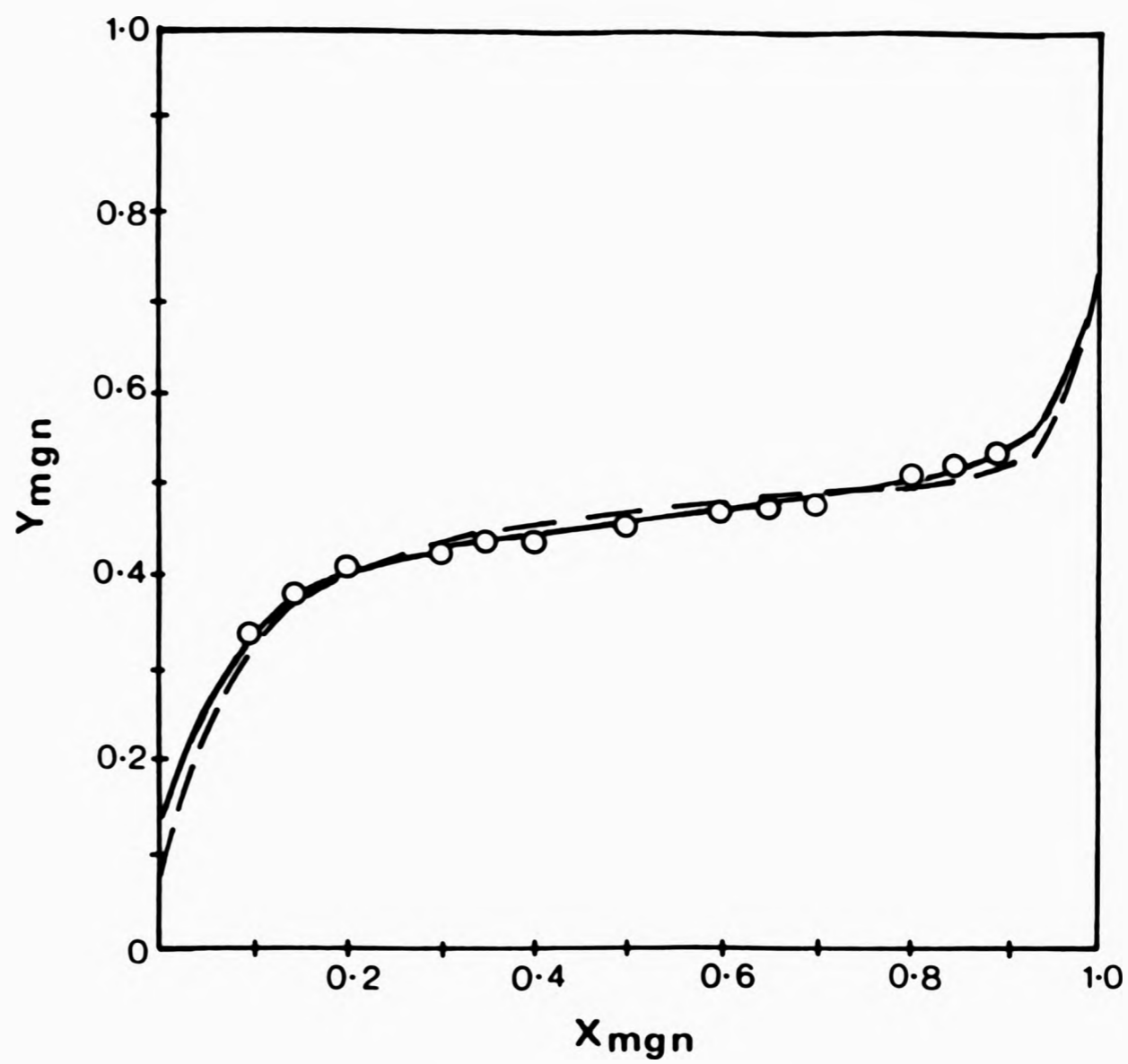


FIGURE 6.4 Copolymer composition curve for the solution copolymerisation of MGN and IP at 333K. (Y_{MGN} = mole fraction MGN in the copolymer; X_{MGN} = mole fraction MGN in the monomer feed; (O) = experimental data; (----) = terminal model fit; (—) = complex participation model fit.

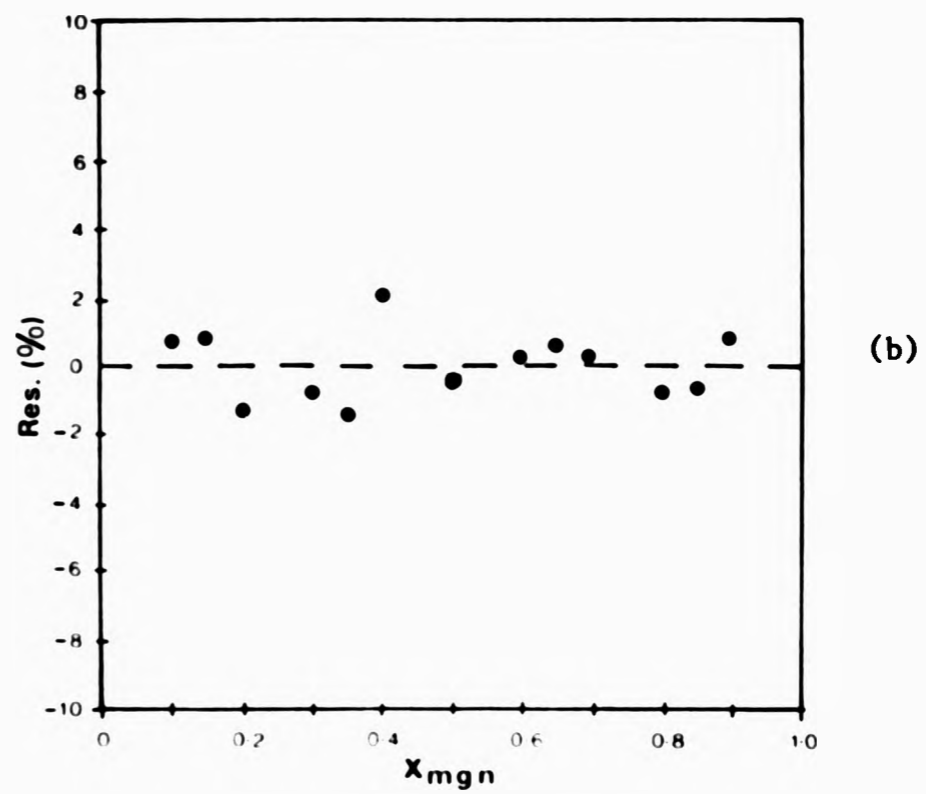
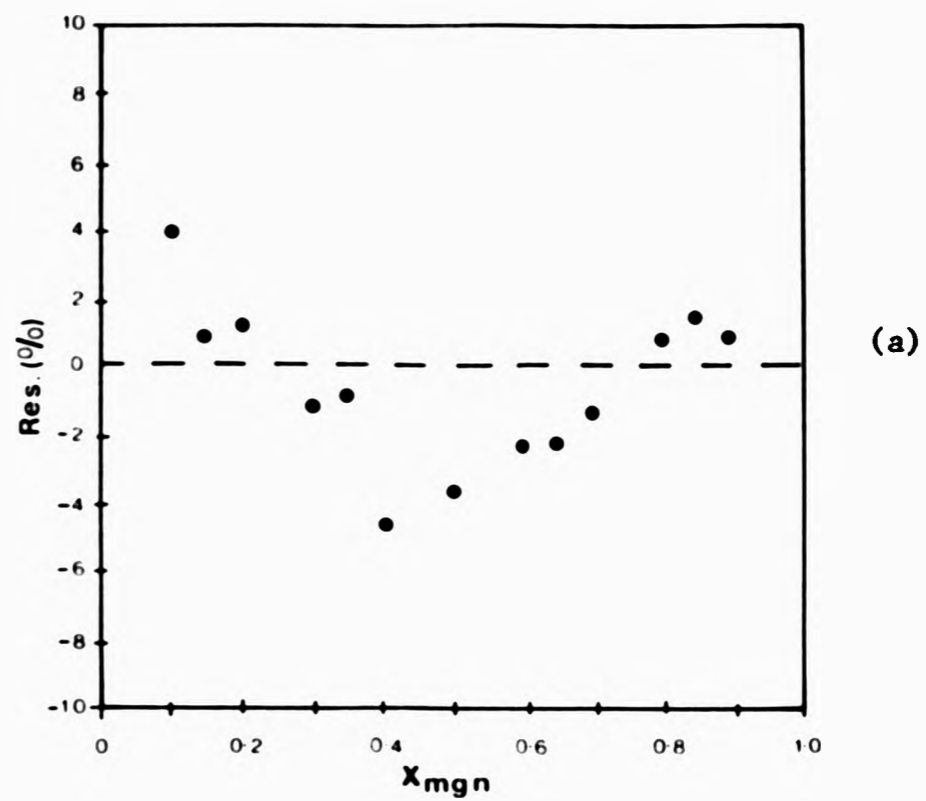


FIGURE 6.5 Residuals for the (a) terminal model fit, (b) complex participation model fit. Residuals are calculated in the form:

$$\text{Res}(\%) = \frac{(Y_{\text{calc}}) - Y_{\text{exp}}}{Y_{\text{exp}}} \times \frac{100}{1}$$

TABLE 6.4
Reactivity Ratios^{a,b} derived using the Terminal or Complex
Participation Models for the Solution Copolymerisation of MGN
and Isoprene at 333K.

<u>Copolymerisation Model</u>	<u>Parameter</u>	<u>Value</u>	<u>Error Range^c</u>
Terminal Model	r_1	0.016	(0.003-0.03)
	r_2	0.109	(0.102- 0.151)
	S.S. ^d	1.36×10^{-3}	-
Complex Participation Model	r_1	0.017	(0.012-0.022)
	r_2	0.152	(0.153-0.172)
	p_1	0.85	(0.116-1.655)
	p_2	0.39	(0.261-0.528)
	s_1	0.18	(0.032-0.372)
	s_2	2.56	(2.055-3.401)
	S.S. ^d	2.50×10^{-4}	-
	K_x^e	0.37	-

- a) Defined for the terminal model in Chapter 4.2 and for the complex participation model, in Chapter 6.1.
- b) The subscript 1 in the reactivity ratios denotes the MGN parameter, subscript 2 the comonomer parameter.
- c) Calculated as defined in Chapter 4.2.
- d) S.S. = Residual Sum of Squares defined as $SS = \sum (Y_{\text{exp}} - Y_{\text{calc}})^2$.
- e) Defined as the mole fraction equilibrium constant fixed at the value determined by nmr analysis.

level) of 3.36, as illustrated in Figure 6.3(b). From this analysis, one may conclude that, as in the MGN-MS copolymerisation system, the expansion of the terminal model to include the participation of a comonomer complex does not significantly improve its ability to describe the experimental monomer feed-copolymer composition data.

However, Figures 6.1 and 6.2, and 6.4 and 6.5, do show that a terminal model analysis of both the MGN-MS and MGN-IP copolymerisation systems produces small systematic deviations between the experimental copolymer compositions and those predicted on the basis of this model (cf. the Kelen-Tüdös analysis of Chapter 5.5.4). There are a number of possible explanations for this observation.

6.3 THE MAYO-LEWIS TERMINAL MODEL: SOURCES OF DEVIATIONS

Kelen and Tüdös have stated²²⁴ that the terminal model cannot be as widely applied to copolymerisation systems as is implicitly assumed in the literature. The inability of this model to describe accurately a copolymer system has been attributed to a number of factors, the most important of which are:

- a) Where one or both of the monomers are capable of association, making it necessary to consider a third polymerisable species³⁸ i.e. EDA complex formation.
- b) If a penultimate unit in the propagating chain influences the reactivity of the chain end radical.³⁵ This situation requires expansion of the Mayo-Lewis model to incorporate three or four kinetically different radicals.
- c) If the copolymerisation is carried out at, or near to the ceiling temperature of one of the monomers it may be necessary to consider, in the kinetic scheme, a depropagation reaction.²²⁵

- d) If one of the monomers is a diene, it may add to a propagating radical in a number of ways, eg. 1,2-, 3,4-, or 1,4- addition.
- e) Experimental error; there is always the possibility that the source of the deviations is analytical in nature.

With respect to the present copolymerisation systems, it is conceivable that a number of the five points raised above may indeed be the source of the small deviations between predicted and experimental copolymer compositions.

A survey of the literature reveals that a number of copolymerisation systems found to deviate from the terminal model involve nitrile monomers, for example the styrene-acrylonitrile,³³ butadiene-acrylonitrile,²²⁶ styrene-fumaronitrile,³² and vinylidene cyanide-maleic anhydride²²⁷ systems. Such observations have been explained either by invoking complex participation, as already discussed but rejected for the present copolymerisation systems, or by proposing a penultimate influence in the system. The latter effect is suggested to be a result of repulsive electrostatic forces between the polar nitrile groups of an incoming nitrile monomer and a penultimate nitrile unit of the propagating radical chain. In view of the chemical structure of MGN one may anticipate a penultimate influence and consequently a small deviation from terminal model copolymer composition predictions.

6.4 THE PENULTIMATE COPOLYMERISATION MODEL

The penultimate model of vinyl copolymerisation, a higher order analogue of the terminal model, proposes that the identity of the penultimate unit, that is the monomer unit adjacent to the radical end group on a growing copolymer chain, can affect the rate of addition of a polymer molecule to a monomer.³¹ The presence of such an influence in a copolymerisation complicates the kinetic analysis and in general

requires eight propagation reactions to describe the system (57-64 below).



four reactivity ratios may be defined as

$$r_1 = \frac{k_{111}}{k_{112}}; \quad r_2 = \frac{k_{222}}{k_{221}}; \quad p_1 = \frac{k_{211}}{k_{212}}; \quad p_2 = \frac{k_{122}}{k_{121}}.$$

Each monomer is therefore characterised by two reactivity ratios.

From this kinetic approach, where a penultimate effect operates in

the system, the instantaneous copolymer composition is given by equation 65,

$$\frac{d[M_1]}{d[M_2]} = \frac{1 + \frac{p_1[M_1]/[M_2](r_1[M_1]/[M_2]+1)}{(p_1[M_1]/[M_2]+1)}}{1 + \frac{p_2(r_2+[M_1]/[M_2])}{[M_1]/[M_2](p_2+[M_1]/[M_2])}} \quad (65)$$

Using this relationship, the iterative non-linear least squares curve fitting procedure may be used to calculate the best fit to the experimental copolymer composition data.

However, it has been pointed out that the distinction between the terminal model and penultimate model of a copolymerisation system based on monomer feed-copolymer composition data is frequently very difficult (although not impossible) to achieve.²²⁸

6.4.1 Penultimate Model Analysis of the MGN(1)-MS(2) Copolymerisation System

In order to analyse the data of Table 6.2 with respect to the penultimate model it is again necessary to assume a negligible effect of EDA comonomer complex on the system.

The calculated copolymer-comonomer feed composition relationship for the penultimate model is compared with the terminal model fit to the experimental data in Figure 6.6. The higher order model does exhibit an improved fit. However, any penultimate effect is not large and the very different polarity of the two monomers is the dominating influence and causes the tendency towards alternation.

The "best estimates" of the penultimate reactivity ratios are given in Table 6.5, their values are indicative of penultimate effects for both MGN and MS ended radicals, i.e. $r_1 \neq P_1$ and $r_2 \neq P_2$. A closer

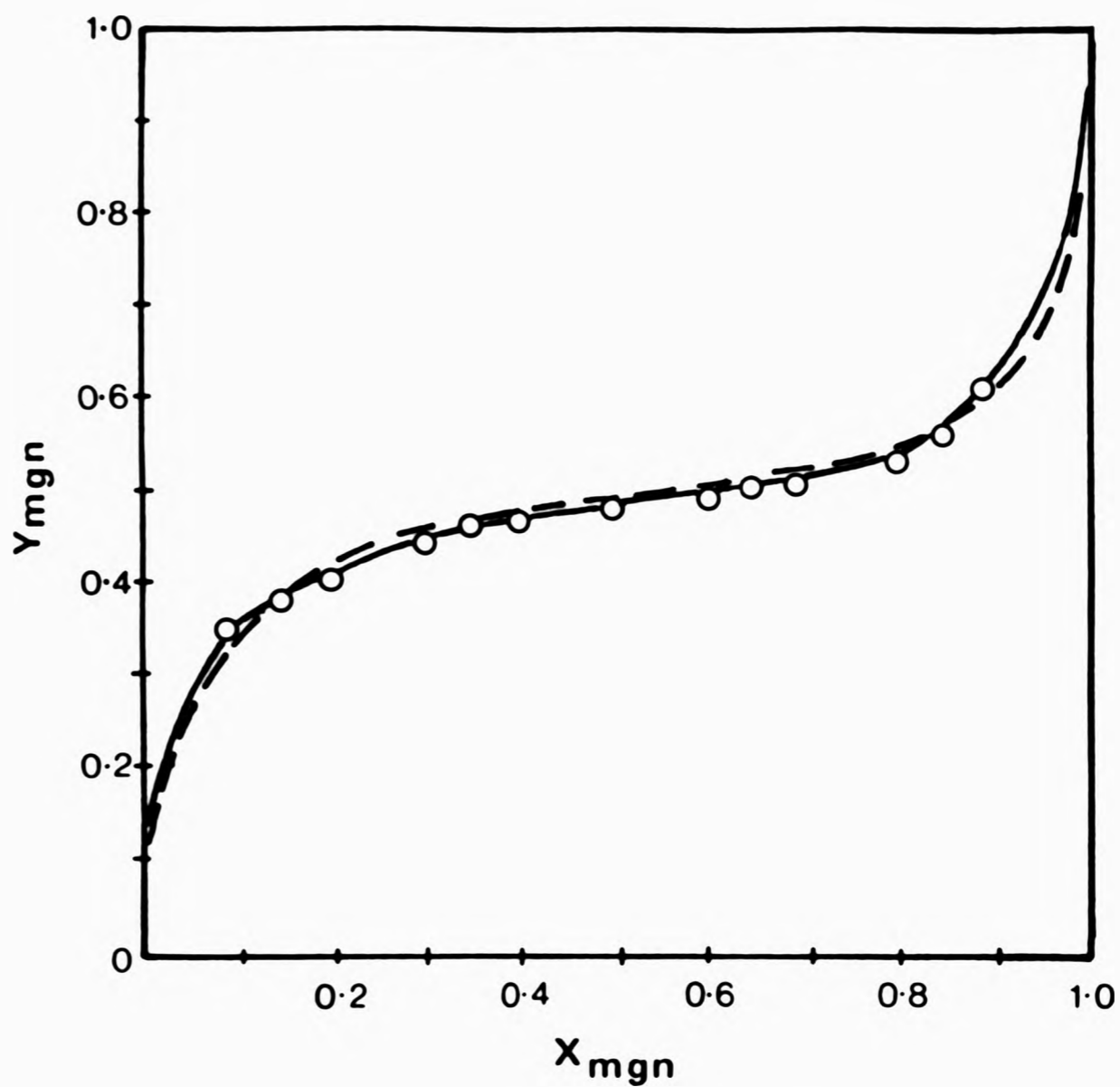


FIGURE 6.6 Copolymer composition curve for the bulk copolymerisation of MGN and α -MS at 323K. (Y_{MGN} = mole fraction MGN in copolymer; X_{MGN} = mole fraction MGN in monomer feed; (O) = experimental data; (---) = terminal model fit; (—) = penultimate model fit.

TABLE 6.5
Reactivity Ratios^{a, b} derived using the Penultimate Model for the
Bulk Copolymerisation of MGN and α -Methyl Styrene (MS) at 323K

<u>Parameter</u>	<u>Value</u>	<u>Error Range^c</u>
r_1	0.159	(0.121-0.196)
r_2	0.069	(0.051-0.085)
p_1	0.031	(0.027-0.035)
p_2	0.134	(0.121-0.153)
S.S. ^d	1.80×10^{-4}	-

a) Defined as in section 6.4.

b) The subscript 1 on the reactivity ratio denotes an MGN parameter.

c) Calculated as defined in Chapter 4.2

d) S.S. = Residual Sum of Squares defined as $SS = \sum (Y_{\text{exp}} - Y_{\text{calc}})^2$.

inspection of these parameters however makes the assignment of a penultimate influence in this system doubtful.

The value of $r_1 \left(\frac{k_{111}}{k_{112}} \right)$ is relatively large in comparison with the other reactivity ratios. Since the numerator of this ratio is the rate constant for the formation of an MGN triad, it is difficult to reconcile the relative magnitude of r_1 with the demonstrated reluctance of MGN to homopolymerise (cf. Chapter 3). Rationalisation of this set of reactivity ratios is therefore dubious, consequently one may not invoke a penultimate influence on the copolymerisation in order to explain the small deviations observed between the experimental copolymer compositions and those predicted on the basis of the terminal model. As specified in section 6.4, however, there are a number of possible alternative explanations of the source of this discrepancy. Specifically, the α -methyl styrene polymerisation has a ceiling temperature of 334K ²²⁹ (this is the temperature above which it is not possible to produce long-chain homopolymer from monomer at unit or lower concentration)²³⁰ therefore, it may be that modification of the terminal copolymer equation to take account of the depropagation of MS sequences could explain the deviations. Such a situation has been advocated by Lowry²³¹ for the styrene- α methyl styrene system.

6.4.2 A Penultimate Model Analysis of the MGN-IP Copolymerisation System

The best fit of the penultimate model to the monomer feed-copolymer composition data is shown in Figure 6.7. The Figure also illustrates that in comparison with the terminal model, this higher order model is in better agreement with the experimental data. The corresponding penultimate model reactivity ratios are shown in Table 6.6. Considering the error range estimated for the four parameters, it is possible that

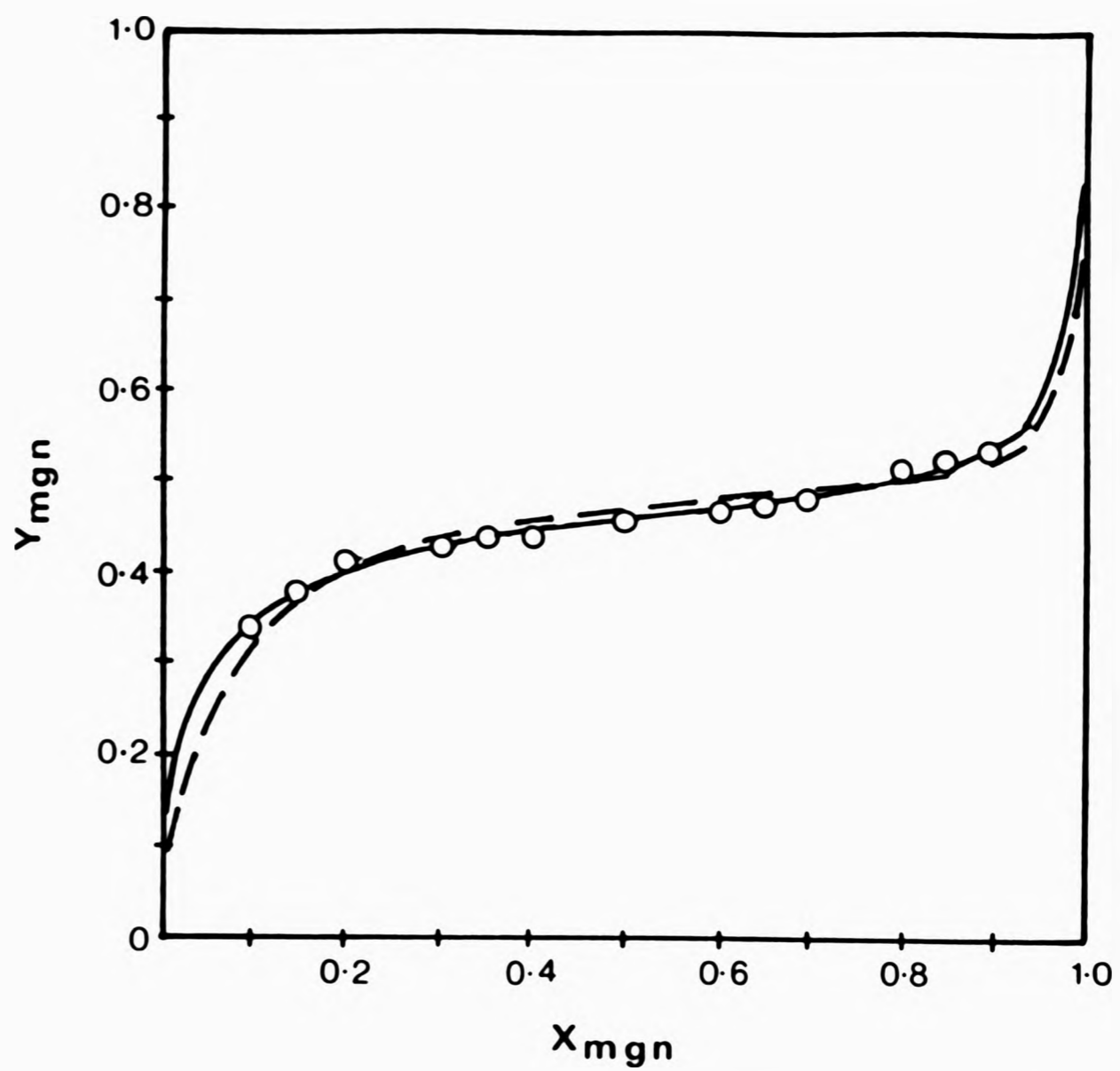


FIGURE 6.7 Copolymer composition curve for the solution copolymer of MGN and IP at 333K. (Y_{MGN} = mole fraction MGN in copolymer; X_{MGN} = mole fraction MGN in monomer feed; (O) = experimental data; (---) = terminal model fit; (—) = penultimate model fit, the 3 and 4 parameter penultimate model fits are indistinguishable.

TABLE 6.6

Reactivity Ratios^{a,b} derived using the Penultimate Model for the
Solution Copolymerisation of MGN and Isoprene (IP) at 333K

<u>Model</u>	<u>Parameter</u>	<u>Value</u>	<u>Error Range^c</u>
Penultimate Model	r_1	0.070	(0.0 -0.131)
	r_2	0.057	(0.042-0.083)
	p_1	0.014	(0.011-0.022)
	p_2	0.182	(0.164-0.213)
	S.S. ^d	4.51×10^{-4}	-
Restricted	r_1	0.019	(0.012-0.026)
Penultimate Model (ie. $r_1 = p_1$)	r_2	0.054	(0.031-0.070)
	p_2	0.189	(0.163-0.221)
	S.S. ^d	4.7×10^{-4}	-

a) Defined as in section 6.4.

b) The subscript 1 on the reactivity ratio denotes an MGN parameter.

c) Calculated as defined in Chapter 4.2

d) S.S. = Residual Sum of Squares defined as $SS = \sum (Y_{\text{exp}} - Y_{\text{calc}})^2$.

this best fit encompasses the situation whereby $r_1 = p_1$, i.e. no penultimate effect exists for the MGN ended radicals. Consequently, the system was re-examined using only three reactivity ratios. The fit of this "restricted" penultimate model is indistinguishable from the original four parameter fit. The resulting reactivity ratios are also presented in Table 6.6.

This analysis suggests a penultimate influence only on the isoprene ended radicals. Such an effect has been noted previously in diene copolymerisations by Vialle et al.²²⁶ and has been invoked as the possible source of deviations from the Mayo-Lewis copolymerisation scheme. It is, however, rather difficult to rationalise this behaviour on the basis of a through space repulsive interaction of polar substituents, bearing in mind that a penultimate MGN unit is separated from an incoming MGN monomer by the four carbon IP moiety.

It may be that what we are observing is not a penultimate effect per se, but is in fact a difference in the reactivity of an —IPIP and —MGNIP propagating species due to the nature of the terminal unit. In Chapter 5.5.4 it was identified that an IP monomer adds to a MGN radical predominantly in a 1,4- fashion (giving an $\text{—MGNIP}_{1,4}$ species). However, IP may add to a propagating IP radical (an increasingly probable situation at high IP feeds) in a 1,2 or 3,4-fashion (giving an $\text{—IPIP}_{1,2}$ or $\text{IPIP}_{3,4}$ species).²²¹ The inherent difference in such species may go some way to explaining the apparent penultimate effect observed on IP ended radicals in this system.

Application of the F test in a comparison of the terminal and the 3 parameter "penultimate model" (see Figure 6.8) shows the higher order model to provide a significant improvement over the Mayo-Lewis model with a level of probability of 0.95. This therefore presents statistical evidence for the use of the three parameter model to describe the MGN-IP

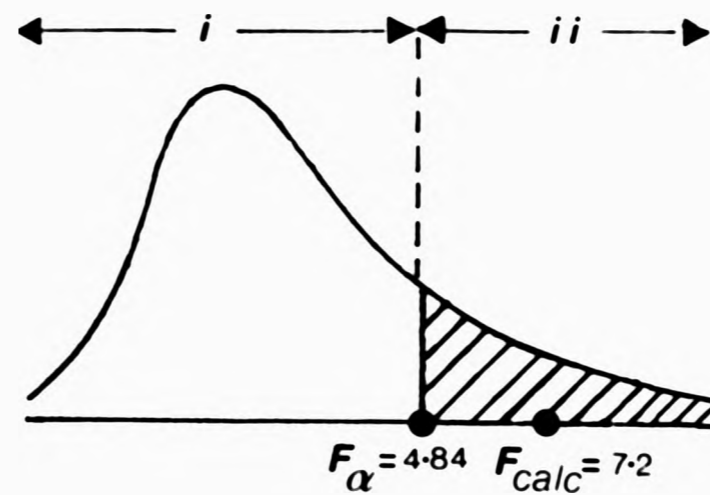


FIGURE 6.8 The F probability of the 0.05 significance level.
 (The whole of F calculated from equation 5, for the terminal model vs. the 3 parameter penultimate model is compared with the critical value of F_{α} (see Appendix 1) for the MGN-IP system.)

Region (i) = a 0.95 probability that there is no significant improvement by employing the higher order model
 Region (ii) = a 0.95 probability that there is a significant improvement.

copolymerisation system.

6.5 THE COPOLYMERISATION OF MGN-MS AND MGN-IP: CONCLUSIONS

This chapter has analysed the experimental monomer feed-copolymer composition data of the bulk MGN-MS and solution MGN-IP systems, in terms of the two copolymerisation models which may be applied to a predominantly alternating copolymerisation, in order to determine the probable copolymerisation mechanism involved. The ability of each model to describe the experimental data was gauged by determining the value of the residual sum of squares of the experimental vs. the calculated copolymer composition behaviour. By employing these values in the F-test, a standard statistical test, it was possible to decide whether any improvement in the fit to the experimental data using the higher order model was statistically significant, ie. the result of the F-test analysis was the criterion upon which the acceptance or rejection of the higher order complex participation model over the simpler terminal model was made. The use of the complex participation model to describe both the MGN-MS and the MGN-IP copolymerisations (under the present conditions), was rejected on the basis that it does not provide a statistically significant improvement in the ability to describe the experimental data over that of the Mayo-Lewis terminal model. Consequently, it is concluded that the alternating tendency observed in both copolymerisation systems is due to the polarity differences between the propagating radical chain end and the incoming monomer, which lowers the energy of activation of cross-propagation compared to the homopropagation reaction, and is not in effect due to significant comonomer complex participation. This then makes it necessary to reconcile the detected presence of a comonomer complex in both copolymerisation systems with the terminal model which excludes such

species. This leads to the proposal that the present systems do not generate a highly reactive comonomer complex able to add to a propagating radical as a single entity, but there occurs merely a weak association between the comonomers, involving a rapid equilibrium which does little to alter the reactivity of either monomer, and should a propagating radical species attack this complex, it promptly dissociates releasing one of the monomers.

The most likely origin(s) of the small deviations observed in both systems, between the experimental monomer feed-copolymer composition, and that predicted on the basis of the terminal model have been detailed. The possible influence of a penultimate effect, a principal source of the deviations observed in several nitrile monomer copolymerisations, on both systems 16 and 19 was examined. On the basis of an unrealistic reactivity ratio, a penultimate model was not considered to be a viable description of the MGN-MS bulk copolymerisation. On the other hand, a "restricted" penultimate analysis (3 reactivity ratios employed) of the MGN-IP system indicated a penultimate effect on the isoprene ended radicals. Application of the F-test in a comparison of this and the terminal model shows the former model to provide a significant improvement in the fit to the experimental data with a level of probability of 0.95. This finding can be explained, not by a penultimate effect per se, but by invoking chain propagation by the diene in more than one chemically distinguishable form.

Ideally, had more time been available, an extension of this copolymerisation study to include an analysis of the monomer sequence distribution in the copolymers prepared across a wide feed range would have been attempted. Hill et al.,²²¹ have found such data to contain valuable information although unlike copolymer composition data, the sequence distribution of monomers cannot always be determined easily.

ed: on the
ive d
ly, 7
ave
of
is
a
h
aris
a
ove
mar
lill
is d
as
g a p
of
ne fo
to
This
at se
ally
e time
dy to
copy
ill
in m
m to

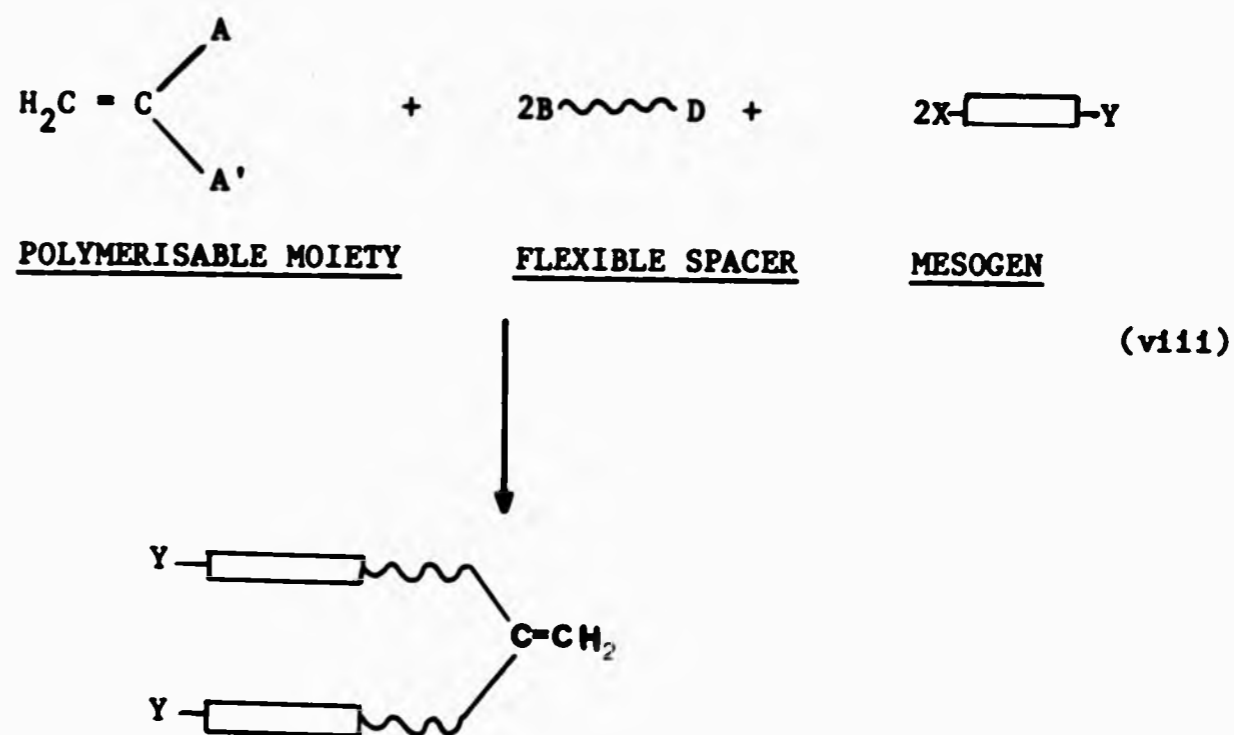
CHAPTER SEVEN

7.1 POSSIBLE APPLICATIONS OF MGN DERIVATIVES

2-Methyleneglutaronitrile's trifunctional structure offers the possibility of preparing, via elementary chemical reactions, a number of novel compounds. For example, complete hydrolysis of MGN yields the α - β unsaturated dibasic acid 2-methyleneglutaric acid which, in view of its structural similarity to itaconic acid, methacrylic acid and acrylic acid, may find similar outlets. Carrying out a controlled partial hydrolysis of MGN allows the preparation of 2-methyleneglutaramide, a difunctional amide offering an additional site for crosslinking over the conventional acrylamide copolymers employed in the preparation of thermosetting acrylic coatings. Alternatively, one may capitalise on the trifunctionality of MGN to prepare cyclic monomers which have the potential to yield high Tg materials eg. 2-methyleneglutaric anhydride or substituted imide derivatives. The experimental procedures for the formation of these, and many other derivatives, have been detailed previously in Chapter 2. These reactions, summarised in Figure 2.3, are an extension of the work proposed by USI.* These potential monomers, however, as derivatives of the dinitrile, may be equally prone to degradative chain transfer upon a radical polymerisation.

As an alternative to the exploratory study of the homopolymerisability-copolymerisability of selected MGN derivatives it was decided to digress somewhat and investigate the suitability of 2-methylene glutaric acid as the "polymerisable moiety" in the synthesis of difunctional cholesteric liquid crystalline side chain monomers, (viii).

* United States Industrial Chemicals Co.



Potential cholesteric monomer if mesogen is optically active.

(where A, A', B, D, X and Y are functional moieties)

7.2 THE PROPOSED SYNTHESIS OF CHOLESTERIC LIQUID CRYSTALLINE MONOMERS-POLYMERS

The intense interest in cholesteric liquid crystalline materials may be traced to the unique optical properties of the mesophase. Although the best known low molar mass substances which form a cholesteric mesophase are esters of cholesterol, non-steroidal liquid crystals that exhibit optical activity may also show a cholesteric mesophase (or as it is now more generally referred to a chiral nematic phase). In turn, cholesteric polymers may be synthesised by polymerising a vinyl monomer which has a low molar mass cholesteric mesogen attached to the alkene group via a flexible alkane spacer as outlined in (viii). However, attempts to obtain a cholesteric liquid crystalline polymer by merely polymerising the corresponding monomer have met with little success. Alternatively, if one copolymerises a cholesteric monomer with a nematic monomer, in analogy with the principle established for low molecular mass systems, polymers exhibiting a cholesteric mesophase can be realised.

This methodology was employed in the present synthesis and is illustrated in Figure 7.1, with the experimental procedures presented below in section 7.2.1.

7.2.1 Experimental Procedure.

Step (1) Friedel-Crafts Acylation (illustrated for biphenyl).

Biphenyl (0.3 mol) was dissolved in 400 cm³ of nitrobenzene to which 0.6 mol. of AlCl₃ was added in portions with stirring. To this solution, 0.3 mol. of ω -bromohexanoyl chloride was added dropwise. The deep red solution was stirred overnight then hydrolysed with a mixture of 100g of ice and 70 cm³ of conc. HCl. The organic layer was isolated and the nitrobenzene and unreacted biphenyl were removed with steam. The solid brown coloured residue was dissolved in toluene and chromatographed on an alumina column (neutral grade). The crude product was recrystallised from toluene.

Yield XXXI = 51%, m.pt. = 385K-392K.

Yield XXXII = 12%, m.pt. = 447K-452K.

Step (2): Illustrated for XXXI

The carbonyl group was reduced to CH₂ with LiAlH₄/AlCl₃ in a mixture of anhydrous chloroform/diethyl ether. 4-(ω -bromohexanol)-biphenyl (0.075 mol) in 250 cm³ of chloroform was added dropwise to a preformed solution of 0.185 mol. LiAlH₄/0.4 mol. AlCl₃ in 140 cm³ of diethyl ether. The reaction mixture was stirred at room temperature for 3 hours and then a mixture of 200 cm³ conc. HCl and 250 cm³ of H₂O was added carefully. The organic layer was isolated, washed with water and dried over Mg SO₄. The solvent was evaporated and the yellow solid purified on an alumina column (neutral grade) with toluene as elutant. The product was recrystallised from toluene.

Yield XXXIII = 80% m.pt. = 298K-301K.

Yield XXXIV = 35% m.pt. = 368K-374K.

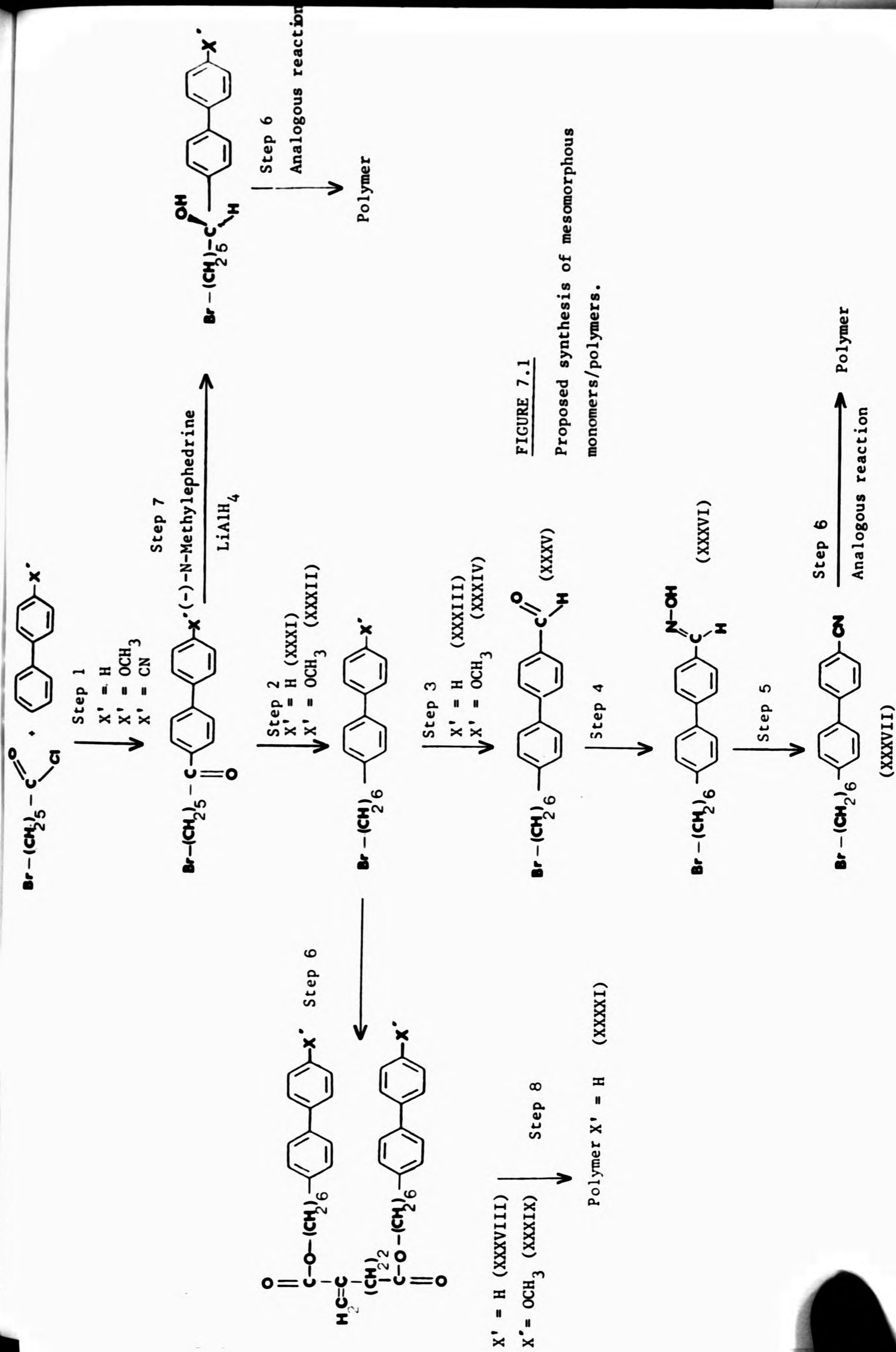


FIGURE 7.1

Proposed synthesis of mesomorphic monomers/polymers.

Step (3).

Prior to this reaction, dichloromethylbutyl ether was prepared. Formyl butanoate, 2.27 mol. (standard esterification) was added to 1.97 mol. P_2O_5 . The homogeneous yellow solution is heated for 15 mins., then distilled under reduced pressure. Yield = 60% b.pt. (0.15 torr) = 323K-330K.

4-(ω -bromohexyl)-4'-formyl biphenyl was prepared as follows.

To a solution of 0.043 mol. of 4-(ω -bromohexyl)-biphenyl in 100 cm^3 of dry dichloromethane cooled to ca. 268K, 0.09 mol. of $TiCl_4$ was added dropwise followed by 0.05 mol. of dichloromethyl butyl ether at such a rate to keep the temperature of the reaction mixture around 268K. The mixture was subsequently stirred at 273K for 40 mins then poured onto ice. The organic layer was isolated, washed with water and sodium bicarbonate, and dried over $Mg SO_4$. The solvent was removed and the yellowish solid aldehyde was used in step 4.

Step (4).

To 0.02 mol. of 4-(ω -bromohexyl)-4'-formylbiphenyl was added 0.04 mol. of hydroxylamine hydrochloride, 0.07 mol. of pyridine, and 6 cm^3 of methanol. The reaction mixture was refluxed for 2.5 hrs, cooled to room temperature, and solvent removed. The mixture was purified on an alumina column (neutral grade) using dichloromethane as solvent.

Yield XXXVI (steps 3 and 4) = 20% m.pt. = 388K-392K.

Step (5).

Preparation of 4-(ω -bromohexyl)-4'-cyanobiphenyl. A mixture of 8×10^{-3} mol. of oxime and 0.05 mol. of acetic anhydride was refluxed for 3 hrs, cooled to room temperature, then poured onto ice. The organic layer was dissolved in chloroform, washed with water then dried with $M SO_4$. The removal of the solvent yielded a sweet smelling oil, which was chromatographed on a silica gel column using chloroform as

solvent. The product nitrile was recrystallised from methanol.

Yield XXXVII = 30% m.pt. 338K-341K.

Step (6). Monomer Preparation: This reaction is illustrated for XXXI.

4-(ω -bromohexyl)-biphenyl (0.033 mol) and 0.015 mol of the dicesium salt of 2-methylene glutaric acid were added to 40 cm³ of dry DMF. The heterogeneous reaction was stirred at 353K in an inert atmosphere for 48 hrs. The precipitated CsBr was removed by filtration, and solvent taken off on the rotary evaporator.* The product was recrystallised from ethyl acetate.

(a) Yield XXXVIII = 30% m.pt. = 330K-334K $c \rightarrow I$ (where c = crystalline, I = isotropic melt, N = nematic mesophase, Ch = cholesteric mesophase).

nmr (CDCl₃) δ ppm: 0.0 (TMS), 1.3-2.0 (m, 16H), 2.8-3.0 (t, 4H), 3.5 (s, 4H), 4.2-4.5 (t, 4H), 5.8 (s, 1H), 6.4 (s, 1H), 7.1-7.8 (m, 18H).

(b) Yield XXXIX = 25% m.pt. = 393K $c \rightarrow N$; 400K $N \rightarrow I$

nmr (CDCl₃) δ ppm: 0.0 (TMS), 1.1-2.1 (m, 16H), 2.9-3.3 (m, 4H), 3.5 (s, 4H), 3.5-3.7 (t, 4H), 4.0 (s, 3H), 5.85 (s, 1H), 6.5 (s, 1H), 6.9-7.9 (m, 16H).

(c) Yield XXXX = 10% m.pt. = 283K $c \rightarrow Ch$; 305K $Ch \rightarrow I$

nmr (CDCl₃) δ ppm: 0.0 (TMS), 0.6-2.5 (m, 39H), 2.9-3.1 (t, 4H), 3.4 (s, 4H), 3.7 (s, 3H), 4.0-4.2 (t, 4H), 5.8 (s, 1H), 6.4 (s, 1H).

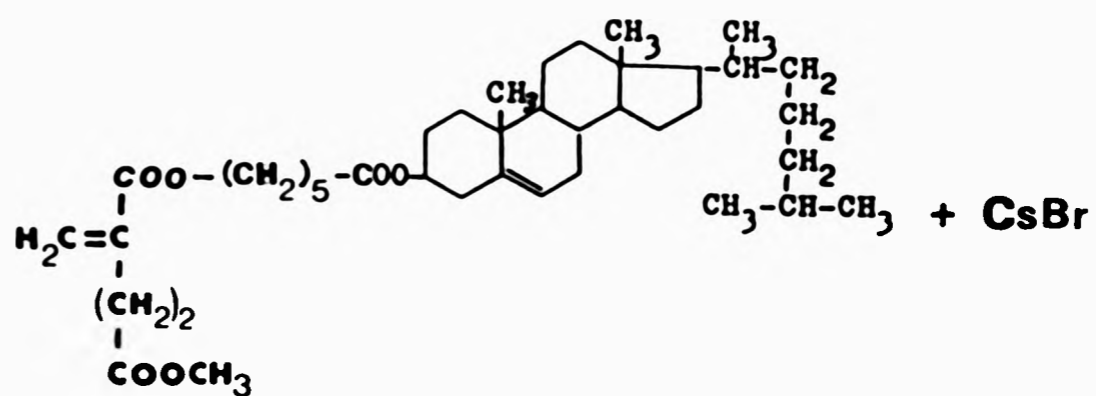
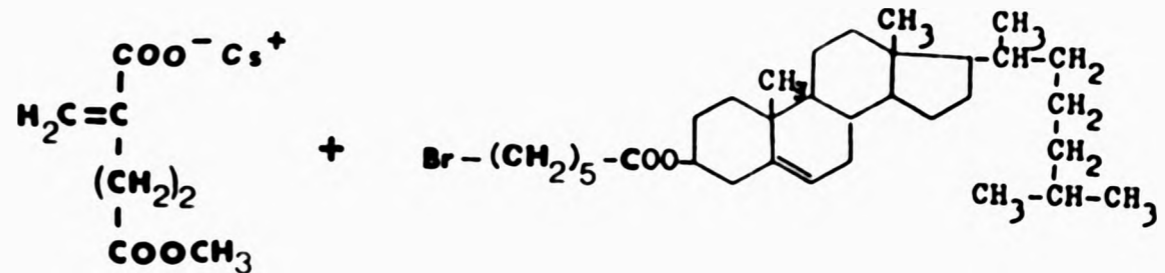
* In the synthesis of the monomer XXXX the crude reaction product was chromatographed on an alumina column using a CHCl₃/hexane (3:1) mixture as solvent.

7.2.2 Discussion

The choice of the biphenyl moiety in the present work was made on the basis of early studies by Gray,²³² who has shown the propensity of 4,4-disubstituted biphenyls to form a liquid crystalline phase.

The Freidel-Crafts acylation reaction (step 1) in addition to attaching the flexible spacer to the mesogenic moiety, also introduces a carbonyl function α to the aromatic system. Asymmetric reduction of this functionality (step 7) could lead to the synthesis of a novel class of cholesteric mesogens.

The acylation reaction proceeds smoothly using the unsubstituted biphenyl. Performing the analogous reaction upon p-methoxybiphenyl gives a low yield of the desired 4,4-substituted product, due primarily to competing acylation reactions, eg. ortho substitution of the ether phenyl ring. The third acylation attempted, that upon p-cyanobiphenyl gave a complex mixture of products and attempts to chromatograph a working amount of the 4,4-substituted compounds proved fruitless. The alternative procedure to 4-(ω -bromohexyl)-4'-cyanobiphenyl of Shibaev²³³ was therefore adopted, but unfortunately this also gave a low yield of the desired material (ca. 4%). Consequently, continuation of the proposed synthesis of Figure 7.1 was restricted to the use of the biphenyl compounds XXXIII and XXXIV. Additionally, the difficulty in obtaining the asymmetric reducing reagents proposed for step 7 meant the adoption of a more conventional approach to the synthesis of a cholesteric monomer ie. the preparation of a monomer based on cholesterol itself (Figure 7.2). To accomplish this synthesis and complete that of the two biphenyl monomers, the SN_2 reaction between the ω -alkyl bromide (the aliphatic spacer-mesogen species) and the chosen carboxylic cesium salt (step 6) was carried out. This reaction proved successful to a varying extent in all three cases, however as in the analogous methyl



CHOLESTERIC MONOMER (XXXX)

FIGURE 7.2 Preparation of cholesteric monomer based on cholesterol.

methacrylate systems, column chromatography was necessary to isolate the low yield of cholesteric monomer XXXX.

Monomers XXXIX and XXXX were shown to be mesomorphous by optical microscopy. The former is mesomorphous over the range 313K-400K, exhibiting what is probably a nematic mesophase, Plate 1 Figure 7.3. The monomer XXXX shows a planar cholesteric mesophase (the helical axes of the molecular arrangement of the molecules is perpendicular to the bounding surfaces) and is capable of reflecting light at the visible region over the range 288K-305K as evidenced by Plate 2 of Figure 7.3.

An examination of the optical properties of the corresponding homopolymers/copolymers was hampered by the poor yields of the preceding monomer syntheses. Only monomer XXXVIII was prepared in a sufficient amount to allow polymerisation. That this monomer is not mesamorphous does not preclude the formation of a mesophase by the homopolymer, as the polymer backbone has been found to enhance the degree of order of a biphenyl side group. In fact if a monomer is nematic, in most cases a smectic polymer results, only a few examples are known where both the monomer and polymer are nematic.

The homopolymer XXXXI was prepared, and examined by DSC and by complimentary studies with the hot stage microscope. Differential scanning calorimetry revealed two features (Figure 7.4) a) a T_g at 283K and b) a melting endotherm at 325K. Without more detailed analysis of the enthalpy of transition it is difficult to ascertain whether this thermal behaviour is that of a conventional semi-crystalline material, comprising both crystalline and amorphous domains, or a mesomorphous polymer. However, the inability to observe any identifiable mesophase, subsequent to annealing the material at 300 K for 24 hours, does, tend to suggest a semicrystalline rather than a mesomorphous polymer.



PLATE 1 MONOMER (XXXIX)

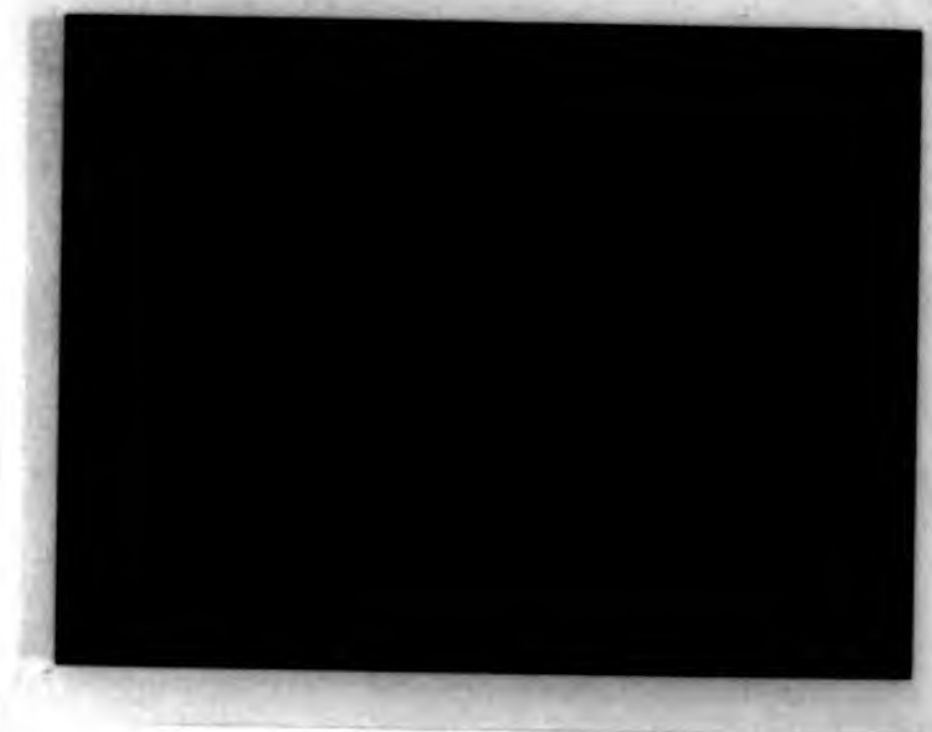


PLATE 2 MONOMER (XXXX)

FIGURE 7.3 (Plate 1) Optical micrograph of monomer XXXIX (crossed polarisers, magnification x 10, 315K) showing probable nematic mesophase.
(Plate 2) Optical micrograph of monomer XXXX (crossed polarisers, magnification x 10, 290K) showing chiral nematic mesophase (planar texture).

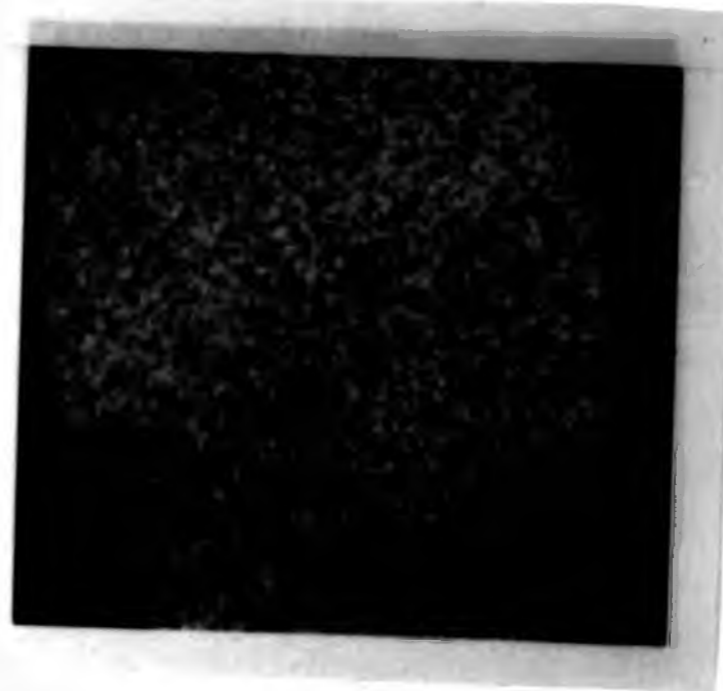


PLATE 1 MONOMER (XXXIX)

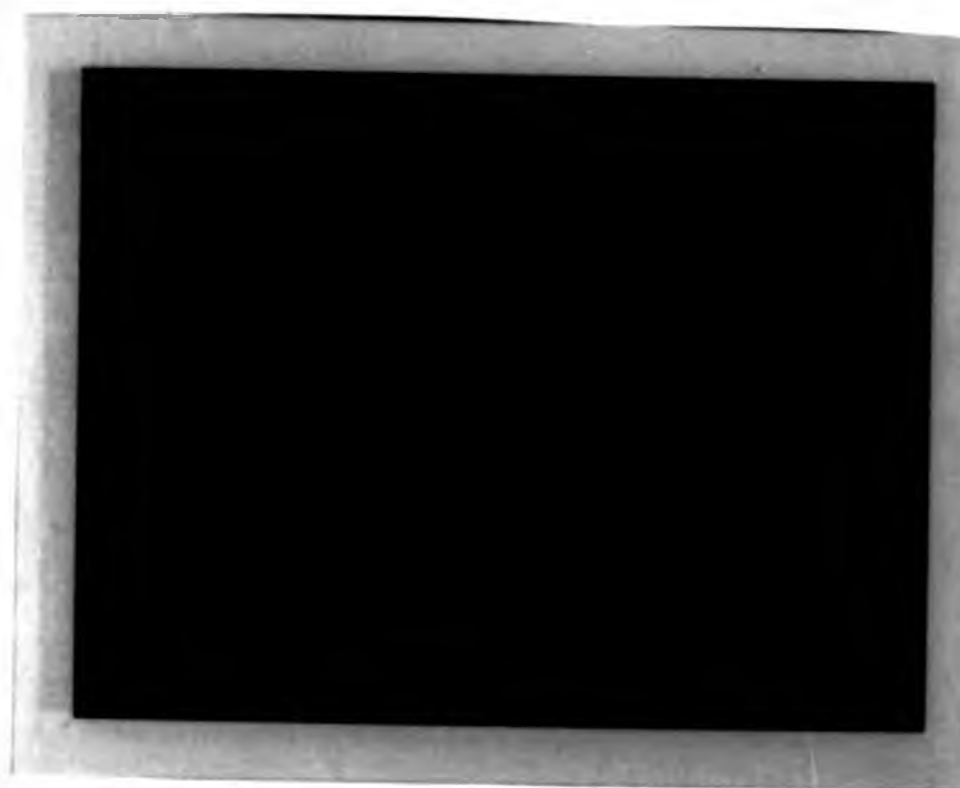


PLATE 2 MONOMER (XXXX)

FIGURE 7.3 (Plate 1) Optical micrograph of monomer XXXIX (crossed polarisers, magnification x 10, 315K) showing probable nematic mesophase.
(Plate 2) Optical micrograph of monomer XXXX (crossed polarisers, magnification x 10, 290K) showing chiral nematic mesophase (planar texture).

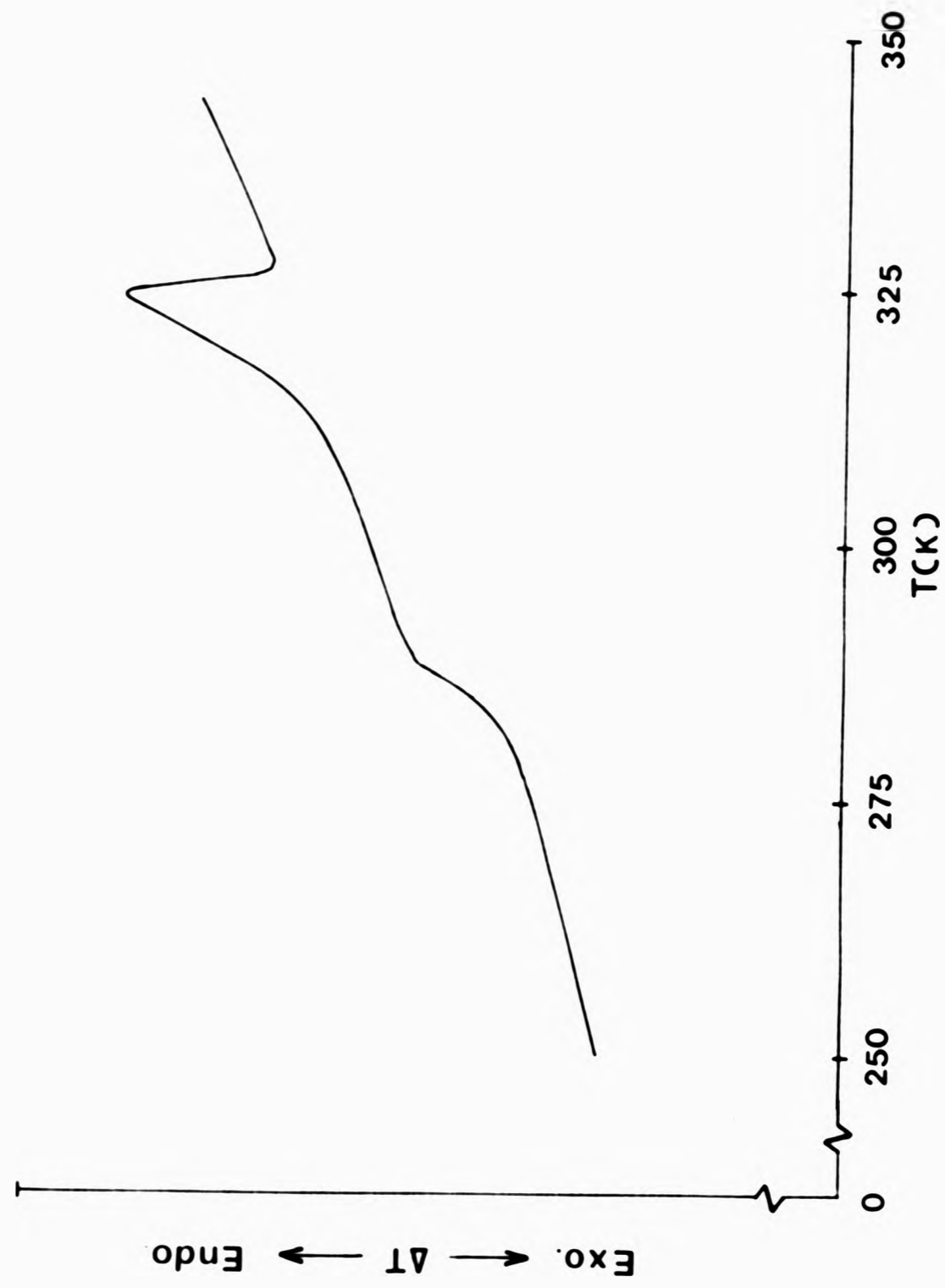


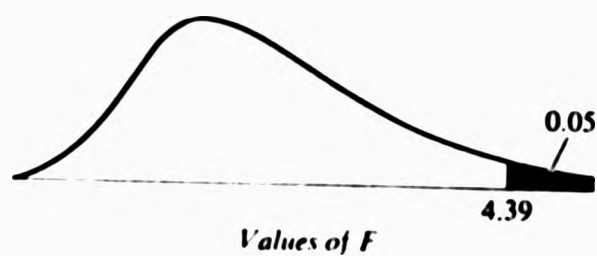
FIGURE 7.4 D.S.C. thermogram of polymer (XXXXI).

7.3 CONCLUSION

The present exploratory study has shown the possibility of preparing a number of interesting monomers by simple chemical transformation of MGN. The feasibility of synthesising liquid crystalline monomers based on 2-methyleneglutaric acid (MGA) has been demonstrated. Such systems have inherent advantages over the ubiquitous methyl methacrylate mesogens. For example, the difunctionality of MGA allows the synthesis of a monomer comprising two different mesogenic moieties, one of which could be cholesteric. The difunctionality may also permit the realisation of a polymeric mesophase at a low concentration of mesogen, ie the mesophase could be observed as a result of the liquid interaction between the pairs of mesogens. Additionally, the unsymmetrical nature of MGN, by virtue of the ethyl moiety, may go some way to reducing the propensity of mesogenic monomers to yield highly ordered smectic structures.

APPENDIX

THE F DISTRIBUTION



Example In an F -distribution with $\nu_1 = 5$ and $\nu_2 = 6$ degrees of freedom, the area to the right of an F value of 4.39 is 0.05. The value on the F -scale to the right of which lies .05 of the area is in lightface type. The value on the F -scale to the right of which lies .01 of the area is in boldface type. $\nu_1 =$ number of degrees of freedom for numerator; $\nu_2 =$ number of degrees of freedom for denominator.

$\nu_2 \backslash \nu_1$	1	2	3	4	5	6	7	8	9	10	20	30	40	50	100	200	∞	ν_2
1	161 4.052	200 4.999	216 5.403	225 5.625	230 5.764	234 5.859	237 5.928	239 5.981	241 6.022	242 6.056	248 6.308	250 6.361	251 6.386	252 6.392	253 6.394	254 6.395	254 6.396	1
2	18.51 98.49	19.00 99.00	19.16 99.17	19.25 99.25	19.30 99.30	19.33 99.33	19.36 99.36	19.37 99.37	19.38 99.39	19.39 99.40	19.44 99.45	19.46 99.47	19.47 99.48	19.47 99.48	19.49 99.49	19.49 99.49	19.50 99.50	2
3	10.13 34.12	9.55 30.82	9.28 29.46	9.12 28.71	9.01 28.24	8.94 27.91	8.88 27.67	8.84 27.49	8.81 27.34	8.78 27.23	8.66 26.69	8.62 26.50	8.60 26.41	8.58 26.35	8.56 26.23	8.54 26.18	8.53 26.12	3
4	7.71 21.20	6.94 18.00	6.59 16.69	6.39 15.90	6.26 15.52	6.16 15.21	6.09 14.90	6.04 14.80	6.00 14.66	5.96 14.54	5.80 14.02	5.80 13.83	5.74 13.74	5.71 13.69	5.66 13.57	5.65 13.52	5.63 13.46	4
5	6.61 16.26	5.79 13.27	5.41 12.06	5.19 11.39	5.05 10.97	4.95 10.67	4.88 10.45	4.82 10.29	4.78 10.15	4.74 10.05	4.56 9.55	4.50 9.38	4.46 9.29	4.44 9.24	4.40 9.13	4.38 9.07	4.36 9.02	5
6	5.99 13.74	5.14 10.92	4.76 9.78	4.53 9.15	4.39 8.75	4.28 8.47	4.21 8.26	4.15 8.10	4.10 7.98	4.06 7.87	3.87 7.39	3.81 7.23	3.77 7.14	3.75 7.09	3.71 6.99	3.69 6.94	3.67 6.88	6
7	5.59 12.25	4.74 9.55	4.35 8.45	4.12 7.85	3.97 7.46	3.87 7.19	3.79 7.00	3.73 6.84	3.68 6.71	3.63 6.62	3.44 6.15	3.38 5.98	3.34 5.90	3.32 5.85	3.28 5.75	3.25 5.70	3.23 5.65	7
8	5.32 11.26	4.46 8.65	4.07 7.59	3.84 7.01	3.69 6.63	3.58 6.37	3.50 6.19	3.44 6.03	3.39 5.91	3.34 5.82	3.15 5.36	3.08 5.20	3.05 5.11	3.03 5.06	2.98 4.96	2.96 4.91	2.93 4.86	8
9	5.12 10.56	4.26 8.02	3.86 6.99	3.63 6.42	3.48 6.06	3.37 5.80	3.29 5.62	3.23 5.47	3.18 5.35	3.13 5.26	2.93 4.80	2.86 4.64	2.82 4.56	2.80 4.51	2.76 4.41	2.73 4.36	2.71 4.31	9
10	4.96 10.04	4.10 7.56	3.71 6.55	3.48 6.09	3.33 5.74	3.22 5.49	3.14 5.21	3.07 5.06	3.02 4.95	2.97 4.85	2.77 4.41	2.70 4.25	2.67 4.17	2.64 4.12	2.59 4.01	2.56 3.96	2.54 3.91	10
20	4.35 8.10	3.49 5.85	3.10 4.94	2.87 4.43	2.71 4.10	2.60 3.87	2.52 3.71	2.45 3.56	2.40 3.45	2.35 3.37	2.12 2.94	2.04 2.77	1.99 2.69	1.96 2.63	1.90 2.53	1.87 2.47	1.84 2.42	20
30	4.17 7.56	3.32 5.39	2.92 4.51	2.69 4.02	2.53 3.70	2.42 3.47	2.34 3.30	2.27 3.17	2.21 3.06	2.16 2.98	1.93 2.55	1.84 2.38	1.79 2.29	1.76 2.24	1.69 2.13	1.66 2.07	1.62 2.01	30
40	4.08 7.31	3.23 5.18	2.84 4.31	2.61 3.83	2.45 3.51	2.34 3.29	2.25 3.12	2.18 2.99	2.12 2.88	2.07 2.80	1.84 2.37	1.74 2.20	1.69 2.11	1.66 2.05	1.59 1.94	1.55 1.88	1.51 1.81	40
50	4.03 7.17	3.18 5.06	2.79 4.20	2.56 3.72	2.40 3.41	2.29 3.18	2.20 3.02	2.13 2.88	2.07 2.78	2.02 2.70	1.78 2.26	1.69 2.10	1.63 2.00	1.60 1.94	1.52 1.82	1.48 1.76	1.44 1.68	50
100	3.94 6.90	3.09 4.82	2.70 3.98	2.46 3.51	2.30 3.20	2.19 2.99	2.10 2.82	2.03 2.69	1.97 2.59	1.92 2.51	1.68 2.06	1.57 1.89	1.51 1.79	1.48 1.73	1.39 1.59	1.34 1.51	1.28 1.43	100
200	3.89 6.76	3.04 4.71	2.65 3.88	2.41 3.41	2.26 3.11	2.14 2.90	2.05 2.73	1.98 2.60	1.92 2.50	1.87 2.41	1.62 1.97	1.52 1.79	1.45 1.69	1.42 1.62	1.32 1.48	1.26 1.39	1.19 1.28	200
∞	3.84 6.64	2.99 4.60	2.60 3.78	2.37 3.32	2.21 3.02	2.09 2.80	2.01 2.64	1.94 2.51	1.88 2.41	1.83 2.32	1.57 1.87	1.46 1.69	1.40 1.52	1.35 1.36	1.24 1.25	1.17 1.25	1.00 1.00	∞

REFERENCES

REFERENCES

1. Hydrocarbon Processing, 11, No 12, (1965).
2. J. Feldman, Brit. Patent 1,224,529, through Chem. Abs., 74, 124894S, (1971).
3. V. Tulio, U.S. Patent 3,567,759, through Chem. Abs., 74, 111603W, (1971).
4. J. McLure, U.S. Patent 3,562,311, through Chem. Abs., 74, 88354e, (1971).
5. T. Kita, Japan Patent, 70,35,288, through Chem. Abs., 74, 141028e, (1971).
6. W. Nemeč et al., Fr. Patent, 1,499,708, through Chem. Abs., 69 76678x, (1968).
7. H. Shinohara, Jap. Patent, 7,004,048, through Chem. Abs., 72, 121037n, (1970).
8. E. Pritchett and P. Kamath, J. Poly.Sci., Poly. Letters, 4, 849, (1966).
9. J. Martinmara and P. Patrakka, Die Makromol. Chemie, 175, 3275, (1974).
10. Fr. Patent, 1452716, National Distillers and Chem. Corp.
11. M. Galin and J. Galin, Eur.Poly. Journal, 9, 1149, (1973).
12. Y. Joh et al., through Chem.Abs., 74, 76818w, (1971).
13. Y. Joh et al., through Chem.Abs., 74, 142600x, (1971).
14. H. Staudinger, Helv.Chim.Acta., 5, 785, (1922).
15. F. Mayo and F. Lewis, J.Amer.Chem.Soc., 66, 1594, (1944).
16. H. Dostal and H. Mark, Trans. Faraday Soc., 54, (1936).
17. T. Alfrey et al., J. Amer.Chem.Soc., 67, 2044, (1945).
18. F. Mayo et al., *ibid.*, 67, 1701, (1945).
19. F. Mayo, F. Lewis and C. Walling, J. Amer.Chem.Soc., 70, 1529, (1948).
20. F. Lewis et al., *ibid.*, 70, 1527, (1948).
21. F. Lewis and F. Mayo, *ibid.*, 70, 1525, (1948).
22. K. Nozaki, J.Polym.Sci., 1, 455, (1946).
23. T. Lipatova et al., Zh.Phys.Chem., 30, 1752, (1956).
24. C. Walling et al., J.Amer.Chem.Soc., 70, 1544, (1948).
25. M. de Wilde et al., J.Polym.Sci., 5, 253, (1950).
26. Y. Shirota et al., Macromolecules, 7, No 1, 4, (1974).
27. T. Alfrey and C. Price, J.Polym.Sci., 2, 101, (1947).
28. G. Ham, *ibid.*, 45, 169, (1960).
29. C. Bamford and W. Barb, Discuss. Faraday Soc., 14, 208, (1953).
30. D. Booth et al., Trans. Faraday Soc., 55, 1293, (1959).

31. E. Merz, T. Alfrey and G. Goldfinger, *J. Polym. Sci.*, 1, 75, (1946).
32. W. Barb, *ibid.*, 11, 117, (1953).
33. G. Ham, *ibid.*, 14, 87, (1954).
34. W. Barb, *ibid.*, 10, 49, (1953).
35. G. Ham, Theory of Copolymerisation in 'Copolymerisation', chapt. 1, Interscience Publications, J. Wiley and Sons, Inc., N.Y., (1964).
36. K. Dodgson and J. Ebdon, *Eur. Poly. Journal*, 13, 791, (1977).
37. P. Deb and G. Meyerhoff, *ibid.*, 20, 713, (1984).
38. R. Barlett and K. Nozaki, *J. Amer. Chem. Soc.*, 68, 1495, (1946).
39. C. Walling et al., *ibid.*, 70, 1537, (1948).
40. F. Lewis et al., *ibid.*, 70, 1537, (1948).
41. F. Lewis, C. Walling, W. Cummings, E. Briggs and E. Mayo, *ibid.*, 70, 1519, (1948).
42. G. Ham, *J. Polym. Sci.*, 61, 9, (1962).
43. M. Litt and F. Bouer, *ibid.*, 67, Part C, 1551, (1967).
44. J. Seiner and M. Litt, *Macromolecules*, 4, 308, (1971).
45. R. Cais, R. Farmer, D. Hill and J.O.'Donnell, *ibid.*, 12, 835, (1979).
46. G. Georgiev and V. Zubov, *Eur. Poly. Journal*, 14, 93, (1978).
47. I. Javani et al., *J. Polym. Sci., Polym. Chem. Ed.*, 20, 977, (1982).
48. G. Kharas and M. Litt, *J. Polym. Sci., Polym. Bulletin*, 12, 65, (1984).
49. J. Furakawa, *J. Polym. Sci., Poly. Letters*, 7, 561, (1969).
50. A. Kawasaki et al., International Rubber Conference, 1975, Tokyo, Full text, p.13, *J. Soc. Rubber Ind., Japan*, 49, 169, (1976).
51. J. Furakawa, *J. Polym. Sci., Polymer Symposium No 51*, 105, (1975).
52. H. Finkelmann and G. Rehage, *Macromol. Chem., Rapid Commun.*, 1, 733, (1980).
53. H. Finkelmann and G. Rehage, *ibid.*, 1, 31, (1980).
54. F. Reintzer, *Monatsh*, 9, 421, (1888).
55. D. Lehmann, *Z. Phys. Chem. (Leipzig)*, 4, 462 (1889).
56. D. Vörländer, *ibid.*, 449, (1927).
57. C. Wiegand, *Z. Naturforsch*, 36, 313, (1954).
58. G. Gray, Materials Science Series; Polymeric Liquid Crystals, Academic Press (1982), Ed. Gifern, Krigbaum and Meyer.
59. G. Gray, Molecular Structure and the Properties of Liquid Crystals, Academic Press, London and New York (1962).
60. S. Chandrasekhar et al., *Pramana*, 9, 471, (1977).

61. G. Gray, 'Liquid Crystals and Plastic Crystals', Ch.4, p103 (1974).
62. Encyclopedia of Chemical Technology, 3rd ed., Vol. 14, p. 395.
63. W. Kast, In Landolt-Bornstein, 6th Ed., Springer, Berlin, Vol. 11, Part 2a, (1960).
64. D. Demus and H. Demus, Flüssige Knstalle in Tabethen, veb Deutscher Verlag für Grundslaggindustne, Leipzig, (1973).
65. G. Gray, 'Liquid Crystals and Plastic Crystals', Ch.2, p.19, (1974).
66. G. Friedel, Annls.Phys., 18, 273, (1922).
67. G. Gray, J.Chem.Soc., 3733, (1956).
68. G. Elliot, Chem. in Brit., 9(s), 213, (1973).
69. J. Ferguson, Sci. Am. 211, 77, (1964).
70. G. Meier et al., Application of Liquid Crystals, Springer Verlag. Berlin, Heidelber, N.Y., (1975).
71. G. Heilmeyer and J. Foldmacher, Proc. IEEE, 57, 34, (1969).
72. G. Brown (ed.), Liquid Crystals, Vol. 2, part 1, p. 217-232, Gordon and Breach, N.Y., (1969).
73. D. Vörländer, Ber., 70B, 1202, (1937).
74. P. Smith, Kolloid, Z. Polym. 250, 27, (1972).
75. C. Beatty et al., Macromolecules, 8, 547, (1975).
76. C. Desper and N. Schneider, Macromolecules, 9, 424, (1976).
77. A. Mousa et al. Polym. Bull., 6, 485, (1982-82).
78. V. Shibaev et al., Macromol. Chem., Rapid Commun., 3, 443, (1982).
79. H. Finkelmann, Polymer Liquid Crystals. Academic Press Inc., Ch.2, p. 35, (1982).
80. P. Morgan, Macromolecules, 10, 1381, (1977).
81. W. Krigbaum, Polymeric Liquid Crystals, Academic Press Inc., Ch.10, p. 275, (1982).
82. H. Finkelmann et al., Die Makromol. Chemie, A8 (10), 2541, (1978).
83. V. Shibaev et al., Eur. Poly. Journal, 16, 277, (1980).
84. V. Shibaev et al., J. Polym. Sci., Polym. Chem. Ed., 17, 1655, (1979).
85. J. Wendorff et al., Mesomorphic Order in Polymers, ACS Symposium Series 74, p. 11, Ed. A. Blumstein, (1978).
86. H. Finkelmann and G. Rehage, Makromol. Chem. Rapid Commun., 1, 31, (1980).
87. N. Platé and V. Shibaev, J. Polym. Sci., Polym. Symp., 67, 1, (1980).
88. V. Shibaev and N. Platé, Adv. Polym. Sci., 60/61, p. 173, (1984).

89. A. Blumstein and E. Hsu, 'Liquid Crystalline Order in Polymers', Ed. A. Blumstein, Academic Press, N.Y., p. 150, (1978).
90. Chemical and Engineering News, May, p. 46, (1984).
91. S. Clough et al., Mesomorphic Order in Polymers, ACS Symposium Series 74, p.1., Ed. A. Blumstein, (1978).
92. H. Finkelmann and G. Rehage, Adv. Polym. Sci., 60/61, p. 99, (1984).
93. I. Konstantinov et al., Eur. Poly. Journal, 20, 1127, (1984).
94. B. Bresci et al., Eur. Poly. Journal, 20, 1127, (1984).
95. F. Goss and C. Ingnd, J. Chem. Soc., 277, 6, (1925).
96. U.S. Patent, 2,232,785.
97. E. Coyner and N. Hillman, J. Amer. Chem. Soc., 71, 324, (1949).
98. J. Feldman, Neth. Appl., 6,402,627, (Sept. 1966), National Distillers and Chem. Corp., through Chem. Abs., 66, 37462, (1967).
99. J. Feldman and B. Saffer, Fr. Pat., 1,388,444, (Feb., 5, 1965), National Distillers and Chem. Corp., through Chem. Abs., 63, 504, (1965).
100. Rhone Poulenc, S.A. Neth. Appl., 6,603,115 (Sept. 1966) through Chem. Abs., 66, 85483, (1967).
101. P. Charbordes et al., Fr. Pat., 1,381,511, (Dec. 1984) through Chem. Abs., 62, 9022, (1965).
102. H. Ito and K. Kimura, Japan Kokai 7,375,514, through Chem. Abs., 80, 47475a, (1974).
103. C. Weis and T. Ninkler, Helv. Chimica Acta, 57, 856, (1974).
104. B. Baker et al., J. Org. Chem., 17, 122, (1952).
105. A. Zilkha and U. Golik, *ibid.*, 28, 2007, (1963).
106. N. Gaylord, U.S. Pat., 345,211, through Chem. Abs., 71, 62373y, (1969).
107. T. Taurney et al., J. Org. Chem., 26, 15, (1961).
108. T. Oishi et al., J. Polym. Sci., Polym. Chem. Ed., 21, 1053, (1983).
109. W. Sorenson and T. Campbell, Preparative Methods of Polymer Chemistry, p. 313, 2nd Ed., (1968), Interscience Publishers.
110. H. Gilman, J. Amer. Chem. Soc., 45, 152, (1923).
111. H. Normant and B. Angelo, Bull. Soc. Chim. Fr., 354, (1960).
112. Y. Joh et al., J. Polym. Sci., A-1, 5, 2503, (1967).
113. R. Dessy et al., J. Amer. Chem. Soc., 79, 3476, (1957).
114. Hanna and Ashbaugh, J. Phys. Chem., 68, 811, (1964).
115. R. Sahai et al., Proc. Nat. Acad. Sci., USA, 71, 1499, (1974).
116. P. Job, Ann. Chim. (Paris), 9, 113, (1928).

117. W. Person, *J. Amer. Chem. Soc.*, 2, 87, (1965).
118. *Techniques and Methods of Polymer Evaluation, Vol. 4, Polymer Molecular Weights Pt 1*, p. 142, (1975), P. Slade, (Ed).
119. D.J. Meiler, Ed., 'Molecular Basis of Transitions and Relaxations', Gordon and Breach, N.Y., (1978).
120. J.F. Rabek, 'Experimental Methods in Polymer Chemistry', J. Wiley and Sons, N.Y., (1980).
121. E.S. Watson, M.J. O'Neill, J. Justin and N. Brenner, *Anal. Chem.*, 36, 1233, (1964).
122. M.J. O'Neill, *ibid.*, 38, 1331, (1968).
123. J.K. Gillham, Review paper, *AIChE Journal*, 6, 20, 1066, (1974).
124. J.M.G. Cowie, *J. Macromol. Sci.-Phys.*, B, 18, 569, (1980).
125. A. Zilkha et al., *J. Polym. Sci.*, 49, 231, (1961).
126. N. Grassie and I. McNeill, *ibid.*, 33, 171, (1958).
127. N. Grassie, 'Chemical Reactions of Polymers', Edited by E.M. Lettes, Interscience, N.Y., (1964).
128. N. Grassie and R. McGuchan, *Eur. Poly. Journal*, 6, 1277, (1970).
129. R.B. Beevers, *Macromol. Rev.*, 3, 115, (1968).
130. T.G. Fox and S. Loshaek, *J. Polym. Sci.*, 15, 371, (1955).
131. R.B. Beavers, *ibid*, Part A, 2, 5257, (1964).
132. C. Schildknecht, 'Alkyl Compounds and their Polymers', *High Polymers Vol. XXVIII*, Wiley-Intersciences, N.Y., (1973).
133. G. D'Alelia, *U.S. Pat.*, 2,339,058.
134. E. Leonard, 'Vinyl and Diene Monomers', *High Polymers Vol. XXIV, Part 2*, Wiley-Interscience, N.Y., (1971).
135. G. Coates et al., 'Organometallic Compounds' Vol. 1, 3rd Ed., Methven, (1967).
136. J.R. Collins, Unpublished work, see reference 129, p. 117.
137. N. Kanabata and T. Tsuruta, *Macromol. Chem.*, 86, 231, (1965).
138. A. Tsukamoto, *J. Polym. Sci.*, A3, 2767, (1965).
139. B. Erusalimskii et al., *Russ. Chem. Rev.*, 37 (11), 874, (1968).
140. 'Reactivity, Mechanism and Structure in Polymer Chemistry', Interscience, A. Ledwith and A. Jenkins (Eds.) (1974).
141. M. Szwarc, in 'Carbanions, Living Polymers and Electron Transfer Processes', Interscience, J. Wiley and Sons Inc., (1968).
142. T. Tsuruta and Y. Yasuda, *J. Macromol. Sci.*, Part A, 2, 943, (1968).
143. R. Houtz, *J. Textile Res.*, 20, 786, (1950).

144. N. Batty and J. Guthrie, *Makromol. Chem.*, 182, 71, (1981).
145. N. Grassie and J. Hay, *J. Polym. Sci.*, 56, 189, (1962).
146. T. Wagner-Jauregg, *Chem. Ber.*, 63, 3213, (1930).
147. H. Gilbert et al., *J. Amer. Chem. Soc.*, 78, 1669, (1956).
148. F. Lewis et al., *J. Amer. Chem. Soc.*, 70, 1523, (1948).
149. G. Butler et al., *J. Macromol. Sci., Chem. Ed.*, A2, 1533, (1972).
150. K. Fujimori, *Aust. J. Chem.*, 33, 189, (1980).
151. B. Kamo et al., *Polymer J.*, 6, 121, (1974).
152. I. Skeist, *J. Amer. Chem. Soc.*, 68, 1781, (1946).
153. W. Richardson, *J. Polym. Sci.*, 10, 353, (1953).
154. F. Billmeyer in 'Experiments in Polymer Science', p. 216, Wiley-Interscience Publication, (1973).
155. J. Moacawin and R. Simha, *J. Chem. Phys.*, 45, 964, (1966).
156. G. Mortimer and P. Tidwell, *J. Polym. Sci.*, A3, 369, (1965).
157. G. Lowry, *ibid*, 12, 463, (1960).
158. K. O'Driscoll and J. Dickson, *J. Makromol. Sci. - Chem.*, A2, 449, (1968).
159. G. Ham, *J. Polym. Sci.*, 54, 1, (1961).
160. G. Smets, *Bull. Soc. Chim. Belges*, 59, 13, (1950).
161. A. Rudin et al., *J. Macromol. Sci. - Chem.*, A7, 1203, (1973).
162. H. Johnston and A. Rudin, *Macromolecules*, 4, 661, (1971).
163. M. Mortimer and P. Tidwell, *J. Macromol. Sci. Rev.*, 4, 281, (1970).
164. R. Leicht and J. Fuhrmann, *J. Polym. Sci., Poly. Chem. Ed.*, 21, 2215, (1983).
165. C. Walling, 'Free Radicals in Solutions', Ch.4, J. Wiley and Sons Inc., N.Y., (1957).
166. L. Peebles, in G. Ham (Ed.), 'Copolymerisation', p. 564-573, Interscience Publishers, J. Wiley and Sons Inc., N.Y., (1964).
167. S. Iwatsuki and T. Itah, *Macromol. Chem.*, 180, 663, (1979).
168. T. Alfrey et al., 'Copolymerisation', Interscience, N.Y. (1952).
169. H. Coover Jr. et al., *J. Polym. Sci.*, A4, 2563, (1966).
170. R. Greenly, *J. Macromol. Sci.*, A4, 2563, (1966).
171. High Polymers, Vol. XXIV, Vinyl and Diene Monomers Part 1, p. 68, E. Leonard (Ed.), Wiley-Interscience Pub., (1970).
172. L. Young, *J. Polym. Sci.*, 54, 411, (1961).
173. T. Fox, *Bull. Amer. Phys. Soc.*, 1, 123, (1956).
174. M. Hirooka and T. Kato, *J. Poly. Chem. Poly. Letts. Ed.*, 12, 31, (1974).
175. N. Johnston, *Macromolecules*, 6 (3), 453, (1973).

176. N. Johnston, *Poly. Prepr. Amer. Chem. Soc., Div. Polym. Chem.*, 10 (2), 609, (1969).
177. I. Schneider, *J. Polym. Sci., Poly. Sympos.*, 64, 95, (1978).
178. J. Heijboer, 'Static and Dynamic Properties of the Polymer Solid State', *Proc. N.A.T.O. Adv. Study Institute, Glasgow* (1981). R. Pethrick and R. Richards (Eds.), D. Reidel (Publ.).
179. A. Yee and S. Smith, *Macromolecules*, 14, 54, (1981).
180. N. McCrum et al., 'An Elastic and Dielectric Effects in Polymer Solids', *J. Wiley, London*, (1967).
181. R. Boyer, in 'Proceedings of Conf. on Poly. Structure and Mechanical Properties', *U.S. Army Natick Laboratories, Natick, M.A.*, (1967).
182. L. Nielsen, *Poly. Eng. Sci.*, 17, 713, (1977).
183. S. Aharoni, *J. Apply. Poly. Sci.*, 16, 3275, (1975).
184. S. Brannstein et al., *Macromolecules*, 6, 715, (1973).
185. H. Günther, 'NMR Spectroscopy', p. 299, *J. Wiley and Sons Inc.*, (1980).
186. G. Gatti and A. Carbonaro, *Die Macromol. Chemie*, 175, 1627, (1974).
187. I. Kuntz and N. Chamberlain, *J. Polym. Sci., Poly. Chem. Ed.*, 12, 1695, (1974).
188. C. Bamford et al., *Nature*, 209, 292, (1966).
189. H. McConnell, *J. Chem. Phys.*, 28, 430, (1958).
190. H. Benesi and J. Hildebrand, *J. Amer. Chem. Soc.*, 71, 2703, (1949).
191. G. Scatchard, *Ann. N.Y. Acad. Sci.*, 51, 660, (1949).
192. D. Deranleau, *J. Amer. Chem. Soc.*, 91, 4050, (1969).
193. R. Drago et al., *ibid.*, 95, 6645, (1973).
194. G. Johnson and R. Bowen, *ibid.*, 87, 1655, (1965).
195. W. Schneider, *J. Phy. Chem.*, 66, 2653, (1962).
196. E. Tsuchida et al., *Die Macromol. Chem.*, 151, 245, (1972).
197. P. Curran, unpublished work, *University of Stirling*, (1984).
198. P. Hyde and A. Ledwith, in 'Molecular Complexes', Vol. 2, R. Foster (Ed.), P. Elek (Pub.), *London*, (1974).
199. S. Iwatsuki et al., *Macromolecules*, 16, 1571, (1983).
200. H. Scott et al., *Tetrahedron Letts.*, 1073, (1963).
201. C. Walling, *J. Amer. Chem. Soc.*, 71, 1930, (1949).
202. N. Gaylord, 'Polymerisation Reactions and New Polymers', *Advances in Chemistry, Series 129*, N. Platzer (Ed.), *Amer. Chem. Soc., Washington D.C.*, (1973).

203. L. Ellinger, *Polymer*, 5, 559, (1964).
204. T. Natsuime et al., *Chem. Commun.*, 189, (1969).
205. S. Aoki and J. Stille, *Macromolecules*, 3, 472, (1970).
206. C. Bamford et al., *Proc. Roy. Soc.*, A, 241, 364, (1957).
207. M. Hirooka et al., *J. Polym. Sci.*, B, 5, 47, (1967).
208. V. Kabanov et al., *J. Polym. Sci., Poly. Chem. Ed.*, 15, 1777, (1977).
209. M. Imoto et al., *Makromol. Chem.*, 65, 174, (1963).
210. J. Furukawa et al., *Polymer J.*, 1, 155, (1970).
211. T. Kelen and F. Tüdös, *J. Macromol. Sci., Chem.*, A9 (1), 1, (1975).
212. T. Kelen et al., *J. Polym. Sci., Poly. Chem. Ed.*, 13, 2277, (1975).
213. K. O'Driscoll et al., *J. Polym. Sci., Polym. Lett. Ed.*, 18, 81, (1980).
214. R. Mulliken and W. Person, 'Molecular Complexes: A lecture and Reprint Volume', Wiley-Interscience, N.Y., (1969).
215. K. Fukui, *Acc. Chem. Res.*, 4, 57, (1971).
216. N. Allinger, *Quantum Chem. Proc. Ex.*, No. 11, (1976).
217. Gaussian, '79 *Quantum Chem. Proc. Ex.*, I.B.N., 360/370, (1971). Modified for VAX 11/780 Computer.
218. R. Le Fevre and K. Sundaram, *J. Chem. Soc.*, 3547, (1963).
219. D. Pollock et al., *J. Polym. Sci.*, 15, 87, (1955).
220. K. Fukui et al., *J. Polym. Sci.*, 20, 537, (1956).
221. D. Hill et al., *Macromolecules*, 15, 960, (1982).
222. E. Tsuchida and T. Tohono, *Makromol. Chem.*, 141, 265, (1971).
223. E. Wilson, 'An Introduction to Scientific Research', p. 204, McGraw-Hill, N.Y., (1952).
224. T. Kelen and F. Tüdös, *J. Polym. Sci., Polym. Symposium*, No. 50, 109, (1975).
225. G. Lowry, *J. Polym. Sci.*, 42, 463, (1960).
226. J. Vialle et al., *J. Macromol. Sci., Chem.*, A5, (6), 1031, (1971).
227. H. Gilbert et al., *J. Amer. Chem. Soc.*, 78, 1669, (1956).
228. C. Pittman and T. Rounsefell, *Macromolecules*, 8, 46, (1975).
229. D. Worsfold and S. Bywater, *J. Polym. Sci.*, 26, 299, (1957).
230. F. Dainton and K. Ivin, *Quart. Rev. Chem. Soc.*, 12, 61, (1958).
231. G. Lowry, *J. Polym. Sci.*, 47, 463, (1960).
232. G. Gray, *J. Phys. Paris*, 36, 337 (1975).
233. V. Shibaev et al., *Eur. Poly. J.*, 18, 651, (1982).